Biogeochemical evidence for chemosymbiosis in the fossil record

Edine Pape

Submitted in accordance with the requirements for the degree of
Doctor of Philosophy

The University of Leeds
School of Earth and Environment

September 2016

The candidate confirms that the work submitted is his/her own and that appropriate credit has been given where reference has been made to the work of others.

Acknowledgements

Firstly I would like to thank my supervisors Fiona Gill, Rob Newton and Cris Little for introducing me to the magical worlds of chemistry and the deep sea. I am particularly grateful for the continuous support and encouragement from Fiona, even when I moved away from Leeds.

In addition I want to thank the many persons and institutions that have given funding, performed analyses, helped me during research trips, and provided samples. All these contributions have greatly helped with this research project.

I am also grateful for the many wonderful people in Leeds, that have provided both general merriment and advice, in particular Caroline, Jamie, Rhian, Laura, Daniela, James, Toby, Ben, Simon, and Lucy “like it or limpet” Campbell. Finally I want to thank my mum Cobi, my dad Johan, my sisters Hilde and Marieke, and the three family cats, for being the most loving and fun family anyone could wish for.

Abstract

Chemosymbiotic invertebrates obtain nutrition from harbouring bacteria that oxidize reduced chemicals to produce energy for carbon fixation. This allows the animals to thrive in the extreme conditions of the deep sea, because the high concentrations of sulphide (thiotrophy) and methane (methanotrophy) at cold seeps and hydrothermal vents can be utilized by the symbiotic bacteria. This research investigates whether the key role of chemosymbiosis in shaping modern deep sea ecosystems can be traced through geological time, by using the stable isotope composition ($\delta^{13}C$, $\delta^{15}N$, $\delta^{34}S$) of organic matter in invertebrate shells. Shell-bound organic matter (SBOM) was isolated using various shell removal techniques, and method comparison suggests that the original isotopic signal is least affect by using EDTA or acetic acid. Multi-isotope analysis of SBOM obtained from (deep sea) molluscs and brachiopods confirms that the main types of chemosymbiosis can be differentiated from non-symbiotic heterotrophic nutritional strategies. In particular chemosymbiotic SBOM $\delta^{13}C$ is characteristically depleted, with defined ranges for the presence of either methanotrophic or thiotrophic symbionts across environmental settings. In suspected thiotrophic taxa from ancient cold seeps, the preservation of this modern range (SBOM $\delta^{13}C$ -35‰ to -29‰) is limited to young subfossil specimens, but the upper threshold is only exceeded in pre-Pliocene samples. Moreover, the protected intra-crystalline SBOM pool retains a distinct $\delta^{13}C$ signal up to the Miocene, and available $\delta^{34}S$ and $\delta^{15}N$ data of intra-crystalline SBOM do not overlap between heterotrophy and thiotrophy. For methanotrophy ($\delta^{13}C$ -65‰ to -36‰ at modern cold seeps) a residual $\delta^{13}C$ biosignature does appear to be present in total SBOM from Miocene samples. This encouraging finding, together with the discovery of intra-crystalline original proteins in a fossil of Cretaceous age, suggests that future work on other well-preserved specimens could trace the evolution of chemosymbiosis deep into geological time.

Table of Contents

List of Tables

List of Figures

Chapter 1
Introduction

The discovery of deep sea ecosystems fuelled by chemical energy drastically changed scientific views on marine biodiversity, and this unique way of life was found at two types of settings: cold seeps and hydrothermal vents (Corliss et al., 1979; Paull et al., 1984). Both ecosystems are sustained by reducing compounds that are emitted from the subsurface, but there are also marked differences between them (reviewed by e.g. Van Dover, 2000; and Tunnicliffe et al., 2003). Hydrothermal vents occur mostly at mid-oceanic ridges, and the presence of a magma chamber causes water to become heated (up to 60°C) and enriched in reduced compounds, such as sulphide and metals. Whereas cold seeps are located along continental margins, and are characterized by the reduction of organic matter that produces methane and other hydrocarbons to seep to the seafloor (at an ambient seawater temperature of 1° to 3°C). Because of the high concentrations of methane, not all of the methane is metabolized by sulphate-driven anaerobic oxidation of methane (AOM), and the consumption of methane and sulphate produces the large amounts of hydrogen sulphide present at cold seeps (Boetius et al., 2000).

Seep and vent ecosystems are located well below the euphotic zone, and primary production comes from chemoautotrophic bacteria. The presence of terminal electron acceptors (oxygen or nitrate) allows them to oxidize the inorganic reduced compounds (sulphide, methane), and use the released energy for carbon fixation (Jannasch and Mottl, 1985; Van Dover et al., 2002). Invertebrate animals can harbour such chemosynthethic bacteria within modified cells of their gill tissues, a nutritional strategy known as chemosymbiosis. The food sources provided by the bacteria allow chemosymbiotic invertebrates to overcome low food availability, and to thrive in the extremely inhospitable conditions of the deep sea (Conway et al., 1994). In this symbiotic relationship the invertebrate host steadily provides the bacteria with reduced compounds and the oxidant oxygen, often by bridging the oxic/anoxic interface (Stewart et al., 2005). The role of nitrate in symbiont respiration is still debated (e.g. evidence for nitrate respiration in Hentschel et al., 1993) and would allow chemosymbiosis to occur in completely anoxic conditions (Roeselers and Newton, 2012).

Symbioses with chemoautotrophic bacteria have been found in a remarkable number of animals, and are most widespread amongst bivalves. All five bivalve families that have evolved symbioses contain the bacteria within specialized bacteriocytes in their very enlarged gills (Stewart et al., 2005).

Three main types of chemosymbiosis can be identified: methanotrophic bacteria that use methane for energy generation, thiotrophic bacteria that utilize hydrogen sulphide, or both types of bacteria in dual symbiosis (Dubilier et al., 2008; Taylor and Glover, 2010) Multiple symbioses with additional bacterial types have been recognized, but their energy sources and nutritional contribution are poorly understood (Taylor and Glover, 2010; Duperron et al., 2013). In addition, Petersen et al. (2011) has demonstrated that thiotrophic bacteria are capable of using hydrogen present at vents as an energy source. The flexibility in bacterial types, and the environmental sources they utilize, allows their hosts to optimally utilize the geochemical sources of the deep sea, that can be very variable in time and space (LeBris & Dupperon, 2010).

Cold seeps and hydrothermal vents with their associated faunas have also been recognized in the fossil record, dating back to the Silurian (e.g. Barbieri et al., 2004). Despite the importance of chemosymbiosis in modern deep sea environments, there is currently very little evidence as to whether ancient seep and vent dwellers were capable of using this nutritional strategy. This is largely because methods demonstrating chemosymbiosis in modern specimens, such as histological, genetic and lipid biomarker analyses (e.g. Duperron et al., 2007; Decker et al., 2013) require soft tissues. A chemosymbiotic lifestyle is therefore usually inferred from modern chemosymbiotic representatives of a fossil species. However, more ancient deep sea ecosystems also contain invertebrate animals whose nutritional strategy cannot be determined, because they have either gone extinct, or because they are no longer present at modern seeps and vents. Knowledge about the nutritional strategies of such fossil seep dwellers is critical to our understanding of the evolution of deep sea fauna, and it is very likely that the capability of chemosymbiosis strongly influenced the composition of deep sea ecosystems.

To obtain new evidence about the ecology of fossil invertebrates, we aimed to test and apply a novel biogeochemical method to analyse ancient shell material to directly reconstruct nutritional strategies. It is well known that an animal's soft tissues reflect the isotopic composition of its nutritional sources for carbon ($\delta^{13}C$), nitrogen ($\delta^{15}N$), and sulphur ($\delta^{34}S$), following the "you are what you eat" principle

(DeNiro and Epstein, 1976; McCutchan et al., 2003). In biomineralizing invertebrates the soft tissues also produce organic templates necessary for biomineralisation, the shell-bound organic matter (SBOM), that is thought to reflect soft tissues values (O'Donnell et al., 2003). In particular it could be possible to identify different types of chemosymbiosis using SBOM, because the unique chemical sources they utilize have distinctive isotopic signatures compared to photosynthetic sources. It has already been proven possible to distinguish shallow water thiotrophic bivalves from heterotrophic feeders based on the carbon, sulphur and nitrogen composition of the SBOM from their shells (Dreier et al., 2012; Dreier et al., 2014).

Analysis of stable isotope signatures of SBOM from cold seep fossil shells could therefore potentially reveal methanotrophic, thiotrophic or dual chemosymbiosis in extinct organisms. Successful application of this novel proxy is dependent on the preservation of the organic molecules, and the retention of their original isotopic signal. From modern molluscs it is known that the majority of SBOM consists of a variety of proteins (amino acids linked by peptides), carbohydrates (complex sugars) are present in much lower abundance, and a very small fraction is made up by lipids (diverse hydrophobic molecules) (Marin et al., 2012). Lipids are generally most resistant to decay and are regularly found in Palaeozoic samples, whilst proteins and polysaccharides are not well preserved on geological timescales (Gupta & Briggs, 2011). However, the mineral-bound proteins of SBOM have the advantage of being protected from degradation compared to organically preserved fossils, and proteins have been identified from e.g. mid-Miocene gastropods (Nance et al., 2015) and have been reported up to the Silurian (Jope et al., 1967). SBOM within fossil shells is however still at risk of degradation via a variety of diagenetic pathways, including the incorporation of components from the surrounding sediment (Penkman et al., 2008). In addition to 'total' SBOM, a particular focus has therefore been placed on the isotopic signature of the intra-crystalline SBOM pool. Whereas the inter-crystalline SBOM surrounds the mineral crystals, the smaller intra-crystalline fraction becomes encased in the growing crystals (Crenshaw, 1972; Lowenstam and Weiner, 1989). Because of this protection from the external environment, intra-crystalline SBOM has an even greater potential to be protected from degradation and preserve over longer timescales (Sykes et al., 1995; Penkman et al., 2008).

1.1 Aim, objectives and thesis structure

The aim of this thesis is to use the stable isotopic analysis of SBOM to trace the evolution of chemosymbiotic lifestyles through geological time. The application of SBOM as a dietary proxy in modern specimens has thus far been very limited, particularly with respect to different nutritional strategies and invertebrate taxa. In addition, the isotopic effects of chemical SBOM isolation are largely unknown. To be able to use stable isotope analysis of SBOM in a reliable manner on fossil specimens, this research was devised around several research questions

- **Research question 1:** Is the stable isotopic composition of SBOM influenced by chemical extraction from shell carbonate?
- **Research question 2:** Does the stable isotopic composition of SBOM relate in a predictable way to that of soft tissues?
- **Research question 3:** Can different nutritional strategies be identified in SBOM (and soft tissues) by their distinct isotopic compositions?
- **Research question 4:** Are SBOM and its original stable isotopic composition preserved over geological time?

These research questions are discussed in three data chapters that are presented in manuscript format, including further introduction to the main research questions. Chapter 2 focusses on method comparison of shell removal techniques and their potential effects on the stable isotopic values ($\delta^{13}C$, $\delta^{15}N$, $\delta^{34}S$) of total SBOM and intra-crystalline SBOM (**Research question 1**), using three test species. Because the isotopic relationship between SBOM and soft tissues of bivalves is poorly understood, the soft tissues of several individual specimens were also analysed (**Research questions 2 and 3** for heterotrophic filter-feeders). In Chapter 3 **Research question 2 and 3** are investigated for a wide range of modern invertebrates from cold seeps and hydrothermal vents, including methanotrophic, thiotrophic, and dual symbiotic bivalves and gastropods. The suite of modern samples also includes brachiopods.

In Chapter 4 the results concerning **Research question 4** are presented. Stable isotope compositions of SBOM were obtained from ancient cold seeps specimens. To assess the preservation of these biosignatures molecular and visual analyses have been performed.

Chapter 2

Stable isotopic comparison of four different methods to isolate shell-bound organic matter in bivalves

Edine Pape[a], Fiona Gill[a], Robert J. Newton[a], Crispin T.S. Little[a], Geoffrey D. Abbott[b].

[a] School of Earth and Environment, University of Leeds, Leeds LS2 9JT, United Kingdom

[b]School of Civil Engineering and Geosciences, Newcastle University, Newcastle upon Tyne NE1 7RU, United Kingdom

Author contribution

EP performed the SBOM extractions, prepared SBOM/soft tissues for stable isotope and Py-GC/MS analysis, helped with stable isotope analysis, and wrote the paper. RJN carried out stable isotope analysis and supervised the contribution of EP therein, FG supervised EDTA extractions, and CTLS supervised bivalve dissection. GDA generated Py-GC/MS results, that were interpreted by EP, FG and GDA. EP, FG, RJN and CTLS designed the research and commented on the manuscript.

Relevant research questions

This chapter focusses on the methodological aspects of obtaining SBOM for stable isotope analysis, presented in the introductory chapter as **Research question 1: Is the stable isotopic composition of SBOM influenced by chemical extraction from shell carbonate*?*** In addition, the stable isotope analysis of soft tissues ($\delta^{13}C$, $\delta^{15}N$, $\delta^{34}S$) as well as SBOM for several individual specimens of the heterotrophic test species will provide information regarding **Research question 2: Does the stable isotopic composition of SBOM relate in a predictable way to that of soft tissues?**

2.1 Introduction

Shell-bound organic matter (SBOM) is the small organic component of mollusc and brachiopod shells, consisting of a proteinaceous framework surrounding the mineral crystals (inter-crystalline SBOM), and a minor fraction that is present within the single crystals (intra-crystalline SBOM), together making up the total SBOM (Lowenstam and Weiner, 1989). The SBOM of molluscs is secreted by mantle epithelial cells, and regulates biomineralisation by controlling the growth, mineralogy and structural organisation of newly formed crystallites (Marin et al., 2012).

As a decay-resistant alternative to the animal's soft tissues, SBOM has great potential as an isotopic proxy for nutrition in both modern and fossil shelled invertebrates (e.g. O'Donnell et al., 2003; Mae et al., 2007; Dreier et al., 2012). Stable isotope analysis of SBOM requires its separation from the mineral component of the shell, because the minerals carry an environmental isotopic signal derived from surrounding seawater, and they are much more abundant than SBOM in the shell. Both the carbon ($\delta^{13}C$) and sulphur ($\delta^{34}S$) isotopic signature of SBOM would be strongly influenced by the presence of calcium carbonate minerals and carbonate associate sulphate (CAS), respectively. CAS is trace sulphate incorporated into the lattice of carbonate minerals (Kampschulte and Strauss, 2004).

The isotopic effects of chemical extraction on SBOM are poorly understood and have not been rigorously tested, even though small isotopic deviations can indicate different food source or different trophic levels (Michener and Kaufman, 2007), and potentially confound interpretations about an animal's ecology and environment. Therefore we have directly compared the most commonly applied techniques for shell removal: ethylenediaminetetraacetic acid (EDTA), hydrochloric acid (HCl), acetic acid (AA), and cation exchange resin (RESIN). Using these methods, total SBOM and intra-crystalline SBOM were obtained from a large sample of homogenized shell powder from three modern filter-feeding bivalve species: the blue mussel *Mytilus edulis*, the grooved carpet shell *Ruditapes decussatus*, and the common cockle *Cerastoderma edule*. The intra-crystalline SBOM pool can be isolated by removing the inter-crystalline pool of total SBOM through prolonged chemical oxidation (Penkman et al., 2008), and the bulk stable isotope signature of intra-crystalline SBOM of molluscs has not previously been determined. To confirm working hypotheses about compositional differences between total SBOM and intra-crystalline SBOM, the molecular constituents of both SBOM pools were

characterized and compared using pyrolysis gas chromatography mass spectrometry (Py-GC/MS). Previous molecular investigations of SBOM have focussed on soluble components, in particularly proteins (Farre et al., 2009; Marin et al., 2012), but Py-GC/MS can be used on insoluble organic matter, and provides insights into the overall composition of SBOM, by producing a suite of thermal break-down products indicative of different types of macromolecules.

The four chemical treatments for SBOM isolation are known to have different advantages and disadvantages. Acidification is the most common method used in ecological studies to obtain biological organics from carbonate-rich samples, whereby inorganic carbon is expelled as CO_2. In general, the published literature shows that acidification can both deplete or enrich $\delta^{13}C$ and $\delta^{15}N$ values to varying extents. In many cases the exact mechanisms for these changes have remained undetermined, but potential causes are loss or chemical transformation of organic matter, particularly due to the break-up of protein complexes and the solubilisation of proteins (Schlacher and Connolly, 2014). No information could be found on the potential effects of acidification for $\delta^{34}S$ stable isotope analysis. Carmicheal et al. (2008) studied potential acidification effects on $\delta^{15}N$ of SBOM, and report no significant alteration compared to untreated shell powder. In this study two different strengths of the commonly used acid HCl were tested, as well as the weaker acetic acid.

An alternative method to acidification is the calcium-chelating agent EDTA (Albeck et al., 1996; Mae et al., 2007; Dreier et al., 2012) that isolates SBOM by binding calcium in a very stable manner, and compared to acidification has the benefit of working at neutral pH (Meenakshi et al., 1971). However, EDTA can be very difficult to remove from the SBOM without specialized filtration systems due to the formation of EDTA-calcium-protein complexes (Curry et al., 1991). Because EDTA molecules contain carbon and nitrogen, this technique could potentially influence SBOM isotope $\delta^{13}C$ and $\delta^{15}N$ ratios by introducing exogenous carbon and nitrogen.

The cation exchange resin method of shell removal (Albeck et al., 1996; Gotliv et al., 2003) does not introduce any additives, and isolates SBOM by binding calcium ions, whilst releasing carbon dioxide. Here we present a novel set-up of this method, aimed at performing large batches of these extractions. In addition we test the possibility of this method to simultaneously obtain CAS for $\delta^{34}S$ isotope analysis, which was precipitated from the demineralising solution.

In addition to stable isotope analysis of chemically isolated SBOM, the $\delta^{15}N$ value of total SBOM can be obtained from untreated shell powder because SBOM is the

only nitrogen pool in the shell. Unfortunately the intra-crystalline SBOM pool forms only a minor fraction of total SBOM, and sample size limitation of isotope analysis means that the amounts of intra-crystalline SBOM present in bleached shell powder would be insufficient for $\delta^{15}N$ stable isotope analysis. For nitrogen it will thus be possible to compare total SBOM results to the 'true' $\delta^{15}N$ SBOM values of untreated shell powder to assess the effect of the different extraction techniques directly.

In the second part of this study the isotopic relationship ($\delta^{13}C$, $\delta^{15}N$, $\delta^{34}S$) between total SBOM and soft tissues for individual specimens of the three test species is investigated. Because the isotopic values of the food sources consumed by the test species are unknown, soft tissues are used as a proxy, because food sources are incorporated into soft tissues with known fractionation. This fractionation reflects a trophic level, and is approximately +3-5‰ for $\delta^{15}N$ and +0.2-1‰ for $\delta^{13}C$, whilst $\delta^{34}S$ does not change between producers and consumers (Michener et al., 2007). To be able to use SBOM to identify nutritional sources and nutritional strategies, they should therefore directly reflect soft tissue values, or show consistent offsets that make it possible to calculate the values of food sources. Previous stable isotopic investigations of SBOM from modern filter-feeding bivalves have been limited to a relatively small number of species (shown in Fig. 2.11) and the exact nature of the isotopic relationship between SBOM and soft tissues is still poorly constrained, and has previously suggested to vary between species (Kovacs et al., 2010),

Because this study investigates two different issues concerning the application of SBOM as an alternative to soft tissues as a dietary proxy, the data is presented and discussed separately. Part I shows the results of method comparison experiments, and the potential isotopic effects of different shell removal techniques on the original SBOM, and Part II focusses on the isotopic relationship between SBOM and soft tissues.

2.2 Material & Methods

2.2.1 Material

Chemical treatments were compared using homogenized shell samples from the bivalve taxa *Mytilus edulis* (blue mussel), *Ruditapes decussatus* (grooved carpet shell) and *Cerastoderma edule* (common cockle). These species are primary consumers that filter feed on suspended organic matter from the water column, *M. edulis* has an epifaunal lifestyle whilst the other two species are infaunal sediment dwellers. Material for this study was obtained from the local fish market in Leeds (UK) in October/November 2012, and comprises 1 kilogram of live specimens each originating from Wales, UK (*M. edulis*), southern France (*R. decussatus*) and Dorset, UK (*C. edule*). The shells were first washed in deionised water and the soft tissue was then excised (separated into gill, mantle, foot, adductor muscle and rest), rinsed three times with DI water and frozen. The extracted soft tissues were freeze-dried and homogenized (where necessary with liquid nitrogen) in a ceramic mortar and pestle. The shells were then cleaned of remaining organic material (internal soft tissues, periostracum and ligament) using a scalpel and a Dremel rotary tool, rinsed with DI water and air-dried. The dry valves were ground using a ceramic mortar and pestle, and sieved to <125µm particle size in a stainless steel sieve, and homogenized for SBOM extraction. For five randomly selected individuals from each species the soft tissues and SBOM were analysed separately.

2.2.2 Isolation of SBOM

2.2.2.1 SBOM isolation using cation exchange resin

SBOM was isolated using cation exchange resin (Dowex 50WX8 50-100 mesh, Acros Organics, New Jersey, USA) based on a modification of the methodologies from Albeck et al. (1996) and Gotliv et al. (2003). Approximately 2 grams of shell powder suspended in DI water were placed inside a dialysis bag (3500D, Spectra Por 3, 18mm width, SpectrumLab, Inc., Rancho Dominguez, USA). The dialysis bag was placed in a glass vial with 75 ml resin and 25 ml DI water. The dialysis tube was vented through the lid of the vial and the reaction vessel was placed in a horizontal shaker for two weeks. The pH of the solution stays constant around 1.5-2. After shell dissolution was completed, the dialysis bag with SBOM was dialysed for five days in DI water, frozen and freeze-dried. Dried SBOM was weighed for calculation of recovery.

2.2.2.2 SBOM isolation using EDTA

For the EDTA technique, the methodology of Dreier et al. (2012) was followed (see also, Mae et al., 2007). Circa 2 grams of shell powder were suspended in DI water within dialysis tubing, and placed in 100ml 0.5M EDTA (VWR International, Leuven, Belgium) made up with MilliQ water (adjusted to pH 7.4 using potassium hydroxide) in glass beakers. Shell dissolution was complete after two weeks, and the dialysis bag with SBOM was dialysed for five days in MilliQ water changed daily. Subsequently, the SBOM was placed in centrifuge tubes, centrifuged and rinsed three times with MilliQ water, before freezing and freeze-drying.

2.2.2.3 SBOM isolation using acid

For HCl dissolution of the mineral component (following Mae et al., 2007) 10ml 6M HCl (Sigma-Aldrich, Steinheim, Germany) was slowly added to 2 grams of shell powder in a 50ml centrifuge tube, dissolution using 10% HCl 40 ml was added to the shell powder in a glass vial. The SBOM was subsequently centrifuged and rinsed three times with DI water to de-acidify the organics. A similar procedure was followed with acetic acid 10% v/v (Aldrich, Dorset, England), whereby 40ml acid was slowly added to 2 grams of shell powder in glass vials left overnight. The SBOM was centrifuged and rinsed three times with DI water. The SBOM samples obtained using HCl and acetic acid were then frozen and freeze-dried.

2.2.3 Removal of inter-crystalline SBOM

Intra-crystalline SBOM samples were obtained following the procedure of Penkman et al. (2008) and Demarchi et al. (2012) to remove the inter-crystalline SBOM pool. Prepared shell powder (maximum of 2 grams) was oxidized with 12% w/v NaOCl (VWR International, Carnot, France) for a 48 hour period within a glass beaker (50 µL per mg of shell powder). After completion the samples were dialyzed a minimum of three times against DI water and air-dried on 20-25 µm filter paper. For isolation of the intra-crystalline SBOM the samples were treated in the same way as unbleached shell powder.

2.2.4 CAS isolation using resin or HCl

Carbonate-associated sulphate (CAS) was obtained from the DI water containing the cation exchange resin. The water was filtered using 20-25 µm filter paper to remove residual resin, then placed in clean glass beakers, and the pH was adjusted

to 2-3 using 10% HCl or 10% NH_4. To precipitate the $BaSO_4$ for isotopic analysis the solutions were heated to ~70°C on a hot plate, 10% BaCl was added as 10% of the total volume, and the solution was kept at this temperature for an hour. After having cooled down overnight, the precipitated $BaSO_4$ was vacuum filtered out on 0.45µm cellulose/nitrate filter paper, that were left to dry in a drying cabinet (~50°C) and stored in glass vials. As a control for the cation exchange resin method, CAS was also isolated from *C. edule* bulk shell material using 10% HCl, and precipitated as described for the resin method.

2.2.5 Stable isotope analyses and elemental concentration

$\delta^{13}C$, $\delta^{15}N$ and $\delta^{34}S$ analyses were performed on freeze-dried SBOM and soft tissues, and additional analyses were performed on untreated shell powder to derive a measurement of SBOM $\delta^{15}N$ unaffected by an extraction procedure. To test for possible isotopic effects from the addition of nitrogen during extraction, a subsample of the batch of EDTA used for the extractions was analysed for $\delta^{15}N$. Similarly, a subsample of the cation exchange resin was analysed for $\delta^{13}C$ and $\delta^{34}S$.

All C, N and S isotopic analyses were performed on an Isoprime continous flow mass spectrometer coupled to an Elementar Pyrocube Elemental Analyser. For all analyses the sample was weighed into 8 x 5 mm tin cups and combusted to N_2, CO_2 and SO_2 at 1150°C in the presence of pure oxygen (N5.0) injected into a stream of helium (CP grade). Quantitative conversion to N_2, CO_2 and SO_2 was achieved by passing the combustion product gas through tungstic oxide packed into the combustion column. Excess oxygen was removed by reaction with hot copper wires at 850°C and water was removed in a Sicapent trap. All solid reagents were sourced from Elemental Microanalysis, UK, and all gases were sourced from BOC, UK. One aliquot of each SBOM and soft tissue sample was analysed for its carbon isotope composition whilst duplicate larger aliquots were analysed for their nitrogen and sulphur isotope composition in the same run. Samples for nitrogen and sulphur isotope analysis were analysed in duplicate because of a small sulphur isotopic memory effect imparted during processing of SO_2 gas in the Pyrocube. In all analyses, N_2 produced by combustion continued through the system to unchecked whilst CO_2 and SO_2 were removed from, and re-injected into, the gas stream using temperature controlled adsorption/desorption columns.

The $\delta^{13}C$ of the sample is derived from the integrated mass 44, 45 and 46 signals from the pulse of sample CO_2, compared to those in an independently introduced pulse of CO_2 reference gas (CP grade). These ratios are then calibrated using urea and C4 sucrose lab standards assigned values of -11.93‰ and -46.83‰ respectively. These values were assigned by calibration using the international standards LSVEC (-46.479‰), CH7 (-31.83‰), CH6 (-10.45‰), and CO-1 (+2.48‰) to the Vienna-Pee Dee Belemnite (V-PDB) scale. The precision obtained for repeat analysis of standard materials is generally 0.2‰ or smaller (1 standard deviation). Repeat analyses of a lab C3 sucrose produced an average of -26.5‰ with a standard deviation of 0.1‰.

The $\delta^{15}N$ is derived using the integrated mass 28 and 29 signals relative to those in a pulse of N_2 reference gas (N5.0). These ratios are calibrated to the international AIR scale using USGS-25 and USGS-26 (both ammonium sulphate) which have been assigned values of -30.4‰ and +53.7‰ respectively. The precision obtained for repeat analyses of standard materials is generally 0.3‰ or smaller (1 standard deviation). Repeat analyses of a yeast sample produces an average of -0.8‰ with a standard deviation of 0.1‰.

The $\delta^{34}S$ is derived using the integrated mass 64 and 66 signals relative to those in a pulse of SO_2 reference gas (N3.0). These ratios are calibrated to the international V-CDT scale using an internal lab barium sulphate standard derived from seawater (SWS-3) which has been analysed against the international standards NBS-127 (+20.3‰), NBS-123 (+17.01‰), IAEA S-1 (-0.30‰) and IAEA S-3 (-32.06‰) and assigned a value of +20.3‰, and an inter-lab chalcopyrite standard CP-1 assigned a value of -4.56‰. The precision obtained for repeat analyses of standard materials is generally 0.5‰ or smaller (1 standard deviation) for SBOM, and 0.2‰ or smaller (1 standard deviation) for CAS. Repeat analyses of a sulphanilamide sample produced an average of -0.2‰ with a standard deviation of 0.3‰.

Weight percent nitrogen and sulphur data were calculated by the Pyrocube software using a calibration based on multiple analyses of sulphanilamide samples with a range of weights. Relative standard deviations on analyses of the concentrations of the nitrogen and sulphur contents of the isotope calibration materials were 5% or better. The very small amount of material needed for carbon isotope analysis meant that the sample size was below the calibration range for carbon and were highly variable. The carbon concentration data are therefore considered unreliable and are not reported.

2.2.6 Pyrolysis Gas Chromatography Mass Spectrometry analysis of SBOM

Pyrolysis GC/MS analysis of total and intra-crystalline SBOM from bulk *M. edulis* (obtain using cation exchange resin) was performed on a CDS Pyroprobe 1000 via a CDS1500 valved interface (320°C), to a Hewlett-Packard 6890GC split injector (320°C) linked to a Hewlett-Packard 5973MSD (electron voltage 70eV, filament current 220uA, source temperature 230°C, quadrupole temperature 150°C, multiplier voltage 2200V, interface temperature 320°C). The acquisition was controlled by a HP kayak xa chemstation computer, in full scan mode (50-650amu). Approximately 0.3mg of the SBOM sample was weighed into a quartz tube with glass wool end plugs. The chemical reagent tetramethylammonium hydroxide (TMAH) and the internal standard androstane were added to the samples. The tube was then placed into a pyroprobe platinum heating coil and then sealed into the valved interface. The sample was pyrolysed at 610°C for 10 seconds with the split open. At the same time the GC temperature programme and data acquisition commenced. Separation was performed on a fused silica capillary column (60m x 0.25mm i.d) coated with 0.25um 5% phenyl methyl silicone (HP-5). Initially the GC was held at 50°C for 5 minutes and then temperature programmed from 50°C-320°C at 5°C per min and held at the final temperature for 5 minutes, total run time 65 minutes, with helium as the carrier gas (constant flow 1ml/min, initial pressure of 50kPa, split at 30 mls/min). Peaks were identified and labelled after comparison of their mass spectra with those of the NIST05 library.

Part I – Method comparison for SBOM isolation

2.3 Results

Total SBOM and intra-crystalline SBOM were successfully isolated using all shell removal methods. The weight percent (wt%) of total SBOM obtained from the shell powder varied between species (*M. edulis* = 0.7% to 1.0%; *R. decussatus* = 0.2% to 0.4% ; *C. edule* = 0.1% to 0.4% using ion-exchange resin) and the intra-crystalline fraction makes up a small percentages of the total (shell wt%: *M. edulis* = ~ 0.01%, *R. decussatus* and *C. edule* = ~ 0.005%, using ion-exchange resin). SBOM is voluminous, and has a uniform colour for each species. The dark blue shelled *M. edulis* contains SBOM with a dark brown colour. The other two species have lighter beige/brown shells and contain SBOM with a beige or light brown colour.

2.3.1 Isotopic values of bulk SBOM and CAS obtained using various shell carbonate removal techniques

This section presents the method comparison results for aliquots of homogenized shell powder from the three test species. For each species the stable isotope composition of SBOM obtained using the different methods are statistically compared using unpaired t-tests (significance threshold: p=<0.05), these results are presented for each isotope system (carbon, nitrogen, sulphur). The data is also shown as box-and-whisker plots, allowing the identification of outliers (values outside 1.5* inter-quartile range). The outliers are expected to be caused by experimental error, and because of their strong influence on statistical analysis they are discussed separately. The mean values for each method are reported with and without outliers.

2.3.1.1 Carbon

The $\delta^{13}C$ data for each method are given in Table 2.1 (total SBOM) and Table 2.2. (intra-crystalline SBOM), the distribution of $\delta^{13}C$ is also shown as box-and-whisker plots in Fig. 2.1 (total SBOM) and Fig. 2.2 (intra-crystalline SBOM). No elemental carbon concentration data is available for the analysed samples. The carbon isotope values of the shell removal agents are $\delta^{13}C$ -39.0‰ (±0.6, n=2) for EDTA, and $\delta^{13}C$ -29.2‰ (n=1) for cation exchange resin.

Total SBOM

Total SBOM isolated using cation exchange resin has lower mean $\delta^{13}C$ values than the other four methods (Fig. 2.1). For *M. edulis* this difference is statistically significant versus EDTA (p=0.0039), 10%HCl (p=0.0037), and 50%HCl (p=0.0110), for *R. decussatus* versus 10%HCl (p=0.0155), and for *C. edule* versus EDTA (p=0.0008), 10%HCl (p=0.0007), 50%HCl (p=0.0059), and acetic acid (p=0.0047). In addition, total SBOM data obtained using $\delta^{13}C$ cation exchange resin is generally the most variable method, particularly in *R. decussatus* and *C. edule*.

Excluding cation exchange resin, comparison between the other four methods shows that total SBOM obtained using 50% HCl has the lowest median value in all three species. In *M. edulis* the $\delta^{13}C$ data from the 50%HCl method is significantly depleted in comparison to EDTA (p=0.0409), and 10%HCl (p=0.0339), and in *R. decussatus* compared to 10%HCl (p=0.0006). Alternatively this could be interpreted

as an enrichment of 10%HCl/EDTA compared to 50%HCl total SBOM samples, particularly because the 10%HCl total SBOM $\delta^{13}C$ values are also statistically enriched compared to those of acetic acid *R. decussatus* total SBOM samples ($p=0.0003$). There are no further statistically significant $\delta^{13}C$ differences between EDTA, acetic acid, and 10%HCl obtained total SBOM. It should however be noted that for acetic acid, the $\delta^{13}C$ total SBOM distribution is very wide and enriched in *M. edulis* (ranging from -18.4‰ to -12.5‰, n=3), and contains an enriched outlier in *C. edule*.

Table 2.1 $\delta^{13}C$ values of bulk total SBOM for method comparison

SBOM was obtained from aliquots of homogenised shell powder from *Mytilus edulis*, *Ruditapes decussatus* and *Cerastoderma edule*. SBOM was isolated using the shell removal techniques: cation exchange resin (RESIN), EDTA, acetic acid (AA), 10%HCl and 50%HCl. For sample sets in which outliers have been identified (Fig. 2.1), mean values without outliers are also given and are underlined.

$\delta^{13}C$ (‰, ±SD)	***M. edulis***	***R. decussatus***	***C. edule***
RESIN	-18.7 ±3.3 (n=7) <u>-17.5 ±0.9 (n=6)</u>	-21.1 ±2.0 (n=6)	-22.8 ±1.8 (n=7) <u>-22.3 ±1.3 (n=6)</u>
EDTA	-16.7 ±2.2 (n=4) <u>-15.6 ±0.2 (n=3)</u>	-19.2 ±0.4 (n=4)	-18.8 ±0.2 (n=4)
10%HCl	-15.6 ±0.1 (n=3)	-18.4 ±0.2 (n=5)	-18.7 ±0.2 (n=6)
50%HCl	-16.8 ±1.2 (n=5) <u>-16.3 ±0.4 (n=4)</u>	-19.5 ±0.4 (n=5)	-19.1 ±0.7 (n=3)
AA	-15.2 ±3.0 (n=3)	-19.3 ±0.2 (n=4)	-18.6 ±1.1 (n=4) <u>-19.1 ±0.3 (n=3)</u>

Figure 2.1 Box-and-whisker plots of $\delta^{13}C$ values from bulk total SBOM for method comparison.

SBOM was obtained from aliquots of homogenised shell powder from *Mytilus edulis*, *Ruditapes decussatus* and *Cerastoderma edule*. SBOM was isolated using the techniques: cation exchange resin (RESIN), EDTA, acetic acid (AA), 10%HCl and 50%HCl. Soft tissue ranges show the minimum and maximum $\delta^{13}C$ value of the gill/mantle/foot/muscle from individual specimens of the three species (presented in Fig. 2.11, n=60). In the plots, the horizontal line presents the median, and the limits of the box and whiskers contain 50% and 100% of the data, respectively. If outliers are present, they fall outside 1.5*inter-quartile range (which is then indicated by the length of the whiskers). The number of analyses for each method are given in Table 2.1.

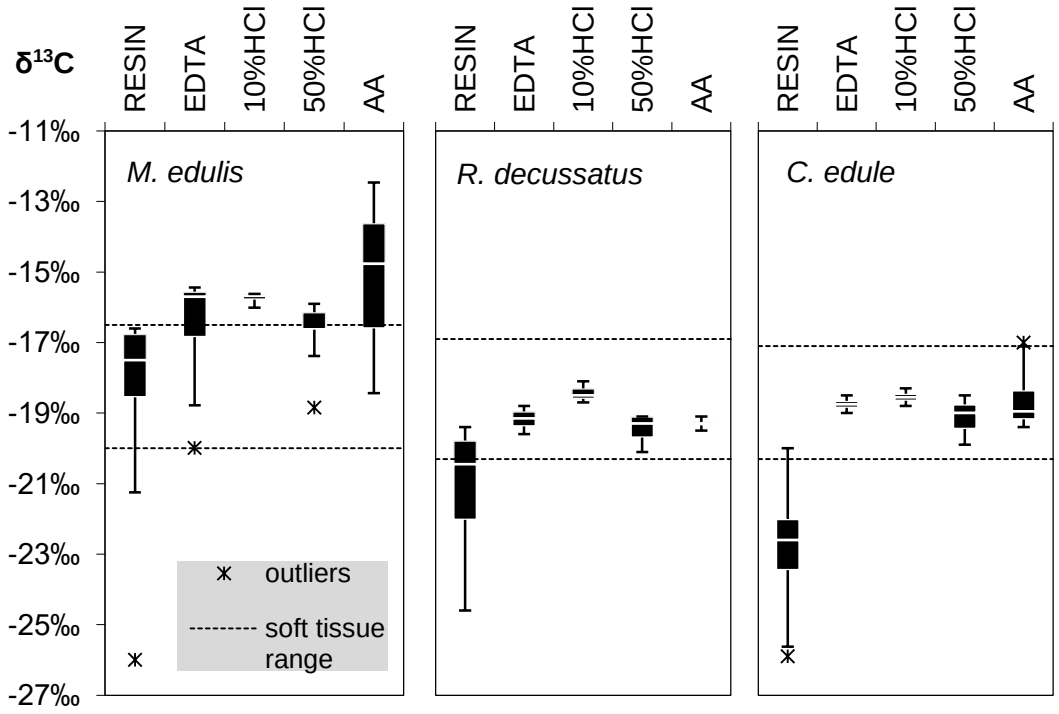

Comparison between total SBOM data and soft tissue $\delta^{13}C$ values (Fig 2.1, -20.0‰ to -16.5‰) from *M. edulis* shows that only SBOM obtained using cation exchange resin (-16.7‰ to -18.7‰, outlier -26.0‰, n=6) overlaps with the isotopic range of the soft tissues. The majority of total SBOM values isolated using EDTA, 10%HCl, 50%HCl, or AA, are more enriched than soft tissue values. For *R. decussatus* total SBOM data obtained using all methods falls inside the range of soft tissue values ($\delta^{13}C$ -21.1‰ to -16.9‰), with the exception of two depleted resin values (-22.5‰ and -25.1‰). With the exception of one value, all of the *C. edule* total SBOM samples isolated using resin (-25.6‰ to -20.0‰) are more depleted than the range of soft tissues (-20.3‰ to -17.1‰) from this species. Total SBOM obtained using other methods have similar values (ranging from -19.9‰ to -17.0‰) to the soft tissue data

Intra-crystalline SBOM

Table 2.2 $\delta^{13}C$ values of bulk intra-crystalline SBOM for method comparison
See Table 2.1 for further details, outliers are identified in Fig. 2.2.

$\delta^{13}C$ (‰, ±SD)	***M. edulis***	***R. decussatus***	***C. edule***
RESIN	-24.8 ±1.7 (n=6) -24.1 ±0.5 (n=5)	-25.7 ±1.3 (n=5) -25.1 ±0.3 (n=4)	-25.7 ±1.6 (n=4)
EDTA	-23.5 ±0.3 (n=3)	-26.1 ±0.1 (n=3)	-26.1 ±0.2 (n=4)
10%HCl	-21.9 ±1.5 (n=8)	-24.8 ±0.5 (n=4)	-22.9 ±0.7 (n=5)
50%HCl	-23.2 ±0.7 (n=3)	-26.1 ±0.3 (n=4)	-25.7 ±1.4 (n=5)
AA	-25.2 ±7.2 (n=6) -22.0 ±0.9 (n=5)	-29.0 ±7.4 (n=6) -26.0 ±1.4 (n=5)	-28.4 ±8.8 (n=6) -25.1 ±4.1 (n=5)

Figure 2.2 Box-and-whisker plots of $\delta^{13}C$ values from bulk intra-crystalline SBOM for method comparison.

See Figure 2.1 for further details, soft tissue ranges are not visualised because all the intra-crystalline SBOM data falls below these ranges. $\delta^{13}C$ values for AA outliers are given in the plots, the whisker for AA of *C. edule* extents to -35.4‰. Number of analyses are given in Table 2.2.

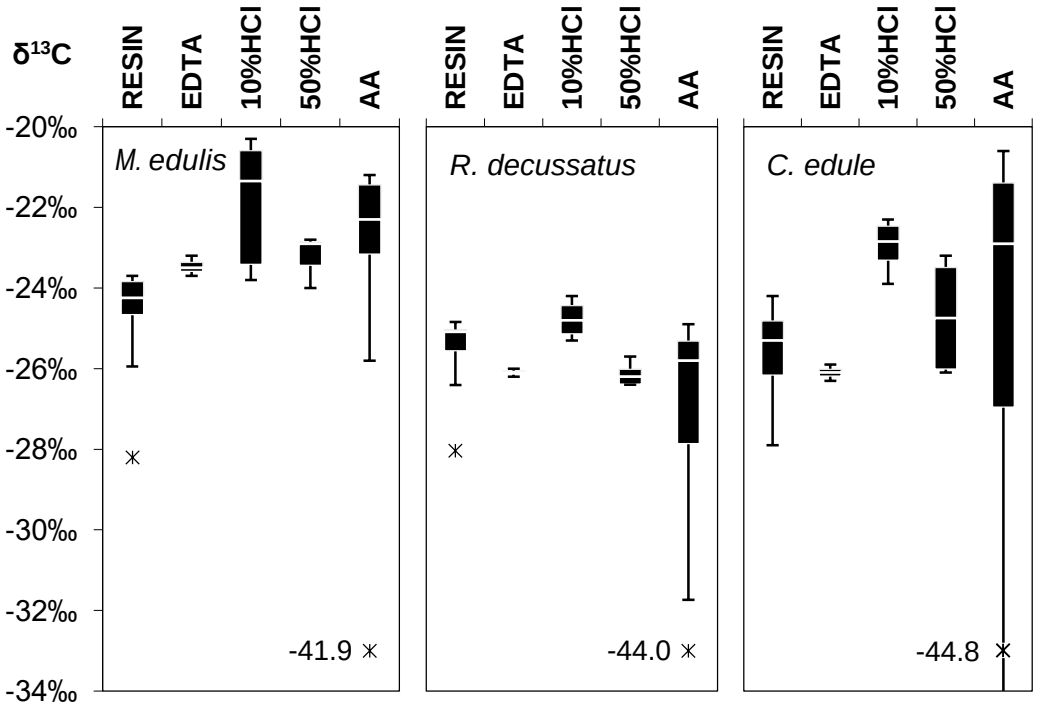

Intra-crystalline SBOM is significantly depleted compared to total SBOM from bulk aliquots of the same species, for each of the five different methods. Mean differences between the two pools across the different methods are: $\delta^{13}C$ -6.8‰ ±0.7 for *M. edulis*, -6.8‰ ±0.7 for *R. decussatus*, and -5.4‰ ±2.0 for *C. edule*.

The intra-crystalline data is shown as box-and-whisker plots in Fig. 2.2., and the most notable difference between the methods are extremely depleted outliers for intra-crystalline SBOM obtained using acetic acid ($\delta^{13}C$ > -40‰) in each test species. Due to the limited number of analysed samples, the isotopic variation of this method is therefore very large for each species.

In *M. edulis* intra-crystalline SBOM isolated using cation exchange resin is significantly depleted in $\delta^{13}C$ compared to EDTA (p=0.0001), 10%HCl (p=0.0030), and acetic acid (p=0.0001). For *R. decussatus* and *C. edule* is cation exchange resin does not have the most depleted values of the different methods. Potentially this is related to the differences in mean intra-crystalline $\delta^{13}C$ values of *M. edulis* (-22.7‰, mean of the four other methods) compared to *R. decussatus* (-25.8‰) and *C. edule* (-25.0‰).

For all three species the mean/median values of 50%HCl/EDTA are more depleted than 10%HCl/acetic acid values. This difference could be statistically confirmed using t-tests between *M. edulis* EDTA vs. acetic acid (p=0.0346), *R. decussatus* EDTA vs. 10%HCl (p=0.0074) and 50%HCl vs. 10%HCl (p=0.0043), and for *C. edule* EDTA vs. 10%HCl (p=0.0001) and 50%HCl vs. 10%HCl (p=0.0054). No statistical differences exist between intra-crystalline samples obtained using EDTA and those isolated using 50%HCl, or between the methods 10%HCl and acetic acid.

Key observations

- Total SBOM isolated using cation exchange resin has more depleted and more variable $\delta^{13}C$ values than the other shell removal methods, this ^{13}C depletion also exists compared to soft tissue $\delta^{13}C$ ranges (with the exception of *M. edulis*). For intra-crystalline SBOM samples the ^{13}C depletion of cation exchange obtained samples is only present in *M. edulis*.

- Intra-crystalline SBOM obtained using 50%HCl/EDTA can have depleted $\delta^{13}C$ values compared to 10%HCl/acetic acid samples, and total SBOM 50%HCl samples also have depleted $\delta^{13}C$ values compared to 10%HCl

- Acetic acid $\delta^{13}C$ data contains several enriched $\delta^{13}C$ values for total SBOM, and extremely $\delta^{13}C$ depleted values for intra-crystalline SBOM

- For all test species intra-crystalline SBOM is depleted by $\delta^{13}C$ - 5-7‰ compared to total SBOM, and $\delta^{13}C$ values fall below the soft tissue ranges

2.3.1.2 Nitrogen

The $\delta^{15}N$ results and the distribution of the values are reported in Table 2.3 and 2.4, and Figure 2.3 and 2.4. In addition the elemental concentration of nitrogen (%N) could be obtained for each isotopic measurement, and for each analysed aliquot of bulk shell powder $\delta^{15}N$ and %N are plotted against each other in Fig. 2.5.The nitrogen value of the EDTA used for the extractions is $\delta^{15}N$ +1.5‰ ±0.6 (n=2).

Total SBOM

Statistical tests between $\delta^{15}N$ of total SBOM (Table 2.3) show that there are no differences in $\delta^{15}N$ values between the different shell removal methods, with the exception of *C. edule* 10%HCl samples that are significantly depleted compared to EDTA, 50%HCl and AA obtained samples.

Table 2.3 $\delta^{15}N$ values and elemental nitrogen concentrations (%N) of bulk total SBOM for method comparison

(p. 19 and 20) SBOM was obtained from aliquots of homogenised shell powder from *Mytilus edulis*, *Ruditapes decussatus* and *Cerastoderma edule*. SBOM was isolated using the shell removal techniques: cation exchange resin (RESIN), EDTA, acetic acid (AA), 10%HCl and 50%HCl. Three *M. edulis* total SBOM samples isolated using EDTA underwent the cation exchange resin method (EDTA-RESIN) and were subsequently re-analysed. For sample sets in which outliers have been identified (see Fig. 2.3), mean values without outliers are also given and underlined.

$\delta^{15}N$ (‰, ±SD)	***M. edulis***	***R. decussatus***	***C. edule***
RESIN	+12.8 ±0.8 (n=7) +<u>12.5 ±0.5 (n=6)</u>	+8.3 ±1.9 (n=8) +<u>7.7 ±0.8 (n=7)</u>	+11.3 ±1.2 (n=8)
EDTA	+12.2 ±0.1 (n=4)	+7.3 ±0.3 (n=4)	+12.3 ±0.2 (n=3)
EDTA-RESIN	+12.1 ±0.3 (n=3)	n/a	n/a
10%HCl	+12.3 ±0.3 (n=6)	+6.8 ±0.2 (n=5)	+12.0 ±0.3 (n=4) +<u>11.8 ±0.1 (n=3)</u>

50%HCl	+12.2 ±0.1 (n=4)	+7.1 ±0.4 (n=3)	+12.4 ±0.1 (n=3)
AA	+12.3 ±0.4 (n=3)	+7.1 ±0.1 (n=3)	+12.3 ±0.1 (n=4)
UNTREATED	+11.6 ±0.1 (n=3)	+6.8	n/a
%N	*M. edulis*	*R. decussatus*	*C. edule*
RESIN	+11.7 ±3.8 (n=7)	+9.4 ±1.5 (n=8)	+7.0 ±2.2 (n=8)
EDTA	+14.9 ±0.7 (n=4)	+12.9 ±1.5 (n=4)	+11.6 ±0.4 (n=3)
EDTA-RESIN	+13.1±1.3 (n=3)	n/a	n/a
10%HCl	+17.1 ±1.9 (n=6)	+14.2 ±0.5 (n=5)	+11.5 ±0.3 (n=4)
50%HCl	+13.6 ±2.3 (n=4)	+8.3 ±3.6 (n=3)	+10.1 ±0.9 (n=3)
AA	+5.2 ±1.5 (n=3)	+12.6 ±0.6 (n=3)	+11.3 ±1.2 (n=3)
UNTREATED	+0.2 ±0.1 (n=3)	+0.1	n/a

Figure 2.3 Box-and-whisker plots of $\delta^{15}N$ values from bulk total SBOM for method comparison.

Further information on the plots is given at Fig. 2.1. The number of analyses for each method is shown in Table 2.3. The soft tissue range for *R. decussatus* is very wide ($\delta^{15}N$ 3.2‰ to 14.8‰) and is therefore not shown.

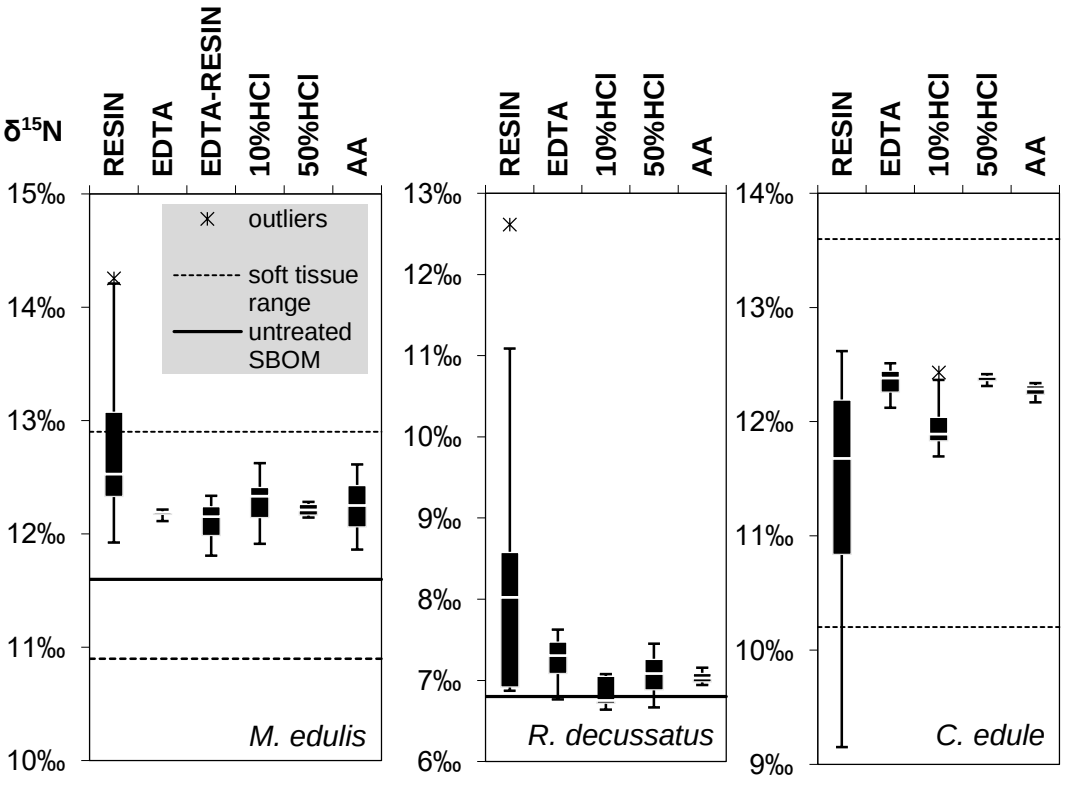

It should however be noted that box-and-whisker plots of the $\delta^{15}N$ data (Fig. 2.3) show a much larger variation for samples obtained using cation exchange resin, than for the other methods. This difference is also apparent from the standard variation of the three test species when using cation exchange resin (0.5‰ to 1.2‰), compared to the other methods (0.1‰ to 0.4‰). To further analyse the isotopic effect of cation exchange resin extraction on total SBOM, several EDTA extracted samples were re-extracted using resin (Table 1). This re-extraction did not change the isotopic signature of the three samples (EDTA: 12.2‰ ±0.1, n=3, EDTA-resin: 12.1‰ ±0.3, n=3), or the elemental concentration between EDTA (14.7% ±0.7, n=3) and EDTA-resin samples (13.1% ±1.3, n=3), although the variation slightly increased for both sets of measurments.

Untreated total SBOM data could be obtained for *M. edulis* ($\delta^{15}N$: +11.6‰ ±0.1, n=3) and *R. decussatus* (+6.8‰, n=1). Untreated *M. edulis* total SBOM is significantly depleted compared to all other methods (p= 0.005 – 0.0424, n=5), and this difference is generally limited to ~ -0.7‰. Untreated *R. decussatus* total SBOM only overlaps with the majority of 10%HCl obtained values (6.8‰ ±0.2, n=5), total SBOM samples isolated using EDTA/50%HCl/acetic acid are enriched by ~ +0.3‰, and for cation exchange resin ~ +1.0‰, compared to untreated $\delta^{15}N$ values.

The elemental concentration of nitrogen (%N) of total SBOM differs between methods. Most notable, the %N of total SBOM samples from *M. edulis* obtained using acetic acid (5.2% ±1.5, n=3) is approximately half that of the other methods (mean values ranging from 10.9% to 14.9%, n=4) but this statistically significant depletion is not reflected in the other two species.

Resin obtained $\delta^{15}N$ outliers are not related to a difference in %N, as shown in Fig. 2.5. The elemental concentration of nitrogen is generally the most variable for samples obtained using cation exchange resin, and also considerable lower compared to other methods: for *M. edulis* vs. 10%HCl (p=0.0130), for *R. decussatus* vs. EDTA (0.0034), vs. 10%HCl (0.0001) and acetic acid (0.0068), and for *C. edule* vs. EDTA (0.0069), 10%HCl (0.0026), 50%HCl (0.0466), and acetic acid (p=0.0119). In addition 50%HCl samples were statistically depleted compared to 10%HCl for *M. edulis* (p=0.0300), to EDTA (0.0369) and 10%HCl (0.0043) for *R. decussatus*), and to 10%HCl for *C. edule* (p=0.0307). Total SBOM samples isolated using EDTA are not statistically enriched in elemental nitrogen concentration compared to 10%HCl for all three test species, and compared to acetic acid for *R. decussatus* and *C. edule*.

Intra-crystalline SBOM

Where total and intra-crystalline SBOM could be compared, intra-crystalline SBOM $\delta^{15}N$ values are significantly depleted compared to total SBOM for all methods/species, with the exception of *M. edulis* SBOM obtained using acetic acid (total SBOM: +12.3‰ ±0.4, n=3 / intra-crystalline SBOM: +11.2‰ ±0.6, n=3) and *R. decussatus* SBOM isolated using cation exchange resin (total SBOM: +7.7‰ ±0.8, n=7 / intra: +7.0‰ ±0.6, n=5). The mean difference between the two SBOM pools is around 1-2‰ for *M. edulis*, 0.5-1‰ for *R. decussatus*, and 1-2.5‰ for *C. edule*, for cation exchange obtained samples this difference is much larger for *M. edulis* (mean difference: 7.9‰) and *C. edule* (5.5‰).

The elemental nitrogen concentration (%N) of intra-crystalline SBOM is also significantly lower than the %N of total SBOM using the following methods: for *M. edulis* EDTA (-10.9%), 10%HCl (-11.1%), 50%HCl (-12.4%), but not for cation exchange resin (-3.3%) and acetic acid (-1.0%). For *R. decussatus* there is a statistically significant difference between total and intra-crystalline SBOM %N for resin (-5.4%) and AA (-9.6%), No data is available for the other methods. The depletion in %N is significant for *C. edule* intra-crystalline SBOM in: 10%HCl (-9.5%), 50%HCl (8.6%), AA (-6.8%), but not for cation exchange resin obtained samples (-3.3%). The general difference in elemental concentration between total SBOM and intra-crystalline SBOM is also shown in Fig. 2.5.

Because of to the lower amounts of intra-crystalline SBOM in the shell and the lower elemental concentration of nitrogen compared to total SBOM, it was not always possible to obtain $\delta^{15}N$ data for intra-crystalline SBOM. The available data (Fig. 2.4) shows that for *M. edulis* cation exchange resin obtained samples are statistically depleted by ~2‰ and more variable than SBOM obtained using the other methods (EDTA, 10%HCl, 50%HCl, acetic acid). The same pattern is observed for *C. edule* intra-crystalline $\delta^{15}N$ data, whereby cation exchange samples are ~4‰ depleted compared to the other methods for which data is available (10%HCl, 50%HCl, acetic acid). For *R. decussatus* $\delta^{15}N$ data for intra-crystalline SBOM is only available for cation exchange resin and acetic acid samples, but there is no statistical difference between these two methods. Potentially this is related to the lower $\delta^{15}N$ value of intra-crystalline SBOM for that species, as is evident from acetic acid obtained mean $\delta^{15}N$ values: +11.2‰ for *M. edulis*, and +11.0‰ for *C. edule*, compared to +6.7‰ for *R. decussatus*.

Table 2.4 $\delta^{15}N$ values and elemental nitrogen concentrations (%N) of bulk intra-crystalline SBOM for method comparison

See Table 2.3 for further details.

$\delta^{15}N$ (‰, ±SD)	***M. edulis***	***R. decussatus***	***C. edule***
RESIN	+4.6 ±0.8 (n=5)	+7.0 ±0.6 (n=5)	+5.8 ±0.9 (n=2)
EDTA	+11.1 ±0.2 (n=3)	n/a	n/a
10%HCl	+9.9 ±0.2 (n=5)	n/a	+9.7 ±1.3 (n=2)
50%HCl	+10.3 ±0.2 (n=3)	n/a	+10.0 ±0.6 (n=2)
AA	+11.2 ±0.6 (n=3)	+6.7 ±0.3 (n=2)	+11.0 ±0.9 (n=3)
%N	***M. edulis***	***R. decussatus***	***C. edule***
RESIN	7.6 ±2.1 (n=5)	4.0 ±0.8 (n=5)	3.7 ±0.5 (n=2)
EDTA	4.0 ±0.5 (n=3)	n/a	n/a
10%HCl	4.8 ±0.9 (n=5)	n/a	2.6 ±1.5 (n=2)
50%HCl	2.2 ±1.0 (n=3)	n/a	1.5 ±0.2 (n=3)
AA	4.2 ±0.7 (n=3)	3.3 ±0.1 (n=2)	4.5 ±2.5 (n=3)

Figure 2.4 Box-and-whisker plots of $\delta^{15}N$ values from bulk intra-crystalline SBOM for method comparison.

Further information on the plots is given at Fig. 2.1. The number of analyses for each method is shown in Table 2.4.

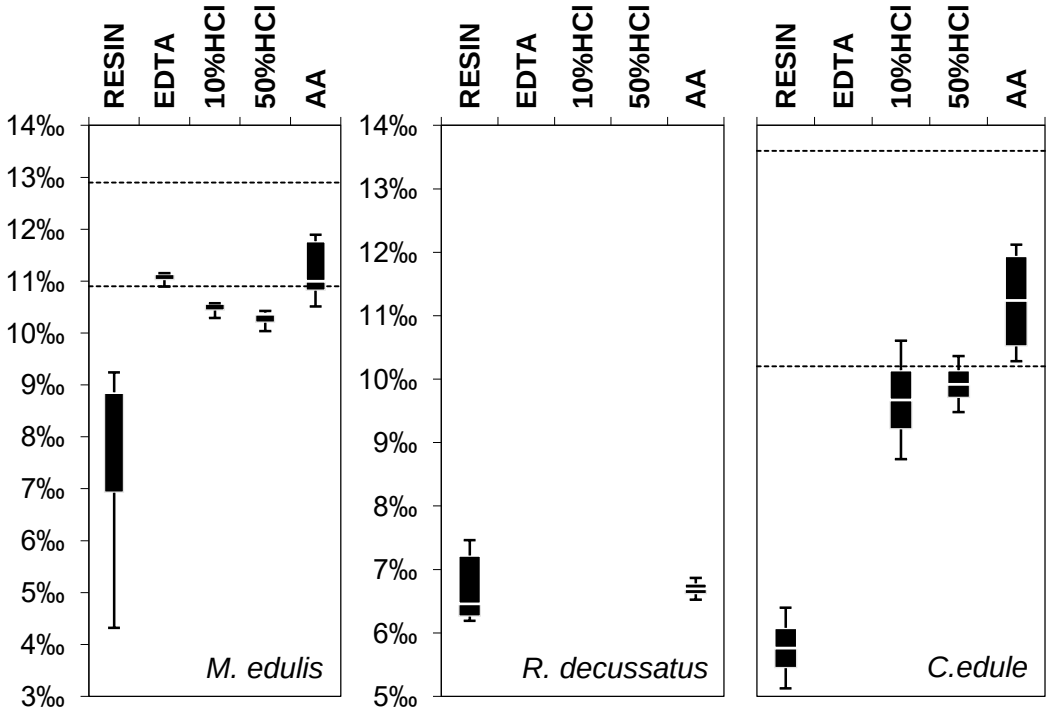

Comparison between the shell removal methods EDTA, 10%HCl, 50%HCl and acetic acid for *M. edulis* shows that the mean $\delta^{15}N$ values of the methods do not vary by more than 1‰. But due to very small intra-method variability (S.D for the various methods: 0.2‰ to 0.6‰), 10%HCl samples are statistically depleted compared to EDTA (p=0.0002) and acetic acid (0.0035), and 50%HCl is statistically depleted compared to EDTA (0.0080). For *C. edule* the intra-method $\delta^{15}N$ variability is greater (0.6‰ to 1.3‰), and no statistical differences exist between the different shell removal methods.

The elemental nitrogen concentration of intra-crystalline SBOM samples obtained using cation exchange resin are statistically enriched compared to all other methods (for which data could be obtained) in *M. edulis* (p=0.0065 to 0.0384, n=4), and for *C. edule* compared to 50%HCl (p=0.0054). For *R. decussatus* the elemental concentration does not differ between intra-crystalline samples using cation exchange resin or acetic acid. In addition to ion exchange resin, statistically lower concentration of nitrogen where found in *M. edulis* 50%HCl samples when compared to EDTA (p=0.0494), 10%HCl (0.0089), and acetic acid (0.0470) samples.

SBOM compared to soft tissue ranges

All *M. edulis* total SBOM $\delta^{15}N$ values obtained using the various techniques overlap with the soft tissue $\delta^{15}N$ range (+10.9‰ to +12.9‰, n=20), with the exception of two enriched cation exchange resin values. Intra-crystalline SBOM *M. edulis* $\delta^{15}N$ values overlap (EDTA, acetic acid) with the ^{15}N depleted end of the soft tissue range, or are more depleted than the soft tissue range (cation exchange resin, 10%HCl, 50%HCl).

R. decussatus has a wide soft tissue $\delta^{15}N$ range (+3.2‰ to +14.8‰, n=20) due to the large isotopic variation between individual specimens, that have average soft tissue $\delta^{15}N$ of +5.6‰, +6.1‰, +7.7‰, +10.2‰, and +14.3‰. The soft tissue range therefore encompasses all total SBOM and intra-crystalline SBOM $\delta^{15}N$ values.

With the exception of one resin $\delta^{15}N$ value (+9.1‰) all total SBOM data is within the range of soft tissue $\delta^{15}N$ values from *C. edule* specimens (+10.2‰ to +13.6‰, n=20). Intra-crystalline SBOM samples obtained using acetic acid completely overlap with the soft tissue range, whilst 10%HCl/50%HCl data generally falls ~0.5‰ below that range. Cation exchange resin intra-crystalline SBOM $\delta^{15}N$ values from *C. edule* are ~4‰ depleted below the soft tissue range.

Figure 2.5 $\delta^{15}N$ isotopic composition and elemental nitrogen (%N) concentration of bulk SBOM for method comparison

(p.26 and 27) Data for individual aliquots of homogenised shell powder as reported in Table 2.3 and 2.4.

M. edulis

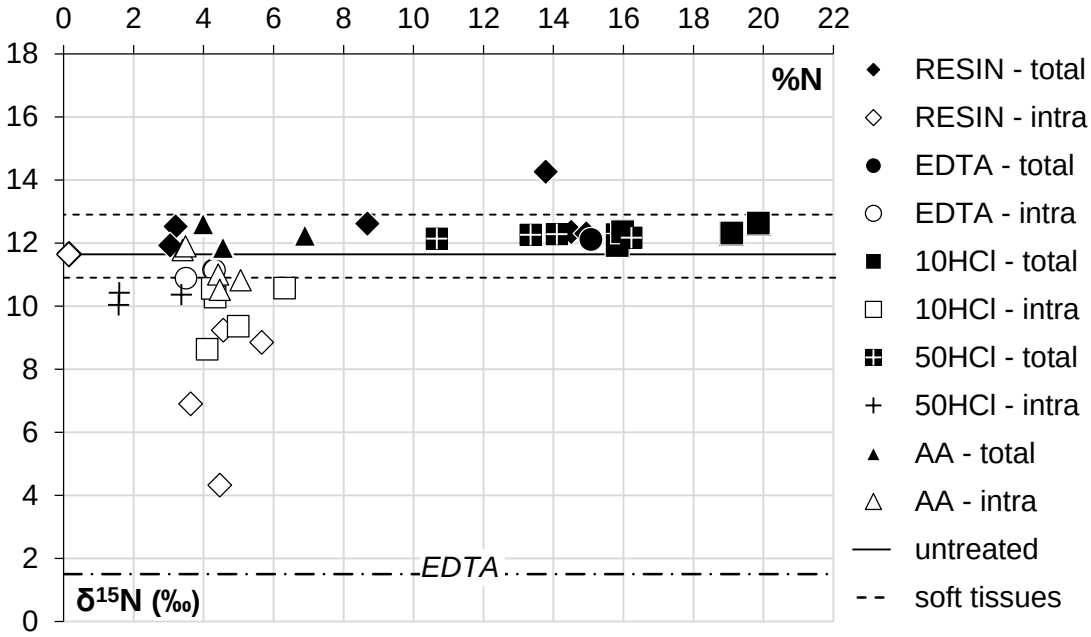

R. decussatus

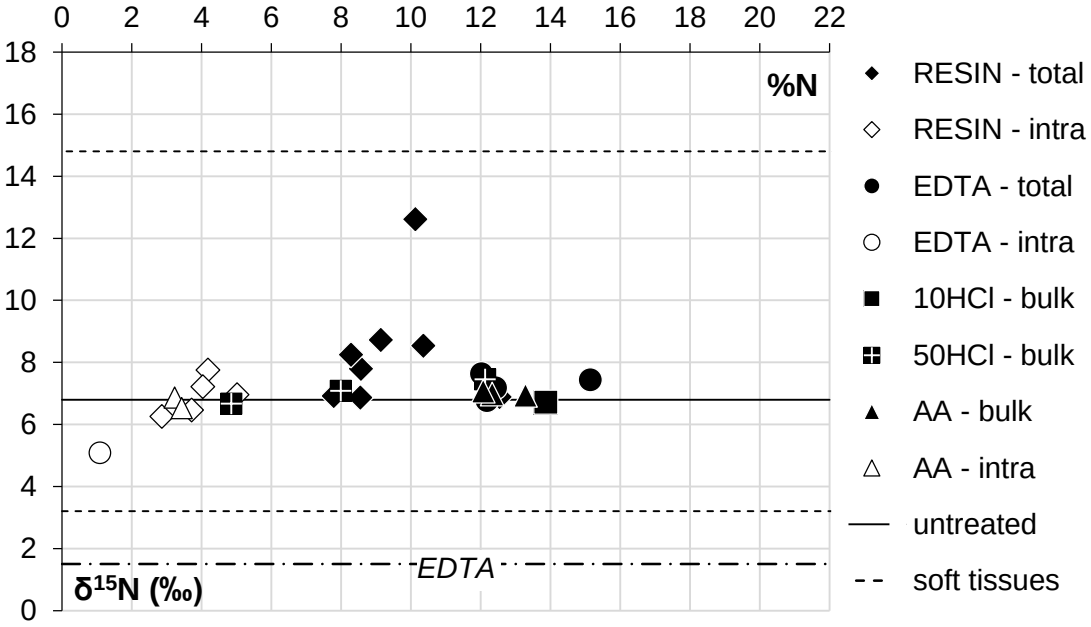

C. edule

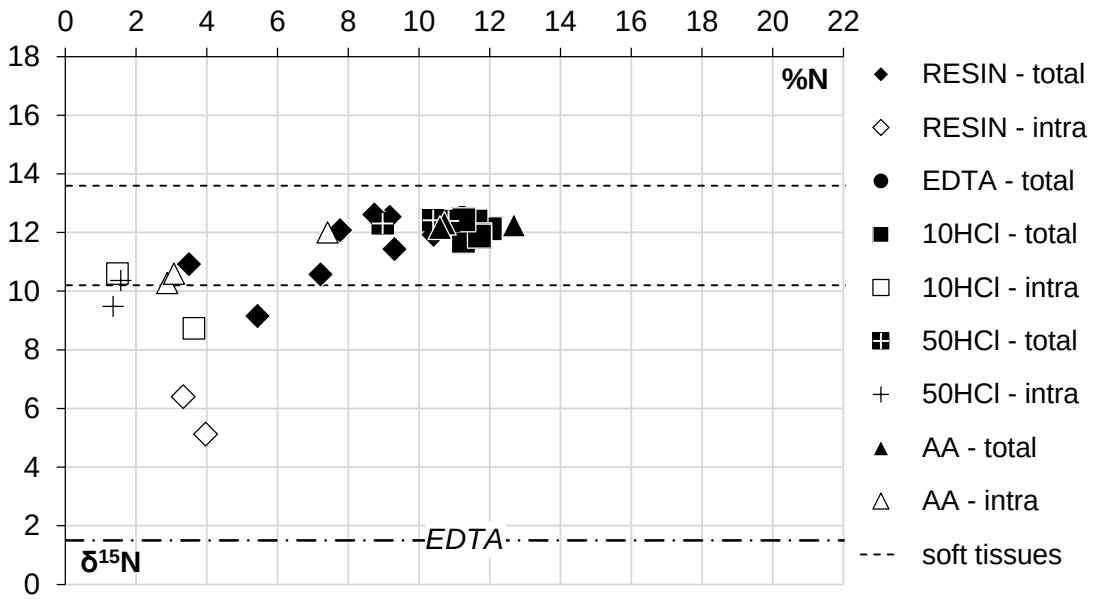

Key observations

- For total SBOM there are generally no statistical differences in $\delta^{15}N$ between the different methods, although $\delta^{15}N$ variation is greatest when cation exchange resin is used. %N is lower in cation exchange resin total SBOM samples compared to other methods, of these 50%HCl obtained samples are lower in %N than 10%HCl/EDTA samples.

- For two test species cation exchange resin $\delta^{15}N$ intra-crystalline SBOM values are depleted by several per mille compared to the other methods.

- Untreated *M. edulis* total SBOM shows very little $\delta^{15}N$ variation and is statistically depleted in $\delta^{15}N$ compared to all chemical methods, this depletion is also observed for *R. decussatus* (with the exception of 10%HCl obtained samples)

- Intra-crystalline SBOM has depleted $\delta^{15}N$ values (1-2‰) compared to total SBOM, and is also lower in elemental nitrogen concentration

- Total SBOM overlaps with the $\delta^{15}N$ soft tissue ranges, but intra-crystalline SBOM $\delta^{15}N$ values can be more depleted than soft tissue values depending on the species and shell removal method

2.3.1.3 Sulphur

The stable isotope $\delta^{34}S$ results and the distribution of the values are reported in Table 2.5 and 2.6, and Figure 2.6 and 2.7. In addition the elemental concentration of sulphur (%S) could be obtained for each isotopic measurement, and for each analysed aliquot of bulk shell powder $\delta^{34}S$ and %S are plotted against each other in Figure 2.8. The sulphur value of the cation exchange resin used for the extractions is $\delta^{34}S$ -1.5‰ (n=1).

Total SBOM

Table 2.5 $\delta^{34}S$ values and elemental sulphur concentrations (%S) of bulk total SBOM for method comparison

See Table 2.3 for further information, outliers are identified in Fig. 2.6.

$\delta^{34}S$ (‰, ±SD)	***M. edulis***	***R. decussatus***	***C. edule***
RESIN	+2.4 ±3.4 (n=6)	+1.8 ±2.8 (n=4)	+0.1 ±1.7 (n=2)
EDTA	+10.6 ±0.8 (n=5) +10.9 ±0.3 (n=4)	+11.0 ±0.4 (n=4)	+7.4 ±0.6 (n=4)
EDTA-RESIN	+3.2 ±0.1 (n=2)	n/a	n/a
10%HCl	+9.7 ±0.7 (n=5) +10.2 ±0.3 (n=4)	+10.3 ±0.4 (n=5) +10.5 ±0.1 (n=4)	+5.2 ±0.4 (n=4)
50%HCl	+10.6	n/a	+5.4 ±0.7 (n=3)
AA	+11.0 ±0.2 (n=3)	+9.3 ±1.3 (n=5) +9.8 ±0.3 (n=4)	+6.5 ±0.5 (n=3)
%S	***M. edulis***	***R. decussatus***	***C. edule***
RESIN	3.7 ±3.5 (n=6)	5.4 ±1.4 (n=4)	5.1 ±2.5 (n=2)
EDTA	0.8 ±0.2 (n=4)	1.8 ±0.1 (n=4)	2.3 ±0.2 (n=4)
EDTA-RESIN	2.8 ±0.1 (n=2)	n/a	n/a
10%HCl	0.9 ±0.4 (n=3)	1.6 ±0.2 (n=3)	2.7 ±0.5 (n=4)
50%HCl	1.3	n/a	2.3 ±0.2 (n=3)
AA	0.3 ±0.7 (n=3)	2.2 ±0.4 (n=3)	2.8 ±0.7 (n=3)

Total SBOM $\delta^{34}S$ data from *M. edulis* obtained using resin is significantly depleted in isotopic value (2.4‰ ±3.4, n=6) and shows a significant increase in elemental concentration (3.7% ±3.5, n=6) compared to all other methods (combined values for other extractions, including outliers: $\delta^{34}S$ 10.3‰ ±3.5, n=13 and %S 0.7% ±0.5, n=11) (Fig. 2.8). The same pattern is found for *R. decussatus* resin total SBOM isotope data (1.8‰ ±2.8, n=4) and elemental concentration (5.4% ±1.4 (n=4) compared to all other methods: $\delta^{34}S$ 10.1‰ ±1.1, n=10, and %S 1.9% ±0.3, n=10. Similarly this difference can be seen for *C. edule*: $\delta^{34}S$ 0.1‰ ±1.7 (resin, n=2) vs. 6.2‰ ±1.1 (other methods, n=14), and in concentration: %S 5.1% ±2.5 (resin, n=2) vs. 2.5% ±0.5 (other methods, n=14). The %S and isotopic $\delta^{34}S$ value are strongly correlated, with R-squared of 0.62 for *M. edulis*, 0.47 for *R. decussatus* and 0.33 for *C. edule*, whereby $\delta^{34}S$ becomes more depleted with increasing %S. *M. edulis* EDTA samples that were treated using resin show a similar shift, with a decrease in isotopic value (before: 10.1‰ ±1.1, n=2; after: 3.2‰ ±0.1, n=2) and an increase in elemental concentration (before: 0.8% ±0.2, n=2; after: 2.8% ±0.1, n=2).

Figure 2.6 Box-and-whisker plots of $\delta^{34}S$ values from bulk total SBOM for method comparison

Further information on the plots is given at Fig. 2.1. The number of analyses for each method is shown in Table 2.5.

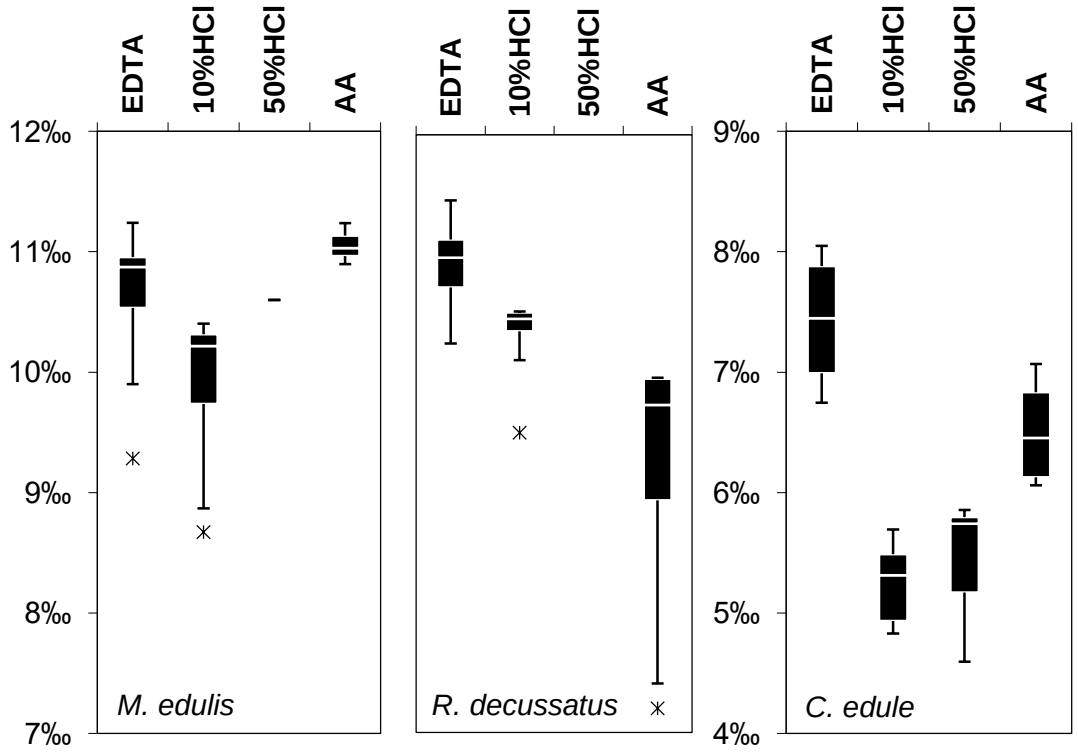

When comparing the other shell removal methods against each other, the EDTA obtained total SBOM $\delta^{34}S$ values are be generally enriched compared to the acidification methods (Fig. 2.7). This difference is significant for *M. edulis* between EDTA vs. 10%HCl (p=0.0164), *R. decussatus* EDTA vs. acetic acid (0.0030), and *C. edule* EDTA vs. 10%HCl (0.0009) and 50%HCl (0.0095). The relationship between the different acidification methods is variable, but significant differences exist between 10% HCl and acetic acid for all three test species (p=0.044 to 0.0121, n=3). Multiple $\delta^{34}S$ measurements of total SBOM obtained using 50%HCl could only be done for *C. edule*, and results are statistically similar to 10%HCl. Sulphur concentrations of total SBOM are not statistically different between any of the shell removal techniques for the three test species.

Intra-crystalline SBOM

Method comparison for intra-crystalline SBOM shows that resin samples show the same systematic relationship observed in total SBOM resin values and concentrations (Fig. 2.8). For *M. edulis* there is a strong depletion in isotopic value for resin (-0.9‰ ±0.4, n=4) compared to all other methods (7.2‰ ±4.0, n=13), as well as an increase in sulphur concentration between resin (6.6‰ ±1.1, n=4) and the other methods (1.2‰ ±0.6, n=11). The same relationship can be found for *R. decussatus*: $\delta^{34}S$ -0.9‰ ±0.9 (resin, n=4) vs. 5.0‰ ±3.7 (other extraction methods, n=5); and %S 5.1% ±1.3 (resin, n=4) vs. 1.3% ±0.2 (other, n=5), as well as for *C. edule*: $\delta^{34}S$ -0.9‰ ±0.1 (resin, n=2) vs. 4.9‰ ±0.9 (other, n=8), and %S 2.8% ±0.1 (resin, n=2) vs. 1.5% ±0.8 (other, n=8).

For other methods used to isolate intra-crystalline SBOM, several very depleted $\delta^{34}S$ values where observed for 10%HCl and 50%HCl in *M. edulis*, *R. decussatus* and *C. edule* (Fig. 2.7 and 2.8). In *M. edulis* this leads to a significant difference of $\sim +7$‰ between EDTA vs. 10%HCl (p=0.0075), and vs. acetic acid (p=0.0005), and very large variation in 50%HCl $\delta^{34}S$ values. Unfortunately EDTA values could not be obtained for the other two test species, acetic acid total SBOM samples are also significantly enriched in $\delta^{34}S$ compared to 50%HCl in *R. decussatus* (p=0.0007) by $\sim +6$‰, but there are no statistical differences between the acidification methods for *C. edule*. Sulphur concentrations of total SBOM are not statistically different between any of the shell removal techniques for the three test species.

Table 2.6 $\delta^{34}S$ values and elemental sulphur concentrations (%S) of bulk intra-crystalline SBOM for method comparison

See Table 2.3 for further information

$\delta^{34}S$ (‰, ±SD)	***M. edulis***	***R. decussatus***	***C. edule***
RESIN	-0.9 ±0.4 (n=4)	-0.9 ±0.9 (n=4)	-0.9 ±0.1 (n=2)
EDTA	+9.3 ±1.1 (n=2)	n/a	n/a
10%HCl	+2.0 ±1.3 (n=3)	n/a	+4.2 ±1.5 (n=2)
50%HCl	+7.1 ±4.6 (n=3)	+1.0 ±0.1 (n=2)	+5.0 ±1.1 (n=3)
AA	+10.2 ±0.5 (n=3)	+7.6 ±0.6 (n=3)	+5.3 ±0.2 (n=3)
%S	***M. edulis***	***R. decussatus***	***C. edule***
RESIN	6.6 ±1.1 (n=4)	5.1 ±1.3 (n=4)	2.8 ±0.1 (n=2)
EDTA	1.8 ±0.6 (n=2)	n/a	n/a
10%HCl	1.5 ±0.6 (n=3)	n/a	1.5 ±1.2 (n=2)
50%HCl	1.7 ±0.7 (n=3)	1.1 ±0.2 (n=2)	1.7 ±0.9 (n=3)
AA	0.9 ±0.2 (n=3)	1.4 ±0.2 (n=3)	1.3 ±0.6 (n=3)

Figure 2.7 Box-and-whisker plots of $\delta^{34}S$ values from bulk intra-crystalline SBOM for method comparison.

Further information on the plots is given at Fig. 2.1. The number of analyses for each method is shown in Table 2.6.

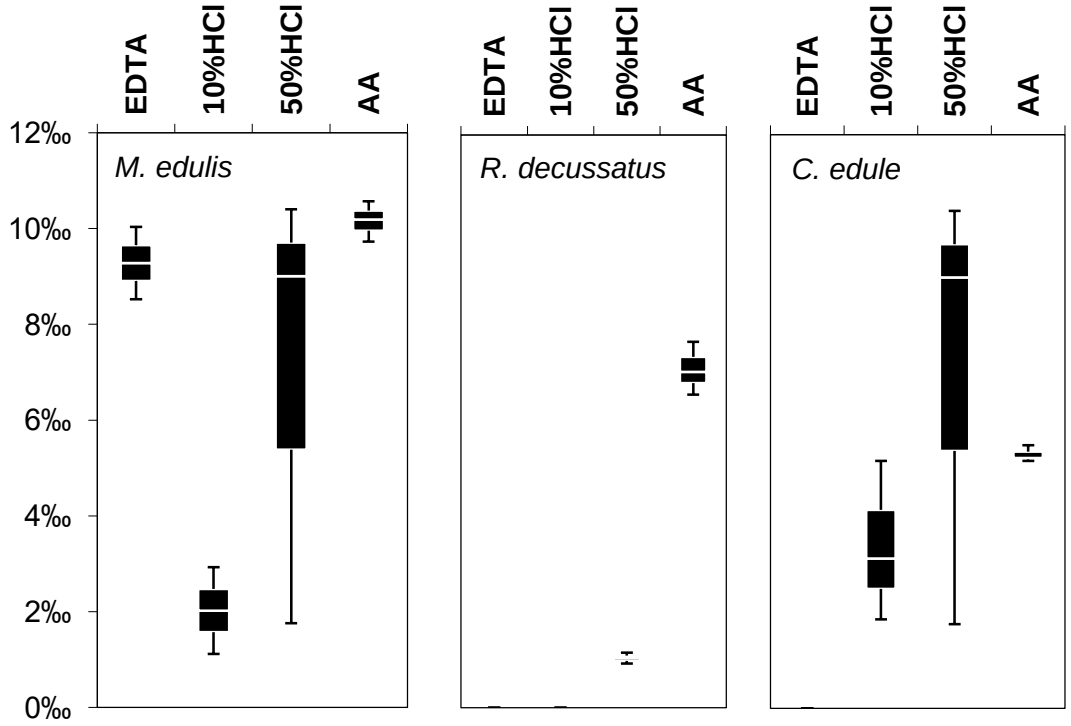

A comparison between the results of total SBOM and intra-crystalline SBOM of the different shell removal methods (if available) does not give a consistent relationship for either sulphur isotopic value or elemental concentration between the two pools. Acetic acid SBOM data could be compared for all three test species: both pools are similar in isotopic composition and elemental concentration for *M. edulis*, but for the other two species the intra-crystalline SBOM $\delta^{34}S$ is statistically depleted by 1-2‰ compared to total SBOM ($p=0.0013$ and 0.0181), and also statistically depleted in elemental concentration ($p=0.0363$ and 0.0479). EDTA obtained SBOM could only be compared for *M. edulis* and shows a small statistical depletion (~ -1‰, $p=0.0385$) in intra-crystalline SBOM compared to total SBOM, but %S is statistically higher (+1%) in intra-crystalline SBOM. 10%HCl samples from *M. edulis* show a large $\delta^{34}S$ depletion in intra-crystalline SBOM (~ -8‰), but a similar elemental concentration. For 10% HCl obtained total and intra-crystalline SBOM from *C. edule*, both $\delta^{34}S$ and %S are statistically similar between the two pools. This was also observed for 50%HCl SBOM samples from the same species.

SBOM compared to soft tissue ranges

SBOM results are differently related to $\delta^{34}S$ soft tissue values for the three test species (Fig. 2.9). For *M. edulis* the large majority of total SBOM $\delta^{34}S$ values (except some depleted 10%HCl values) overlap with the soft tissue $\delta^{34}S$ range. For intra-crystalline SBOM from *M. edulis* only acetic acid obtained SBOM, and some EDTA/50%HCl overlap with the soft tissue range, but none of the 10%HCl samples. For *R. decussatus* only a minority of EDTA $\delta^{34}S$ values overlaps with the soft tissue range, whilst total SBOM obtained using other methods is more depleted. In addition, all intra-crystalline SBOM from *R. decussatus* is more depleted than the soft tissue $\delta^{34}S$ range. Lastly, for *C. edule* all total and intra-crystalline SBOM has depleted $\delta^{34}S$ values compared to the soft tissue range of that species.

Figure 2.9 $\delta^{34}S$ isotopic composition and elemental sulphur (%S) concentration of bulk SBOM for method comparison

(p.32) Data for individual aliquots of homogenised shell powder as reported in Table 2.5 and 2.6.

M. edulis

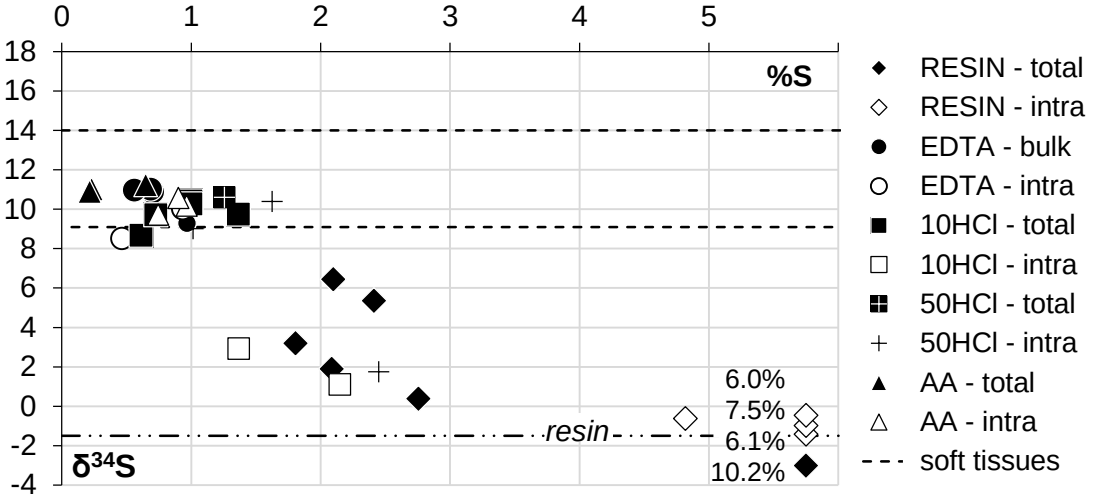

R. decussatus

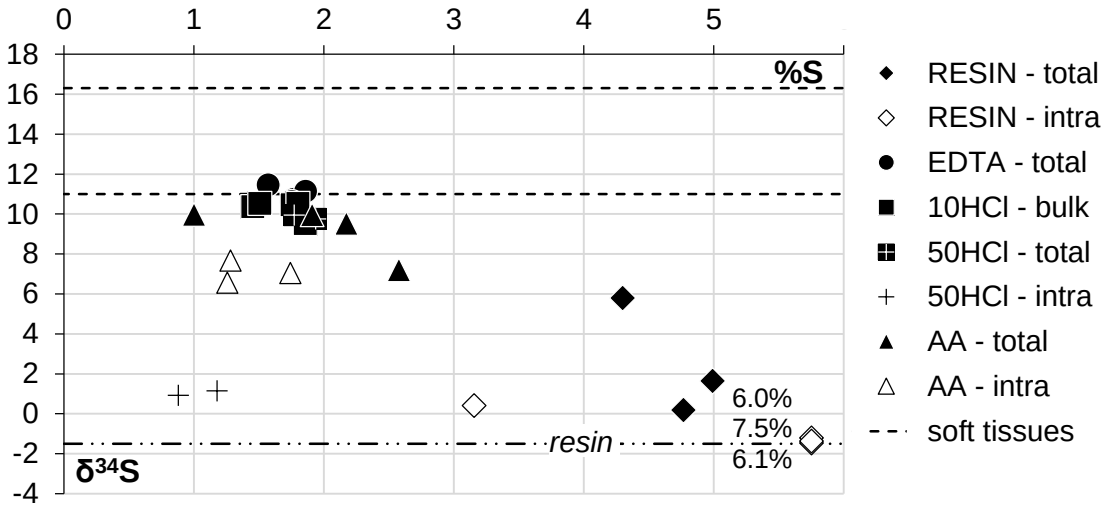

C. edule

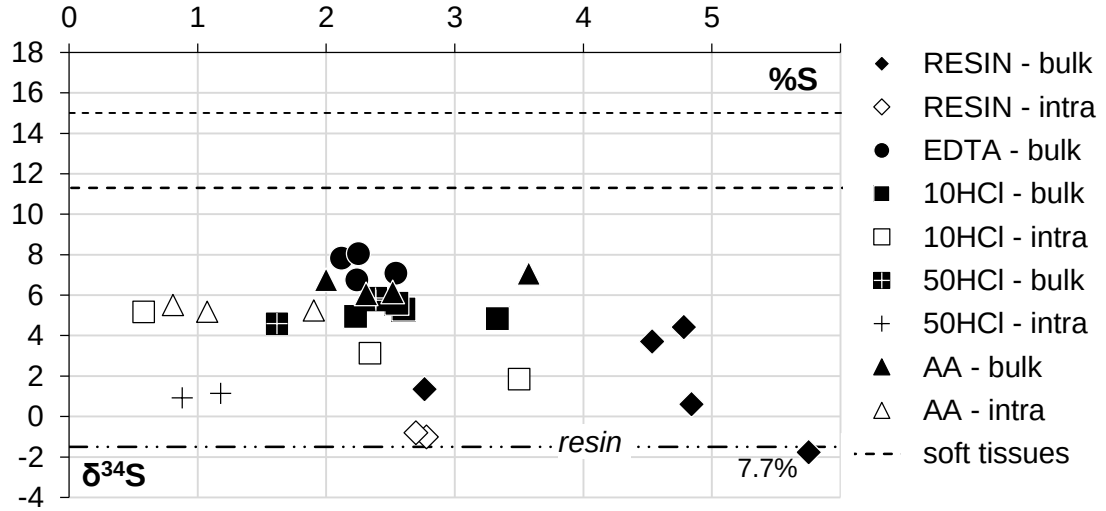

Key observations

- Total and intra-crystalline SBOM obtained using cation exchange resin is depleted in $\delta^{34}S$ and enriched in %S compared to the other shell removal methods

- Total SBOM obtained using EDTA is generally enriched for $\delta^{34}S$ compared to acidification methods, and for intra-crystalline SBOM very depleted $\delta^{34}S$ values have been observed for samples obtained using 10%HCl and 50%HCl

- The relationship between total SBOM and intra-crystalline SBOM for $\delta^{34}S$ and %S is unclear, and varies between the different methods and species.

- Total SBOM and some intra-crystalline SBOM $\delta^{34}S$ values of *M. edulis* overlap with the soft tissue range, for the other two test species the SBOM $\delta^{34}S$ values are generally depleted outside of the soft tissue range

Carbonate-associated sulphate (CAS)

CAS data is shown in Table 2.7. *C. edule* CAS obtained using HCl (20.3‰ ±0.3 (n=2) is significantly enriched compared to *C. edule* CAS (total SBOM) obtained from resin water (11.9‰ ±0.7, n=2, (p=0.0041), with a mean difference of +8.4‰. There is no difference in %S between the two extraction methods (p=0.5442). *C. edule* CAS HCl is also significantly different from all resin CAS data (combined: 11.0‰ ±2.3, n=11, excluding outlier shown in Table 3.1), with a p-value of 0.0002. Similarly there is no difference in %S (11.4% ±0.8, n=11, p=0.3503).

Table 2.7 $\delta^{34}S$ isotopic composition of CAS

(p. 34) CAS was obtained using cation exchange resin (RESIN) or 10%HCl from aliquots of homogenised shell powder from *Mytilus edulis*, *Ruditapes decussatus* and *Cerastoderma edule*. Elemental sulphur concentration is shown as %S. The outlier values are not from the same sample.

Species	**Method**	**SBOM**	**$\delta^{34}S$** (‰ ±SD)	**%S** (%)
M. edulis	RESIN	total	+14.5 (n=1)	11.8 (n=1)
		intra	+11.1 ±1.5 (n=3), outlier 0.7	11.2 ±0.6 (n=3), outlier 3.3
R. decussatus	RESIN	total	+12.6 (n=1)	12.0 (n=1)
		intra	+5.4 (n=1)	12.6 (n=1)
C. edule	RESIN	total	+11.9 ±0.7 (n=2)	11.6 ±0.5 (n=2)
		intra	+10.5 ±0.6 (n=3)	10.9 ±1.0 (n=3)
	10%HCl	total	+20.3 ±0.3 (n=2)	12.0 ±0.6 (n=2)

2.3.2 Pyrolysis GC/MS comparison of total and intra-crystalline bulk SBOM

The molecular composition of total and intra-crystalline SBOM (isolated using cation exchange resin) from *M. edulis* was analysed using Py-GC/MS, whereby the molecular components are separated using gas chromatography and identified using mass spectrometry (Fig. 2.10). Pyrolysis GC/MS results show that the majority of SBOM consists of proteins, and that lipids (in the form of saturated fatty acids) are also present, which is in agreement with published literature (Goulletquer & Wolowicz et al., 1989; CoBabe & Pratt, 1995). Comparison between the two samples shows that intra-crystalline SBOM has a simple make-up with only several high intensity peaks of pyrolysis products, particularly compared to the more complex total SBOM sample. The most abundant component of intra-crystalline SBOM is the lipid C16:0 (palmitic acid), and there are also clear peaks for other saturated fatty acids (C14:0, C15:0, C17:0, C:18:10, C). Palmitic acid is the most abundant and widespread natural saturated acid, and its occurrence is ubiquitous (Gunstone et al., 2007). Other major pyrolysis products are break-down components of proteins, and toluene. Toluene is also abundant in the total SBOM sample, which is furthermore dominated by phenol and indole. The generation of toluene, phenol and indole is associated with the presence of aromatic amino acids in proteins (Moldoveanu, 1998). The C16:0 peak has a much lower relative abundance in total SBOM than in the intra-crystalline SBOM sample. No identifiable cation exchange resin products were detected in the samples.

Figure 2.10 Total ion chromatograms from pyrolysis GC/MS for total SBOM and intra-crystalline SBOM of *M. edulis*

SBOM samples were isolated using cation exchange resin. Identified pyrolysis products are numbered and listed in the table below.

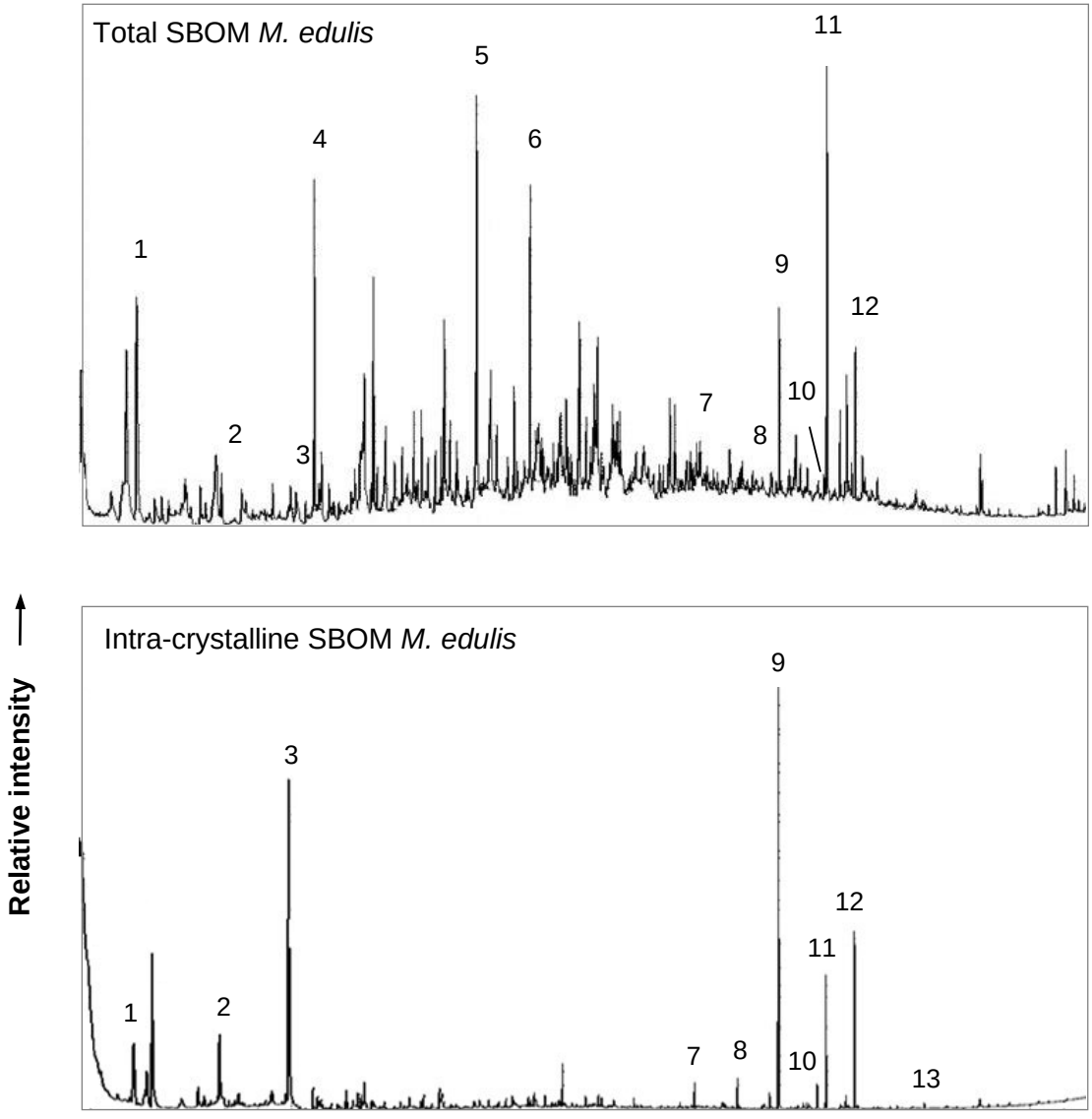

1	Toluene	**7**	C14:0
2	Styrene	**8**	C15:0
3	TMAH	**9**	C16:0
4	Phenol	**10**	C17:0
5	1-Methylindole	**11**	Androstane
6	1,3-Dimethyl indole	**12**	C18:0
		13	C20:0

2.4 Discussion

2.4.1 Isotopic and compositional comparison between total SBOM and intra-crystalline SBOM

Consistent isotopic differences between total SBOM and intra-crystalline SBOM were observed for all three test species, irrespective of shell removal method: both $\delta^{13}C$ (- 5-7‰) and $\delta^{15}N$ (- 1-2‰) values of intra-crystalline SBOM are statistically depleted compared to total SBOM samples, and generally also compared to the soft tissue ranges. In addition, the intra-crystalline fraction has a lower in elemental nitrogen concentration than the total SBOM fraction. This isotopic and elemental difference can be explained by the higher relative proportion of lipids in the intra-crystalline fraction. Of the macromolecular groups lipids are characteristically depleted in ^{13}C due to enzymatic discrimination (DeNiro & Epstein, 1978), and high lipid content would result in the observed lower $\delta^{13}C$ values of intra-crystalline SBOM. In addition lipids contain very limited amounts of nitrogen, and this would therefore also explain the elemental difference between the two pools. The lower $\delta^{15}N$ values of intra-crystalline SBOM could be due to the presence of e.g. ^{15}N depleted lipoprotein compounds, that have previously been suggested to explain $\delta^{15}N$ enrichment of soft tissues after lipid removal (Ruiz-Cooley, 2011). Alternatively, other difference in protein compounds (with different $\delta^{15}N$ values) could contribute to the observed difference (see: 2.4.2). In either scenario, the $\delta^{13}C$ and $\delta^{15}N$ components of inter-crystalline SBOM are more similar to those of soft tissues, because total SBOM reflects soft tissue values much closer. Unfortunately due the limited $\delta^{34}S$ data it is unclear if there is a consistent difference in sulphur stable isotope values and concentration between the two SBOM pools.

The difference in macromolecular composition between inter- and intra-crystalline SBOM suggests that they are secreted following different biochemical pathways, and it is likely that these differences are related to different functions of the two pools in the biomineralisation process. The role of lipids in biomineralisation is not yet deciphered, but has been suggested to be important (Farre and Dauphin, 2009). In addition, the relationship between intra-crystalline SBOM and the mineral is not completely understood, but is also crucial and crucial in biomineralisation, and has been shown to control shell microstructures (Okumara et al., 2013).

For our study the compositional difference of the two pools is important to take into account when comparing shell removal methods, and their potentially different influences on these two SBOM pools. These results are furthermore relevant for

palaeontological investigations. In general, the intra-crystalline SBOM pool is often preferred for biochemical analysis of fossil specimens because it is physically protected from external diagenetic pathways by the mineral (Sykes et al., 1995). This study however shows that when this pool is used for stable isotope analysis, the results will be very different from original soft tissue/total SBOM values, and subsequent reconstruction of the precise nutritional sources of the animal will be much more difficult.

In addition, a change in the isotopic off-set between total SBOM and intra-crystalline SBOM in fossil specimens (compared to modern taxa) could indicate degradation or contamination of either the inter-crystalline pool or both SBOM pools. Hypothetically, inter-crystalline SBOM would be first affected because of the difference in preservation potential compared to intra-crystalline SBOM.

2.4.2 Evaluation criteria for the success of shell removal methods

With the exception of total SBOM $\delta^{15}N$, it is not possible to assess the effects of shell removal methods by comparing the obtained isotope data to untreated samples. Because of the lack of true controls, the success of the different methods is evaluated using the following characteristics for the SBOM results: (i) low variation, and (ii) isotopic similarity to soft tissue values, these two criteria are presented in more detail below.

(i) **Low isotopic variation.** It is likely that isotopic heterogeneity of SBOM exists within individual specimens, and between individual specimens of the same species. However, because of the extensive homogenization of bulk shell powder in this study, the analysed aliquots of the bulk material are expected to have a uniform isotopic signal. This assumption is confirmed by the $\delta^{15}N$ analysis of total SBOM from *M. edulis* ($\delta^{15}N$ 11.6‰ ±0.1, n=3), that showed isotopic variation within measurement error. Therefore low variation and absence of outliers are expected for the stable isotope values of SBOM obtained using the different methods.

(ii) **Similarity to soft tissue values.** Soft tissues are often used as a stable isotopic proxy for untreated SBOM (e.g. Carmichael et al., 2008). Within this specific study it is not possible to compare the bulk shell powder to “bulk” soft tissue values, because of the difficulty of homogenising soft tissues,

particularly for such a large amount of individual animals. As a preferred alternative, the bulk SBOM results are compared to the range of stable isotope values obtain from the different tissues (gills, mantle, foot, muscle, rest) of several individual specimens.

Isotopic differences between the soft tissue ranges and bulk SBOM can be caused by inherent differences between the two organic pools instead of methodological effects. Some of these potential causes can also be responsible for isotopic variation between the different soft tissues (and potentially SBOM values of different species), and below these are discussed in combination where appropriate.

a) SBOM synthesis fractionation. The different molecular components of the SBOM are secreted by epithelial cells that line the outer margin of the mantle (Lowenstam & Weiner, 1989), potentially in combination with specialized hemocytes (blood cells) (Johnstone et al., 2015), and it has been proposed that their cells and cell products combine SBOM with nanocrystals in vesicles to form multi-crystalline composites, and progressively organised shell structures (Johnstone et al., 2015). The formation of SBOM is therefore a complex cellular process that involves many different secretory cell types and their products (Myers et al., 2007). However, data about the synthesis and routing of SBOM components are very scarce, and it is unknown how this affects isotopic discrimination of the different macromolecules.

   For essential amino acids the fractionation between soft tissues and SBOM is expected to be limited. Because essential amino acids cannot be synthesized by the animal, they are taken up from the diet and directly routed to soft tissues with minimal isotopic alteration. If these are also directly routed into SBOM, they have very similar values (McCullagh et al., 2005). Whilst carbon and nitrogen are present in both essential and non-essential amino acids, sulphur can only be present in proteins as the essential amino acid methionine, and as cysteine, a semi-essential amino acid that can be synthesized from methionine (no isotopic information is available for that process) (Nehlich et al., 2015). Both methionine and cysteine have been observed in SBOM (e.g. Marin et al., 2016), and high isotopic similarity in $\delta^{34}S$ between diet, soft tissues and SBOM is expected.

b) Compositional differences. Different soft tissues and SBOM can differ in isotopic value due to isotopic routing: whereby certain biochemical components are preferentially allocated to certain organs (Schwarcz 1991). In general, carbohydrates are used for energy metabolism, proteins to build and repair tissues, and fatty acids are present in fat reserves. Because these different components have different isotopic values, compositional differences can cause isotopic differences between soft tissues, and potentially SBOM. This is of particular concern for the carbon stable isotope ratios, because sulphur is only present in proteins (and restricted to the amino acids cysteine and methionine), and similarly protein is the major source of nitrogen (present in all amino acids), since lipids only contain negligible amounts of nitrogen. Carbon however is supplied by dietary proteins, lipids, and carbohydrates, which may differ in their carbon isotope composition. This is further complicated by non-essential amino acids, that can be synthesized using carbon from other macronutritional sources than protein, such as the carbohydrates and lipids (e.g. Jim et al., 2006). As discussed in section 2.4.1, lipids are characteristically depleted in ^{13}C (Hobson and Welch, 1992), causing more depleted $\delta^{13}C$ values in tissues with high-lipid content, and $\delta^{13}C$ enriched values for those rich in protein. This ^{13}C enrichment has particularly been noted for protein-rich bivalve muscle tissue (e.g. DeNiro & Epstein, 1976; Mateo et al., 2008; Ruiz-Cooley et al., 2011).

   In addition to differences in macromolecular composition, significant isotopic variation also exists between compounds of the same macromolecular group. E.g. different amino acids in a single tissue can in $\delta^{13}C$ and $\delta^{15}N$ by more than 15‰, due to differences in enzymatic discrimination (e.g. Hare et al., 1991). As different proteins contain distinction proportions of amino acids, differences in protein composition among tissue types can yield dissimilar isotopic compositions that are unrelated to nutritional sources.

c) Represented time periods. An important difference between SBOM and soft tissues is the time period over which stable isotope values are averaged: in SBOM they represent a life-time average, whilst soft tissues represent a specific time period, related to tissue growth and isotopic turnover (Versteegh et al., 2011; Fry and Arnold, 1992). The represented time periods differ between tissues, and muscle tissue is

generally regarded as having the slowest turnover rate (e.g. Hill & McQuaid, 2009), potentially followed by the gills, and other soft tissues (Fertig et al., 2010).

2.4.3 Method comparison of shell removal techniques

In this section the analytical results will be discussed per shell removal technique, but particular attention will be given to consistent isotopic differences between methods that could be indicative of method-specific effects on isotope values.

2.4.3.1 Comparison to untreated $\delta^{15}N$ values of total SBOM

Untreated *M. edulis* total SBOM shows very little $\delta^{15}N$ variation and is statistically depleted in $\delta^{15}N$ compared to all chemical methods, this depletion is also observed for *R. decussatus* (with the exception of 10%HCl obtained samples). This depletion is generally small and the mean differences between untreated SBOM and treated SBOM range from -0.6‰ to -1.2‰ for the different methods. This does suggest that all SBOM isolation methods remove a $\delta^{15}N$ enriched protein component from the total SBOM pool. It is difficult to identify the precise mechanisms and source of this change, because the SBOM matrix contains at least dozens of different proteins that can be hugely diverse, in biochemical properties and sequence information (Marin et al., 2012; 2016).

2.4.3.2 Cation exchange resin

Cation exchange resin was tested as an alternative method to isolate SBOM for stable isotope analysis, and no disadvantages of the method were previously known. However, in this study significant differences in the isotopic values of SBOM obtained using resin versus other shell removal methods were observed. The most significant effect was found for $\delta^{34}S$ SBOM values, whereby increasing elemental sulphur concentrations cause a depletion in $\delta^{34}S$ values. This negative correlation suggests that the depletion is caused by an accumulating residual component from the cation exchange resin ($\delta^{34}S$ -1.5‰). Although in a very limited number of samples resin beads were observed, the physical size of the resin makes it impossible to penetrate the dialysis bag (3500 dalton). It is likely that for the small number of samples resin has become attached to the (knots of the) dialysis bag and were freeze-dried with the SBOM samples, but a different mechanism involving

the release, transport and trapping a dissolved species is necessary to explain the ^{34}S depletion in all of the samples. The chemical formula of the cation exchange resin does however not contain any sulphur, but solely consists of carbon and hydrogen (http://www.sigmaaldrich.com/catalog/product/sial/217492?lang=en&region=NL, accessed 18 September 2016). One possibility is bacterial contamination of the re-usable resin, that could be incorporating resin into the SBOM they are feeding on. A similar contamination mechanism could be possible for the carbon and nitrogen values discussed below.

Residual resin compound also appears to effect CAS obtained from resin water ($\delta^{34}S$ +11.0‰ ±2.3, n=11), that is significantly depleted in ^{34}S compared to the expected seawater sulphate value (+20.3‰). *C. edule* CAS values obtained using HCl (+20.3‰ ±0.3, n=2) accurately reflect seawater sulphate $\delta^{34}S$, and confirm this conclusion. The %S between resin and HCl samples is very similar, and it is possible that the sulphur is exchanging with the resin, or the %S increase is too small to detect. The ^{34}S enrichment of CAS provides insights into the mechanisms of residual resin contamination. Because the resin water is filtered before precipitation residual resin beads cannot be the contaminant, and either the contamination is precipitated with CAS from inorganic sulphate, or is present as organic sulphur and co-precipitated with $BaSO_4$.

In summary, the residual inorganic sulphur compound of cation exchange resin remains unidentified, but has a $\delta^{34}S$ value -1.5‰. The effect of the contaminant is variable, and increases with higher %S towards the depleted value of the resin. Because both the %S of samples and the $\delta^{34}S$ value of the contaminant are known, it will still be possible to identify large ^{34}S differences between sulphur sources, particularly if these for instance have negative $\delta^{34}S$ values. This possibility is further explored in Chapter 3.

In addition to an effect on $\delta^{34}S$ SBOM values, cation exchange resin also causes a ^{13}C depletion for total and intra-crystalline SBOM values compared to the other methods, for values heavier than $\delta^{13}C \sim$ -23‰ in this study. These values are also depleted compared to soft tissue ranges, with the exception of *M. edulis* (discussed below). It is likely that this depletion is also caused by (the same) residual resin component, since resin has a depleted $\delta^{13}C$ value of -29.2‰. This is also in agreement with several depleted outliers (up to -28.2‰), that could potentially be caused by increased amounts of residual resin compounds, potentially incorporated by bacteria. The effect on the total and intra-crystalline SBOM $\delta^{13}C <$ -23‰ is limited to minus 1-2‰.

Lastly, cation exchange resin showed the largest variation in $\delta^{15}N$ total SBOM values, as well as lower elemental nitrogen concentration (%N). Whereas for two test species intra-crystalline SBOM $\delta^{15}N$ are significantly depleted compared to other methods, and have higher %N. This suggests that cation exchange resin can both remove and add nitrogen sources, but mechanisms for this are currently unknown. In general however, the $\delta^{15}N$ total SBOM are statistically similar to the other shell removal methods, and can be used to identify trophic levels and differentiate nitrogen sources.

2.4.3.3 EDTA

Several possible disadvantages of using EDTA for SBOM isolation were outlined in the introduction, the primary concern being that residual EDTA (containing carbon and nitrogen) would become incorporated with SBOM and influence its stable isotope values. The carbon value of EDTA ($\delta^{13}C$ -39.0‰) was determined, but no depletion in $\delta^{13}C$ values was observed in total SBOM isolated using EDTA compared to the other shell removal methods. However, for intra-crystalline SBOM obtained using EDTA the $\delta^{13}C$ values are depleted compared to the 10%HCl/acetic acid methods, and mean differences can encompass 2‰. Therefore it is possible that the smaller amounts of intra-crystalline SBOM (0.1% of shell weight vs. ~1% in total SBOM) is more strongly effected by residual EDTA. The $\delta^{15}N$ data of EDTA obtained SBOM is similar in value and variability to other shell removal methods.

EDTA SBOM samples generally have enriched $\delta^{34}S$ values compared to acidification methods, and they more closely reflect soft tissue ranges for both total and intra-crystalline SBOM. For both *R. decussatus* and *C. edule* however, the EDTA $\delta^{34}S$ total SBOM values are still depleted compared to soft tissue ranges. This depletion is unexpected, because of the (semi)essential amino acids containing sulphur were predicted to be routed directly into SBOM. The most likely explanation is that ^{34}S enrichment occurs when the amino acids are transported from the soft tissues into SBOM (via the extrapallial fluid), or alternatively this fractionation could occur during isolation of SBOM. Our observation is in agreement with previously obtained differences in $\delta^{34}S$ between total SBOM (obtained using EDTA) and soft tissues: O'Donnell (2003) found a depletion in SBOM of *Mercenaria mercenaria* (+13.6‰ ±0.2 for SBOM and +15.4‰ ±0.8 for soft tissues, n=unknown), as did Dreier *et al*., (2012) for *Venerupis aurea* (+13.6‰ for SBOM, +18.0‰ for gills, n=1). This suggests that $\delta^{34}S$ total SBOM does not reflect the values from soft tissues for heterotrophic filter feeders.

2.4.3.4 Acidification methods

The results for methods using 10%HCl, 50%HCl and acetic acid are discussed together because all three methods are based on acidification. In the introduction it was noted that the effects of acidification on stable isotope values have led to both more enriched and more depleted $\delta^{13}C$ and $\delta^{15}N$ values, as well as no effects, and that the mechanisms behind these changes often remain undetermined. In this study statistical differences in $\delta^{13}C$ values of SBOM obtained using the different acidification methods were found: 50%HCl samples are most depleted for total and intra-crystalline SBOM compared to 10%HCl and acetic acid, in addition the elemental nitrogen concentration of 50%HCl samples is lower than for 10%HCl/EDTA samples. Together these observations suggest that the stronger 50%HCl acid has a greater influence on the $\delta^{13}C$ values of SBOM by removing ^{13}C depleted protein compounds. Loss of acid-soluble organic carbon (amino acids/carbohydrates) has previously been reported, and can cause $\delta^{13}C$ depleted values if acid-insoluble lipids are preferentially retained for example, since these are characteristically ^{13}C depleted (Schlacher & Connelly, 2014). This could also explain the depleted $\delta^{15}N$ values for both 50%HCl/10%HCl obtained intra-crystalline SBOM versus the weaker acetic acid. In addition, deviating values were observed for $\delta^{13}C$ values of SBOM obtained using acetic acid. The enriched $\delta^{13}C$ values for total SBOM could be explained by remaining inorganic carbonate (that has a very enriched $\delta^{13}C$ value) due to the weakness of the acid. The extremely depleted $\delta^{13}C$ values for intra-crystalline SBOM are best explained by residual acid, as there are very few mechanisms that could result in a depletion of -20‰.

As discussed in the EDTA section, sulphur SBOM data obtained using acidification is generally depleted compared to EDTA obtained samples, and neither reflect soft tissue $\delta^{34}S$ accurately. Moreover, several 10%HCl/50%HCl extremely low values ($\delta^{34}S$ < 2.0‰, n=7, species=3) are present in intra-crystalline samples, that are not present in EDTA or acetic acid samples. This suggests strong depletion/fractionation of $\delta^{34}S$ values, that did not result in statistically different elemental sulphur concentrations between the different methods. It is known that the sulphur containing amino acids can become unstable, which would could be a potential explanation for this effect (Dreier et al., 2012).

Part II – Isotopic relationship between individual SBOM and soft tissues

In Part I bulk shell powder was used to obtain SBOM for stable isotope analysis, which could only be generally compared to soft tissues isotope values. In this section the isotopic comparison between SBOM and soft tissues is done on an individual basis, and individual SBOM is compared to multiple soft tissues of the same individual bivalve. Because these experiments were conducted before the results of the Part I were known, the SBOM was obtained using cation exchange resin. SBOM was additionally isolated using 10%HCl for specimens with sufficient remaining shell powder.

2.5 Results

The isotopic offset between different soft tissues and SBOM is shown in Fig. 2.10, showing the mean difference (±SE) amongst the different individuals.

Carbon and nitrogen

Species-specific variation can be observed in $\Delta_{SBOM-ST}$: *M. edulis* has a positive $\Delta_{SBOM-ST}$ for both $\delta^{15}N$ and $\delta^{13}C$ (soft tissues are more enriched compared to SBOM), whilst *R. decussatus* and *C. edule* have a negative relationship (soft tissues are more depleted compared to SBOM).

Isotopic differences can be found between the different tissues compared across five individual specimens. Particularly noticeable is the statistically significant $\delta^{13}C$ depletion in muscle tissue compared to several other tissues for both *M. edulis* and *R. decussatus*. Across the three species and for both carbon and nitrogen, muscle is always least positive/most negative difference for both $\delta^{13}C$ and $\delta^{15}N$ compared to SBOM values. The ‘rest’ and ‘mantle’ tissues are amongst the most positive/least negative differences for both $\delta^{13}C$ and $\delta^{15}N$.

Isotopic comparison between individual total SBOM for $\delta^{13}C$ and $\delta^{15}N$ obtained using both cation exchange resin and 10%HCl does not show a clear pattern for nitrogen (difference: $\delta^{15}N$ +0.3‰ ±1.1, n=4), but carbon is generally more depleted using ion-exchange resin ($\delta^{13}C$ -0.7‰ ±1.0, n=6). Due to species-specific variation, using HCl values causes the $\Delta_{SBOM-ST}$ for *M. edulis* to increase, and for *R. decussatus*/*C. edule* to generally decrease. For nitrogen the effects on $\Delta_{SBOM-ST}$ were variable.

Figure 2.11 Isotopic comparison ($\delta^{13}C$ and $\delta^{15}N$) between total SBOM and soft tissues for individual specimens

The three test species used in this study are underlined, total SBOM was obtained using cation exchange resin. Published results (and methodology) from: [a]Versteegh et al., 2011 (simple combustion), [b]LeBlanc, 1989 (EDTA, acidification), [c]Watanabe et al., 2009 (acidification), [d]O'Donnell et al., 2003 (acidification), [e]Carmicheal et al., 2008 (acidification), [f]Dreier et al., 2012 (EDTA), [g]Kovacs et al., 2010 (acidification). Data is compared between average values of individual specimens for SBOM and soft tissues ('specimen comparison'), or mean values of SBOM and soft tissues for multiple specimens ('means comparison'). The bold error range shows values without one outlier, that showed very large variation between the different soft tissues (as explained in the text).

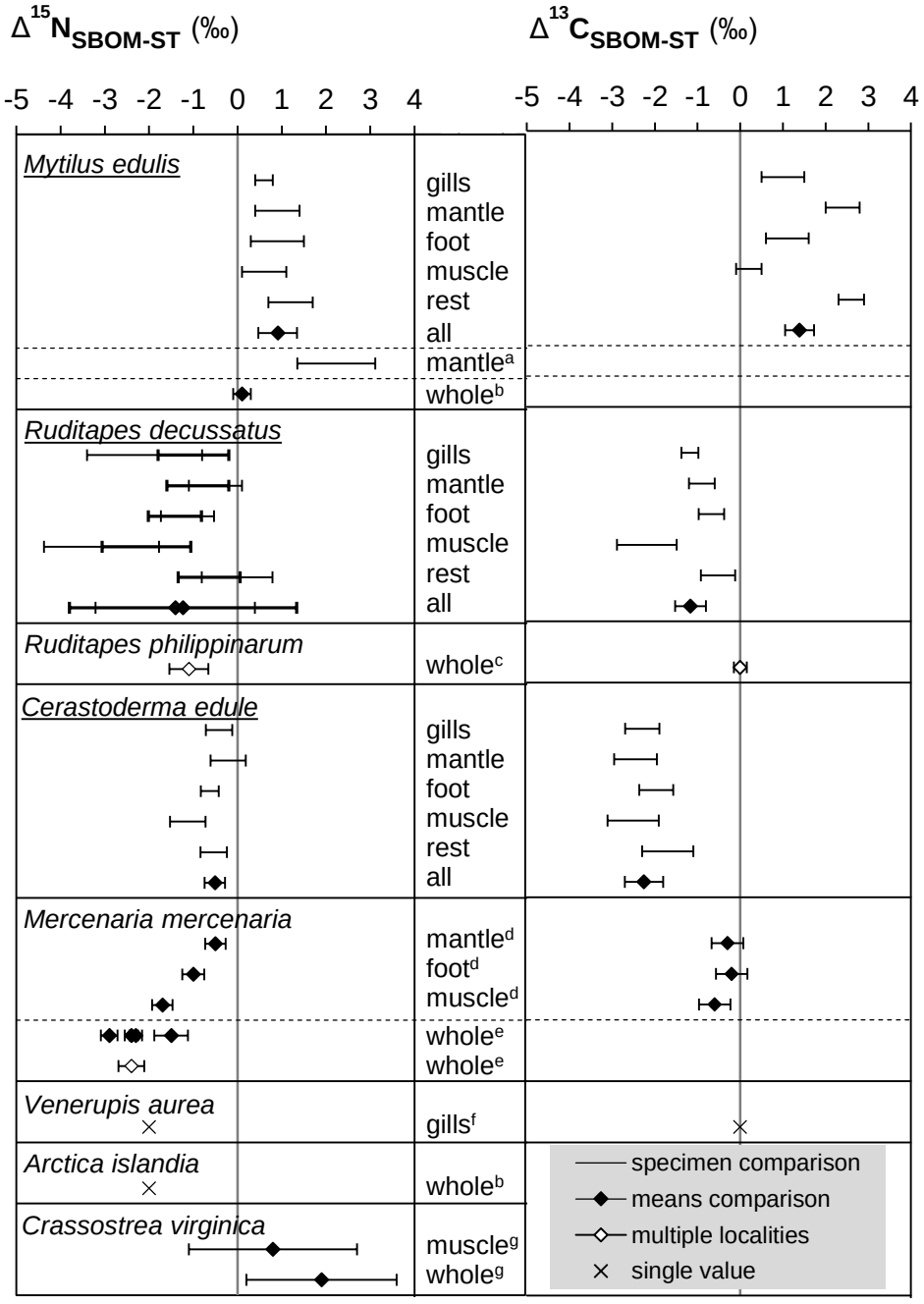

Sulphur

$\delta^{34}S$ total SBOM isolated using cation exchange resin values from individual specimens (-1.4‰ to +11.9‰) were unrealistically variable, and not compared to related soft tissues. Therefore SBOM was also isolated using 10%HCl for a limited number of specimens. $\delta^{34}S$ total SBOM obtained using HCl (+5.2‰ to +9.5‰, n=5 specimens of three species) is strongly depleted compared to mean soft tissue values of the species (+12.0‰ to +15.2‰), with a mean difference of -6.2‰ ±1.5

2.6 Discussion

Carbon and nitrogen

In section 2.4.2 possible reasons for isotopic variation in soft tissues/SBOM are listed. The enriched $\delta^{13}C$/ $\delta^{15}N$ values of muscle tissue can be explained by high protein content, that is generally enriched in ^{13}C compared to lipids.

Our dataset confirms previous reports of species-specific variation in $\Delta_{SBOM-ST}$ of bivalves species in for $\delta^{13}C$ and $\delta^{15}N$. For *M. edulis* soft tissues are consistently more enriched compared to SBOM, and for *R. decussatus* and *C. edule* soft tissue are more depleted for both isotope systems, even though all species were isolated using cation exchange resin that was shown to cause a 1-2‰ depletion in $\delta^{13}C$ values. Published values (shown in Fig. 2.11) confirm this positive relationship for $\Delta_{SBOM-ST}$ of *M. edulis* in $\delta^{15}N$ (LeBlanc, 1989; Versteegh et al., 2011), that is also found in the species *C. virginica* (Kovacs et al., 2010).

Assumed isotopic similarity of SBOM vs. soft tissues can give a false impression of a successful extraction method: bulk resin $\delta^{13}C$ total SBOM of *M. edulis* (Part I, this chapter) obtained using cation exchange resin overlaps with the species' soft tissue $\delta^{13}C$ range, whilst total SBOM obtained using the other methods appears to be $\delta^{13}C$ enriched. The 'depleting effect' of cation exchange resin therefore causes the off-set between SBOM and soft tissues for *M. edulis* to decrease. This effect would likely also have been observed for bulk resin $\delta^{15}N$ total SBOM in Part I if soft tissue ranges were smaller.

The $\delta^{13}C$/$\delta^{15}N$ enrichment of *M. edulis* SBOM in relation to soft tissue values has previously been attributed to the thin shell of this species (Carmichael et al., 2008). However, that does not explain the similar results for thick-shelled *C. virginica*. Alternatively, both *M. edulis* and *C. virginica* are distinct from the other bivalve

species because of the presence of calcite within their shells: *M. edulis* consists of both calcite and aragonite (Lorens and Bender, 1980) and *C. virginica* is completely calcitic (Lombardi et al., 2013). In addition, differences exist in the shell ultrastructure in *M. edulis* and *C. virginica* compared to the other species, in particular the absence of crossed-lamellar layers and the presence of nacre/nacre-like structures (Bourgoin, 1988; Checa et al., 2007; Lombardi et al., 2013).

SBOM is responsible for forming shell structure, as well as the $CaCO_3$ polymorph (Marin et al., 2012). Although it is still not understood how SBOM works (Marin et al., 2016), it is known that different shell structures are related to different SBOM compositions, as e.g. Liao et al. (2015) identified multiple unique proteins to different shell layers of *Mytilus coruscus* (nacre, fibrous prism, myostracum). It is very likely that these different proteins differ in $\delta^{13}C$ and $\delta^{15}N$ due to difference in synthesis, which would explain the differences ΔSBOM-ST within our data.

Sulphur

Total SBOM obtained using 10%HCl showed a strong isotopic depletion of SBOM sulphur composition (-6.2‰ ±1.5, n=5 specimens for three species) compared to soft tissues. This is in agreement with our observations for bulk SBOM, which show that SBOM $\delta^{34}S$ values do not closely reflect soft tissue $\delta^{34}S$ values.

2.7 Conclusions

This study shows that the largest isotopic influence on SBOM $\delta^{13}C$ and $\delta^{15}N$ composition is the species-specific off-set compared to soft tissue values, likely caused by differences in SBOM protein composition. Understanding the SBOM-soft tissue relationship is therefore critical for identifying nutritional strategies and nutritional sources.

The impact of the shell removal methods is of secondary influence on isotopic SBOM values, and generally the isotopic variation between shell removal methods is less than the soft tissue ranges of the species. Of the different methods EDTA, 10%HCl and 50%HCl are most suitable for $\delta^{13}C$ analysis of total and intra-crystalline SBOM. These methods, as well as acetic acid, are also preferred for $\delta^{15}N$ total SBOM, whilst intra-crystalline SBOM should best be isolated using EDTA or acetic acid. EDTA is the preferred method for $\delta^{34}S$ SBOM analysis, although the relationship between SBOM and soft tissues needs to be further investigated. Ultimately the important of such isotopic differences will depend on the research question that are investigated.

Chapter 3

Identifying chemosymbiosis in modern bivalves using stable isotope analysis of shell-bound organic matter

Edine Pape[a], Fiona Gill[a], Robert J. Newton[a], Crispin T.S. Little[a], Emma Stirk[a], Freya Howden[a], Cindy L. Van Dover[b], Elizabeth Harper[c], John Taylor[d], Paul Dando[e], Adrian Boyce[f], and Geoffrey D. Abbott[g]

[a] School of Earth and Environment, University of Leeds, Leeds LS2 9JT, United Kingdom

[b] Division of Marine Science and Conservation, Duke University, Beaufort NC 28516, United States

[c] Department of Earth Sciences, University of Cambridge, Cambridge CB2 3EQ, United Kingdom

[d] Department of Life Sciences, Natural History Museum, London SW7 5BD, United Kingdom

[e] ?

f Scottish Universities Environmental Research Centre, East Kilbride, G75 0QF, United Kingdom

[g] School of Civil Engineering and Geosciences, Newcastle University, Newcastle upon Tyne NE1 7RU, United Kingdom

Author contribution

EP performed the great majority of SBOM extractions, prepared SBOM/soft tissues for stable isotope analysis, carried out stable isotope analysis, and wrote the paper. EP, FG, RJN and CTLS designed the research and commented on the manuscript. RJN carried out stable isotope analysis and supervised the contribution of EP therein. ES performed SBOM extractions of hydrothermal vent specimens, FH carried out the SBOM extractions on cold seep specimens using EDTA. The material in this study was provided by CLVD (cold seep and hydrothermal vent taxa), EH (brachiopods), and JT/PD (shallow reducing taxa). AB generated the $\delta^{13}C$

values of shell carbonate. GDA generated Py-GC/MS results, that were interpreted by FG and GDA.

Relevant research questions

The aim of the research presented in this thesis is to reconstruct the occurrence of chemosymbiosis through geological time using stable isotope analysis of shell-bound organic matter (SBOM), and to investigate the influence of chemosymbiosis on the evolution of deep sea fauna and ecosystems. This chapter focusses on **Research question 3: Can different nutritional strategies be identified in SBOM by their distinct isotopic compositions?** As well as **Research Question 2: Does the stable isotopic composition of SBOM relate in a predictable way to that of soft tissues?** for those specimens analysed that include soft tissues in addition to shell material. If it is possible to identify biosignatures for chemosymbiosis in the modern suite of samples, these can subsequently be compared to analytical results from fossil taxa.

The majority of the results were obtained before the method comparison data (presented in Chapter 2) could be analysed, and therefore cation exchange resin was used to isolate the SBOM for analysis. The potential isotopic effects of the cation exchange resin method are discussed in the Material & Methods section of this chapter. For samples with sufficient shell material additional SBOM extractions were performed using 10%HCl, and a small part of the data could also be compared to a pilot study using EDTA. Because the stable isotope composition of SBOM from chemosymbiotic taxa is expected to differ from heterotrophic filter-feeders, the potential isotopic effects of the three shell removal techniques on SBOM could also be different. The comparison between cation exchange resin, 10%HCl and EDTA provides further insights regarding **Research question 1: Is the stable isotopic composition of SBOM influenced by chemical extraction from shell carbonate*?***

3.1 Introduction

Chemosymbiosis is an unusual nutritional strategy whereby invertebrates obtain nutrition from living in symbiosis with chemoautotrophic bacteria that oxidize reduced chemicals to produce energy for carbon fixation. The invertebrate host then directly digests the bacteria, or receives nutrition via translocation of nutrients (Fisher, 1990). Chemosymbiotic animals are characterized by either the presence of methanotrophic bacteria that use methane for energy generation and as a carbon source, or by thiotrophic bacteria that utilize hydrogen sulphide. It is also possible for both types of bacteria to be present as a dual symbiosis (Dubilier et al., 2008; Taylor & Glover, 2010). The identification of these chemosymbiotic strategies in macroinvertebrates not only reveals their nutritional sources, but is also indicative of an array of physiological and behavioural adaptions. In addition, it provides insights into local environmental conditions, as well as about the distribution of chemosymbiotic nutrition itself. Unfortunately the existing techniques to determine the presence of symbionts require the animal's soft tissues, and can therefore only be performed on animals that are collected alive. This methodological issue hampers the identification of chemosymbiosis in dead specimens, as well as in subfossil and more ancient taxa. To overcome this limitation, the stable isotope composition of shell-bound organic matter (SBOM) is tested as a decay-resistant alternative to soft tissue analysis. SBOM consists of a framework of organic molecules produced by the mantle, and therefore reflects the stable isotope composition of soft tissues (O'Donnell et al., 2003), although the precise relationship between soft tissues and SBOM is not well understood and can be species-specific (as discussed in Chapter 2).

The carbon ($\delta^{13}C$), sulphur ($\delta^{34}S$), and nitrogen ($\delta^{15}N$) stable isotope values of bivalve and gastropod soft tissues have been very important in revealing nutritional strategies (e.g. Childress et al., 1986; McAvoy et al., 2008). Most commonly used for the identification of methanotrophic chemosymbiosis is an extremely depleted carbon value, because the bacteria incorporate methane with $\delta^{13}C$ values of -50 to -110‰ (Whiticar, 1999), whereas heterotrophic bivalves consume particular organic matter ($\delta^{13}C$ -22‰ to -18.5‰, Hoefs, 2015). Because thiotrophic bacteria rely on depleted hydrogen sulphide ($\delta^{34}S$ -10 to -50‰, Bottrell and Raiswell, 2000) as an energy and sulphur source, thiotrophic chemosymbiosis can be distinguished from bivalves with heterotrophic lifestyles who derive their sulphur from seawater-sulphate producing a much more positive range of values ($\delta^{34}S$ +15‰ to +20‰, as reviewed in Mae et al 2008). The nitrogen sources of seep and vent organisms are

not well known (e.g. Dreier et al., 2012; Feng et al., 2015), but many chemosymbiotic bivalves have the ability to directly utilize ^{15}N depleted nitrate and ammonium (Lee and Childress 1994; Lee et al., 1992), differentiating them from animals relying on photosynthetically derived nutrition ($\delta^{15}N$ +0‰ to +15‰, Michener et al., 2007)

Published studies using the stable isotope composition of SBOM from chemosymbiotic bivalves have analysed a limited number of thiotrophic and methanotrophic species originating from shallow reducing environments (Dreier et al., 2012 and 2014) or deep sea hydrothermal vents (Mae et al., 2007). Missing from this dataset are taxa from cold seep localities, in particular bivalves relying on dual symbiosis. Cold seeps represent an important type of chemosynthesis-based ecosystem in the deep sea, that differ from hydrothermal vents in the chemical composition of seeping fluids, as well as their longevity. Moreover, ancient cold seeps have been recognized in the fossil record and contain well-preserved shell material (Kiel, 2010; Campbell, 2006), whereas fossil vent specimens are notoriously difficult to study (Little et al., 2004).

To identify the isotopic ranges of each nutritional strategy, 19 species from 9 different cold seep localities were analysed. To effectively compare isotopic variation between environmental settings, additional hydrothermal vent families and shallow-water bivalves were included. In addition to the complete SBOM fraction (total SBOM), the intra-crystalline SBOM pool from these samples was also analysed. This SBOM fraction is present within the minerals and more likely to be protected from external diagenesis (Sykes et al., 1995). Therefore intra-crystalline SBOM could be very important in the study of fossil samples. In Chapter 2 it was shown that intra-crystalline SBOM carries a different stable isotope signal to the total SBOM pool for heterotroph species, that does not closely reflect soft tissue values. It was suggested that this isotopic off-set is related to differences in the chemical composition of the two pools. A similar isotopic and compositional difference can be expected for chemosymbiotic taxa. To further investigate compositional differences, both SBOM pools and related shell powder were analysed using pyrolysis gas chromatography mass spectrometry (pyrolysis GC/MS) for a thiotrophic seep vesicomyid.

Our suite of samples includes several brachiopods species from shallow non-reducing environments. These animals were analysed because at pre-Cretaceous cold seeps dense assemblages of mono-specific brachiopods are common (Sandy, 2010). This high abundance has led some to suggest a chemosymbiotic lifestyle,

even though modern brachiopods are suspension-feeders and generally absent from cold seeps Brachiopods also secrete SBOM (Jope, 1967) but the bulk isotope signal of total or intra-crystalline SBOM has not previously been determined. In future studies the stable isotope values of heterotrophic brachiopods can be compared to suspected chemosymbiotic brachiopods from the fossil record.

Lastly, the extensive suit of samples analysed within this study provides the opportunity to investigate whether nutritional strategies can be differentiated using the $\delta^{13}C$ values of shell carbonate (e.g. Lietard and Pierre, 2009). Whilst most of the shell carbonate is derived from seawater DIC, a small proportion of the shell is made up of metabolic CO_2, that can be reconstructed using $\delta^{13}C$ of SBOM and/or soft tissues (McConnaughey et al., 2008). Because nutrition only determines a minor part of the $\delta^{13}C$ signal, shell carbonate is expected to be a much less effective proxy for nutritional strategies than SBOM.

Research questions

The main aim of this study is to investigate whether it is possible to differentiate nutritional strategies using the isotopic values of total and/or intra-crystalline SBOM. In addition, the possibility of shell carbonate $\delta^{13}C$ as a nutritional proxy is further investigated. To be able to extrapolate conclusions based on our dataset to all modern and ancient ecosystems, the reasons for isotopic variability within and between nutritional strategies must be fully understood. Such intra-strategy variation could be related to e.g. differences in (isotopic values of) environmental sources, or the animal's physiology and behaviour.

In addition, a better understanding of the isotopic relationship between soft tissues and SBOM is critical to evaluate whether SBOM can differentiate nutritional strategies to the same degree as soft tissue values. It can also provide insights into the reconstruction of isotopic source values based on SBOM, since isotopic fractionation between sources and soft tissues is relatively well understood.

In summary, this study aims to identify isotopic differences between nutritional strategies in i) total SBOM, ii) intra-crystalline SBOM, and to a lesser degree in iii) shell carbonate. These observations need to be placed in context to be fully understood, and therefore the isotopic dataset obtained in this study will be used to answer several inter-connected research questions:

- **Total SBOM**
    - What causes isotopic variability of total SBOM within the same nutritional strategy?
    - What is the isotopic relationship between total SBOM and soft tissues?
    - Can different nutritional strategies be identified across environments by distinct isotopic values of total SBOM?
- **Intra-crystalline SBOM**
    - What is the isotopic and compositional relationship between intra-crystalline SBOM and total SBOM?
    - Can different nutritional strategies be identified across environments by distinct isotopic values of intra-crystalline SBOM?
- **Shell carbonate**
    - What causes isotopic variability of shell carbonate within the same nutritional strategy?
    - Can different nutritional strategies be identified across environments by the distinct isotopic values of shell carbonate?

3.2 Materials & methods

3.2.1 Material

An overview of all the specimens analysed is shown in Table 3.2. In Table 3.1 a summary is given of the number of species analysed per nutritional strategy for each environmental setting. Whilst cold seep ecosystems have been reported to frequently include heterotrophic species (MacAvoy et al., 2008), they appear to not be frequently collected and unfortunately very few deep sea heterotrophs were available for analysis (Table 3.1).

Table 3.1 Summary of samples by nutritional strategy and environmental setting

Number of analysed species is given with the number of specimens between brackets, total numbers for the nutritional strategies and environmental settings are shown in italics. Collated specimens were counted as 1 specimen.

	Nutritional strategy (n=)				
Environmental setting (n=)	Methanotrophic symbionts	Dual symbiosis	Thiotrophic symbionts	Heterotrophy	
Cold seeps	1 (10)	3 (19)	13 (62)	2 (2)	*19 (93)*
Hydrothermal vents			10 (29)	1 (1)	*11 (30)*
Shallow reducing			9 (14)	2 (2)	*11 (16)*
Shallow non-reducing				4 (28)	*4 (28)*
	1 (10)	*3 (19)*	*32 (105)*	*9 (33)*	

Figure 3.1 shows a map the different localities, and published isotopic values of environmental sources for these localities are reported in Table 3.3, Table 3.4. and Table 3.5 for carbon, nitrogen and sulphur, respectively. Table 3.2 includes the nutritional strategies of chemosymbiotic species. It should be noted that whilst *B. heckerae* is reported as dual symbiotic, the range of symbiotic bacteria appears to be more diverse, and specimens have been reported to contain two types of thiotrophic bacteria, one methanotrophic type of bacteria, and a methylotrophic phylotype. The metabolism of these symbionts has however not yet been investigated (Duperron et al., 2007; Duperron et al., 2013). The analysed material includes specimens from several chemosymbiotic bivalve families, that are all characterized by different behavioural and physiological strategies. Bathymodiolin mussels are epibenthic, and live attached to hard substrates (Duperron, 2010). Vesicomyid clams usually live shallowly burrowed in the sediment, whereas solemyid, lucinid and thyasirid bivalves are sediment dwellers that can produce long burrows to span the oxic-anoxic interface in the seafloor sediment (Stewart and Cavanaugh, 2006; Taylor and Glover, 2010). Further information on the ecology of the families, and information on shell mineralogy, can be found in Chapter 4.

Table 3.2 Overview of samples

(p. 56-59) The total number of specimens analysed is shown under “n”, when this number is between brackets multiple specimens were collated to obtain sufficient shell material for SBOM isolation. For species that are underlined soft tissues were also analysed.

species	**n**	**nutritional strategy**	**locality**	**storage**
Cold seeps				
Bathymodiolus childressi	10	methanotrophic symbionts	Gulf of Mexico, Green Canyon, GC234, GC233, GC185	air-dried
Calyptogena ponderosa	3	thiotrophic symbionts	Gulf of Mexico, Green Canyon, GC272	air-dried
Vesicomya cordata	3	thiotrophic symbionts	Gulf of Mexico, Green Canyon, GC272	air-dried

Bathymodiolus heckerae (adult)	6	dual symbiosis	Gulf of Mexico: Florida Escarpment	air-dried
Bathymodiolus heckerae (juvenile)	5	dual symbiosis	Gulf of Mexico: Florida Escarpment	ethanol
Vesicomya cf. *kaikoi*	(4)	thiotrophic symbionts	Gulf of Mexico: Florida Escarpment	ethanol
Paralepetopsis floridensis	(12)	heterotrophy	Gulf of Mexico: Florida Escarpment	ethanol
Bathymodiolus heckerae	6	dual symbiosis	Blake Ridge Diapir	air-dried
Vesicomya cf. *venusta*	5	thiotrophic symbionts	Blake Ridge Diapir	ethanol
Bathymodiolus sp.	3	unknown / dual symbiosis	Barbados accretionary prism	air-dried
"*Calyptogena valvidae*"	3	thiotrophic symbionts	Barbados accretionary prism	air-dried
Calyptogena kilmeri	5	thiotrophic symbionts	Extrovert Cliffs, Monterey Bay	ethanol and/or formalin
Calyptogena starobogatovi	5	thiotrophic symbionts	Oregon Subduction zone	ethanol and/or formalin
Calyptogena packardana	5	thiotrophic symbionts	Monterey Canyon, Monterey Bay	ethanol and/or formalin
Calyptogena pacifica	5	thiotrophic symbionts	Guaymas Basin, Mexico	ethanol and/or formalin
Calyptogena stearnsii	5	thiotrophic symbionts	Monterey Canyon, Monterey Bay	ethanol and/or formalin
Ectenogena elongata (PSC44)	5	thiotrophic symbionts	Fossil Hill, Southern California	ethanol and/or formalin
Ectenogena elongata (other push cores)	9	thiotrophic symbionts	Fossil Hill, Southern California	air-dried
Ectenogena elongata (large)	3	thiotrophic symbionts	Fossil Hill, Southern California	air-dried (broken)
Ectenogena elongata	3	thiotrophic symbionts	San Diego Through, Southern California	air-dried

Solemyidae sp.	1	thiotrophic symbionts	San Diego Trough, Southern California	air-dried
Lucinidae sp.	1	thiotrophic symbionts	San Diego Trough, Southern California	air-dried
Delectopecten sp.	1	thiotrophic symbionts	San Diego Trough, Southern California	ethanol and/or formalin
Hydrothermal vent localities				
Bathyaustriella thionipta	5	thiotrophic symbionts	Macauley Cone, Kermadec Ridge, NZ	air-dried
Alvinoconcho hessleri	3	thiotrophic symbionts	South Su, Manus Basin	ethanol and/or formalin
Ifremeria nautilei	3	chemoautotrophic symbionts	South Su, Manus Basin	ethanol and/or formalin
Bathymodiolus manusensis	3	thiotrophic symbionts	South Su, Manus Basin	ethanol and/or formalin
Lepetodrilus elevatus	(7)	grazing / suspension feeding	East Wall, East Pacific Rise	ethanol and/or formalin
Bathymodiolus thermophilus	2	thiotrophic symbionts	East Wall, East Pacific Rise	
Bathymodiolus thermophilus	2	thiotrophic symbionts	Buckfield, East Pacific Rise	
Peltospiroidea sp.	(3)	unknown / thiotrophic symbionts	East Scotia Ridge	frozen
Vesicomyidae sp.	3	thiotrophic symbionts	East Scotia Ridge	air-dried
Bathymodiolus brevior	3	thiotrophic symbionts	Kilo Moana, Lau Basin	ethanol and/or formalin
Bathymodiolus brevior	3	thiotrophic symbionts	Tow Cam, Lau Basin	ethanol and/or formalin
Shallow reducing environments				
Codakia oricularis	2	thiotrophic symbionts	Little Duck Keys, Florida Keys (seagrass)	ethanol and/or formalin

Pegophysema philippiana	2	thiotrophic symbionts	Magellan Bay, Mactan Island (unknown)	ethanol and/or formalin
Ctena orbiculata	2	thiotrophic symbionts	Ramrod Key, Florida Keys (seagrass)	ethanol and/or formalin
Loripes lucinalis	1	thiotrophic symbionts	Houmt Souk, Djerba, Tunisia (seagrass/sand)	ethanol and/or formalin
Ctena imbricatula	2	thiotrophic symbionts	Bocas del Toro, Panama (mangrove)	
Lucina adansoni	2	thiotrophic symbionts	Sal Rei Village, Boavista Island, Cape Verde Islands (sand)	ethanol and/or formalin
Myrtea spinifera	(2)	thiotrophic symbionts	Skogsvågen, Norway (fjord ecosystem)	air-dried
Myrtea spinifera	(9)	thiotrophic symbionts	Gåsevik, Sweden (fjord ecosystem)	ethanol and/or formalin
Thyasira sarsi	(7)	thiotrophic symbionts	Gåsevik, Sweden (fjord ecosystem)	ethanol and/or formalin
Abra alba	(16)	deposit feeder	Gåsevik, Sweden (fjord ecosystem)	ethanol and/or formalin
Ennucula tenuis	(6)	deposit feeder	Gåsevik, Sweden (fjord ecosystem)	ethanol and/or formalin
Shallow non-reducing environments				
Terebratella sanguinea	5	filter-feeding	Big Hope Bay, New Zealand	air-dried
Terebratella sanguinea	7	filter-feeding	Tricky Cove, New Zealand (fjord ecosystem)	air-dried
Notosaria nigricans	5	filter-feeding	Tricky Cove, New Zealand (fjord ecosystem)	air-dried
Liothyrella neozelanica	7	filter-feeding	Tricky Cove, New Zealand (fjord ecosystem)	air-dried
Liothyrella uva	4	filter-feeding	Tricky Cove, New Zealand (fjord ecosystem)	air-dried

Figure 3.1 Locality map of samples analysed in this study, including the location of mid-ocean ridges

Cold seeps (black): (A) Gulf of Mexico, (B) Blake Ridge, (C) Barbados accretory prism, (D) Monterey Bay, (E) Oregon Subduction Zone, (F) Guaymas Basin, (G) Southern California localities, Hydrothermal vents (dark grey): (H) Kermadec Ridge, (I) Manus Basin, (J) East Pacific Rise localities, (K) East Scotia Ridge, (L), Lau Basin localities

Shallow reducing environments (medium grey): (M) Florida Keys, US, (N) Mactan Island, Philippines, (O) Houmt Souk, Tunesia, (P) Bocas del Toro, Panama, (Q) Boavista Island, Cape Verde Islands, (R) Skogsvågen, Norway, (S) Gåsevik, Sweden

Shallow non-reducing environments (light grey): (T) New Zealand localities.

Figure modified from http://pubs.usgs.gov/gip/dynamic/baseball.html, accessed September 1 2016.

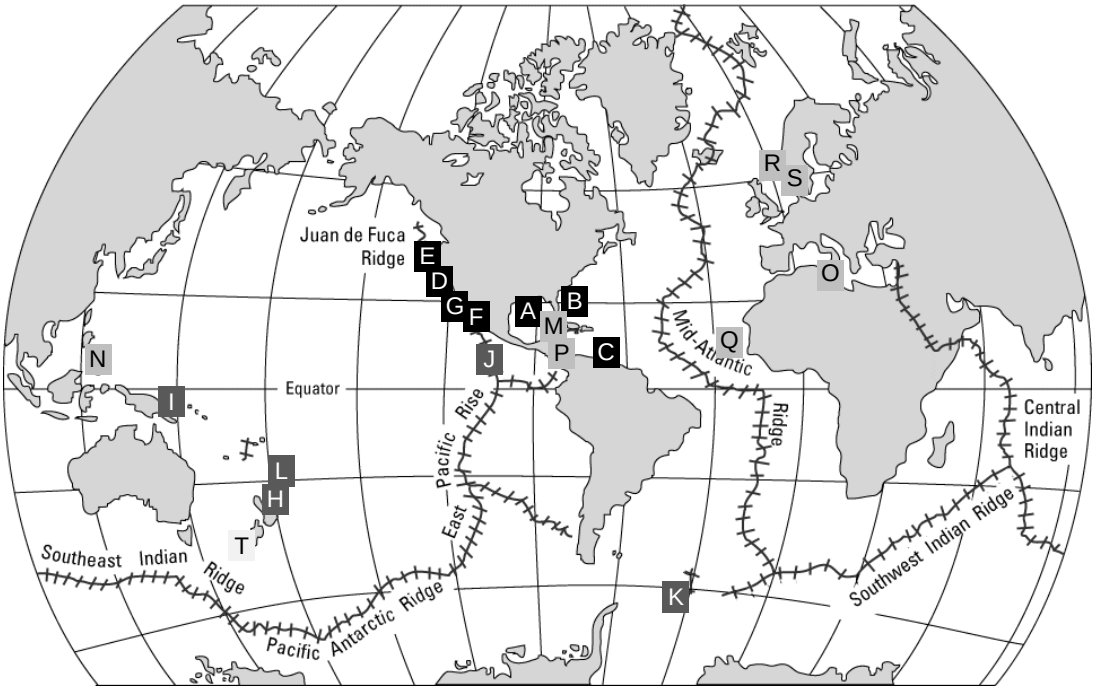

Table 3.3 Published carbon stable isotope values ($\delta^{13}C$ in ‰) of environmental sources at sample localities

Abbreviations: DIC (dissolved inorganic carbon), POM (particulate organic matter), SOM (sedimentary organic matter), SPOM (suspended particulate organic matter). References: [1] Rau et al. (1982), [2] Hoefs (2015), [3] Anderson & Arthur (1983), [4] Whiticar (1999), [5] Aharon et al. (1991), [6] Goni et al. (1998), [7] Wells & Rooker (2009), [8] Milkov (2005), [9] Feng et al. (2009), [10] Joye et al. (2004), [11] Sassen et al. (1999), [12] Sassen et al. (2004), [13] Hu et al. (2010), [14] Pohlman et al. (2005), [15] Sassen et al. (2009), [16] Paull et al. (1992), [17] Martens et al. (1991), [18] Paull et al. (1992), and Paull et al. (2000), [19] Martin et al. (2004), [20] Reid et al. (2013), [21] De Ronde et al. (2007), [22] Baker et al. (2015), [23] and Freeman and Thacker (2011), [24] Cornelisen et al. (2007), [25] McLeod & Wing (2007), [26] Demopoulos et al. (2010).

Locality	**Seawater DIC**	**Pore water DIC**	**POM**	**Methane**
Surface seawater	+1 to +2 [1]		-22 to -18.5 [2]	
Deep sea	+0 [3]			
Cold seeps				
General	+0 [3]	-45 to +18 [24]		-110 to -20 [4]
Gulf of Mexico	+1 [5]		-20 [6] -21.5 [7]	-74.7 to – 42.2 [8]
Green Canyon, GOM	+0.6 [9]		-19.8 ±0.7 (-23.3 to -15.9) [26]	
GC185, GOM			-25 [10]	-46.0, -44.1 [11] -45.4 [12]
GC233, GOM	-0.3 [12]	-24.8 to -47.1 [12] (up to 17cm)	-25 [10]	-65.5, -64.3 [11]
GC234, GOM		-49.3 [13]		-49.4 [14] -48.7 [15]
Florida Escarpment, GOM	-0.4 to +0.4 (mean -0.1) [16]	-17.3 to -48.2 [16]	-67.9 to -25.3 (SOM) [16]	-94 to -61 [17]
Blake Ridge		-31.4 to -8.9 [18]		-72.1 to -62.5 (mean -68.4) [18]
Extrovert Cliffs	-3 [19] (2 cm depth)	up to -9 [19]		
Hydrothermal vents				
East Scotia Ridge	+0.1 ±0.1 [20]			
Macauley Cone, Kermadec Ridge	+1.0 [21]			
Shallow reducing environments				
Bocas del Toro	+0 [22]		-23 [23]	

Table 3.4 Published nitrogen and sulphur stable isotope values ($\delta^{15}N$ and $\delta^{34}S$ in ‰) of environmental sources at sample localities

References: [1] Cline and Kaplan (1975), [2] Fry, personal comments in Riekenberg, 2012 [3] Rooker et al. (2006) ; Wells & Rooker (2009); [4] Peterson and Fry (1987), [5] Michener et. (2007), [6] Demopoulos et al., (2010)

Locality	**Nitrate – bottom water**	**Nitrate - pore water**	**Ammonium**	**Particulate organic matter**
General			-20 to +10 [4]	
Seawater	+5 to +19[1]			-2 to +11 [4]
Deep sea	+4 to +6 [4]			> +6 [5]
Cold seeps				
Gulf of Mexico	+5 to +7 [2]			+2 to +8 [3]
Green Canyon				+0.3 to +9.6 (mean 3.5 ±0.7) [6]

References: [1] Canfield (2001), [2] Rees et al. (1978), [3] Aharon & Fu (2003), [4] Formolo and Lyons (2013), [6] Petersen & Fry, [7] Shanks (2001).

Locality	**Sulphate – Bottom water**	**Sulphate pore water**	**Sulphide - bottom water**	**Sulphide – pore water**	**POM**
Seawater	+20.3 [2]		depletion of -30 to -70 w.r.t. sulphate[1]		+17 to +21 [5]
Cold seeps					
Gulf of Mexico	+20.3 [3]				
GC233, GOM [4]	+23.4	+25.5 to +26.3	-20.3	-20.8 to -20.0	
GC234, GOM [4]	+20.1 to +36.8	+19.9 to +54.1	-0.4 to +8.0	+2.1 to +19.7	
Blake Ridge [6]	+20.2	up to +21.3		-18.8 to 1.6 (mean -1.3 ±1.4)	
Hydrothermal vents					
General			-5 to +8 [7]		

3.2.2 Methods

Methods used in this study are described in Chapter 2, and include: preparation of the shell material/soft tissues, stable isotope analysis and elemental concentration, and SBOM isolation using cation exchange resin, 10%HCl, or EDTA. Figure 3.4 shows which SBOM isolation method was used on which samples, although the large majority of the samples SBOM was isolated using cation exchange resin. The methodology for carbon stable isotope analysis of shell carbonate is given in Chapter 4. To reconstruct the sulphate $\delta^{34}S$ composition of local sources, the analysis of carbonate-associated sulphate using cation exchange resin was attempted but unsuccessful due to the presence of residual resin (see: Chapter 2).

3.2.2.1 Pyrolysis GC/MS

Pyrolysis GC/MS analysis was performed on total SBOM and intra-crystalline SBOM from *Calyptogena ponderosa* (Gulf of Mexico) obtained using cation exchange resin. In addition shell powder from this species was analysed. The analyses were performed by CDS Analytical (Oxford, PA), and no further methodological details are available at the moment.

3.2.2.2 Isotopic effects of SBOM isolation

The shell removal technique using ion exchange resin was assumed to be superior to other shell removal techniques. A later method comparison test however showed that the resin could potentially influence the original stable isotope signature of SBOM (Chapter 2). For species with sufficient remaining shell material, SBOM was therefore also isolated using 10%HCl. In addition, SBOM isolated using EDTA is available for two cold seep species. This section discusses if, and how, the different methods could influence the stable isotope values of SBOM, and whether observations made for SBOM from heterotrophic filter-feeders (total SBOM $\delta^{13}C$: -21‰ to -16‰, $\delta^{15}N$: +4‰ to +14‰, $\delta^{34}S$: +8‰ to +16‰) also apply to the more depleted SBOM values of chemosymbiotic animals.

To be able to directly compare different methods, individual specimens were used of which SBOM was isolated using multiple methods (samples analysed by multiple methods can be found in Fig. 3.4). The isotopic off-set of 10%HCl and EDTA obtained SBOM compared to cation exchange resin SBOM is shown in Fig. 3.2.

Figure 3.2 Method comparison of the stable isotope composition ($\delta^{13}C$, $\delta^{15}N$) of SBOM from individual specimens

The isotopic differences between the methods are shown as an offset (Δ) of 10%HCl/EDTA values versus cation exchange results (zero line). If multiple specimens from the same species were analysed, the offset is shown as a mean with standard deviation (vertical bar)

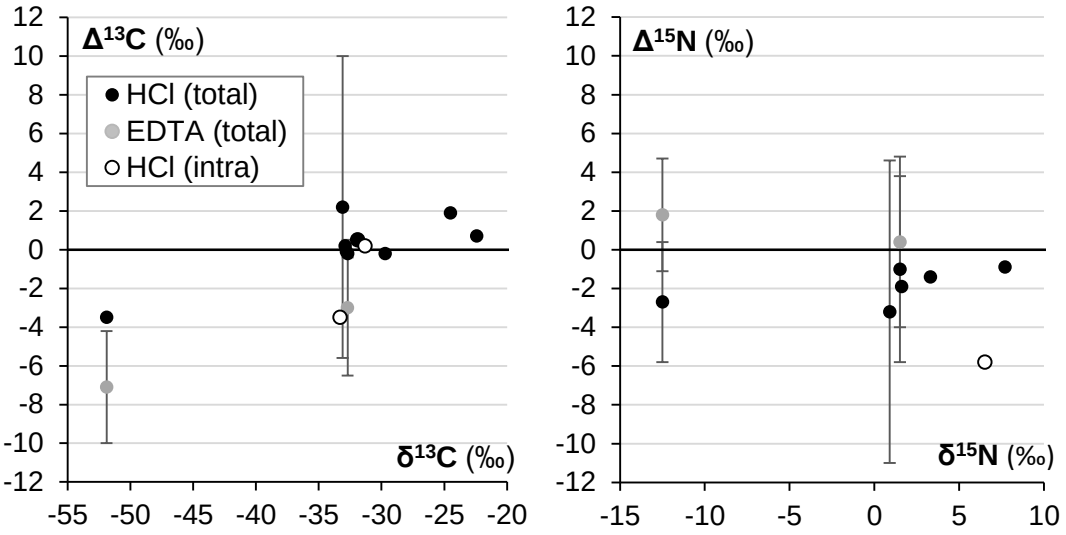

Isotopic effects on $\delta^{13}C$ and $\delta^{15}N$

The effect of cation exchange resin on the $\delta^{13}C$ composition of chemosymbiotic species is in agreement with the conclusions from Chapter 2, that show a slight depletion of 1-2‰ compared to the other methods, presumably caused by the incorporation of residual resin components with a value of $\delta^{13}C$ -29.2‰. In samples from this study (Fig. 3.2) the difference between 10%HCl and ion exchange resin values is non-existent for total SBOM values between $\delta^{13}C$ -35‰ to -30‰, presumably because these values are more similar to the resin value than those of heterotrophic filter feeders ($\delta^{13}C$ -21‰ to -16‰). For SBOM $\delta^{13}C$ -51.9‰ the enrichment (> 4‰) compared to 10%HCL/EDTA obtained samples is suggested to be caused by the residual resin. Particularly because the 10%HCl and EDTA samples are very similar ($\delta^{13}C$ +0.3‰ ±0.4, n=2). The isotopic effect of cation exchange resin on SBOM is unlikely to affect this study, because of the large isotopic differences in $\delta^{13}C$ between the nutritional strategies. Particularly because very depleted carbon values are presumably most strongly affected by resin, and that range of values will still be distinctly different from other nutritional strategies.

The depletion of EDTA values compared to resin/10%HCl for the $\delta^{13}C$ -32.7‰ sample could point to residual EDTA ($\delta^{13}C$ -39.0‰), although this effect was not found Chapter 2.

In Chapter 2 no statistical differences in $\delta^{15}N$ values were found between cation exchange resin obtained total SBOM samples and other shell removal techniques, and $\delta^{15}N$ variation was ~1‰. The same observations are made for this study (Fig. 3.2). The isotopic off-set between cation exchange resin samples and 10%HCL/EDTA is either < ±2‰ or highly variable. The use of cation exchange resin is therefore not expected to cause a consistent bias.

Very limited data is available for methodological differences in intra-crystalline SBOM for both $\delta^{13}C$ and $\delta^{15}N$, but the possible isotopic effects of cation exchange resin appear to be variable, which was also observed in Chapter 2. In this study cation exchange resin as well as 10%HCl have often been used to isolate SBOM for different specimens of the same species, and combining both methods per species will limit potential isotopic effects of either method.

Isotopic effects on $\delta^{34}S$

In Chapter 2 it was shown that SBOM isolated using cation exchange resin is influenced by a sulphur component from cation exchange resin, causing SBOM values to become more similar to the resin value ($\delta^{34}S$ -1.5‰) with increasing elemental concentrations of sulphur (%S). However, because the source of contamination is known it should still be possible to identify large isotopic difference between samples, until the original SBOM $\delta^{34}S$ signature is completely replaced with the resin value. Hypothetically, bivalves relying on seawater sulphate ($\delta^{34}S$ +20.3‰) should have signatures more positive than $\delta^{34}S$ -1.5‰, and bivalve using sulphide ($\delta^{34}S$ depleted up to -50‰) should have values more negative than $\delta^{34}S$ -1.5‰. To determine the thresholds at which $\delta^{34}S$ values and %S concentrations from these different sulphur sources can still be distinguished (and investigate the isotopic variation of cation exchange resin), total SBOM samples with known $\delta^{34}S$ values for soft tissues were divided into three distinct categories: 1) 10‰ to 20‰, 2) -10‰ to 0‰, and 3) -25‰ to -15‰, shown in Fig. 3.3. The data displayed in Figure 3.3 confirms the linear relationship between $\delta^{34}S$ and %S of total SBOM for the category 10-20‰ (R-squared: 0.46), but this is not evident for the other two categories (R-squared: 0.05 and 0.02). Based on Figure 3.3 it is not possible to distinguish intermediate values (-10‰ to 0‰) from the enriched (10‰ to 20‰) and depleted (-15‰ to -25‰) categories, because of overlap between the three

categories. Nutritional strategies with positive $\delta^{34}S$ values (relying on seawater sulphate) can only be identified with certainty for values above +3‰ (as intermediate negative values also display positive SBOM results) and represent soft tissues values up to 20‰. Nutritional strategies with negative sulphur values for soft tissues, can be identified below -3‰ (no more overlap with positive categories), more depleted values $\delta^{34}S$ based on hydrogen sulphide can be identified using resin total SBOM values below -5‰, and represent soft tissue values depleted up to -25‰. It is advised not to use SBOM samples with > 5% sulphur, as these show extremely depleted values for the 10-20 category. (These depleted values show that the value of resin can be lower than -1.5‰, although generally high concentration samples are around the -1.5‰ value). It was noted that smaller specimens often have higher %S, possibly because < 2 grams of shell material was used which increase the ratio of SBOM:resin. In general, Fig. 3.3 shows a large enrichment of the -25 to -15 and -10 to 0 categories, as well as a large depletion of the +10 to +20 categories for all total SBOM samples, seemingly unrelated to %S. This suggests that $\delta^{34}S$ of isolated SBOM does not closely reflect $\delta^{34}S$ of soft tissue values, which was also concluded in Chapter 2 and is further discussed in section 3.4.2.2.

In Figure 3.3 the $\delta^{34}S$ categories based on soft tissue values are compared for intra-crystalline SBOM, according to %S This graph show that it is not possible to distinguish any of the three categories for the majority of the samples. Only a very broad distinction can hypothetically be made between negative (< -2‰) and positive (> 2‰) $\delta^{34}S$ values of SBOM to indicate soft tissues values, for samples with %S lower than 5%. Likely the impact of resin is stronger on intra-crystalline SBOM because of the small amounts of SBOM, explaining why most samples fall around the resin values of -1.5‰ and many have high %S values.

Figure 3.3 Sulphur stable isotope comparison between soft tissues versus total SBOM and intra-crystalline SBOM for individual specimens

SBOM $\delta^{34}S$ values (isolated using cation exchange resin) are separated into three categories according to the $\delta^{34}S$ composition of associated soft tissue (ST) values. The $\delta^{34}S$ soft tissue range of the each category is shown as a box. The SBOM values are displayed according to their elemental concentration of sulphur (%S) The value of resin ($\delta^{34}S$ -1.5‰) is displayed as a dashed line. The plot shows that above 5%S in total SBOM the $\delta^{34}S$ value is dominated by the isotopic signal of cation exchange resin, below that concentration widely different sulphur sources can be identified.

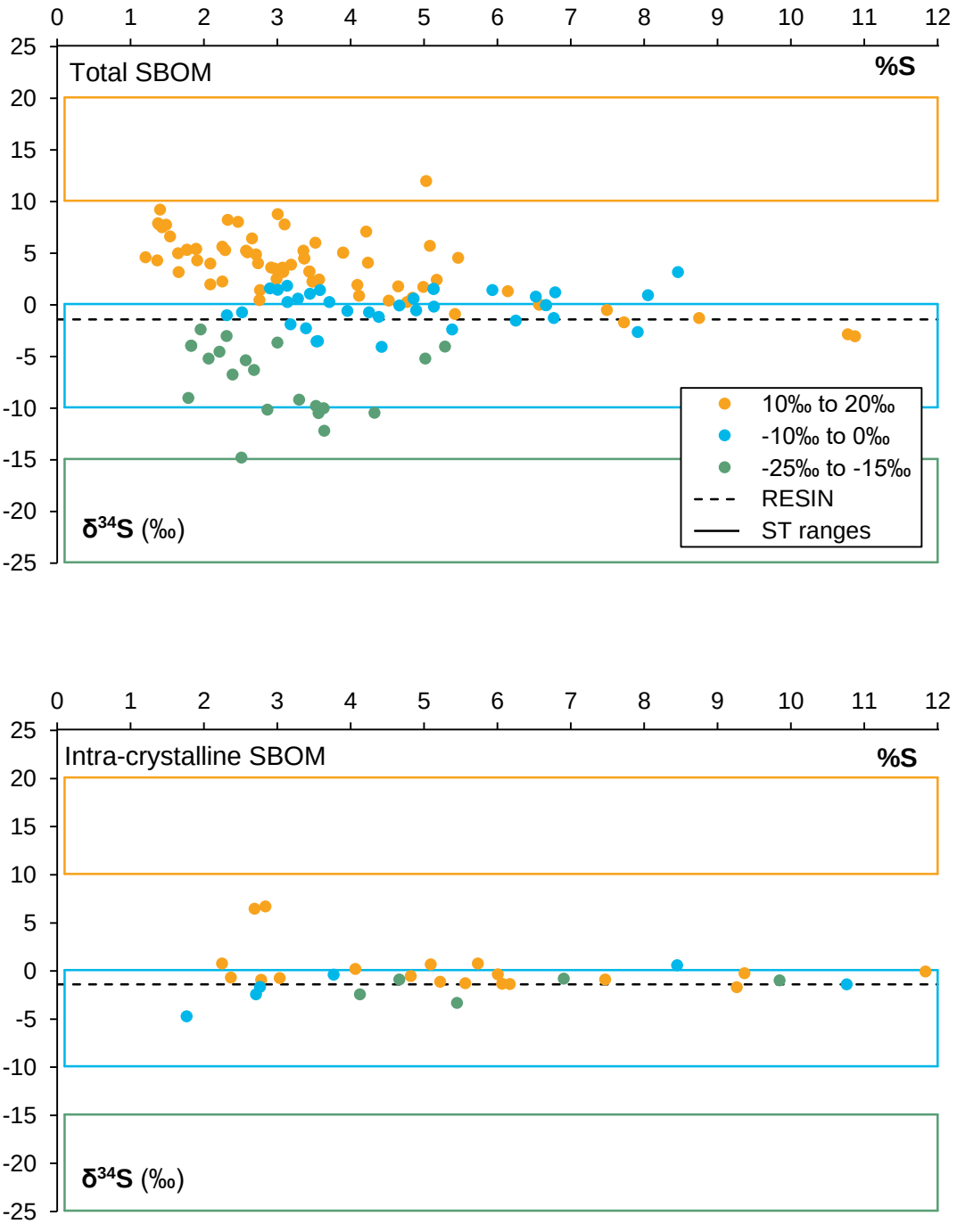

A comparison between the $\delta^{34}S$ total SBOM obtained using 10%HCl and EDTA from the same specimens of *Bathymodiolus childressi* and *Calyptogena ponderosa* is shown in Table 3.6. It should be noted that several very enriched EDTA $\delta^{34}S$ values (shown in Fig. 3.4) were excluded from further data analysis. These subsamples were noted to have a lighter colour than the majority of the total SBOM, and likely to represent intra-crystalline SBOM. For positive $\delta^{34}S$ total SBOM (*B. childressi*) shell removal using 10%HCl is accompanied by a large isotopic depletion: total SBOM obtained using EDTA is significantly enriched (+7.4‰ and +11.7‰) and more similar to published soft tissue values. This suggests that 10%HCl is removing a sulphur compound with enriched $\delta^{34}S$ values, which was also observed for several SBOM samples in Chapter 2. The higher elemental sulphur concentration in the 10%HCl samples in this study suggests that a sulphur poor compound (relative to the bulk %S) is removed, increasing the %S of the sample. The EDTA and 10%HCl methods report similar $\delta^{34}S$ values for the depleted total SBOM samples of *C. ponderosa*, and the difference in elemental concentration is smaller than for *B. childressi*.

Table 3.5 Method comparison of the sulphur stable isotope composition ($\delta^{34}S$) total SBOM from individual specimens, isolated using cation exchange resin, 10%HCl and EDTA

*Soft tissue values from previous studies, not directly measured from the specific samples analysed are obtained from Kennicutt II et al. (1992), Riekenberg et al., 2016, and Dattagupta et al. (2004).

Species	**Soft tissues**	**RESIN**	**HCl**	**EDTA**	**$\Delta_{HCl-EDTA}$**
B. childressi (GC233)	12.3* (mean, n=9)	+1.0‰ (3.9%)	-3.2‰ (1.7%)	+8.4‰ (0.7%)	**-11.7‰ (-59%)**
	-1.1 to 13.9* (10.3± 2.9, n=128)	+2.0‰ (2.7%)	+6.5‰ (2.0%)	+13.9‰ (0.5%)	**-7.4‰ (-75%)**
C. ponderosa (GC272)	-10 to +10* (n=7)	-4.2‰ (4.4%)	-6.0‰ (2.4%)	-5.6‰ (1.6%)	**-0.4‰ (-33%)**
		-1.0‰ (4.7%)	-6.0‰ (1.6%)	-4.6‰ (1.4%)	**-1.4‰ (-12.5%)**

Possible effects of liquid preservation and freeze drying

Several of the analysed specimens were preserved in liquid (ethanol, formalin), which theoretically could have an isotopic effect due to incorporation of lighter carbon of the preservatives or through extraction of organic compounds from tissues (Hobson et al., 1997). Reports about isotopic shifts in the tissues of bivalves and gastropods due to liquid preservation range from no observed systematic effect (Sarakinos et al, 2002) or small and predictable (DeLong and Thorp, 2009), to around or > 1 per mille difference for both carbon and nitrogen (e.g. Lui et al., 2013), particularly when formalin is used (e.g. Sarakinos et al., 2002; Carabel et al., 2009; Lui et al., 2013) The duration of liquid preservation generally does not seem to be of influence, as alterations happen in the early phase (Lui et al., 2013), possibly because an equilibrium is reached (Kaehler and Pakhomov, 2001). The extent of the shift appears to be species-specific (Lui et al., 2013; Kaehler & Pakhomov, 2001), and is unfortunately not known for our seep- and vent specimens. However, due to the large differences in carbon and nitrogen sources in deep-sea ecosystems, the relatively small influence of liquid preservation is unlikely to confound interpretations. Similarly, the effect of freezing (as part of the freeze-drying process, or long-term preservation) of soft tissues was reported by Lui et al. (2013) to be less than 1 per mille enrichment for both carbon and nitrogen.

Only one study compares SBOM obtained from dry-stored shells, compared to those preserved in ethanol for over 70 years. Versteegh et al. (2011) found a nitrogen depletion of -5.9 (+/- 2.2) per mille in the SBOM of ethanol-preserved shells, the effects of short-term storage are however not known.

3.3 Results

SBOM was successfully obtained from all species. SBOM obtained from *Bathymodiolus* species had a dark brown colour, whereas the SBOM from other specimens was generally light brown. Notable red and dark grey coloured SBOM was observed for the brachiopod genera *Terebratella* and *Notosaria*, respectively. The colours are similar to the shell colour of these brachiopods. The results from stable isotope analysis of SBOM, soft tissues and shell carbonate are shown in Fig. 3.4, and the isotopic relationships between SBOM and soft tissues are given in Table 3.6.

The stable isotope results are presented in the following order: isotopic system ($\delta^{13}C$, $\delta^{15}N$, $\delta^{32}S$), subdivided by environmental setting (cold seeps, hydrothermal vents, shallow reducing environments, shallow non-reducing environments), of which the isotopic data is discussed per nutritional strategy (methanotrophy, dual symbiosis, thiotrophy and/or heterotrophy), and furthermore by the different isotopic pools that were analysed (total SBOM, intra-crystalline SBOM, soft tissues, and/or shell carbonate). By presenting the data this way the analysed isotopic pools can be compared between nutritional strategies of the same locality, whereas the discussion of the results will mainly focus on broad differences between environmental settings.

For statistical comparisons the mean value of multiple isotopic measurements of SBOM/soft tissues were used. The mean soft tissue value was calculated using the mean values of the various soft tissues of individual specimens. If SBOM was obtained for individual specimens using multiple different methods, the reported isotopic data is a mean value of the results. Where $\delta^{34}S$ values of SBOM obtained using resin are used, this will be specifically mentioned.

Figure 3.4 $\delta^{13}C$, $\delta^{15}N$ and $\delta^{34}S$ values of SBOM, soft tissues and shell carbonate from analysed specimens

Results are presented per environmental setting:

A. Cold seep localities, samples include *Bathymodiolus* species
B. Cold seep localities, samples exclude *Bathymodiolus* species
C. Hydrothermal vent localities
D. Shallow reducing environments
E. Shallow non-reducing environments (brachiopod species)

Overview of the species and localities is given in Table 3.1 and Fig. 3.1, locality names are indicated in the plots were possible or given as abbreviations next to the species name. Symbol key is presented below, and each column represents an individual specimen (collated specimens are indicated in Table 3.1). $\delta^{34}S$ values obtained from SBOM samples isolated using cation exchange resin are not shown in the plots, but are reported in the text.

Local methane values are given in Table 3.2., references for soft tissue data for the Gulf of Mexico specimens: Dattagupta et al., 2004; Macavoy et al., 2008; Becker et al., 2010; Riekenberg et al., 2016.

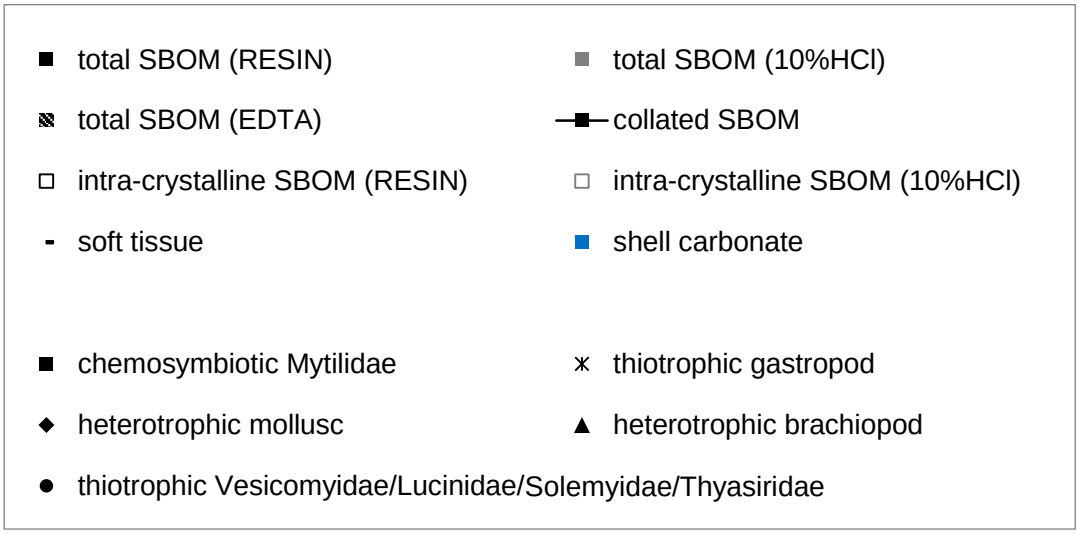

Figure 3.4A Cold seep localities, samples include *Bathymodiolus* species

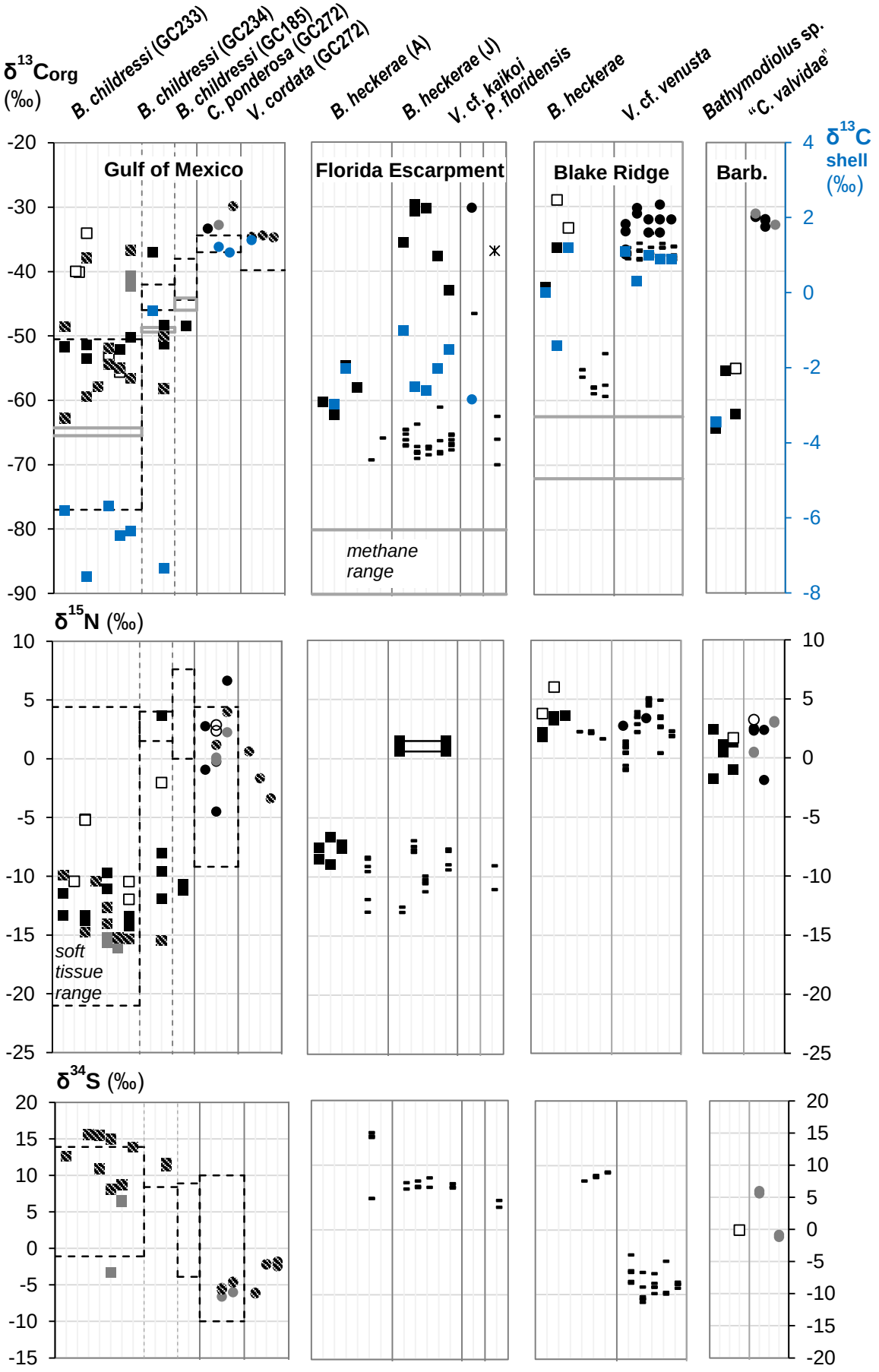

Figure 3.4B Cold seep localities, samples exclude *Bathymodiolus* species

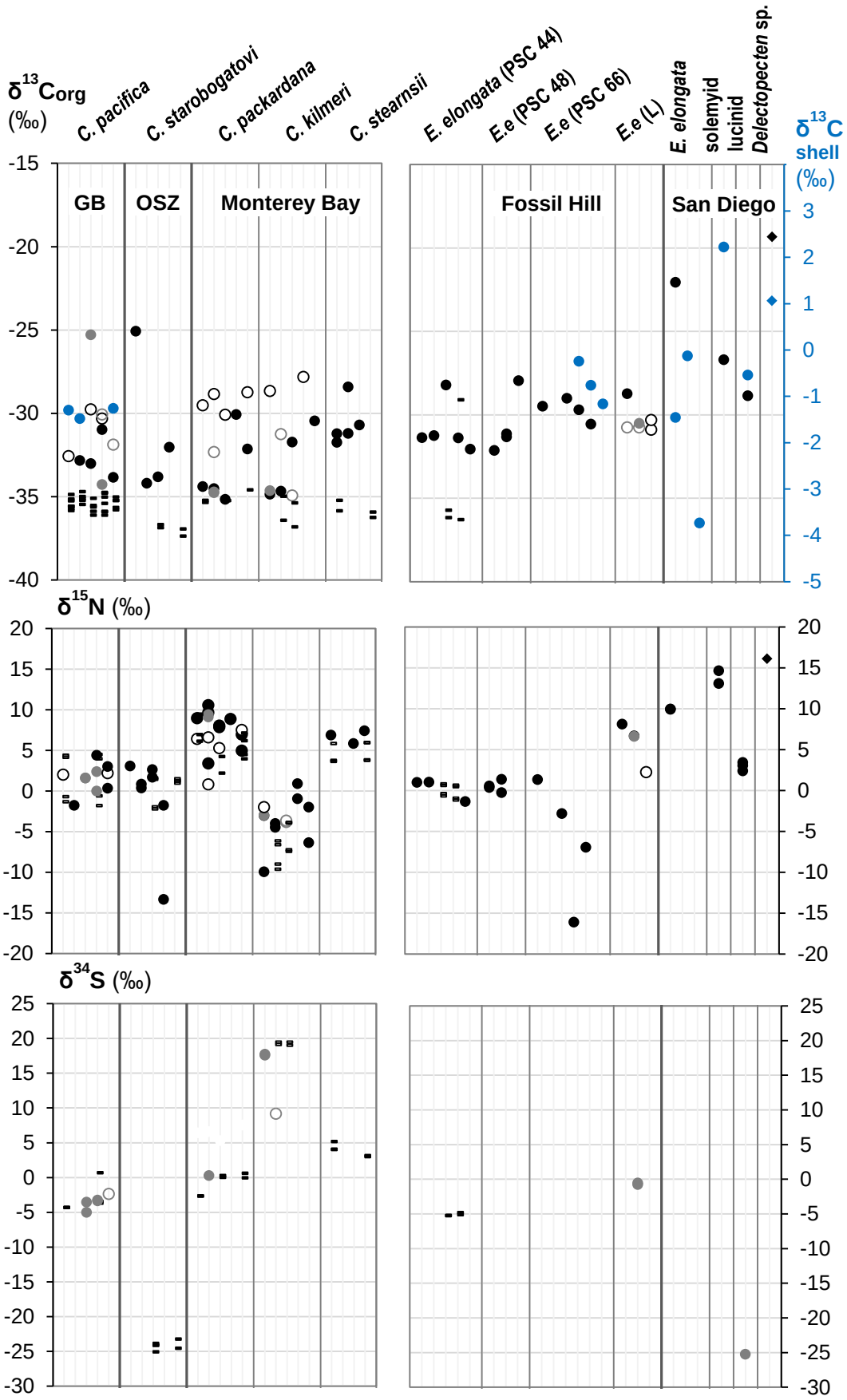

Figure 3.4C Hydrothermal vent localities

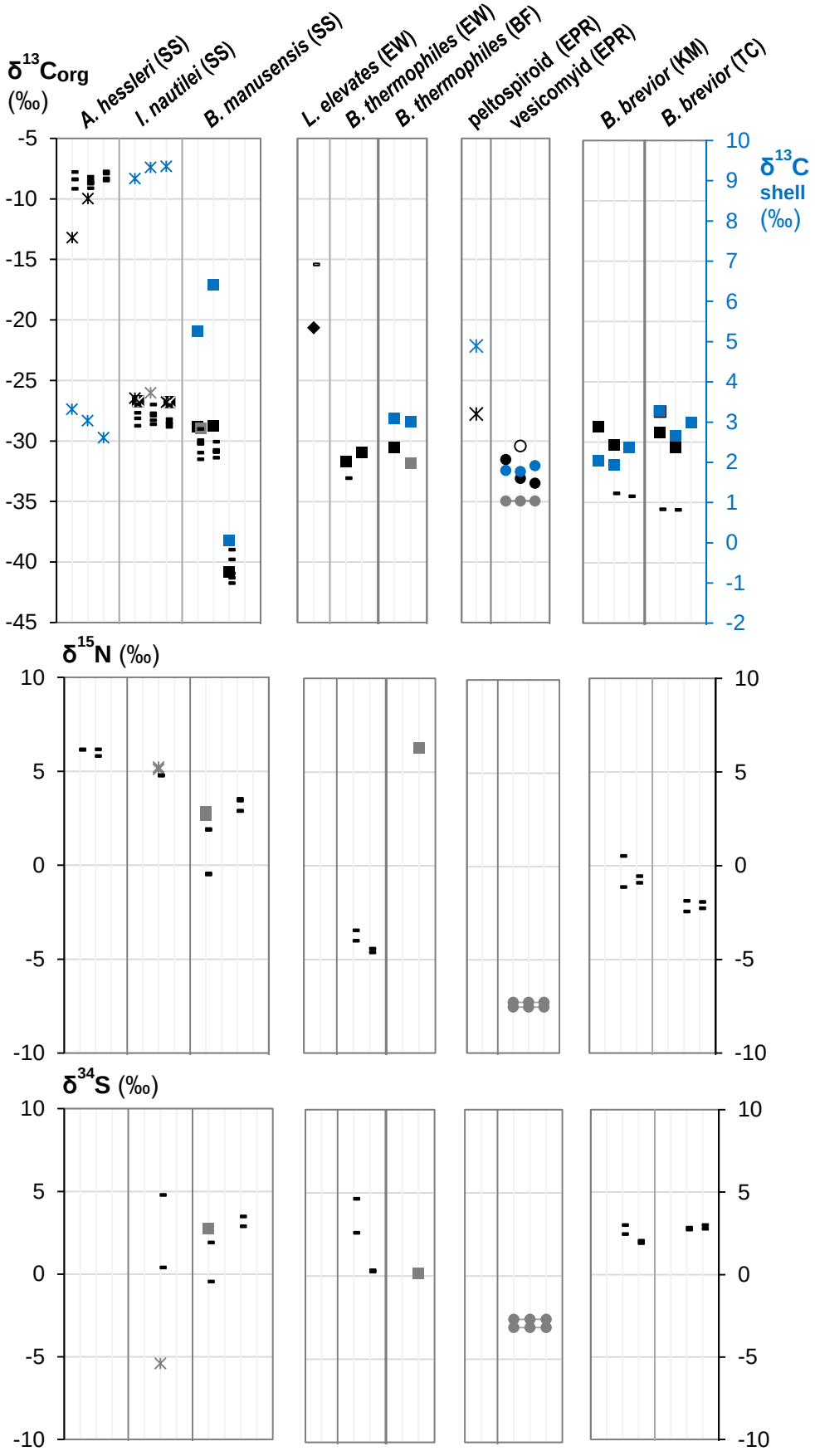

Figure 3.4D Shallow reducing environments

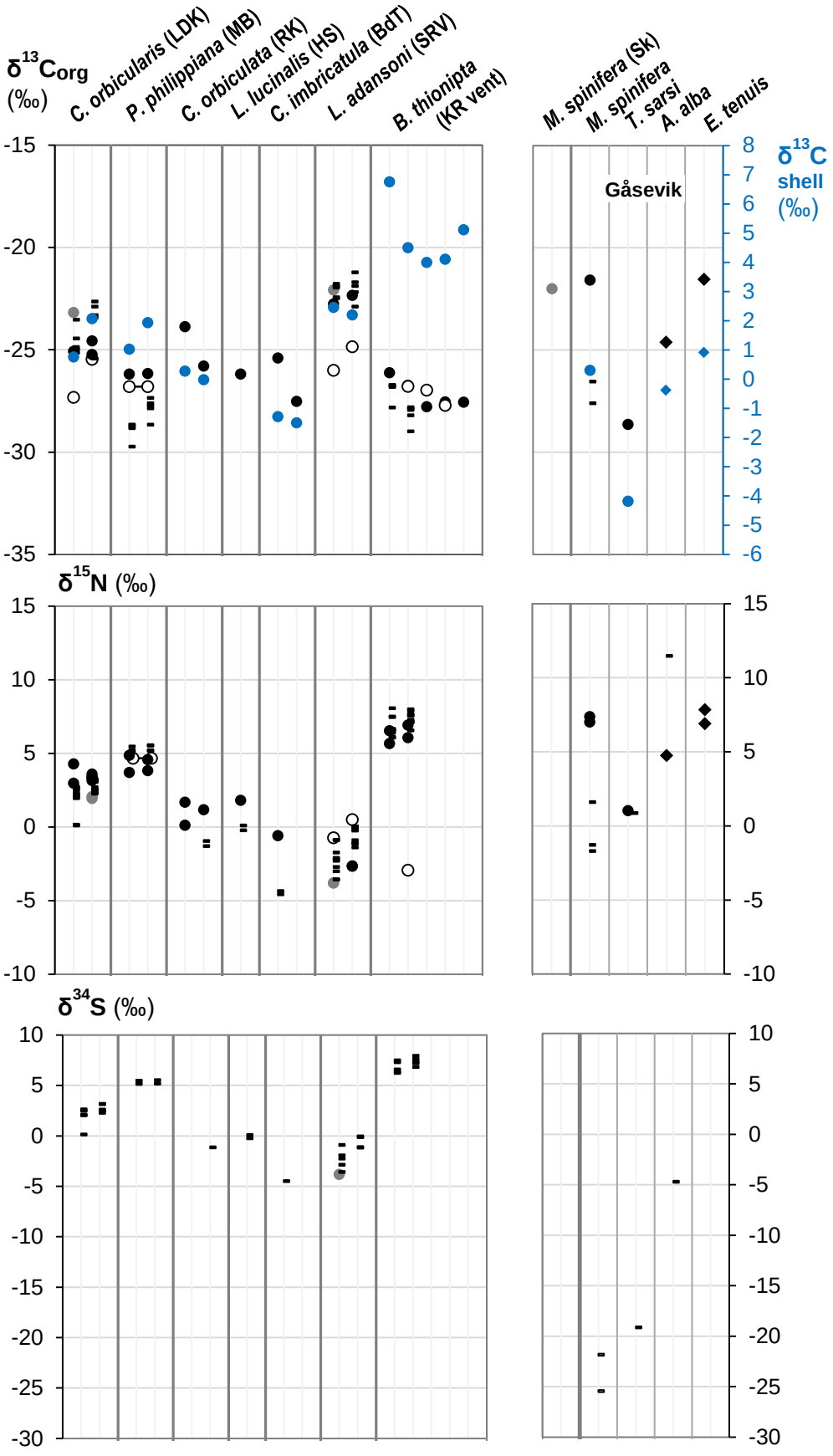

Figure 3.4E Shallow non-reducing environments

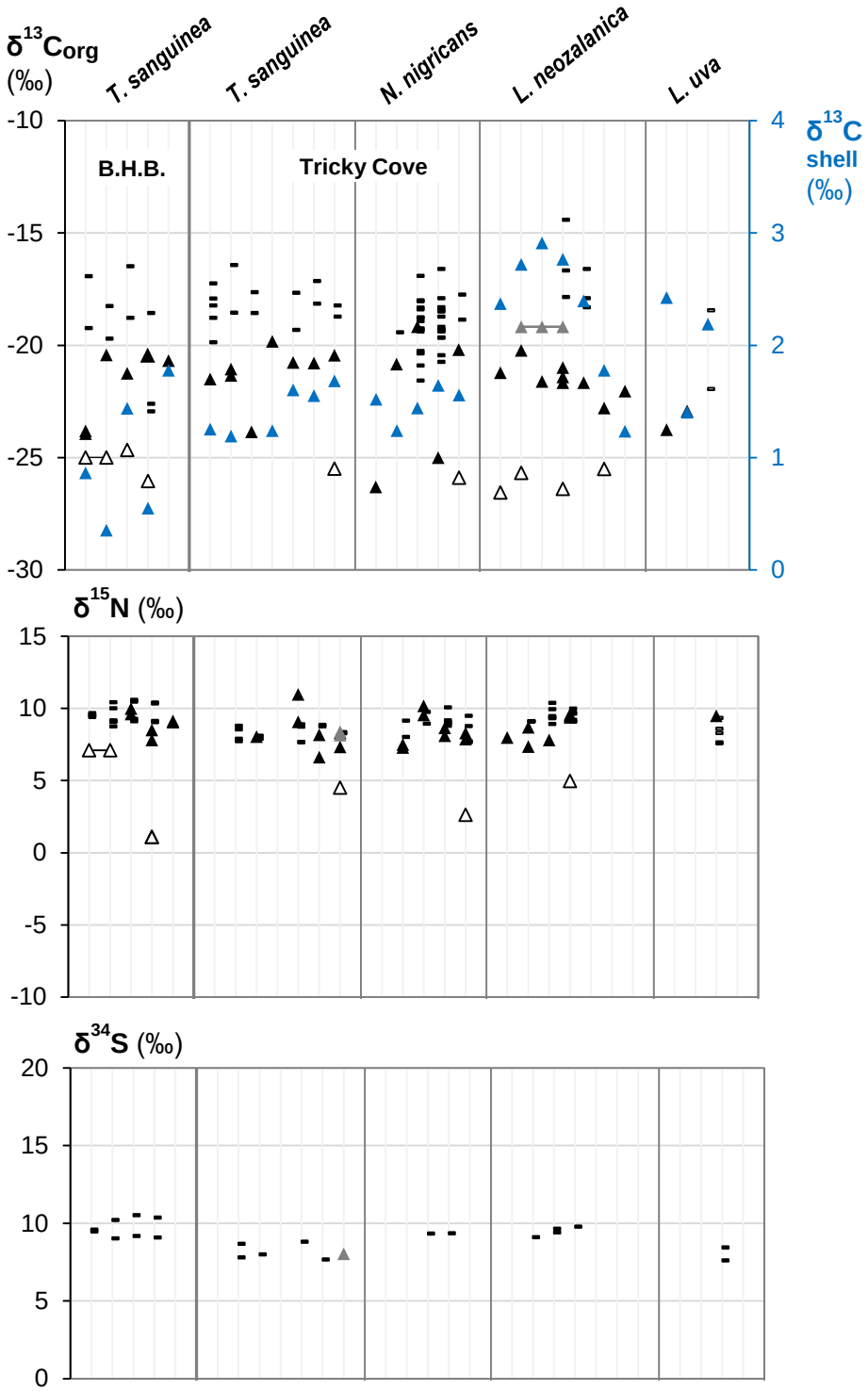

Table 3.6 Isotopic relationship between SBOM and various soft tissues

Individual SBOM values ($\delta^{13}C$, $\delta^{15}N$ and $\delta^{34}S$) are compared to related soft tissues, a positive value indicates that the SBOM is more enriched than the soft tissue. In addition, the gills and rest are compared to the other soft tissues (mantle, foot, and/or muscle), and the order of depletion amongst the soft tissues is given (from the most enriched to the more depleted value: g=gills, ma=mantle, f=foot, mu=muscle, r=rest). The mean soft tissue value of each specimen (mean value of all available soft tissue measurements) is also given, as well as the mean difference between SBOM and the mean soft tissue value between multiple specimens of the same species.

δ (‰)	total SBOM	mean soft tissue	Δ SBOM–gills	Δ SBOM–mantle	Δ SBOM–foot	Δ SBOM–muscle	Δ SBOM–rest	Δ gills–others	Δ rest–others	order of depletion
COLD SEEPS										
***B. heckerae*, juvenile (Florida Escarpment)**										
^{13}C	-35.6	-65.3	+30.1	+29.6	+28.9	+30.3		-0.5		f-ma-g-mu
	-42.9	-66.0	+22.3	+23.7	+22.5	+24.0		+1.1		g-f-ma-mu
	-30.2	-66.9	+33.5	+38.8	+36.9	+37.9		+4.5		g-f-mu-ma
	-30.2	-67.5	+38.2	+36.9	+36.9	+37.3		-1.1		f-g/ma-mu
	-37.7	-65.9	+23.3	+30.5	+30.2	+28.5		+6.5		g-mu-f-ma
	Δ+31.5 ±6.0		◄ *mean SBOM-soft tissue difference*							
^{15}N		-8.5						-1.4		ma-g
		-7.5								mu-f
		-10.4								f-ma
^{34}S		6.8						-0.6		ma-g
		6.8								f-mu
		7.3								f-ma
***V. venusta* (Blake Ridge)**										
^{13}C	-37.0	-37.2	+0.2	+0.2	+0.4	-0.1	+1.0	-0.0	-0.9	mu-ma/g-f-r
	-31.1	-37.2	+7.2	+7.2	+6.9	+5.6	+5.8	-1.4	-0.1	ma-mu-r-f-g
	-33.0	-36.2	+4.4	+4.4	+4.2	+1.1	+4.8	-1.5	-1.9	mu-ma-f-g-r
	-32.1	-36.2	+4.2	+4.2	+4.3	+3.6	+5.5	-0.2	-1.4	mu-ma/g-f-r
	-30.2	-37.6	+8.0	+6.0	+8.0	+8.0	+7.5	-0.8	1.3	r-ma-mu-f/g
	Δ +4.2 ±2.8									
^{15}N		0.5						-1.6	+0.6	r-f-ma-g
		4.8							+0.1	f-r-ma
		3.2						-0,6	-0,7	f-r-g
		2.0						-2,4	+1,4	r-f-ma-g
		2.0							+0,2	r/f, ma

δ (‰)	total SBOM	mean soft tissue	Δ SBOM–gills	Δ SBOM–mantle	Δ SBOM–foot	Δ SBOM–muscle	Δ SBOM–rest	Δ gills–others	Δ rest–others	order of depletion
^{34}S		-6.0						-4,2	-2,6	ma-r-g
		-8.2							-1,7	ma-f-r
		-9.7						-0,4	-2,1	f-g-r
		-7.3							-4,9	ma-r
		-8.4							-0,5	f-ma-r
***C. pacifica* (Guaymas Basin)**										
^{13}C		-35,4						+0.5	+0.8	r-g-ma-f/mu
	-32.8	-35,1	+2.2	+2.3	+2.6	+2.4	+1.9	+0.3	+0.6	r-g-ma-mu-f
	-29.1	-35,6	+6.5	+6.4	+6.7	+7.0	+5.9	+0.2	+0.7	r-ma-g-f-mu
	-32.6	-35,4	+2.1	+2.8	+3.2	+3.4	+2.4	+1.0	+0.8	g-r-ma-f-mu
	-33.8	-35,4	+1.9	+1.4	+1.8	+1.4	+1.2	-0.4	+0.4	r-ma/mu-f-g
	Δ +2.3 ±0.6									
^{15}N		1,6						-5.3		mu-g
	2.3	1,5	+3.5			-1.9		-5.4		mu-g
^{34}S	-3.3	-1.4	-4.2			+0.2		+4.2		g-mu
C. packardana										
^{13}C	-34.4	-35.4	+1.0			+0.8		-0.1		mu-g
	-35.1	-35.2	+0.1							
	-32.1	-34.6				+2.4				
	Δ +1.1 ±1.2									
^{15}N	9.0	8.0	-2.4			-0.4		-2.9		mu-g
C. starobogatovi										
^{13}C	-33.8	-36.8	+2.9			+3.1		+0.2		g-mu
		-37.1						+0.4		g-mu
^{15}N	2.2	-0.3	+3.2			+0.7		-3.6		mu-g
		1.2						-0.3		mu-g
^{34}S		-24.3						+0.6		g-mu
		-23.9						+1.3		g-mu
C. kilmeri										
^{13}C	-34.7	-35.7	+0.3			+1.8		+1.4		g-mu
	-31.7	-36.1	+3.7			+5.1		+1.4		g-mu
	Δ +2.7 ±2.5									
^{15}N	-4.2	-7.8	+5.1			+2.1		-3.0		mu-g
		-5.6						-3.4		mu-g

δ (‰)	total SBOM	mean soft tissue	Δ SBOM–gills	Δ SBOM–mantle	Δ SBOM–foot	Δ SBOM–muscle	Δ SBOM–rest	Δ gills–others	Δ rest–others	order of depletion
C. stearnsii										
^{13}C	-31.5	-35.5 -36.1	+4.4			-3.7		-0.6 -0.3		mu-g mu-g
^{15}N	6.9 7.4	4.8 4.9	+3.2 +3.6			+1.1 +1.5		-2.1 -2.2		mu-g mu-g
	Δ +2.3 ±0.3									
^{34}S		4.6 3.1						-1.1 -0.2		
E. elongata **(PSC44, Fossil Hill)**										
^{13}C	-28.2 -31.4	-35.9 -32.7	+7.9 +4.9	+7.5 -2.3				-0.4 -7.2		mu-g mu-g
	Δ +2.3 ±0.3									
^{15}N		0.1 -0.3						-1.2 -1.6		mu-g mu-g
HYDROTHERMAL VENTS										
B. thionipta										
^{13}C	-26.1 -26.7	-28.2 -27.0	+2.9 +1.1	+1.8 +0.0	+1.7 +0.0	+2.1 +0.1	+1.7 +0.1	-1.0 -1.1	+0.1 -0.1	f/ma-r/mu-g f-ma/r-mu-g
	Δ +1.1 ±1.3									
^{15}N	6.1 6.5	7.4 6.8	-1.2 -0.3	-0.3 -0.9	-1.4 -1.1	-0.5 -1.4	-0.2 -0.7	-0.8 -0.8	-0.9 -0.4	mu-ma-f-g-r mu-f-ma-r-g
	Δ -0.8 ±0.1									
^{34}S		-12.6 -6.2						+2.0 +11.9	+8.7 +5.9	r-ma-g-f-mu g-ma-r-f-mu
A. hessleri **(South Su)**										
^{13}C	-13.2 -10.0	-8.4 -8.7 -8.1	-4.8 -1.6	-4.8 -1.2	-5.4 -1.5		-4.1 -0.8	-0.3 +0.2 -0.7	-1.1 -0.5 -0.5	f-g/m-r f/g-m-r m-f-r-g
	Δ -3.0 ±2.5									
I. hessleri **(South Su)**										
^{13}C	-26.5	-27.9	+2.3	+1.2	+0.5		+1.7	-1.4	-0.8	f-ma-r-g
	-26.0	-27.7	+2.3	+1.0	+1.7		+1.9	-0.9	-0.6	ma-f-r-g
	-26.1	-28.2	+2.4	+2.4	+0.9		+2.5	-0.8	-0.9	f-ma/g-r
	Δ +1.7 ±0.4									

δ (‰)	total SBOM	mean soft tissue	Δ SBOM–gills	Δ SBOM–mantle	Δ SBOM–foot	Δ SBOM–muscle	Δ SBOM–rest	Δ gills–others	Δ rest–others	order of depletion
^{15}N	5.2	4.8	+0.4							
^{34}S	-5.4	-7.1	+1.7							
B. manusensis										
^{13}C	-28.9	-30.2	2.6	0.1	1.3	1.1	1.4	-1.8	-0.5	ma-mu-f/r-g
	-28.7	-30.8	2.7	2.0	1.3	2.1	2.2	-0.8	-0.4	f-ma-mu/r-g
	-40.8	-39.4	1.0	0.1	-1.8	-1.3	-4.8	-2.0	+3.8	r-f-mu-ma-g
	Δ +1.7 ±1.8									
^{15}N	2.8	1.4	+3.3			+0.9		-2.4		mu-g
								-0.6		mu-g
^{34}S	-8.1	-8.3	-0.8			+1.0		+1.8		g-mu
		2.0						+1.8		g-mu
***B. brevior* (Kilo Moana)**										
^{13}C	-30.2	-34.2	whole tissue							
***B. brevior* (Tow Cam)**										
^{13}C	-29.2	-35.6	whole tissue							
	-30.4	-35.6	whole tissue							
SHALLOW REDUCING ENVIRONMENTS										
C. orbicularis										
^{13}C	-24.1	-24.6	+0.9	+0.8	+0.3	+1.0	-0.6	-0.2	+1.3	r-f-g-ma-mu
	-23.5	-23.5	-2.2	-2.0	-1.6	-1.5	0.5	+0.6	-2.2	g-ma-f-mu-r
	Δ -0.7 ±0.4									
^{15}N	3.6	1.9	+1.6	+1.2	+1.6	+1.0	+3.5	-0.3	-2.3	mu-ma-f/g-r
	2.9	2.8	+0.6	-0.3	-0.3	+0.3	+0.4	-0.5	+0.4	mu/r-g-ma-f
	Δ +1.2 ±0.8									
^{34}S									-0.2	f-ma-r-mu
	-9.9	-16.2	+3.7	+2.5	+7.5	+11.5		+3.4		ma-g-f-mu
P. philippiana										
^{13}C	-26.2	-28.9	3.5	2.5	2.6	2.5	2.6	-1.0	-0.1	ma/mu-f/r-g
	-26.2	-27.8	2.5	1.2	1.6	1.4	1.7	-1.1	-0.3	ma-mu-f-r-g
	Δ +2.2 ±0.8									
^{15}N	4.3	5.3	-0.9			-1.2		-0.3		mu-g
	4.2	5.4	-1.3			-1.0		+0.3		g-mu

δ (‰)	total SBOM	mean soft tissue	Δ SBOM–gills	Δ SBOM–mantle	Δ SBOM–foot	Δ SBOM–muscle	Δ SBOM–rest	Δ gills–others	Δ rest–others	order of depletion
	Δ +1.1 ±0.0									
^{34}S		-20.4 -19.6						-1.5 +0.0		mu-g mu/g
C. orbiculata										
^{15}N	**1.2**	-1.1				+2.3				
L. lucinalis										
^{15}N	**1.8**	-0.1				+1.9				
C. imbricatula										
^{15}N	-0.6	-4.5				+3.9				
L. adansoni										
^{13}C	-22.4 -22.3	-22.1 -22.0	0.0 0.6	-0.5 -0.6	-0.6 -1.1	-0.5 -0.5	0.1 -0.1	-0.6 -1.3	-0.6 -0.6	f-ma-mu-g-r f-ma-mu-r-g
	Δ -0.3 ±0.0									
^{15}N	-3.8 -2.6	-2.3 -0.6	-0.2 -1.5	-1.6	-1.9 -2.5	-2.9 -2.5	-0.9 -1.5	-1.9 -1.1	-1.2 -1.0	mu-f-ma-r-g mu/f-r/g
	Δ -1.8 ±0.4									
^{34}S	-20.3	-15.6 -13.7	-5.8	-7.3	-1.7	-0.9	-7.9	+2.5	+4.6 +7.0	r-ma-g-f-mu r-ma-g-mu
***M. spinifera* (Gåsevik)**										
^{13}C		-27.1						-1.1		ma-g
^{15}N		0.1						-3.1		ma-g
^{34}S		-23.6						-3.6		ma-g
SHALLOW NON-REDUCING ENVIRONMENTS										
***T. sanguinea* (Big Hope Bay)**										
^{13}C	-23.9 -20.4 -21.2 -20.4	-18,1 -19,0 -17,4 -21,4	-4.6 -2.2 -3.0 2.5	 2.1		-6.9 -0.7 -4.8 -1.9		-2.3 1.5 -1.8 -2.4		mu-l l-mu mu-l mu-ma-l
	Δ -2.9 ±2.9									

δ (‰)	total SBOM	mean soft tissue	Δ SBOM–gills	Δ SBOM–mantle	Δ SBOM–foot	Δ SBOM–muscle	Δ SBOM–rest	Δ gills–others	Δ rest–others	order of depletion
^{15}N		9.5								ma-mu
		9.6						+1,2		l-mu
	9.8	9.9	-0.7			+0.6		+0.7		l-mu
	8.2	9.7	-2.2			-0.9		+1.3		l-mu
	Δ -0.8 ±1.1									
^{34}S		16.6								mu-ma
		17.0						+1.0		l-mu
		16.2						-1.2		mu-l
		16.0						+4.0		l-mu
***T. sanguinea* (Tricky Cove)**										
^{13}C	-21.5	-18.4	-2.7	-3.3	-4.3	-3.6	-1.6	-1.0	-2.1	p-mu-ma-l-r
	-17.5	-17.5	1.1			-1.1		-2.1		mu-l
	-23.9	-18.1	-5.3			-6.2		-0.9		mu-l
	-20.8	-18.5	-3.1			-1.5		1.6		l-mu
	-20.8	-17.6	-2.6			-3.7		-1.0		mu-l
	Δ -2.9 ±2.1									
^{15}N		8.2						+0.9		l-mu
	8.1	8.0				+0.1				
	10.0	8.2	+1.2			+3.3		+1.1		l-mu
	7.4	8.8				-1.4				
	Δ +0.1 ±1.6									
^{34}S		13.7						+0.4		l-mu
		16.6						+1.2		l-mu
N. nigricans										
^{13}C	-20.8	-19,4				-1.4				
	-19.2	-19,0	0.3	0.4	-1.2	-1.2	0.9	-0.9	-1.5	p/mu-l-ma-r
	-25.0	-19,1	-5.6	-5.7	-7.1	-6.5	-4.7	-0.9	-1.7	p-mu-ma-l-r
	Δ -2.5 ±3.0									
^{15}N	7.4	8.6				-1.2				
	9.9	9.3		+0.6						
	8.4	9.1		-1.0	-0.4	-0.8				ma-mu-p
	Δ -0.5 ±0.9									
^{34}S		15.6								p-ma

δ (‰)	total SBOM	mean soft tissue	Δ SBOM–gills	Δ SBOM–mantle	Δ SBOM–foot	Δ SBOM–muscle	Δ SBOM–rest	Δ gills–others	Δ rest–others	order of depletion
L. neozelanica **(Tricky Cove)**										
^{13}C	-21.7	-16.9				-4.7				
	-21.4	-16.7	-5.9			-3.6				ma-mu
	-22.0	-14.4	-3.7	-13.7		-5.4		-5.8		ma-mu-l
	Δ -5.7 ±1.7									
^{15}N	8.0	9.1				-1.1				
	7.8	9.5		-1.6		-1.8				mu-ma
	9.5	9.5		-0.3		+0.3				ma-mu
	8.0	9.6	-2.4	-1.1		-1.4		+1.0		l-mu-ma
		8.5						+1.4		l-mu-p
	Δ -1.1 ±0.8									
^{34}S		16.1								ma-mu
		12.0								ma-mu
								-1.0		mu-ma-l
L. uva **(Tricky Cove)**										
^{13}C	-21.9	-17.7	-3.5		-4.3	-5.0				mu-p-l
^{15}N		8.5						+1.4		l-mu-p
^{34}S		18.1						-2.6		p-l/mu

3.3.1 $\delta^{13}C$ of SBOM, soft tissues and shell carbonate

3.3.1.1 Cold seep: Green Canyon, Gulf of Mexico (Fig. 3.4A)

Bivalves harbouring methanotrophic symbionts

SBOM was obtained from *Bathymodiolus childressi* from three Green Canyon (GC) localities. $\delta^{13}C$ total SBOM values ranged from: -48.4‰ (GC185, n=1), -53.1‰ to -57.9‰ (GC233, n=6), and -52.6‰ to -37.0‰ (GC234, n=2). No statistical difference between GC233 (n=6) versus GC234 (n=2) exists, but when data from GC234 and GC185 (n=1) are combined the difference with GC233 is significant (p=0.0489). Intracrystalline SBOM $\delta^{13}C$ values have a range of -41.4‰ to -36.0‰ (GC233, n=4) and -34.8‰ (GC234, n=1). The total and intra-crystalline SBOM could be compared for several individuals, showing that the intra-crystalline pool mean value is +16.7‰ ±5.8 (n=4) enriched compared to total SBOM.

The $\delta^{13}C$ of shell carbonate ranged from -7.6‰ to -5.7‰ (GC233, n=4), and -0.5 to -7.3 (GC234, n=2), thus overlapping in isotopic ranges between localities. It should be noted that the most enriched total SBOM sample (-37.0‰) also has the most enriched shell carbonate value (-0.5‰).

Bivalves harbouring thiotrophic symbionts

Two thiotrophic vesicomyid clam species from GC272 were analysed. Total SBOM of *Calyptogena ponderosa* had $\delta^{13}C$ values ranging from -33.3‰ to -31.6‰ (n=3), and for *Vesicomya cordata* from -34.7‰ to -34.4‰ (n=3). The isotopic difference in total SBOM $\delta^{13}C$ between these two species is statistically significant (P=0.0250). A single intra-crystalline value (-29.2‰) of *C. ponderosa* could be compared to total SBOM (-33.1‰) of the same specimen, showing a +3.9‰ enrichment.

The $\delta^{13}C$ of shell carbonate for both species overlap in ranges, for *Calyptogena* values range 1.1‰ to 1.2‰ (n=2), and for *Vesicomya* from 1.0‰ to 1.4‰ (n=3).

Comparison between nutritional strategies at this locality

$\delta^{13}C$ total SBOM of methanotrophic *B. childressi* (-51.9 ±5.8‰, n=9, all sublocalities) is significantly depleted compared to thiotrophic *C. ponderosa* and *V. cordata* (-33.6‰ ±1.2, n=6), which is expected because *B. childressi* uses depleted methane as a carbon source. Similarly, $\delta^{13}C$ shell carbonate for the *Bathymodiolus* specimens (-5.7‰ ±2.4, n=7) is much more depleted than the two thiotrophic species (1.2‰ ±0.2, n=5). The singular intra-crystalline value of *C. ponderosa* (-29.2‰) is more enriched than the intra-crystalline SBOM values of *B. childressi* (-37.7‰ ±2.9, n=4), but cannot be statistically compared.

3.3.1.2 Cold seep: Florida Escarpment, Gulf of Mexico (Fig. 3.4A)

Bivalves harbouring dual symbionts

Bathymodiolus heckerae harbours both methanotrophic and thiotrophic symbionts, and both adult (max. length of 10.5 to 20.5cm) and juvenile specimens (circa 1.5 cm) of the species were investigated. $\delta^{13}C$ SBOM of both developmental stages is significantly different, the $\delta^{13}C$ total SBOM of adult *B. heckerae* ranges from -62.2‰ to -54.6‰ (n=4), whilst the juvenile specimens are circa +20‰ more enriched, showing values from -42.9‰ to -30.2‰ (n=5). Soft tissue $\delta^{13}C$ values from the two groups are however similar: -67.5‰ ±2.4 (adult, n=2) and -66.3‰ ±0.8 (juvenile, n=5). Shell carbonate $\delta^{13}C$ values also do not show a statistical difference between the two age groups: -2.5‰ ±0.7 (adult, n =2) and -1.9‰ ±0.7 (juvenile, n=5).

The soft tissues analysed for adult *Bathymodiolus* could not be related to individual specimens, but for the overall group total SBOM (-58.7‰ ±3.3, n=4) is on average +8.8‰ more enriched than soft tissues (-67.5‰ ±2.4, n=2). It was possible to make individual comparisons for the juvenile specimens, this showed that their total SBOM is +31.0‰ ±6.0 (n=5) enriched compared to the soft tissues of the specimens. Because of this extreme offset the isotopic relationship between different soft tissues of individuals and individual SBOM values will not be further discussed. A comparison between the different soft tissues of individual specimens did not reveal clear trends, although it should be noted that in the majority of specimens the gills are the most enriched tissue of the animals (3 out of 5).

Bivalves harbouring thiotrophic symbionts

For the analysis of the very small *Vesicomya* cf. *kaikoi* specimens from Florida Escarpment it was necessary to collate multiple specimens. The $\delta^{13}C$ total SBOM value of the species was -30.2‰, whilst the soft tissues had a much more depleted value of -46.5‰. The $\delta^{13}C$ shell carbonate value of the species was -2.8‰.

Heterotrophic limpet

Specimens from the small limpet species *Paralepetopsis floridensis* had to be collated to obtain sufficient total SBOM, this analysis gave a total SBOM $\delta^{13}C$ value of -36.8‰. The collated soft tissues of the specimens were ~30‰ more depleted in $\delta^{13}C$ than the total SBOM (-66.1‰ ±3.7, n=3), and the species had a shell carbonate value of $\delta^{13}C$ -8.3‰.

Comparison between nutritional strategies at this locality

The $\delta^{13}C$ total SBOM values of dual symbiotic *Bathymodiolus* (adult, -58.7‰ ±3.3, n=4) are distinct from thiotrophic *Vesicomya* (-30.2‰) and heterotrophic *Paralepetopsis* (-37.7‰), because *B. heckerae* harbours both thiotrophic and methanotrophic bacteria, of which the latter use depleted methane as a carbon source. *Vesicomya* and *Paralepetopsis* do however have overlap in value with the $\delta^{13}C$ total SBOM range of juvenile *Bathymodiolus* specimens (-35.3‰ ±5.4, n=5). When comparing soft tissue values, there is no statistical difference between adult *Bathymodiolus* (-67.5‰ ±2.4), juvenile *Bathymodiolus* (-66.3‰ ±0.9) and *Paralepetopsis* (-66.1‰ ±3.7), but thiotrophic *Vesicomya* (-46.5‰) is more enriched. The $\delta^{13}C$ shell carbonate value of juvenile and adult *Bathymodiolus* (-2.1‰ ±0.7, n=7) is similar to *Vesicomya* (-2.8‰), whilst the shell carbonate of *Paralepetopsis* is much more depleted than the other chemosymbiotic species at -8.3‰. Due to the limited amount of SBOM/shell carbonate measurments of

Vesicomya and *Paralepetopsis* it was not possible to make any statistical comparisons between different nutritional strategies for those isotopic pools.

3.3.1.3 Cold seep: Blake Ridge (Fig. 3.4A)

Bivalves harbouring dual symbionts

$\delta^{13}C$ total SBOM of dual symbiotic *B. heckerae* ranged from -42.4‰ to -36.4‰ (n=2), and intra-crystalline SBOM from -33.3‰ to -29.0‰ (n=2). The isotopic difference between these two SBOM pools is not statistically significant (P=0.1549), but comparison between total and intra-crystalline SBOM for one individual specimen showed an enrichment of +7.4‰ in the latter.

Whole tissues of *B. heckerae* specimens had a mean $\delta^{13}C$ value of -56.8 ±1.4 (n=3). These could not be compared to individual SBOM values, but mean total SBOM (-39.4‰ ±4.3, n=2) is +17.4‰ heavier than the soft tissues.

The $\delta^{13}C$ value of shell carbonate varied between -1.4‰ and 1.2‰ (n=3).

Bivalves harbouring thiotrophic symbionts

Total SBOM, soft tissues and shell carbonate were analysed for five thiotrophic *V. venusta* specimens (size of circa 1.5 cm). The total SBOM $\delta^{13}C$ values for this species ranged from –37.0‰ to -30.2‰ (n=5). Individual comparison between total SBOM and mean soft tissue values (combined mean*:* $\delta^{13}C$ -36.9‰ ±0.6, n=5) of the specimens showed that SBOM is always more enriched, but very variable (range: +0.2 to +7.4, mean is +4.2 ±2.8, n=5). Because of this variation the isotopic relationship between SBOM and specific soft tissues will not be further discussed.

Comparison of $\delta^{13}C$ from different soft tissues of the individual specimens revealed that the gills (5 out of 5, -0.8‰ ±0.7, n=5) and rest (4 out of 5, -0.6‰ ±1.3, n=5) are more depleted than the other tissues (*mean value of mantle and/or foot and/or muscle*). Muscle is the most ^{13}C enriched tissue in the majority of the specimens (3 out of 5), the mantle tissue is either most or second most enriched tissue in these specimens.

Shell carbonate $\delta^{13}C$ values of *V. venusta* ranged from 0.3‰ to 1.1‰ (n=5).

Comparison between nutritional strategies at this locality

Total SBOM $\delta^{13}C$ from dual symbiotic *Bathymodiolus* (-39.4‰ ±4.3, n=2) is significantly more depleted than thiotrophic *V. venusta* (-32.7‰ ±2.6, n=5, p=0.0452) by -6.7‰, because *Bathymodiolus* partly relies on depleted methane. The difference between the soft tissue values of the two species (-56.8‰ ±1.4, n=3

and -36.9 ±0.6, n=5, resp.) is however much larger (19.9‰) and significant (p=<0.0001). The $\delta^{13}C$ shell carbonate of *V. venusta* (-0.8 ±0.3, n=5) is not statistically different from *B. heckerae* (-0.1 ±1.3, n=3), but carbonate values are much more variable in the dual symbiotic species.

3.3.1.4 Cold seep: Barbados (Fig. 3.4A)

Bivalves with unknown nutritional strategy

Currently the nutritional strategy of *Bathymodiolus* sp. (circa 10cm. length) from Barbados is unknown. The $\delta^{13}C$ total SBOM of this species ranged from -64.4‰ to -55.4‰ (n=3), a single intra-crystalline SBOM sample had a value of -55.1‰. Comparison at the individual specimen level showed that the intra-crystalline value was +7.1‰ more enriched than the total SBOM. The $\delta^{13}C$ shell carbonate of one specimen was measured: -3.4‰.

Bivalves harbouring thiotrophic symbionts

Thiotrophic *Calyptogena valvidae* has a $\delta^{13}C$ total SBOM range of -32.4 to -31.4. No intra-crystalline measurments are available for this species. A single shell carbonate $\delta^{13}C$ value was reported at 1.3‰.

Comparison between nutritional strategies at this locality

Total SBOM of *Bathymodiolus* of unknown nutritional strategy ($\delta^{13}C$ -60.7 ±4.7, n=2) is on average -28.8‰ more depleted than thiotrophic *C. valvidae* (-31.9 ±0.5, n=3), and therefore partly or completely relies on a more depleted carbon source, probably methane. The shell carbonate $\delta^{13}C$ measurement of *Bathymodiolus* is -4.7‰ more depleted than the measurement of *Calyptogena*, but due to the limited amount of data they cannot be statistically compared.

3.3.1.5 Cold seep: Guaymas Basin (Fig. 3.4B)

Bivalves harbouring thiotrophic symbionts

Specimens of thiotrophic *Calyptogena pacifica* (4.0-4.5 cm) were analysed for individual total SBOM, intra-crystalline SBOM, shell carbonate and soft tissue $\delta^{13}C$ values. $\delta^{13}C$ total SBOM values ranged from -33.8‰ to -29.1‰ (n=4), with a mean total SBOM value of -33.1‰ ±0.5 (n=4).

$\delta^{13}C$ for intra-crystalline SBOM ranged from -32.6‰ to -29.8‰, and the two SBOM pools are statistically different (p=0.0162). Comparison between total and intra-

crystalline SBOM for individual specimens showed that the latter pool is -2.6‰ ±0.7 (n=4) enriched. Soft tissues values of the individual specimens have a very limited $\delta^{13}C$ range from -35.6‰ to -35.1‰, that is significantly depleted by -2.5‰ (p= <0.0001) compared to mean total SBOM. For the individual SBOM-soft tissue relationships of specimens a similar depletion of -2.3‰ ±0.6 (n=4) was found.

Investigation into the isotopic relationship between individual total SBOM and individual soft tissues (n=4) (Table 3.6) revealed that gill tissue to be the least variable (SBOM-tissue difference: +2.2 ±0.3) and muscle tissue to be most variable (+2.6 ±0.9), with the other tissues showing intermediate values, for both SBOM-soft tissue difference and variation. Comparison between the different tissues shows that gills are generally enriched compared to the other tissues (4 out 5, +0.3‰ ±0.5) and rest is always more enriched (5 out of 5, +0.6‰ ±0.2), the muscle tissue is generally most depleted (3 out of 5).

Shell carbonate $\delta^{13}C$ values of *C. pacifica* fall within a narrow range from -0.9‰ to -0.7‰ (n=3).

3.3.1.6 Cold seep: Oregon Subduction Zone (Fig. 3.4B)

Bivalves harbouring thiotrophic symbionts

$\delta^{13}C$ total SBOM of thiotrophic *Calyptogena starobogatovi* ranged from -34.2‰ to -32.0‰ (n=3), with one more enriched value of -25.1‰. Mean soft tissue values were -37.1‰ and -36.8‰ (n=2), with soft tissues being on average -5.7‰ depleted. For one specimen the total SBOM and mean soft tissue value could be individually compared, revealing a more limited depletion of -3.0‰.

A comparison between the $\delta^{13}C$ values of gills and muscle tissue for two specimens showed that the gills are most enriched (+0.2 and +0.4) out of these two tissues.

3.3.1.7 Cold seep: Monterey Bay (Fig. 3.4B)

Bivalves harbouring thiotrophic symbionts

Three thiotrophic vesicomyid species from Monterey Bay were analysed. Total SBOM $\delta^{13}C$ values for *Calyptogena packardana* range from -35.1‰ to -30.1‰ (n=5), for *Calyptogena kilmeri* from -34.7‰ to -30.4‰ (n=4), and for *Calyptogena stearnsii* from -31.5‰ to -29.8‰ (n=3). $\delta^{13}C$ values for intra-crystalline SBOM of the three species range from -30.6‰ to -29.5‰ (n=4) for *C. packardana*, and from -34.9‰ to -27.8‰ (n=4) *C. kilmeri*. $\delta^{13}C$ values of soft tissues for *C. packardana*

range from -35.3‰ to -34.6‰ (n=3), from -36.1‰ to 35.7‰ (n=2) for *C. kilmeri*, and from -36.1‰ to -35.5‰ (n=2) for *C. stearnsii*. There is not statistical difference between the three species in $\delta^{13}C$ of total SBOM, intra-crystalline SBOM, or soft tissue values.

For *C. kilmeri* $\delta^{13}C$ total (-32.9‰ ±2.2, n=4) and intra-crystalline (-30.7‰ ±3.2, n=4) SBOM are not statistically different. This is also reflected in the total-intra SBOM relationship of the individual specimens, showing that the intra-crystalline SBOM can be both more depleted (-6.1‰ and -3.5‰), as well as more enriched (+3.2‰) than the total SBOM values. Total SBOM of *C. kilmeri* was more enriched than the related soft tissue mean (+1.0 and +4.4). Isotopic comparison between the gill and muscle tissue showed that the latter is always more depleted (+1.4 and +1.4).

Intra-crystalline SBOM $\delta^{13}C$ of *C. packardana* (-29.7‰ ±0.8, n=4) is statistically more enriched than the total SBOM (-33.3‰ ±2.1, n=5) of the species. For individual specimens the isotopic difference between the two pools is +4.4‰ ±0.8 (n=4). There is no statistical difference between mean total SBOM and soft tissues $\delta^{13}C$ values, but by comparing this for individual specimens it is shown that total SBOM is always more depleted (-2.4‰ to -0.1‰, n=3). Due to the limited amount of soft tissue data no further conclusions can be drawn about the different soft tissues.

C. stearnsii soft tissue $\delta^{13}C$ values (-35.8 ±0.4, n=2) are significantly depleted compared to total SBOM values (-30.7 ±0.8, n=3), with p=0.0040. This depletion could be determined for on individual specimen at -4.1‰.Further comparison between the different soft tissue showed that gills are more enriched than muscle tissue (+0.3‰ and +0.6‰).

3.3.1.8 Cold seep: Fossil Hill (Fig. 3.4B)

Bivalves harbouring thiotrophic symbionts

Ectenogena elongata specimens from several different push cores (PSC) at Fossil Hill were analysed (4-5cm), as well as larger broken (older?) pieces of the species, to investigate whether small-scale isotopic differences in SBOM exist at a single locality. $\delta^{13}C$ total SBOM of *E. elongata* ranged from -32.1‰ to -28.2‰ (PSC44, n=5), -32.1‰ to -28.0‰ (PSC48, n=3), -30.6‰ to -29.0‰ (PSC66), and -30.5‰ to -28.7‰ (broken, n=2). No statistical difference exists in $\delta^{13}C$ values of total SBOM between the four different sub-localitites of Fossil Hill, and the data can be combined for comparisons between localities (-30.3‰ ±1.5, n=13).

Gills and muscle tissue of two *E. elongata* specimens from PSC44 were analysed, this gave mean soft tissue values of $\delta^{13}C$ -35.9‰ and -32.7‰. Individual SBOM-soft tissue comparison shows that the total SBOM is always more enriched than soft tissues by +4.5‰ ±4.5 (n=2). The large variation in this isotopic relationship is caused by one very enriched muscle tissue measurment (-29.1‰). When excluding this outlier, the mean difference between all total SBOM (-30.9‰ ±1.5, n=5) and all soft tissues (-36.1‰ ±0.2, n=2) is +5.2‰.

$\delta^{13}C$ shell carbonate of *E. elongata* from PSC66 ranged from -1.2‰ to -0.2‰ (n=3).

Intra-crystalline $\delta^{13}C$ values of SBOM from larger *E. elongata* specimens had a narrow range, from -30.7‰ to -30.6‰ (n=3). The difference between all total SBOM (-29.6 ±1.3, n=2) and all intra-crystalline SBOM (-30.7 ±0.1, n=3) is a +1.1‰ enrichment in total SBOM. For individual specimens this enrichment is also +1.1‰ (±1.3, n=2).

3.3.1.9 Cold seep: San Diego Trough (Fig. 3.4B)

Thiotrophic bivalves from the cold seep localitites described thus far all belong to the family Vesicomyidae. At San Diego Trough it was possibly to also analyse single specimens from the thiotrophic families Solemyidae (solemyid) and Lucinidae (lucinid).

Bivalves harbouring thiotrophic symbionts

From each thiotrophic species only a single specimen could be analysed, these show $\delta^{13}C$ total SBOM values of -22.1‰ (*E. elongata*), -26.7‰ (solemyid) and -29.1‰ (lucinid), the large variation between the species is evident from a standard deviation of ±3.6‰ on these values.

The $\delta^{13}C$ shell carbonate values of *E. elongata* ranged from -3.7 to -0.1. The other two thiotrophic species had values of 2.2‰ (solemyid) and -0.5‰. (lucinid). The variation on mean values of the three species is ±2.0‰.

Total SBOM was obtained from lucinid using resin as well as HCl, the variation between obtained $\delta^{13}C$ values with a variation of ±0.3‰.

Heterotrophic bivalves

Total SBOM of *Deltopecten* had an ‰ value of -19.3‰ (n=1), the $\delta^{13}C$ shell carbonate value of the specimen was 1.1‰.

Comparison between nutritional strategies at this locality

Despite the large isotopic differences between the thiotrophic species (-26.0 ±3.6, n=3), the mean difference with heterotrophic *Deltopecten* (-19.3‰) shows a +6.7‰ enrichment in total SBOM ‰ for the latter species. This difference is expected because *Deltopecten* relies on enriched photosynthetically derived material, which is generally much more enriched in ^{13}C and ^{15}N than chemosynthetically derived material at colds seeps (McAvoy, 2008).

The $\delta^{13}C$ shell carbonate value from *Deltopecten* (1.1‰) falls within the variation of the mean thiotrophic shell carbonate value (-0.7 ±2.2, n=5).

3.3.1.10 Hydrothermal vent: South Su (Fig. 3.4C)

Gastropods harbouring thiotrophic symbionts

Two chemosymbiotic gastropod species are present at South Su: *Alviniconcha hessleri* and *Ifremeria nautilei*. The total SBOM $\delta^{13}C$ values for *A. hessleri* vary between -13.2‰ to -10.0‰ (n=2) and soft tissues between -8.7‰ and -8.1‰ (n=3). Statistically $\delta^{13}C$ of total SBOM and soft tissues are not different, but individually the SBOM is always more depleted (-4.8‰ and -1.3‰). Shell carbonate values range from 2.6‰ to 3.3‰ (n=3).

I. nautilei has a total SBOM range from -26.5‰ to -26.0‰ (n=3), intra-crystalline SBOM from -26.8‰ to -26.7‰ (n=2), and soft tissues from -28.2 to -27.7. These organic pools are all statistically different from each other. For individual specimens, total SBOM is in comparison between +0.3‰ and +0.7‰ (n=3) more enriched than intra-crystalline SBOM, and between +1.4‰ and +2.0‰ (n=3) more enriched than mean soft tissue values. Comparison between the different soft tissues shows that the gills (-1.0‰ ±0.4, n=3) and rest (-0.7‰ ±0.4, n=3) are always more depleted than the other tissues. Shell carbonate values of *Ifremeria* range from 9.0‰ to 9.3‰ (n=3).

Statistical comparison between shows that *Ifremeria* is significantly more enriched than *Alviniconcha* in $\delta^{13}C$ total SBOM (mean: +14.6‰, p=0.0013) and soft tissues (mean: +19.5‰, p=0.0037), and more depleted for $\delta^{13}C$ shell carbonate (mean: -6.2‰, p=<0.0001).

Bivalves harbouring thiotrophic symbionts

Thiotriophic *B. manusensis* from South Su shows large variation in total SBOM $\delta^{13}C$ values: -40.8‰, -28.9‰, and -28.7‰, the same variation in also found in related

soft tissue $\delta^{13}C$ values of the specimens: -39.4‰, -30.2‰, and -30.8‰, (individual $\Delta_{SBOM\text{-}soft\ tissue}$: 0.7‰ ±1.8, n=3), as well as the shell carbonate $\delta^{13}C$: 0.0‰, 5.2‰ and 6.4‰, respectively.

The value of a single intra-crystalline SBOM value sample was -27.9‰, showing an +0.8‰ enrichment compared to the total SBOM of that specimen.

Comparison between the different soft tissues shows that the gill tissue has the least variation in $\Delta_{SBOM\text{-}soft\ tissue}$ (+2.1‰ ±1.0, n=3), and is always more depleted compared to the other tissues (-1.5‰ ±0.6, n=3).

Comparison between nutritional strategies at this locality

The large isotopic differences between *Alviniconcha* and *Ifremeria* were discussed above. Similar enrichment in *Ifremeria* compared to *Bathymodiolus* was found in the $\delta^{13}C$ values of total SBOM (+21.2‰, p=0.0072) and soft tissues (+25.1‰, p=<0.0011). But where the shell carbonate values of *Ifremeria* was statistically depleted (-6.2‰), the values of *Bathymodiolus* (3.9‰, ±3.4, n=3) and *Alviniconcha* (3.0‰, ±0.4) are similar (p=0.6275), unless the depleted outlier is removed (depletion of -2.8‰ in *Ifremeria*, p=0.0123).

Mussel *Bathymodiolus* and gastropod *Ifremeria* are similar in $\delta^{13}C$ total SBOM (p=0.1731, n=3), but when the depleted outlier (-40.8‰) of *Bathymodiolus* is removed they are statistically different (-28.8‰ ±0.1, n=2 versus -26.2‰ ±0.2, n=3, resp., p=0.0005). The same applies for the shell carbonate values (*included* p=0.0544, and *excluded* p=0.0047). Soft tissues of *Bathymodiolus* (-33.5‰ ±5.2, n=3) are more depleted than those of *Ifremeria* (-27.9‰ ±0.2, n=3), with and without including the depleted mussel specimen. Combined values of *Bathymodiolus* and *Ifremeria* are statistically different from *Alviniconcha* for total SBOM (p=0.0013) and soft tissues (p=<0.0001), but not for shell carbonate (p=0.1390).

3.3.1.11 Hydrothermal vent: East Wall (Fig. 3.4C)

Bivalves harbouring thiotrophic symbionts

Thiotrophic *B. thermophilus* from East Wall has $\delta^{13}C$ total SBOM values ranging from –31.7‰ to -30.9‰ (n=2). A single analysed gill tissue has a value of -33.0‰, which is -1.3‰ more depleted than the individual total SBOM of that specimen.

Heterotrophic gastropod

Multiple *Lepetodrilus elevatus* specimens were combined for a single analysed of $\delta^{13}C$ total SBOM: –20.6‰. Related whole tissues show a value of -15.4‰, and are thus +5.2‰ more enriched than total SBOM.

Comparison between nutritional strategies at this locality

Statistical analysis between thiotrophic *Bathymodiolus* and heterotrophic *Lepetodrilus* is not possible. But a comparison between the means shows that *Lepetodrilus* is +10.7‰ more enriched in $\delta^{13}C$ total SBOM, and +17.6‰ in $\delta^{13}C$ soft tissue values. This enrichment is likely due to *Lepetodrilus* feeding on enriched photosynthetically derived material

3.3.1.12 Hydrothermal vent: Buckfield (Fig. 3.4C)

$\delta^{13}C$ total SBOM of thiotrophic *B. thermophilus* from Buckfield ranges from -31.8‰ to -30.5‰ (n=2). Shell carbonate from this species ranges from 3.0‰ to 3.1‰ $\delta^{13}C$ total SBOM (n=3).

3.3.1.13 Hydrothermal vent: East Scotia Ridge (Fig. 3.4C)

Chemosymbiotic gastropod

The peltospiroid gastropod species (collated?) from East Pacific Rise has a $\delta^{13}C$ total SBOM value of -27.8‰, and $\delta^{13}C$ shell carbonate value of 4.9‰.

Bivalve harbouring thiotrophic symbionts **(suspected)**

The vesicomyid clam species has $\delta^{13}C$ total SBOM that ranges from -33.5‰ to -30.4‰ (n=3), a total SBOM sample of these three samples combined obtained using HCl has a slightly more depleted value of -35‰. A single intra-crystalline SBOM sample had a value of -30.4‰, which was +2.7‰ more enriched than the individual total SBOM of that specimen. Shell carbonate values vary between 1.7‰ and 1.9‰.

Comparison between nutritional strategies at this locality

The peltospiroid gastropod is more enriched in $\delta^{13}C$ total SBOM (mean difference: +4.9‰) and shell carbonate (+3.1‰) than the vesicomyid clams.

3.3.1.14 Hydrothermal vent: Kilo Moana, Lau Basin (Fig. 3.4C)

Bivalve harbouring thiotrophic symbionts

The $\delta^{13}C$ values of thiotrophic *B. brevior* from this locality range from -30.2‰ and -28.7‰ (n=2) for total SBOM, and from -34.4‰ and -34.2‰ for whole tissue values (n=2). Individual $\Delta_{SBOM\text{-}soft\ tissue}$ could be determined for one specimen, and showed a -4.0‰ enrichment in total SBOM. $\delta^{13}C$ shell carbonate values range from 1.9‰ to 2.4‰ (n=3).

3.3.1.15 Hydrothermal vent: Tow Cam, Lau Basin (Fig. 3.4C)

Bivalve harbouring thiotrophic symbionts

Thiotrophic *B. brevior* from Tow Cam shows total SBOM $\delta^{13}C$ values that range from -30.4‰ to -29.2‰ (n=2), and has an intra-crystalline value of -27.5‰. The intra-crystalline SBOM is +1.8‰ enriched compared to the total SBOM of the specimen.

$\delta^{13}C$ values for whole soft tissues range from -35.6‰ to -35.6‰ (n=2). The mean soft tissue value is -5.8‰ more depleted than the mean total SBOM value, compared for individual specimens the depletion is 5.8‰ ±0.8 (n=2).

3.3.1.16 Hydrothermal vent: Kermadec Ridge (Fig. 3.4D)

Bathyaustriella thionipta is the only known vent lucinid and has a thiotrophic lifestyle. $\delta^{13}C$ total SBOM of the species ranges from -27.8‰ to -26.1‰ (n=5), and intra-crystalline SBOM from -27.7‰ to -26.8‰ (n=3). The two SBOM pools are statistically the same (p=1.000), and their relationship for individual specimens is variably enriched or depleted (-0.2 ±0.6 difference, n=3).

Soft tissue $\delta^{13}C$ values of *B. thionipta* are -28.2‰ and -27.0‰. These values are not statistically different from total or intra-crystalline SBOM data. When individual total SBOM values are compared to individual mean soft tissues values, the latter are always more depleted (-0.2‰ and -2.0‰). The differences in this isotopic relationship are similar when specified for the various soft tissues (range from 0.0‰ to -0.1‰, and -2.1‰ to -1.7‰, n=4), with the exception of the more depleted gill tissues (-2.9‰ and -1.1‰). Also in comparison to the other soft tissues (minus rest), the gills are depleted by -1.0 (n=2).

$\delta^{13}C$ shell carbonate values range from 4.1‰ to 6.8‰ (n=5).

3.3.1.17 Shallow reducing environments: Little Ducks Keys (Fig. 3.4D)

Bivalves harbouring thiotrophic symbionts

The lucinid *Codakia orbicularis* has $\delta^{13}C$ total SBOM of -24.9‰ and -24.1‰, intra-crystalline of -27.3‰, and -25.5‰, and soft tissue values of -24.6‰ and -23.5‰. For individual specimens total SBOM is +1.9‰ ±1.9 (n=2) more enriched than intra-crystalline SBOM. The relationship between individual SBOM and soft tissues is variable (-0.4‰ ±1.3, n=2) and will therefore not be discussed in more detail. Also the relationship between the different soft tissues (gills/rest versus other tissues) is variable between the two specimens. $\delta^{13}C$ shell carbonate values are 0.8‰ and 2.1‰.

3.3.1.18 Shallow reducing environment: Magellan Bay (Fig. 3.4D)

Bivalves harbouring thiotrophic symbionts

Pegophysema philippiana has $\delta^{13}C$ total SBOM of -26.2‰ and -26.2‰, an a collated intra-crystalline value (-26.8‰) was obtained that is -0.6‰ depleted compared to both specimens. Soft tissue values are -28.9 and -27.8, that are individually -2.2‰ ±0.8 (n=2) depleted compared to total SBOM. Variation of the different soft tissues for SBOM-soft tissue difference are similar (variation of ±0.9‰ to ±0.7‰), and gill tissues are always more depleted than other tissues by -1.1‰ (±0.0, n=2). Shell carbonate values are 1.0‰ and 1.9‰.

3.3.1.19 Shallow reducing environment: Ramrod Key (Fig. 3.4D)

Bivalves harbouring thiotrophic symbionts

Total SBOM of *Ctena orbiculata* has $\delta^{13}C$ values of -25.4 and -23.9. Shell carbonate $\delta^{13}C$ values are 0.0‰ and 0.3‰.

3.3.1.20 Shallow reducing environment: Houmt Souk (Fig. 3.4D)

Bivalves harbouring thiotrophic symbionts

Lucinid species *Loripes lucinalis* has a total SBOM value of $\delta^{13}C$ -26.2‰.

3.3.1.21 Shallow reducing environment: Bocas del Toro (Fig. 3.4D)

Bivalves harbouring thiotrophic symbionts

Ctena imbricatula has $\delta^{13}C$ values of -27.5‰ and -25.4‰ for total SBOM, and -1.5‰ and -1.3‰ for shell carbonate.

3.3.1.22 Shallow reducing environment: Sal Rei Village (Fig. 3.4D)

Bivalves harbouring thiotrophic symbionts

Thiotrophic *Lucina adansoni* was analysed for total SBOM, intra-crystalline SBOM, soft tissues and shell carbonate. The total SBOM of *L. adansoni* has $\delta^{13}C$ values for total SBOM of -22.4‰ and -22.3‰, for intra-crystalline SBOM of -26.0‰ and -24.9‰, and for soft tissues of -22.1‰ and -22.0‰. Compared to the total SBOM of individual specimens, the intra-crystalline SBOM is -3.0‰ (±0.8, n=2) more depleted, and the soft tissues are +0.3‰ (±0.0, n=2) more enriched. The variation between the two specimens in *SBOM-soft tissue* for the different soft tissues is small, and ranges from ±0.1‰ to ±0.4‰, with the 'rest' tissue being most similar to the total SBOM (+0.0‰ ±0.2, n=2). There is a similar order of depletion in the tissues of the two specimens, and 'gills' and 'rest' are always more depleted than the other tissues (-0.9‰ ±0.5, and -0.6‰ ±0.0, respectively, n=2). Shell carbonate values of *Lucina* are 2.2‰ and 2.4‰.

3.3.1.23 Shallow reducing environment: Skogsvågen (Fig. 3.4D)

Bivalves harbouring thiotrophic symbionts

Multiple specimens of the lucinid *Myrtea spinifera* were collated to obtain a $\delta^{13}C$ total SBOM value of -22.0‰ (using HCl).

3.3.1.24 Shallow reducing environment: Gåsevik (Fig. 3.4D)

All specimens from this locality were collated because of their small size. All other species analysed of shallowing reducing environment discussed thus far belong to the Lucinidae family. In addition to the lucinid *M. spinifera* from this locality, we also analysed collated specimens of the thyasirid *Thyasira sarsi* (Thyasiridae) and the deposit feeders *Abra alba* and *Ennucula tenuis*.

Bivalves harbouring thiotrophic symbionts

M. spinifera from Gåsevik has a $\delta^{13}C$ total SBOM value of -21.6‰, and a soft tissue value of -27.1‰, with soft tissue being depleted by -5.5‰. Shell carbonate for this species has a $\delta^{13}C$ value of 0.3‰.

Thiotrophic thyasirid clam *T. sarsi* shows a total SBOM value of $\delta^{13}C$ -28.6‰, and a soft tissue value of -29.8‰ (-1.2‰ more depleted than total SBOM). The $\delta^{13}C$ value of shell carbonate was -4.2‰.

Heterotrophic bivalves

Despite feeder *A. alba* has a $\delta^{13}C$ value of -24.6‰ for total SBOM, and of -18.8‰ for soft tissue, soft tissue is thus +5.8 more enriched than total SBOM. The shell carbonate of this species is -0.4‰.

The other deposit feeder at this locality is *E. tenuis*, this species shows a $\delta^{13}C$ total SBOM value of -21.5‰. Shell carbonate has a value of 0.9‰.

Comparison between nutritional strategies at this locality

Whilst the total SBOM values for thiotrophic *T. sarsi* and heterotrophic *E. tenuis* are as expected, the -24.6‰ value of *A. alba* (particularly compared to *M. spinifera*) does not show the enrichment known from heterotrophic species feeding on POM, that are generally no more depleted than -22‰. The expected values are observed in the soft tissue values from the specimens.

3.3.1.25 Shallow non-reducing environment: Big Hope Bay (Fig. 3.4E)

Heterotrophic brachiopods

Terebratella sanguinea $\delta^{13}C$ total SBOM values range from -23.9‰ to -20.4‰ (n=5), and intra-crystalline SBOM from -26.0‰ to -23.7‰, and the two SBOM pools are statistically different (p=0.0019). Comparison for individual specimens shows a depletion of -3.7‰ ±1.9 in the intra-crystalline fraction. Soft tissues $\delta^{13}C$ values of Terebratella range from -21.4‰ to -17.4‰, and are not statistically different from total SBOM (p=0.0590), individually soft tissues are more enriched for 3 out 4 specimens (mean: +2.6 ±2.9, n=4) – specifically muscle tissue is always more enriched than SBOM (+3.6‰, ±2.8, n=4);and lophophore is generally more depleted than the other soft tissues (-1.2‰, ±1.8, n=4, 3 out of 4). Shell carbonate $\delta^{13}C$ range from 0.4‰ to 1.8‰.

3.3.1.26 Shallow non-reducing environment: Tricky Cove (Fig. 3.4E)

Heterotrophic brachiopods

Several brachiopod species from Tricky Cove were analysed for $\delta^{13}C$ total SBOM, intra-crystalline SBOM, soft tissues and shell carbonate. *T. sanguinea* is found at

both Big Hope Bay and Tricky Cove. At Tricky Cove the species has $\delta^{13}C$ total SBOM values that range from -23.9 to -17.5, an intra-crystalline value of -25.5‰ (-5.1‰ depleted compared to total SBOM), and soft tissues from -18.5‰ to -17.5‰ (n=5). Soft tissue and total SBOM are not statistically different (p=0.0805), but for individual specimens soft tissues are always similar or more enriched (+2.9‰ ±2.1, n=5). SBOM-soft tissues: muscle is also individually always more depleted (+3.2‰ ±2.1, n=2). Comparison between different tissues, lophophore is generally more depleted (4 out of 5): -0.7‰ (+1.4, n=5).

Notosaria nigricans has total SBOM values that vary from -26.3‰ to -19.2‰, an intra-crystalline value of -25.9‰ (-5.7‰ depleted compared to total SBOM), and soft tissues from -19.4‰ to -18.3‰ (n=4). The total SBOM and soft tissue are not statistically different, but for individual specimens there is a SBOM-soft tissue enrichment of +2.4‰ ±2.5 (n=4). Due to the large variability individual tissue SBOM-soft tissue differences will not be discussed. It can be shown that the gills (-0.9 ±0.0) and rest (-1.6 ±0.1, n=2) are always more depleted compared to the other tissues.

$\delta^{13}C$ total SBOM for *Liothyrella neozelanica* range from -22.8‰to -20.2‰ (n=7), intracrystalline SBOM from -26.6‰ to -25.5‰ (n=4), and soft tissues from -16.9‰ to -14.4‰ (n=3). The intra-crystalline pool is statistically depleted from total SBOM (p=<0.0001), and individual differences are -4.7‰ ±0.9 (n=4). Soft tissues are statistically enriched compared total SBOM (p=<0.0001), by -5.7‰ ±1.7 (n=3) (*not enough data is available for further conclusions about (SBOM-) soft tissues*).

The total SBOM range of the species *Liothyrella uva* ranges from -23.7 to -21.9, and a soft tissue value of -17.7. For the individual specimen there is an SBOM-soft tissue difference of 4.3‰.

Comparison between the different filter-feeding brachiopods species of Tricky Cove shows that there are is only a statistical difference in $\delta^{13}C$ total SBOM between the *Liothyrella* species (p=0.0396).

The intra-crystalline values of *T. sanguinea* (-25.5‰) and *N. nigricans* (-25.9) are within the range of intra-crystalline values of *L. neozelanica* (-26.0 ±0.6, n=4).

Soft tissues values differ between *T. sanguinea* versus *N. nigricans* (p=0.0123) and *L. neozelanica* (p=0.0200) (but overlap with *L. uva*). There is also a statistical difference between *N. nigricans* and *L. neozelanica* (p=0.0097). A mean soft tissue value for these species (-17.8‰ ±1.4) is very similar to the soft tissue value of *L. uva* (-17.7).

The brachiopod species from Tricky Cove have the following ranges for $\delta^{13}C$ shell carbonate: 1.2‰ to 1.7‰ (*T. sanguinea*, n=6), 1.2‰ to 1.6‰ (*N. nigricans*, n=5), 1.2‰ to 2.9‰ (*L. neozelanica*, n=7), and 1.4‰ to 2.4‰ (*L. uva*, n=3). There are statistical differences between *T. sanguinea* and both *Liothyrella* species (p=0.0050, and 0.0314), as well as between *N. nigricans* and *L. neozelanica* (p=0.177) (*Liothyrella* species are statistically similar, p=0.4725).

3.3.2 $\delta^{15}N$ of SBOM and soft tissues

3.3.2.1 Cold seep: Green Canyon, Gulf of Mexico (Fig. 3.4A)

Bivalves harbouring methanotrophic symbionts

B. childressi $\delta^{15}N$ total SBOM values range from -15.6‰ to -10.4‰ (n=10), and intra-crystalline SBOM from -2.0‰ to -12.8‰ (n=5). There is no statistical difference between the total SBOM values of the localities GC233 (-12.7‰ ±2.1, n=8) and GC234 (-11.8‰ ±1.2, n=2).The intra-crystalline SBOM values are very variable (-12.8‰ to -2.0‰, n=4), and statistically different from the total SBOM pool (p=0.0258). For individual specimens the intra-crystalline SBOM is +6.4‰ ±4.0 (n=3) more enriched than the total SBOM values.

Bivalves harbouring thiotrophic symbionts

For *C. ponderosa* the total SBOM $\delta^{15}N$ values range from -0.4‰ to 4.3‰ (n=3). Intra-crystalline SBOM has a value of 2.6‰, which is +3.8‰ enriched compared to the total SBOM value of that specimen.

V. cordata has a range of $\delta^{15}N$ total SBOM from -3.4‰ to 0.6‰.

The total SBOM values between *C. ponderosa* (1.6‰ ±2.4, n=3) and *V. cordata* (2.5‰ ±1.2, n=3) are not statistically different (p=0.0572).

Comparison between different nutritional strategies at this locality

Bathymodiolus total SBOM (-12.5‰ ±1.9, n=10) is statistically different from the more enriched values of thiotrophic *Calyptogena* and *Vesicomya* (0.1‰ ±2.6, n=6). The intra-crystalline value from *Calyptogena* (2.6‰) is also more enriched than the values from *Bathymodiolus* (-7.8‰ ±5.1). These results suggest that methanotrophic *B. childressi* is using a more depleted nitrogen source than the thiotrophic species.

3.3.2.2 Cold seep: Florida Escarpment, Gulf of Mexico (Fig. 3.4A)

Bivalves harbouring dual symbiotic bacteria

Adult *B. heckerae* total SBOM $\delta^{15}N$ values range from -8.0‰ to -7.5‰ (n=3). Soft tissues from a single specimen from that locality have a large variation in $\delta^{15}N$ (-10.1‰ ±1.9, n =6 measurments), that partially overlaps with total SBOM values.

Total SBOM from all juvenile *B. heckerae* specimens were combined for a single $\delta^{15}N$ measurment of 1.1‰, and soft tissue values ranged from -12.8‰ to -7.5‰ (n=4). Therefore, whilst soft tissue values of the two age groups are statistically similar, the juvenile total SBOM value is much more enriched compared to the adult specimens.

Bivalves harbouring thiotrophic symbionts

The single measurment of total SBOM for *Vesicomya* from Florida Escarpment had a $\delta^{15}N$ total SBOM value of 2.8‰.

Heterotrophic limpet

The limpet *P. floridensis* was shown to have a total SBOM $\delta^{15}N$ value of 3.3‰, soft tissues had a value of -10.1‰.

Comparison between nutritional strategies at this locality

No statistical comparisons could be made between $\delta^{15}N$ total SBOM of the different nutritional strategies. However, juvenile *B. heckerae* (1.1‰), *Vesicomya* (2.8‰) and *P. floridensis* (3.3‰) all have similar values, compared to the very depleted adult *B. heckerae* total SBOM data (-7.7‰ ±0.3, n=3). Mean soft tissue values from both juvenile *B. heckerae* (-9.8‰ ±2.3) and *P. floridensis* (-10.1‰) are similar to adult *B. heckerae* (-10.1‰)

3.3.2.3 Cold seep: Blake Ridge

Bivalves harbouring dual symbionts

B. heckerae $\delta^{15}N$ total SBOM ranges from 2.0‰ to 3.6‰ (n=3), intra-crystalline SBOM from 3.8‰ to 6.0‰ (n=2), and the two SBOM pools are not statistically different from each other. However, for individual specimens the intra-crystalline pool is always more enriched. Soft tissue range from 1.6‰ to 2.3‰ (n=3), and values are statistically similar to total SBOM.

Bivalves harbouring thiotrophic symbionts

A combined total SBOM $\delta^{15}N$ value for all *V.* cf. *venusta* specimens (n=5) is 3.1‰. Mean soft tissue values for the individual specimens vary between 0.5‰ and 4.8‰ (n=5)

Comparison between nutritional strategies at this locality

B. heckerae has a mean total SBOM $\delta^{15}N$ value of 2.6‰ ±0.9 (n=3), an intra-crystalline SBOM value of 4.9‰ ±1.6 (n=2), and soft tissue value of 2.0‰ ±0.3 (n=3). Total SBOM of *V. venusta* (3.1‰) falls within the range of *B. heckerae* values, and soft tissue values of *V. venusta* (2.5‰ ±1.6, n=3) are statistically similar to soft tissue values of *Bathymodiolus*.

3.3.2.4 Cold seep: Barbados (Fig. 3.4A)

Bivalves with unknown nutritional strategy

Bathymodiolus from Barbados has $\delta^{15}N$ total SBOM values ranging from 0.2‰ to 0.8‰ (n=3), and an intra-crystalline SBOM value of 1.7‰ (n=1). The intra-crystalline SBOM is +1.5‰ enriched compared to total SBOM of that specimen.

Bivalves harbouring thiotrophic symbionts

$\delta^{15}N$ total SBOM values of *C. valvidae* range from 0.3‰ to 3.2‰ (n=3). Intra-crystalline SBOM had a value of 3.2‰, that was 1.8‰ depleted compared to the total SBOM of that specimen.

Comparison between nutritional strategies at this locality

$\delta^{15}N$ total SBOM of *Bathymodiolus* (0.4‰ ±0.4, n=3) and *Calyptogena* (1.6‰ ±1.5, n=3) is statistically similar between the two species (p=0.2516).

3.3.2.5 Cold seep: Guaymas Basin (Fig. 3.4B)

Bivalves harbouring thiotrophic symbionts

Total SBOM $\delta^{15}N$ values from *C. pacifica* fall between -1.8‰ and 2.3‰ (n=4), intra-crystalline SBOM has a value of 2.2‰ (+0.5‰ enriched compared to total SBOM of that specimen). Soft tissue means ranged from 1.5‰ to 1.6‰ (n=2), but variability within the species was large, with gills being -5.4‰ (±0.1, n=2) more depleted.

3.3.2.6 Cold seep: Oregon Subduction Zone (Fig. 3.4B)

Bivalves with thiotrophic bivalves

The total SBOM $\delta^{15}N$ values of *C. starobogatovi* ranged from 0.6‰ to 2.2‰ (n=3), and include one specimen with a very depleted mean value of -7.6‰. Soft tissues had mean values of -0.3‰ and 1.2‰.

3.3.2.7 Cold seep: Monterey Bay (Fig. 3.4B)

Bivalves harbouring thiotrophic symbionts

C. packardana has $\delta^{15}N$ total SBOM values ranging from 6.0‰ to 9.7‰ (n=5), and intra-crystalline SBOM values from 5.3‰ to 7.5‰ (n=4). The intra-crystalline values are -2.6 ±4.0 (n=4) depleted/enriched compared to total SBOM for individual specimens. Soft tissue values fall between 3.2‰ to 8.0‰ (n=3). These $\delta^{15}N$ values are similar to *C. stearnsii*: total SBOM results range from 5.8‰ to 7.4‰ (n=3), soft tissues values are 4.8‰ and 4.9‰.

Total SBOM values of *C. kilmeri* are much more depleted, and range from $\delta^{15}N$ -4.9‰ to 0.0‰ (n=3), and intra-crystalline SBOM has a value of -3.7‰. Mean soft tissue values are -7.8‰ and -5.6‰ (n=2).

3.3.2.8 Cold seep: Fossil Hill (Fig. 3.4B)

Bivalves harbouring thiotrophic symbionts

E. elongata from PSC48 has $\delta^{15}N$ total SBOM values of 0.5‰ and 0.6‰, PSC52 of 1.3‰, and PSC66 of -6.9‰. Compared to the push core specimens, large *E. elongata* has statistically more enriched total SBOM values of 6.6‰ and 8.1‰, and an intra-crystalline value of 2.3‰.

3.3.2.9 Cold seep: San Diego Trough (Fig. 3.4B)

Bivalves harbouring thiotrophic symbionts

$\delta^{15}N$ total SBOM from the thiotrophic vesicomyid *E. elongata* is 10.0‰. A solemyid specimen shows a total SBOM value of 13.9‰. These two specimens are enriched compared to a lucinid specimen of the same locality, that has a total SBOM value of 3.0‰.

Heterotrophic bivalves

Delectopecten sp. has a total SBOM $\delta^{15}N$ value of 16.1‰.

3.3.2.10 Hydrothermal vent: South Su (Fig. 3.4C)

Gastropods harbouring thiotrophic symbionts

A. hessleri mean soft tissue $\delta^{15}N$ values are 6.2‰ and 6.0‰.

I. nautilei total SBOM has a $\delta^{15}N$ value of 5.2‰, and a soft tissue value of 4.8‰.

Bivalves harbouring thiotrophic symbionts

$\delta^{15}N$ values for *B. manusensis* are 2.8‰ for total SBOM, and 0.7‰ for mean soft tissue value.

3.3.2.11 Hydrothermal vent: East Wall (Fig. 3.4C)

Bivalves harbouring thiotrophic symbionts

B. thermophilus $\delta^{15}N$ values for soft tissues are -4.5‰ and -3.7‰.

3.3.2.12 Hydrothermal vent: Buckfield (Fig. 3.4C)

Bivalves harbouring thiotrophic symbionts

$\delta^{15}N$ total SBOM for *B. thermophilus* is 6.3‰.

3.3.2.13 Hydrothermal vent: East Scotia Ridge (Fig. 3.4C)

Bivalves harbouring thiotrophic symbionts

Vesicomyidae sp. has a $\delta^{15}N$ total SBOM value of 7.4‰.

3.3.2.14 Hydrothermal vent: Kilo Moana, Lau Basin (Fig. 3.4C)

Bivalve harbouring thiotrophic symbionts

Whole tissues of *B. brevior* have $\delta^{15}N$ values of -0.3‰ and -0.8‰.

3.3.2.15 Hydrothermal vent: Tow Cam, Lau Basin (Fig. 3.4C)

Bivalves harbouring thiotrophic symbionts

B. brevior $\delta^{15}N$ soft tissues values are -2.2‰ and -2.1‰.

3.3.2.16 Hydrothermal vent: Kermadec Ridge (Fig. 3.4D)

Bivalve harbouring thiotrophic symbionts

B. thionipta has $\delta^{15}N$ total SBOM values of 6.1‰ and 6.5‰, and an intra-crystalline SBOM value of -2.9 (individually -9.5‰ more depleted). Mean soft tissue values are 6.8‰ and 7.4‰, and individually they are +0.8‰ ±0.1 (n=2) more enriched than the individual total SBOM values.

3.3.2.17 Shallow reducing environments: Little Ducks Keys (Fig. 3.4D)

Bivalves harbouring thiotrophic symbionts

C. orbicularis has $\delta^{15}N$ total SBOM values of 3.4‰ and 3.6‰. Mean soft tissues values are 1.9‰ and 2.8‰, that are individually -1.2‰ ±0.8 (n=2) more depleted than total SBOM.

3.3.2.18 Shallow reducing environment: Magellan Bay (Fig. 3.4D)

Bivalves harbouring thiotrophic symbionts

Total SBOM for *P. philippinana* has $\delta^{15}N$ values of 4.2‰ and 4.3‰, soft tissues values are 5.3‰ and 5.4‰. For individual specimens, the soft tissues are +1.1‰ ±0.0 (n=2) enriched compared to total SBOM values.

3.3.2.19 Shallow reducing environment: Ramrod Key (Fig. 3.4D)

Bivalves harbouring thiotrophic symbionts

Total SBOM of *C. orbiculata* $\delta^{15}N$ values are 0.9‰ and 1.2‰. Mean soft tissue value of an individual specimen is -1.1‰, which is -2.3‰ depleted compared to individual total SBOM.

3.3.2.20 Shallow reducing environment: Houmt Souk (Fig. 3.4D)

Bivalves harbouring thiotrophic symbionts

L. lucinalis $\delta^{15}N$ total SBOM is 1.8‰, muscle tissue of this specimen has a value of -1.1‰ (-2.3‰ more depleted).

3.3.2.21 Shallow reducing environment: Sal Rei Village (Fig. 3.4D)

Bivalves harbouring thiotrophic symbionts

Total SBOM obtained from *L. adansoni* specimens had $\delta^{15}N$ values of -3.8‰ and -2.6, intra-crystalline SBOM values were -0.7‰ and 0.5‰ (-3.1‰ ±0.1, n=2 more enriched than individual total SBOM). Soft tissue values of the two specimens are -2.3‰ and -0.6‰, showing a mean depletion of -1.8‰ ±0.4 (n=2) compared to total SBOM.

3.3.2.22 Shallow reducing environment: Gåsevik (Fig. 3.4D)

Bivalves harbouring thiotrophic symbionts

The lucinid *M. spinifera* has a total SBOM $\delta^{15}N$ value of 7.2‰, the soft tissue of this specimen had a more depleted value of 0.1‰.

Total SBOM $\delta^{15}N$ of *T. sarsi* (1.0‰) is very similar to the soft tissue value of that specimen (0.9‰).

Heterotrophic bivalves

A. alba $\delta^{15}N$ values are 4.7‰ for total SBOM, and 11.5‰ for soft tissues.

Total SBOM from *E. tenuis* has a value of 7.4‰.

Comparison between different nutritional strategies at this locality

Soft tissue $\delta^{15}N$ values of the two thiotrophic species (0.1‰ and 0.1‰) are very depleted compared to heterotrophic *A. alba* (11.5‰). Total SBOM from *M. spinifera* (7.2‰) does not show this depletion compared to the two heterotrophic species (4.7‰ and 7.4‰).

3.3.2.23 Shallow non-reducing environment: Big Hope Bay (Fig. 3.4E)

Heterotrophic brachiopods

$\delta^{15}N$ total SBOM from *T. sanguinea* ranges from 8.2‰ to 9.9‰ (n=3), and intra-crystalline SBOM has values of 7.1‰ and 1.1‰. Mean soft tissues have a limited range between 9.5‰ and 9.9‰ (n=4).

3.3.2.24 Shallow non-reducing environment: Tricky Cove (Fig. 3.4E)

Heterotrophic brachiopods

T. sanguinea SBOM $\delta^{15}N$ values are between 7.4‰ and 10.0‰ (n=5) for total SBOM, and 4.5‰ for intra-crystalline SBOM. Mean soft tissues values fall between 8.0‰ and 8.8‰ (n=5).

For *N. nigricans* total SBOM ranges from 7.4‰ to 9.9‰ (n=4), intra-crystalline SBOM has a value of 2.6‰. Mean soft tissues values are between 7.7‰ and 9.3‰ (n=5).

3.3.3 $\delta^{34}S$ of SBOM and soft tissues

3.3.3.1 Cold seep: Green Canyon, Gulf of Mexico (Fig. 3.4A)

Bivalves harbouring methanotrophic symbionts

As discussed in the methods section (3.2.2.2), all methods confirm a positive sulphur value for *B. childressi*, with mean values ranging from 8.4‰ to 15.6‰ (n=6), in addition resin total SBOM $\delta^{34}S$ value (3.6‰ to 0.7‰, n=10 measurements) decrease with increasing %S (R-squared: 0.5823). The most positive intra-crystalline values with a mean of 3.1‰ (maximum value 4.3‰, n=8 measurements) also supports this.

Bivalves harbouring thiotrophic symbionts

Total SBOM $\delta^{34}S$ results for *C. ponderosa* were discussed in paragraph 3.2.2. *Sulphur*, and show negative sulphur values for EDTA, HCl and resin. Mean values (excluding resin samples) are: -5.8‰ and -5.1‰. Total resin SBOM measurments (n=5) have a mean value of -2.7‰, and a minimum value of -4.2‰. Total SBOM values obtained using the three different methods suggest that soft tissues from *C. ponderosa* have $\delta^{34}S$ values less depleted than -10‰. The intra-crystalline SBOM value of -2.1‰ also support negative sulphur values.

For *V. cordata* total SBOM was only obtained using EDTA, and total SBOM range from -6.2‰ to -2.1‰. This suggests *V. cordata* was using the same sulfur sources as *C. ponderosa*, that includes depleted hydrogen sulphide utilized by the thiotrophic bacteria they are harbouring.

Comparison between different nutritional strategies at this locality

Negative $\delta^{34}S$ total SBOM values of *C. ponderosa* and *V. cordata* (-4.0‰ ±1.9, n=5) compared to positive values for *B. childressi* (12.1‰ ±2.8, n=10) are expected because the thiotrophic bacteria harboured in the vesicomyid clams are utilizing depleted hydrogen sulphide, whereas the methanotrophic *Bathymodiolus* (also) uses seawater sulphate as a sulphur source.

3.3.3.2 Cold seep: Florida Escarpment, Gulf of Mexico (Fig. 3.4A)

Bivalves harbouring dual symbiotic bacteria

Soft tissue $\delta^{34}S$ data for adult *B. heckerae* consists of a single specimen (whole tissue) with large variation: 11.3‰ ±5.0 (n=6 measurments). For resin the value over 3‰ for one specimen (3.9‰ ±0.7, n=2) confirm the positive sulphur values.

Juvenile *B. heckerae* specimens had soft tissue values similar to the adult specimens, ranging from 6.8‰ to 7.3‰ (n=4).

Heterotrophic limpet

Soft tissue $\delta^{34}S$ for *P. floridensis* has a value of 4.6‰.

Comparison between nutritional strategies at this locality.

All the species that were analysed show positive sulphur values. This is in agreement with absence of thiotrophic bacteria, and suggests that they are all relying on the same sulphur source.

3.3.3.3 Cold seep: Blake Ridge (Fig. 3.4A)

Bivalves harbouring dual symbionts

Soft tissue $\delta^{34}S$ values of *B. heckerae* range from 7.6‰ to 8.9‰ (n=3).

Despite low %S (generally below 3%) total SBOM obtained using resin is very similar to the resin value (-1.0 ±0.4, n=8 measurments), and cannot be used to confirm positive or negative sulphur values of SBOM.

Bivalves harbouring thiotrophic symbionts

Mean soft tissue values ranges from -6.0‰ to -9.7‰ (n=5) for *V. venusta*.

Comparison between nutritional strategies at this locality

V. venusta soft tissue $\delta^{34}S$ values (-7.9‰ ±1.4, n=5) are considerably depleted compared to *B. heckerae* (+8.4 ±0.7, n=3) ($p =< 0.0001$). This expected because the *V. venusta* lives in symbiosis with thiotrophic bacteria that use depleted hydrogen sulphide as a sulphur source.

3.3.3.4 Cold seep: Barbados (Fig. 3.4A)

Bivalves with unknown nutritional strategy

None of the measurments of total SBOM obtained using resin from *Bathymodiolus* sp. are conclusively positive or negative.

Bivalves harbouring thiotrophic symbionts

Total SBOM $\delta^{34}S$ values of *C. valvidae* obtained using HCl had values of 1.0‰ and 5.8‰. A resin value of 3.2‰ confirms the positive values of SBOM and soft tissues, other values are inconclusive.

3.3.3.5 Cold seep: Guaymas Basin (Fig. 3.4B)

Bivalves harbouring thiotrophic symbionts

Total SBOM $\delta^{34}S$ values of *C. pacifica* are -4.3‰ and -3.3‰, and intra-crystalline SBOM has a value of -2.4‰. Mean soft tissues values range from -4.3‰ to -1.3‰ (n=2). As expected for this range of values, they cannot be confirmed using resin total SBOM. Intra-crystalline SBOM obtained using resin (-2.5‰) is in agreement with negative sulphur values.

3.3.3.6 Cold seep: Oregon Subduction Zone (Fig. 3.4B)

Bivalves harbouring thiotrophic symbionts

Soft tissue of *C. starobogatovi* have very depleted $\delta^{34}S$ values, with values of -24.6‰ and -24.0‰. Resin total SBOM (n=3 measurments) confirms very negative sulphur values, ranging from -14.9 (2.5% S) to -5.3 (5.0%) (n=4).

3.3.3.7 Cold seep: Monterey Bay (Fig. 3.4B)

Bivalves harbouring thiotrophic symbionts

C. packardana total SBOM $\delta^{34}S$ value is 0.3‰, which is in agreement with mean soft tissues values that range from -2.7‰ to 0.3‰ (n=3). As expected for this range close to the value of resin, they cannot be confirmed using resin total SBOM. Resin intra-crystalline SBOM however points towards negative sulphur values (-4.8‰, %S 1.8%) for at least some of the specimens.

C. kilmeri has very positive sulphur values for total SBOM (17.7‰), which is in agreement with soft tissue values from this species (19.2‰ and 19.3‰). Intra-crystalline SBOM has (variable) positive values of 2.5‰ and 9.2‰. Resin total SBOM are conclusively positive for several measurments, and range from 7.0‰ to 8.7‰ (n=5).

C. stearnsii from Monterey Bay has soft tissue $\delta^{34}S$ values of 3.1‰ and 4.6‰, total SBOM resin value %S is too high to be reliable.

3.3.3.8 Cold seep: Fossil Hill (Fig. 3.4B)

Bivalves harbouring thiotrophic symbionts

Soft tissue $\delta^{34}S$ values from Fossil Hill *E. elongata* are only known from PSC44: -5.0‰ and -5.1‰. These measurments are in agreement with several negative resin values for all the push cores: -6.1‰ ±2.1 (n=3).

Large *E. elongata* has a total SBOM value of -0.6‰.Resin values are inconclusive or have a high %S.

3.3.3.9 Cold seep: San Diego Trough (Fig. 3.4B)

Bivalves harbouring thiotrophic symbionts

Total SBOM of the lucinid specimens has a $\delta^{34}S$ value of -25.2‰. This very negative value is confirmed by the total SBOM obtained using resin: -10.6‰.

For the solemyid specimens SBOM/soft tissues could also be depleted up to 25‰ because total resin values are negative: -6.7‰ (2.5%) and -4.3‰ (3.7%).

E. elongata SBOM obtained using resin has values up to 4.3‰ (n=2), which is indicative of soft tissue values up to 20‰.

3.3.3.10 Hydrothermal vent: South Su (Fig. 3.4C)

Gastropods harbouring thiotrophic symbionts

$\delta^{34}S$ values of *I. nautilei* are -5.4‰ for total SBOM, and -7.1‰ for mean soft tissues.

Bivalves harbouring thiotrophic symbionts

B. manusensis total SBOM has a $\delta^{34}S$ value of -8.1‰, and mean soft tissues show values of -8.3‰ and -2.0‰. These values are similar to the negative sulphur values of the gastropod *I. nautilei*.

3.3.3.11 Hydrothermal vent: East Wall (Fig. 3.4C)

Bivalves harbouring thiotrophic symbionts

Soft tissues of *B. thermophilus* have $\delta^{34}S$ values of 0.3‰ and 3.6‰.

3.3.3.12 Hydrothermal vent: Buckfield (Fig. 3.4C)

Bivalves harbouring thiotrophic symbionts

Total SBOM of *B. thermophilus* has a $\delta^{34}S$ value of 0.2‰.

3.3.3.13 Hydrothermal vent: East Scotia Ridge (Fig. 3.4C)

Bivalves harbouring thiotrophic symbionts

Vesicomyidae sp. total SBOM value is $\delta^{34}S$ -2.9‰

3.3.3.14 Hydrothermal vent: Kilo Moana, Lau Basin (Fig. 3.4C)

Bivalve harbouring thiotrophic symbionts

Whole tissues of *B. brevior* have $\delta^{34}S$ values of 2.0‰ and 2.7‰.

3.3.3.15 Hydrothermal vent: Tow Cam, Lau Basin (Fig. 3.4C)

Bivalve harbouring thiotrophic symbionts

B. brevior $\delta^{34}S$ soft tissues are 2.8‰ and 2.9‰.

3.3.3.16 Hydrothermal vent: Kermadec Ridge (Fig. 3.4D)

Bivalve harbouring thiotrophic symbionts

B. thionipta mean soft tissue $\delta^{34}S$ values are -14.2‰ (±4.9) and -6.2‰(±7.7) and show large variation between soft tissues. Resin total SBOM values confirm the very negative values, with measurments ranging from -12.3‰ to -9.3‰ (n=3).

3.3.3.17 Shallow reducing environments: Little Ducks Keys (Fig. 3.4D)

Bivalves harbouring thiotrophic symbionts

The lucinid *Codakia orbicularis* $\delta^{34}S$ total SBOM value is -9.9‰, mean soft tissues are more depleted with values of however -16.2‰ (±4.0) and -20.3‰ (±1.6). Total SBOM resin value is in agreement with the depleted values: -6.4‰.

3.3.3.18 Shallow reducing environment: Magellan Bay (Fig. 3.4D)

Bivalves harbouring thiotrophic symbionts

Mean $\delta^{34}S$ values of soft tissues from *P. philippiana* are -20.4‰ and -19.6‰.

3.3.3.19 Shallow reducing environment: Ramrod Key (Fig. 3.4D)

Bivalves harbouring thiotrophic symbionts

For *C. orbiculata* a single soft tissue has a $\delta^{34}S$ value of -17.9‰. Total SBOM obtained using resin confirms the negative sulphur value, ranging from -6.8‰ to -3.1‰ (n=3).

3.3.3.20 Shallow reducing environment: Houmt Souk (Fig. 3.4D)

The muscle tissue of *L. lucinalis* has a $\delta^{34}S$ value of -24.6‰.

3.3.3.21 Shallow reducing environment: Bocas del Toro (Fig. 3.4D)

Bivalves harbouring thiotrophic symbionts

C. imbricatula muscle tissue has a value of $\delta^{34}S$ -24.6‰. Total SBOM obtained using resin is in agreement with negative sulphur values, with a most depleted value of -4.0‰ (n=3 measurments).

3.3.3.22 Shallow reducing environment: Sal Rei Village (Fig. 3.4D)

Bivalves harbouring thiotrophic symbionts

Lucina adansoni has a total SBOM $\delta^{34}S$ value of -20.3‰, and mean soft tissues values are -15.6‰ (±3.2) and -13.7‰ (±4.5).

Total SBOM (-10.1‰) and intra-crystalline SBOM (-2.5‰ and -3.5‰) are in agreement with these very negative sulphur values.

3.3.3.23 Shallow reducing environment: Gåsevik (Fig. 3.4D)

Bivalves harbouring thiotrophic symbionts

M. spinifera soft tissue value: $\delta^{34}S$ -23.6‰. Total SBOM obtained using resin confirms the very low sulphur values, with a minimum value of -5.3‰.

Soft tissues from *T. sarsi* are similarly depleted as *M. spinifera* (-19.1‰). This is also reflected in total SBOM obtained using resin: -10.5‰.

Heterotrophic bivalves

A. alba soft tissue has a $\delta^{34}S$ value of -4.7‰.

Comparison between different nutritional strategies at this locality

The two thiotrophic bivalves species are more depleted than *A. alba*, likely because they are more reliant on depleted hydrogen sulphide as a sulphur source.

3.3.3.24 Shallow non-reducing environment: Big Hope Bay (Fig. 3.4E)

Heterotrophic brachiopods

Soft tissue $\delta^{34}S$ values from *T. sanguinea* range from 16.0‰ to 17.0‰ (n=4). Five measurments of resin total SBOM > 3‰ confirm the positive values, with a maximum of 5.0‰. Intra-crystalline values of 6.4‰ and 6.6‰ are in agreement with this.

3.3.3.25 Shallow non-reducing environment: Tricky Cove (Fig. 3.4E)

Heterotrophic brachiopods

Total SBOM of *T. sanguinea* has a $\delta^{34}S$ value of 13.3‰, and the positive values are confirmed by resin total SBOM (maximum value of 5.3‰ (1.9%), R-squared of 0.94, n=16 measurments). Mean soft tissue values fall between 13.7‰ and 16.7‰ (n=5).

Notosaria nigricans soft tissues range from 15.4‰ to 17.2‰ (n=4). All measured resin total SBOM values are > 3‰, with a maximum of 9.1‰ (n=5).

Soft tissues of *L. neozelanica* range from $\delta^{34}S$ 12.0‰ to 18.1‰ (n=1). Total SBOM values obtained using resin of 4.2‰ and 3.9‰ are in agreement with positive SBOM/soft tissue sulphur values.

L. uva mean soft tissue has a value of 18.1‰.

3.3.4 Pyrolysis GC/MS comparison of total SBOM, intra-crystalline SBOM and shell powder

The molecular composition of total SBOM (isolated using cation exchange resin), intra-crystalline SBOM (isolated using cation exchange resin), and untreated shell powder from *Calyptogena ponderosa* (Gulf of Mexico) were analysed using Py-GC/MS. The results are presented as labelled total ion chromatograms in Fig. 3.5. As expected, the signal from the shell powder was much smaller than for the isolated SBOM (10x less than total SBOM), because the shell consists of mostly inorganic material.

The untreated shell powder contains many of the same components as the SBOM samples, confirming that isolated SBOM is chemically similar to original SBOM. The presence of Phenol, 2,4-bis(1,1-dimethylethyl) (19) in the shell powder sample is unexpected, and potentially a contaminant because it is used as an antioxidant in rubber.

Of particular interest to this study is the difference in peak distribution between total SBOM and intra-crystalline SBOM, in particular the higher abundance of protein break-down products (15-20 minutes) in total SBOM, and higher relative lipid abundance in intra-crystalline SBOM. Because no TMAH was used in these samples the lipids in the shell are cleaved differently from larger molecules, but they are the fatty acids/FAMES that have previously been observed in pyrograms of SBOM (Chapter 2). The presence of phthalate plasticizer (14) in both SBOM samples is likely a contaminant from the isolation procedure.

Figure 3.5 Total ion chromatograms from pyrolysis GC/MS for total SBOM, intra-crystalline SBOM, and shell powder of *C. ponderosa*

(p. 114) SBOM samples were isolated using cation exchange resin.

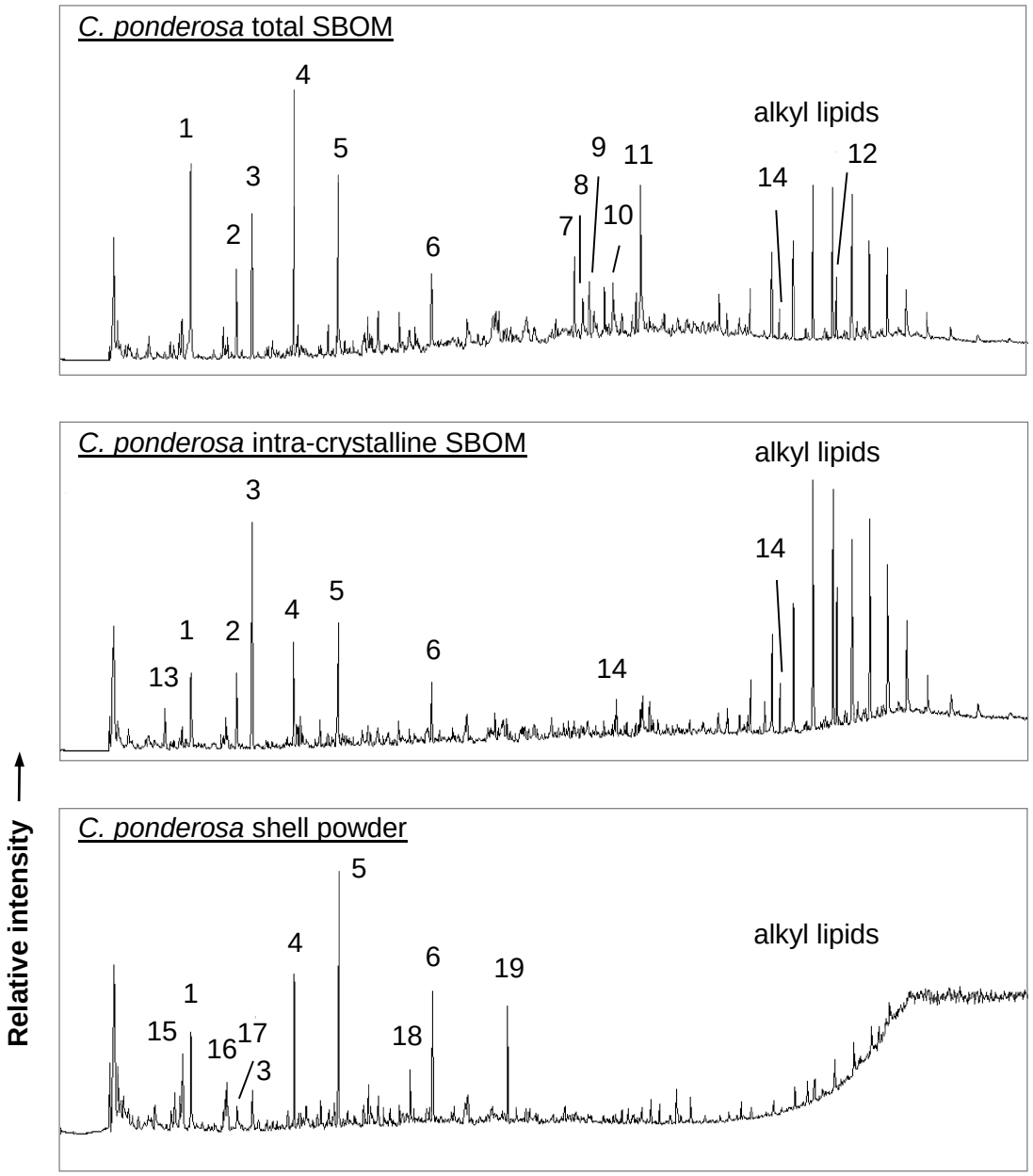

1	Toluene	**11**	5,10-Diethoxy-2,3,7,8-tetrahydro-1H,6H-dipyrrolo[1,2-a;1',2'-d]pyrazine
2	Ethyl Benzene	**12**	Squalene
3	Styrene	**13**	2-Propenoic acid, 2-methyl-, methyl ester
4	Phenol	**14**	phthalate plasticizer
5	Methyl Phenol	**15**	Pyrrole
6	5H-1-Pyrindine	**16**	Pentanenitrile, 4-methyl-
7	Uric Acid	**17**	1,3-Cyclopentadiene, 5-(1-methylethylidene)-
8	1H-Pyrazole-1-carboxaldehyde, 4-ethyl-4,5-dihydro-5-propyl-	**18**	Benzenepropanenitrile
9	Glycyl-L-proline	**19**	Phenol, 2,4-bis(1,1-dimethylethyl)-
10	Pyrrolo[1,2-a]pyrazine-1,4-dione, hexahydro-3-(2-methylpropyl)-		

3.4 Discussion

The aim of this study is to identify the different types of nutritional strategies using the stable isotope values ($\delta^{13}C$, $\delta^{15}N$, $\delta^{34}S$) of total SBOM and intra-crystalline SBOM, as well as shell carbonate. Of these three potential proxies only total SBOM has been shown to closely relate to soft tissues values/nutritional sources (Chapter 2). The presented total SBOM data in this study shows that it is generally possible to differentiate nutritional strategies from the same locality using total SBOM values. They however also reveal large isotopic variability of each nutritional strategy across localities and environmental settings. It is critical to understand the possible ranges of isotopic values for each nutritional strategy (methanotrophy, thiotrophy, dual symbiosis, and heterotrophy), before it can be determined whether it is possible to differentiate nutritional strategies from each other. Therefore total SBOM variability is firstly discussed per nutritional strategy, and subsequently different strategies are compared.

The second part of the discussion focusses on the relationship between total SBOM and intra-crystalline SBOM, and the potential of the latter pool to differentiate nutritional strategies.

In the last section the incorporation of nutritional sources into the $\delta^{13}C$ signal of shell carbonate is discussed, and possible application of shell carbonate to identify nutritional strategies.

3.4.1. Total SBOM variability within nutritional strategies

To be able to use the isotopic value of SBOM to differentiate various nutritional strategies, it is crucial to understand the isotopic SBOM variation within each nutritional strategy. Much of this variation is expected to be caused by different environmental sources, and isotopic variation of these sources. In particular large differences are possible between taxa from the various environmental settings: cold seeps, hydrothermal vent, and shallow (non-)reducing environments, that are characterized by very different biochemical conditions. Cold seeps are stable environments with high concentrations of methane and AOM-produced sulphide, whereas hydrothermal vents are short-lived and vigorous places, with heated fluids enriched in sulphide and metals. Animals living in shallow reducing environments do not have to deal with the food shortage of the deep sea, and their ecosystems are photosynthesis-based, instead of dominated by chemosynthesis. In addition,

the physiology and behavioural strategies of animals can be different between these environmental settings.

In this section, where possible, the isotopic relationship between potential environmental sources and total SBOM was calculated to investigate how the environmental sources are incorporated into SBOM, and whether fractionation occurs during uptake and incorporation. This relationship is discussed per nutritional strategy, and the variation that can be found (i) between localities of the same environmental setting, and (ii) between different environmental settings. In general this section focusses on total SBOM data and discussion of soft tissue data is secondary.

3.4.1.1. Methanotrophy

In this section the carbon, nitrogen and sulphur measurements of *B. childressi* from the Gulf of Mexico seeps are discussed. Our suite of samples only contained methanotrophic/dual symbiotic *Bathymodiolus* taxa from cold seep localities, but both nutritional strategies have also been found in *Bathymodiolus* species from hydrothermal vents.

Cold seeps

Carbon. Bivalves harbouring methanotrophic symbionts use methane from venting fluids, as both an energy source and as a carbon source (Fisher et al., 1990; Petersen & Dubilier, 2009). The production of methane is associated with large kinetic fractionation that discriminates against ^{13}C, which can lead to $\delta^{13}C$ values of methane as negative as -110 (Whiticar, 1999). This methane is used by methanotrophic bivalves following the simplified chemical reaction: oxygen + methane → carbon dioxide + organic matter (nutrition) (Childress & Girguis, 2011). All the symbiotic bacteria are related to Type I methanotrophic Gammaproteobacteria (Duperron, 2010), but the isotopic fraction of methane when incorporated into CO_2 and bacterial biomass is unclear: isotopic discrimination has been reported to be +0‰ at cold seeps (cf. Fisher et al., 1990; as used by Feng et al., 2015), as well as between -35‰ to -5‰ in laboratory conditions, because the microbes involved preferentially use lighter isotopes (Templeton et al., 2006). In general, maximum fractionation will be achieved when there is an excess of methane over oxygen, resulting in only partial methane oxidation. As a hypothesis we predicated the $\delta^{13}C$ of SBOM/soft tissue from bivalves harbouring

methanotrophic symbionts to reflect the isotopic value of the methane source without any fractionation (Table 3.7).

B. childressi from the Gulf of Mexico seeps is the only methanotrophic bivalve species analysed in this study, and the extremely depleted $\delta^{13}C$ total SBOM values (-51.9‰ ±5.8, n=9) confirm the use of methane as a carbon source by this species. The specimens were obtained from three separate seep localities in the Green Canyon area of the Gulf of Mexico: the brine pool GC233, and the gas hydrate seeps GC185 and GC234. The isotopic $\delta^{13}C$ value of methane differs between these three localities (shown in Figure 3.4), and the largest variation is caused by the difference between a relatively depleted biogenic origin of the methane at GC233 ($\delta^{13}C$ -64.3‰ to -65.5‰) and a less depleted thermogenic origin for the other two localities (GC185, $\delta^{13}C$ -44.1‰ to -46.0‰, and GC234, $\delta^{13}C$ -49.4‰ to -48.7‰) (Sassen et al., 2003; Pohlman et al., 2005). This difference exists because biogenic methane is produced from organic matter as a metabolic by-product of methanogenic microbes, whereas thermogenic methane results from the effects of increased pressure and high temperature on organic matter during deep burial (overview in Demirbas, 2010; Whiticar, 1999). The difference in the type of methane is reflected in the total SBOM $\delta^{13}C$ values of methanotrophic *B. childressi* from these localitites, as GC233 (-54.8‰ ±1.7, n=6) is statistically depleted compared to GC234 and GC233 (-46.0‰ ±8.1, n=3) (p=0.0489).

To further investigate the potential fractionation of methane when utilized by the symbiosis, the difference between calculated (0‰ fractionation of the source methane $\delta^{13}C$ value) and measured $\delta^{13}C$ SBOM values is shown in Table 3.7. This overview shows that the isotopic fraction between the methane source and total SBOM is not consistent, and $\delta^{13}C$ of total SBOM is ~ +10‰ enriched compared to local methane values at GC233, depleted by ~ -3‰ at GC185, and both depleted and enriched at GC234 by similar differences. Bacterial fractionation can explain the slight depletion compared to the methane source but the enrichment of total SBOM is unexpected. There are several explanations for this relationship: i) $\delta^{13}C$ of methane utilized by our specimens differs from published values, possibly because the carbon composition/concentration may have varied through time, ii) positive fractionation when $\delta^{13}C$ is incorporated from the soft tissues into SBOM, iii) shell removal techniques cause a positive fractionation of SBOM values $\delta^{13}C < -60‰$, iv) specimens with enriched $\delta^{13}C$ total SBOM supplemented their chemosymbiotic diet by filter-feeding on particulate organic matter with more positive $\delta^{13}C$ values (-25.0‰ to -19.0‰, Table 3.2), since *B. childressi* still retains the ability to filter-feed, although less effectively than heterotrophic bivalves (Page et al., 1990). To

distinguish between these possibilities, the SBOM data from GC233 ($\delta^{13}C$ -57.9‰ to -53.1‰, n=6) can be compared to published soft tissue $\delta^{13}C$ data from the same locality, ranging from -77.0‰ to -50.3‰ (1991/1992 and 2006 samples, n=128, Riekenberg et al., 2016). The complete overlap between data from this study and published values shows that no additional isotopic effect related to SBOM synthesis or isolation is required to explain our dataset, and that $\delta^{13}C$ variability could be attributed to changing methane $\delta^{13}C$ values or filter-feeding. However, because our data falls at the top of the range of published $\delta^{13}C$ values (mean: -62.3‰ ±5.3, n=128), an SBOM-related $\delta^{13}C$ effect can certainly not be excluded.

One specimen from GC234 shows very enriched $\delta^{13}C$ values for both total SBOM (-37.0‰) and shell carbonate (-0.5‰) compared to the other analysed specimens (SBOM: $\delta^{13}C$ -53.7‰ ±2.7, n=7; shell carbonate: -6.5‰ ±0.8, n=7). As explained above in the “Carbon” section, filter feeding on POM could lead to the enrichment of soft tissues/SBOM values compared to the local methane value. Unfortunately no sulphur or nitrogen data are available for this specimen to further support this hypothesis. It has however been suggested that particulate resources are an important part of the nutrition of *B. childressi* from gas hydrate seep GC185 (Riekenberg et al., 2016), and a similar scenario could apply to GC234. (Shell carbonate is further discussed in section 3.4.6)

Table 3.7 Methanotrophic species: calculated and measured $\delta^{13}C$ values for total SBOM and shell carbonate values

Methane source values are given in Table 3.3. $\delta^{13}C$ shell was calculated using [90% DIC + 10% SBOM + 2‰ fractionation], as explained in section 3.4.6.1), the same formula was used to calculate [% metabolic contribution] based on measured $\delta^{13}C$ values. Remarks are made on the difference between calculated SBOM/shell carbonate and measured values.

Specimen	**Methane $\delta^{13}C$**	**$\delta^{13}C$ total SBOM**	**Remarks ΔSBOM-source**	**Calculated $\delta^{13}C$ shell**	**$\delta^{13}C$ shell** (% metabolic carbon)	**Remarks Δcalculated-measured $\delta^{13}C$ shell**
B. childressi (GC233)	-64.3 to -65.5	**-55.4**	enriched ~+10‰	-3.8	**-5.8** (13.5%)	depleted DIC or higher % metabolic C
	-64.3 to -65.5	**-54.8**	enriched ~+10‰	-3.8	**-7.6** (17.5%)	
	-64.3 to -65.5	**-53.1**	Enriched ~+10‰	-3.6	**-5.7** (14%)	

Specimen	**Methane $\delta^{13}C$**	**$\delta^{13}C$ total SBOM**	**Remarks ΔSBOM-source**	**Calculated $\delta^{13}C$ shell**	**$\delta^{13}C$ shell** (% metabolic carbon)	**Remarks Δcalculated-measured $\delta^{13}C$ shell**
	-64.3 to -65.5	**-54.2**	enriched ~+10‰	-3.7	-**6.5** (15%)	
	-64.3 to -65.5	**-53.4**	enriched ~+10‰	-3.6	**-6.3** (15%)	
	-64.3 to -65.5	**-57.9**	enriched ~+10‰			
B. childressi (GC234)	-49.4 to -48.7	**-37.0**	enriched ~+10‰	-1.2	**-0.5** (8%)	enriched DIC or lower % metabolic C
	-49.4 to -48.7	**-52.6**	depleted ~-3‰	-2.7	**-7.3** (18.5%)	depleted DIC or higher % metabolic C
B. childressi (GC185)	-46.0 to -44.1	**-48.4**	depleted ~-3‰			

Nitrogen. Chemosymbiotic bivalves are well-known to exhibit depleted ($\delta^{15}N$ < 6‰), and sometimes negative, nitrogen isotope values of their soft tissues (Conway et al., 1994). Low $\delta^{15}N$ values are thought to indicate nitrogen that is locally assimilated, but for most chemosymbiotic species this is not well understood and direct $\delta^{15}N$ measurements of local inorganic sources are very scarce (e.g. Kennicutt et al. 1992; Becker et al., 2010). Inorganic nitrogen is present at vanishingly small concentrations in surface waters (Ryther and Dunstan, 1971) but very abundant at vents and seeps, in the form of nitrate ($\delta^{15}N$ 4‰ to 6‰, ~ 40 µm concentrations) and ammonium ($\delta^{15}N$ -20‰ to +10‰, present up to millimolar concentrations) (see Table 3.3, and references within Lee & Childress, 1994). Both inorganic nitrogen sources can be assimilated by either the bivalve hosts and/or their symbionts. In particular ammonium $\delta^{15}N$ can be very low due to dissimilatory nitrate reductase, causing a -20‰ to -30‰ fractionation compared to source nitrate (Granger et al., 2008). No evidence has been found for the fixation of nitrogen (N^2), which is an energetically costly process and unlikely in an environment with abundant nitrate and ammonium (Lee et al., 1992 and 1999; Lee and Childress, 1994).

The $\delta^{15}N$ of bivalve soft tissues and SBOM depends on the $\delta^{15}N$ values and proportions of environmental nitrate/ammonium. In addition, laboratory studies have shown that both nitrate and ammonium can undergo fractionations > -20‰, that are

largely dependent on concentration, as well as the types of enzymes used for assimilation (Lee & Childressi 1994; Lee et al., 1999, and references within).

It has also been suggested that photosynthetically derived nitrogen (POM: $\delta^{15}N$ -2‰ to +11‰) obtained via filter-feeding may be an important nutritional component for chemosymbiotic bivalves (shown for *B. childressi* by Pile and Young, 1999). If nitrogen is obtained from POM or the symbiont producers, it is possible that the $\delta^{15}N$ of the bivalve host reflects the higher trophic level as a consumer. Such a trophic step is generally accompanied by a $\delta^{15}N$ +3.4‰ increase, whereas little or no change is expected for carbon and sulphur (DeNiro and Epstein, 1978; Michener et al., 2007). Hypothetically, such a trophic step is only expected when symbionts are digested, instead of through translocation of organic matter from the symbionts. For *B. childressi* specifically both types of nutrient acquisition have been suggested (Fisher and Childress, 1992; Cavanaugh et al., 1992; Barry et al, 2002; Streams et al., 1997).

In summary, because information about environmental nitrogen sources and cycling is largely absent, and the kinetic isotopic effects of cycling and assimilation can be pronounced, it is will be very challenging to identify the nitrogen sources of specimens in detail. Comparison of $\delta^{15}N$ SBOM between nutritional strategies, localities and environmental settings should be handled with caution.

Methanotrophic *B. childressi* has the most depleted total SBOM $\delta^{15}N$ (-12.5‰ ±1.9, n=10) of any species in our data set. And similarly negative $\delta^{15}N$ soft tissue values of this species and locality (-14.8‰ ±4.0, n=128, Riekenberg et al., 2016) have been linked to the use of ammonium (e.g. MacAvoy et al., 2008; Becker et al., 2010), particularly because millimolar concentrations of ammonium have been measured at the Gulf of Mexico (Joye et al., 2005). Although local $\delta^{15}N$ values are not known for any of the localitites in our database, the very negative $\delta^{15}N$ values of SBOM make the use of ammonium as a nitrogen source very likely.

Sulphur. Methanotrophic bacteria reflect the $\delta^{34}S$ signature of ambient seawater sulphate that they use as a sulphur source, and this is also reflected in the bivalve host (Vetter and Fry, 1998). To deal with sulphide toxicity, methanotrophic symbioses are capable of oxidizing hydrogen sulphide to the less toxic thiosulphate (Childress and Girguis, 2011).

The $\delta^{34}S$ values of *B. childressi* SBOM ($\delta^{34}S$ 8.4‰ to 15.6‰) are very similar to published soft tissue values ($\delta^{34}S$ 10.3‰ ±2.9, n=128, Riekenberg et al., 2016), and relatively close to the value of seawater sulphate in the Gulf of Mexico ($\delta^{34}S$ 20.3‰). The data is also similar to the soft tissue $\delta^{34}S$ composition of resident

heterotrophs present at GC233, e.g. the grazing snail *Bathynertia naticoidea* ($\delta^{34}S$ 9.3‰ ±2.0, n=6) and the polychaete *Methanoaricia dendrobranchiata* (16.5‰ ±2.7, n=9) (McAvoy et al., 2008) that are expected to reflect marine phytoplankton that assimilate sweater sulphate (generally $\delta^{34}S$ +15‰ to +20‰). Similarly, total SBOM $\delta^{34}S$ values are comparable to total SBOM obtained from filter-feeding bivalves living in shallow non-reducing environments, ranging from $\delta^{34}S$ ~+7‰ to +11‰ (Chapter 2, soft tissues: ~+11‰ to +16‰).

At cold seeps there is also the possibility of incorporating a ^{34}S depleted sulphate pool, when depleted sulphide is re-oxidized by thiotrophic bacteria with negligible fraction of $\delta^{34}S$. Different degrees of temporal/spatial mixing between seawater sulphate and re-oxidized AOM sulphate could also explain the ~ 5‰ variation observed between specimens at GC233 (Feng et al., 2015).

3.4.1.2 Thiotrophy

Our suite of samples contains thiotrophic bivalves from three environmental settings: cold seeps, hydrothermal vents and shallow reducing environments. In this section the general environmental sources and physiological processes associated with thiotrophy are described first, followed by a comparison of the data across the different environments. Collated specimens from Gåsevik and other localities are generally excluded from the discussion because of an anomalously large difference between SBOM and soft tissue values, which is shown in section in 3.4.2.3.

Current understanding of thiotrophy

Carbon. Thiotrophic bacteria use dissolved inorganic carbon (DIC, usually in the form of CO_2) as a carbon source. The majority of thiotrophic bacteria involved in symbioses belong to the class of Gammaproteobacteria, that fix carbon via the Calvin-Benson-Bassham cycle (CBB) (Nelson & Fisher, 1995; Dubilier et al., 2008). The isotopic fractionation of DIC during this process depends on the specifics of the CO_2-fixing enzyme ribulose bisphosphate carboxylase/oxygenase (RubisCO) (Nakagawa & Takai, 2008). RubisCO can be present in different forms (I, II, III) that all catalyse the same reactions, but have different structures and physiological purposes (overview in Tabita et al., 2008). In addition, Form I RubisCO can be further classified into four types (A, B, C, D) based on the large subunits of RubisCO. Most thiotrophic bivalves harbour bacteria that use Form IA RubisCO (Stewart et al., 2005). The fractionation associated with this type of RubisCO was shown to be around $\delta^{13}C$ -25‰ in laboratory studies (Ruby et al., 1987; Scott et al.,

2004), but has been hypothesized to be as large as -35‰ to -40‰ in nature (Robinson and Cavanaugh, 1995; Robinson et al., 2003). In addition to Form I, Proteobacteria can also use RubisCO Form II, that causes a much smaller carbon isotope fractionation of $\delta^{13}C$ -9-15‰ (Robinson, 2003). This difference in fractionation between the two types of RubisCO is caused by lower discrimination against ^{13}C in Form II.

The reductive tricarboxylic acid cycle (rTCA) is an alternative CO_2 fixation pathway used by Epsilonproteobacteria. Organic carbon produced via the rTCA cycle in the deep sea generally has values more enriched than $\delta^{13}C$ -16‰ (Hügler et al., 2011).

In addition to differences related to CO_2 fixation pathways, DIC $\delta^{13}C$ variability could also be of influence on the $\delta^{13}C$ value of SBOM. In general, the DIC at deep sea environments is more depleted due to conversion of CO_2 into organic matter, which removes ^{12}C and results in ^{13}C enrichment of the residual DIC (Hoefs, 2015).

Nitrogen. A general discussion on the nitrogen sources of chemosymbiotic animals is given in 3.4.1.1, in the nitrogen section. The capability of thiotrophic symbioses to utilize nitrate or ammonium can be confirmed by the presence of key enzymes for their assimilation. Thus far enzymes for the use of ammonium have been detected in species from the families Vesicomyidae, Lucinidae, Solemyidea and Mytilidae and evidence for nitrate assimilation in Mytilidae and Solemyidae, though not all species appear to be capable of using nitrate (Lee and Childress, 1994; Lee et al., 1999). At both vents and cold seeps ammonium concentrations are generally high, up to millimolar concentrations, whereas nitrate is usually present at ~40µm (references within Lee and Childress, 1994).

Sulphur. Thiotrophic bacteria use sulphide as an energy source and as a sulphur source, and the sulphide is utilized with negligible fractionation (Stewart et al., 2005). At cold seeps environmental sulphide is produced when diffusing methane is oxidized anaerobically in the subsurface by sulphate-driven AOM: $CH_4 + SO_4^{2-} \rightarrow HCO_3^- + HS^- + H_2O$, a process that is mediated by methanotrophic archaea and sulphate reducing bacteria (Knittel & Boetius, 2009). The bacterial sulphate reduction results in a kinetic isotope fractionation of sulphide by $\delta^{34}S$ -30‰ to -70‰, dependent on the rate of reduction and openness of the system (Habitcht and Canfield, 2001). The preferential use of the lighter ^{32}S isotope by this process therefore leads to negative $\delta^{34}S$ values for sulphide, that is greatly depleted compared to the $\delta^{34}S$ seawater sulphate (Peterson and Fry, 1987). However due to e.g. mixing and sulphide oxidation, this difference in $\delta^{34}S$ between sulphide and

sulphate may however be limited, e.g. a difference of 15-30‰ between the two pools was observed in clam beds of Blake Ridge (Heyl et al., 2007).

Similar to cold seep ecosystems, in shallow reducing habitats (seagrass beds, mangroves and fjords) ^{34}S depleted sulphide is also produced as a metabolic end product: bacteria anoxically decompose organic matter, whilst using sulphate as an electron acceptor (Jorgensen et al., 1982). The expressed fractionation during this process depends on environmental and physiological factors (Bradley et al., 2016). The organic matter utilized by the bacteria naturally accumulates in the subsurface of seagrass beds and mangrove fringes, but also in fjords from decaying vegetation and sewage (Van der Heide, 2012; Dando and Southward, 1986). In addition, chemosymbiotic taxa can also be found in reducing unvegetated mud and sand (Meyer et al., 2008). Although sulphide concentrations can be very low in these habitats, the constant flux can support a high diversity of chemosymbiotic species, particularly Lucinidae, Thyasiridae and Solemyidae (Dubilier et al., 2008; Taylor and Glover, 2010).

In contrast to both cold seeps and hydrothermal vents, the large majority of sulphide present at hydrothermal vents is geologically derived, and results from chemical interactions between hot rocks and seawater sulphate below the seafloor (Van Dover, 2000). The sulphide within hydrothermal vent fluids generally has a $\delta^{34}S$ composition of -5 to +8‰, and geographical differences are much more limited (Shanks, 2001). Some of the suphide present at hydrothermal vents can be produced by AOM, although this process is much less common (as discussed above). In addition to sulphide, it has been shown that thiotrophic (vent) invertebrates can also oxidize thiosulphate. This is an intermediate sulphur oxidation product, produced from hydrogen sulphide (Beinart et al., 2015).

Unfortunately very few environmental sulphide sources are known for our localities (Table 3.4), and it will be challenging to directly relate $\delta^{34}S$ differences between species to either variation in local sources, or nutritional differences. Particularly because sulphide $\delta^{34}S$ values can be very variable locally (e.g. Rodrigues et al., 2013). But whilst positive $\delta^{34}S$ values cannot be taken as an absence of thiotrophy, negative $\delta^{34}S$ values of total SBOM are likely to indicate the presence of thiotrophic bacteria. Therefore thiotrophy is usually inferred from soft tissue values $\delta^{34}S < 5$‰ (Vetter and Fry, 1998).

Comparison between environmental settings

Carbon. In general $\delta^{13}C$ total SBOM of seep thiotrophs (-31.6‰ ±2.7, n=51) and vent thiotrophs (-29.7‰ ±3.3, n=22) are both consistent with DIC utilized by thiotrophic bacteria using RubisCO Form IA ($\delta^{13}C$ -25‰ to -40‰). The exception is the vent gastropod *Alviniconcha* ($\delta^{13}C$ -11.6‰ ±2.3, n=3), that is discussed separately below.

Interestingly, $\delta^{13}C$ total SBOM from both vent and seep thiotrophs is statistically depleted compared to thiotrophs from shallow reducing environments (24.8‰ ±2.7, n=14) by approximately 5‰ (p= <0.001, which was also found for soft tissue comparison between the environmental settings). Table 3.8 shows that this difference is not due to DIC $\delta^{13}C$ differences between the environments, because calculated total SBOM fractionation between deep sea (-31.0‰ ±2.9, n=75, vents and seeps) versus shallow (-26.1‰ ±2.0, n=14) also shows this distinction (p= < 0.0001). Only for bivalves from the family Lucinidae, total SBOM $\delta^{13}C$ comparisons can be made across the environments: these show that lucinids from cold seeps (-29.1‰, n=1) and hydrothermal vents (-27.1‰ ±0.7, n=5, locality =1) are more depleted than shallow living taxa (-24.9‰ ±1.9, n=11), although the difference is less extreme.

The enriched $\delta^{13}C$ total SBOM values at shallow reducing environments could be caused by different fractionation of DIC due to different environmental conditions, whereby it is possible to fractionate to a greater degree in the deep sea. One explanation is that at vents and seeps there is an increased amount of inorganic carbon as well as a lower pH, that leads to increased environmental CO_2 partial pressure, facilitating CO_2 transport and diffusion to the symbionts (Childress and Girguis, 2011), allowing for greater fractionation. Another possibility is that thiotrophs living at shallow localities are more likely to supplement their diet by filter-feeding ^{12}C enriched POM, which is much more abundant at shallow depth (Dubilier et al., 2008). It however seems unlikely that all analysed species would be supplementing their diet with very similar amounts of filter feeding. In addition, the measured $\delta^{13}C$ total SBOM values would require the majority of nutrition to be derived from POM, which is not reflect in the $\delta^{15}N$ and $\delta^{34}S$ values of these species (as discussed in the nitrogen and sulphur sections below).

Carbon – comparison between families. As noted in the sections above, the differences between Lucinidae from the various environmental settings are less extreme than when the whole dataset is considered. This suggests that family specific $\delta^{13}C$ differences in total SBOM could exist. In particular it was noted that

Vesicomyidae total SBOM $\delta^{13}C$ values from cold seeps (-31.9‰ ±2.2, n=48) and hydrothermal vents (-32.7‰ ±1.0, n=3) are generally depleted compared to the abovementioned Lucinidae from the same environment type, although data is limited. To further investigate this potential difference, soft tissue $\delta^{13}C$ values from seep Vesicomyidae from our dataset (-36.3‰ ±2.5, n=22, range: -46.5‰ to -32.7‰) can be compared to published soft tissue data from cold seep lucinids, because *B. thionipta* is the only known vent lucinid. Three seep species/localities could be found in the literature, and soft tissue $\delta^{13}C$ values range from 30.5‰ to -27.7‰ (Duperron et al., 2007; Olu-Le Roy et al., 2004; Rodrigues et al., 2013). This shows that ^{13}C depletion could be inherent to Vesicomyidae. The physiological functioning of Vesicomyidae is most different from all bivalve families, including vascular haemoglobin to transport oxygen, and a sulphide-binding protein (Childress and Girguis, 2011). This might make Vesicomyidae better adapted to a chemosymbiotic lifestyle than Lucinidae, and able to live without additional filter feeding or ability to fractionate DIC to a greater degree. Alternatively, it should be noted that lucinids from shallow environments are often considered mixotrophic (e.g. Van der Geest, 2014), and this could potentially also apply to deep sea species.

Table 3.8 Thiotrophic species: calculated fractionation of DIC for total and intra-crystalline $\delta^{13}C$ SBOM, calculated and measured $\delta^{13}C$ shell carbonate values

Published DIC data are given in Table 3.2, shell carbonate and metabolic carbon calculations can be found at Table 3.7. If the $\delta^{13}C$ value of DIC was unknown, $\delta^{13}C$ 0% for deep sea localities and 1.5% for shallow environments was used. Calculations using soft tissue values are in between brackets. Remarks are made on the difference between calculated shell carbonate and measured values.

Specimen	**$\delta^{13}C$ total SBOM** [soft tissues]	**ΔDIC-total SBOM** [soft tissues]	**ΔDIC-intra SBOM**	**Calculated $\delta^{13}C$ shell based on SBOM** [based on soft tissues]	**$\delta^{13}C$ shell** (% metabolic carbon)	**Remarks**
Cold seeps						
C. ponderosa (GC272)	**-33.3**	-32.7		-0.8	**1.2** (4%)	enriched DIC or lower % metabolic C
	-33.1	-32.5	-28.6	-0.8	**1.1** (4.5%)	
	-31.6	-31.0		-0.6	**1.4** (4%)	

V. cordata (GC272)	**-34.6**	-34.0		-1.0	**1.0** (5.5%)	enriched DIC or lower % metabolic C
	-34.4	-33.8		-0.9	**1.4** (4.5%)	
	-34.7	-34.1		-0.8	**1.2** (4%)	
V. cf. *kaikoi* (FE)	**-30.2** [-46.5]	-30.1 [-46.4]		-1.4 to -0.7 [-3.0 / -2.2]	**-2.8**	as expected for ST
V. cf. *venusta* (Blake Ridge)	**-37.0** [-37.2]	-37.0 [-37.2]		-1.7 [-1.7]	**1.1** (2.5%)	enriched DIC or lower % metabolic C
	-31.1 [-37.2]	-31.1 [-37.2]		-1.1 [-1.7]	**0.3** (5%)	
	-33.0 [-36.2]	-33.0 [-36.2]		-1.3 [-1.6]	**1.0** (3%)	
	-32.1 [-36.2]	-32.1 [-36.2]		-1.2 [-1.6]	**0.9** (3%)	
	-30.2 [-37.6]	-30.2 [-37.6]		-1.0 [-1.8]	**0.9** (3.5%)	
C. valvidae (Barbados)	**-31.4**	-31.4		-1.1	**1.3** (2%)	enriched DIC or higher % metabolic C
	-31.9	-31.9				
	-32.4	-32.4				
C. pacifica (Guaymas B)		[-35.4]	-32.6	[-3.5]	**-0.7**	
	-32.8	-32.8 [-35.1]		-1.3 [-1.5]	**-0.9** (9%)	as expected. or slightly enriched DIC or higher % metabolic C
	-29.1	-29.1 [-35.6]	-29.8			
	-32.6	-32.6 [-35.4]	-30.2			
	-33.8	-33.8 [-35.4]	-31.9	-1.4 [-1.5]	**-0.7** (8%)	
C. packardana (Monterey Bay)	**-34.4**	-34.4 [-35.3]	-29.5			
	-34.7	-34.7	-30.6			
	-35.1	-35.1 [-35.2]	-30.1			
	-30.1	-30.1				
	-32.1	-32.1 [-34.6]	-28.7			
C. starobogatovi (Oregon)	**-25.1**	-25.1				
	-34.2	-34.2				
	-33.8	-33.8 [-36.8]				
	-32.0	-32.0				

	-37.1	-37.1				
C. kilmeri (Extrovert Cliffs)	**-34.7**	-31.7 [-32.7]	-24.7			
	-34.7	-31.7 [-33.1]	-28.2			
	-31.7	-28.7	-31.9			
	-30.4	-27.4				
C. stearnsii (Monterey Bay)	**-30.7**	-30.7				
	-31.5	-31.5				
	-29.8	-29.8 [-35.5]				
	-36.1	-36.1				
E.elongata (FH. PSC44)	**-31.4**	-31.4				
	-31.2	-31.2				
	-28.2	-28.2 [-35.9]				
	-31.4	-31.4 [-32.7]				
	-32.1	-32.1				
E.elongata (FH. PSC48)	**-32.1**	-32.1				
	-31.2	-31.2				
	-28.0	-28.0				
E.elongata (FH. PSC66)	**-29.0**	-29.0		-0.9	**-0.2** (8%)	as expected. or slightly enriched DIC or higher % metabolic C
	-29.7	-29.7		-1.0	**-0.8** (9.5%)	
	-30.6	-30.6				
E.elongata (FH. large)			-30.6			
	-30.5	-30.5	-30.7			
	-28.7	-28.7	-30.7			
E. elongata (San Diego Trough)	**-22.1**	-22.1		-0.2	**-1.5** (16%)	depleted DIC or higher % metabolic C
solemyid (San Diego Trough)	**-26.7**	-26.7		-0.7	**2.2** (0%)	enriched DIC: 3.2
lucinid (San Diego Trough)	**-29.1**	-29.1		-0.9	**-0.5** (9%)	slightly enriched DIC or higher % metabolic C

Hydrothermal vents						
A. hessleri (South Su)	**-13.2**	-13.2 [-8.4]		0.7 [1.2]	**3.3** (0%)	enriched DIC: 2.9
	-10.0	-10.0 [-8.7]		1.0 [1.1]	**3.0** (0%)	enriched DIC: 2.2
		[-8.1]		[1.2]	**2.6**	enriched DIC: 1.8
I. nautilei (South Su)	**-26.5**	-26.5 [-27.9]	**-**26.7	-0.7 [-0.8]	**9.0** (0%)	enriched DIC: 10.7
	-26.0	-26.0 [-27.7]		-0.6 [-0.8]	**9.3** (0%)	enriched DIC: 11.0
	-26.1	-26.1 [-28.2]	**-**26.8	-0.6 [-0.8]	**9.3** (0%)	enriched DIC: 11.0
B. manusensis (South Su)	**-28.9**	-28.9 [-30.2]		-0.9 [-1.0]	**5.2** (0%)	enriched DIC: 6.8
	-28.7	-28.7 [-30.8]	-27.9	-0.9 [-1.1]	**6.4** (0%)	enriched DIC: 8.1
	-40.8	-40.8 [-39.4]		-2.1 [-1.9]	**0.0** (5%)	enriched DIC or higher % metabolic C
B. thermophilus. (East Wall)	**-31.7**	-31.7 [-33.0]				
	-30.9	-30.9				
B. thermophilus (Buckfield)	**-30.5**	-30.5		-1.1	**4.4** (0%)	enriched DIC: 6.0
	-31.8	-31.8		-1.2	**4.7** (0%)	enriched DIC: 6.5
peltospiroid (East Scotia Ridge)	**-27.8**	-27.9		-0.9	**4.9** (0%)	enriched DIC: 6.3
vesicomyid (East Scotia Ridge)	**-31.5**	-31.6		-1.2	**1.8** (0%)	enriched DIC: 3.3
	-33.1	-33.2		-1.2	**1.7** (0%)	enriched DIC: 3.3
	-33.5	-33.6		-1.3	**1.9** (0%)	enriched DIC: 3.6
B. brevior (Kilo Moana)	**-28.7**	-28.7		-0.9	**2.0** (0%)	enriched DIC: 3.2
	-30.2	-30.2 [-34.3]		-1.0 [-1.4]	**1.9** (0%)	enriched DIC: 3.2
		[-34.5]		[-1.5]	**2.4** (0%)	enriched DIC: 4.3
B. brevior (Tow Cam)	**-29.2**	-29.2 [-35.6]		-0.9 [-1.6]	**2.7** (0%)	enriched DIC: 4.0

	-30.4	-30.4 [-35.6]		-1.0 [-1.6]	**3.0** (0%)	enriched DIC: 4.5
B. thionipta (Macauley Caldera. Kermadec Ridge)	**-26.1**	-27.1 [-29.2]		0.3 [0.1]	**6.8** (0%)	enriched DIC: 8.2
	-26.7	-27.7 [-28.0]	-27.8	0.2 [0.2]	**4.5** (0%)	enriched DIC: 5.7
	-27.8	-28.8	-28.0	0.1	**4.0** (0%)	enriched DIC: 5.3
	-27.6	-28.6	-28.7	0.1	**4.1** (0%)	enriched DIC: 5.4
	-27.6	-28.6		0.1	**5.1** (0%)	enriched DIC: 6.5
Shallow reducing environments						
C. orbicularis (Little Duck Keys)	**-24.1**	-25.6	-28.8	0.9	**0.8** (10%)	as expected
	-24.9	-26.1	-27.0	0.9	**2.1** (5.5%)	enriched DIC or higher % metabolic C
P. philippiana (Magellan Bay)	**-26.2**	-27.7 [-30.4]		0.7 [-0.5]	**1.9** (6%)	enriched DIC or higher % metabolic C
	-26.2	-27.7 [-29.3]		0.7 [-1.4]	**0.6** (9%)	
C. orbiculata (Ramrod Key)	**-23.9**	-25.4	**-**28.8	1.0	**0.3** (13%)	depleted DIC or higher % metabolic C
	-25.4	-26.9	**-**27.0	0.8	**0.0** (13%)	
L. lucinalis (Houmt Souk)	**-26.2**	-27.7				
C. imbricatula (Bocas del Toro)	**-25.4**	-25.4		-0.5	**-1.3** (13%)	depleted DIC or higher % metabolic C
	-27.5	-27.5		-0.8	**-1.5** (13%)	
L. adansoni (Sal Rei Village)	**-22.4**	-23.9 [-23.6]	-27.5	1.1 [1.1]	**2.4** (4.5%)	enriched DIC or higher % metabolic C
	-22.3	-23.8 [-23.5]	-26.4	1.1 [1.1]	**2.2** (5.5%)	
M. spinifera (Skovsvagen)	**-22.0**	-23.5				
M. spinifera (Gåsevik)	**-21.6**	-23.1 [-28.6]		1.0 [0.5]	**0.3** (13%)	depleted DIC or higher % metabolic C
T. sarsi (Gåsevik)	**-28.6**	-30.1 [-31.3]		0.3 [0.2]	**-4.2** (26%)	depleted DIC: -3.7 or extremely high % metabolic carbon

Carbon – *Alviniconcha hessleri*. The $\delta^{13}C$ values of *Alviniconcha hessleri* (total SBOM: $\delta^{13}C$ -11.6‰ ±2.3, n=3; soft tissues: -8.4‰ ±0.4, n=3) are extremely enriched in ^{12}C for both total SBOM ($\delta^{13}C$ -29.7‰ ±3.3, n=22, localities=7) and soft tissues ($\delta^{13}C$ -31.7‰ ±4.0, n=13, localities=5) compared to all other vent thiotrophic specimens ($\delta^{13}C$ total SBOM: -30.0‰ ±3.7, n=87). These heavy values have previously been observed by other workers (e.g. Van Dover et al., 2001, -11.0‰ ±0.1 for soft tissues from *A. hessleri* of the hydrothermal vent Karei Field), and are in agreement with the presence of symbiotic Epsilonproteobacteria that use the rTCA cycle for carbon fixation. Interestingly, for *A. hessleri* from Marina Trough overwhelming evidence has been presented for carbon fixation via the CBB cycle using RubisCO Form IA, including depleted $\delta^{13}C$ values and identification of Gammaproteobacteria (Stein et al., 1990; Suzuki et al., 2005). The presence of two separate lineages of bacteria with different metabolic pathways within the same species is unexpected, but is in agreement with recent genetic work that has identified *A. hessleri* as a species complex. Johnson et al. (2015) confirmed that *A. hessleri* is a cryptic species, and the different taxa can only be differentiated using DNA from mitochondrial genes. Moreover, the specimens from South Su and Karei Field for which the presence of Epsilonproteobacteria is proposed, do not belong to the species *A. hessleri sensu stricto* from Marina Trough, in which Gammaprotebacteria have been identified. The two different carbon fixation pathways therefore seem to be present in different taxa, instead of both being present in the same species.

Carbon – variability across environments. In general, the $\delta^{13}C$ total SBOM variability could be environmental (e.g. difference in DIC $\delta^{13}C$, or the size of the carbon pool affecting fractionation) or biological, through the incorporation of POM (-22‰ to -18.5‰, Table 3.3) via filter-feeding. The latter possibility is suggested to explain the statistical enrichment of several species compared to multiple other taxa: at cold seeps, *E. elongata* (Fossil Hill, $\delta^{13}C$ -30.3‰ ±1.5, n=13) and *C. stearnsii* (Monterey Bay, $\delta^{13}C$ -30.7‰ ±0.8, n=3), as well as for the shallow living *L. adansoni* (Sal Rei Village, $\delta^{13}C$ -22.4 ±0.1, n=2). This conclusion is further supported by the small size (< 4 cm in length) of the two seep vesicomyids, since smaller chemosymbiotic specimens are more dependent on filter-feeding than larger ones (as observed for *Bathymodiolus*, Martin et al., 2008). Although the soft tissue values of these two species are similar to other taxa (around $\delta^{13}C$ -35‰), the two organic pools reflect different time periods, and extensive filter-feeding could have occurred earlier in life. The additional filter feeding of *L. adansoni* could be related to its presence at intertidal sands, instead of seagrass environments.

Nitrogen. The total SBOM $\delta^{15}N$ from thiotrophs largely overlap between the three environmental settings: cold seeps (2.3‰ ±4.6, n=36; range -4.9‰ to +13.9‰), hydrothermal vents (2.4‰ ±4.4, n=14; -4.5‰ to +7.4‰, includes soft tissue values because of limited data), and shallow reducing environments (1.7‰ ±2.3, n=9; range: -3.8‰ to +4.3‰). The large majority of the values is $\delta^{15}N < 6$‰ in all settings, which indicates that most of the nitrogen by the animals is derived from inorganic nitrogen sources. It is likely that for species with values $\delta^{15}N > 6$‰ some nitrogen is obtained via filter-feeding photosynthetically-derived nitrogen, or by the assimilation of ^{15}N enriched nitrate. Similar to conclusions in the carbon section, filter feeding could be related to size: both seep taxa with very positive $\delta^{15}N$ values are small (< 4cm): *C. packardana* (7.7‰ ±1.6, n=5), *C. stearnsii* (6.7‰ ±0.8. n=3), and therefore possibly more likely to rely on POM.

Sulphur. Because of limited total SBOM $\delta^{34}S$ data, the $\delta^{34}S$ values of soft tissues and total SBOM are combined. $\delta^{34}S$ value below +5‰ generally indicate thiotrophy (Vetter and Fry, 1998) and all but one species in our dataset are in agreement with this: cold seeps (-25.2‰ to 4.6‰), hydrothermal vents (-14.2‰ to 2.9‰), shallow reducing environments (-22.7‰ to -9.9‰). It likely that the variability at each environmental setting is caused by $\delta^{34}S$ variation of environmental sulphide between localities, since sulphide $\delta^{34}S$ can become very heavy when a large proportion of the available sulphate pool is consumed during sulphate reduction. Unfortunately local sulphur source values generally are unknown. It can only be shown that the relatively enriched sulphide values of Blake Ridge ($\delta^{34}S$ -1.3 ±1.4) are indeed reflected in total SBOM $\delta^{34}S$ values of *C. valvidae* from that locality (2.4‰ ±4.8, n=2). Sulphide at hydrothermal vents was reported to have $\delta^{34}S$ values between -5‰ and 8‰, but our dataset shows that more depleted $\delta^{34}S$ values are also possible (Fig. 3.9).

C. kilmeri from the Monterey Bay seeps has a total SBOM $\delta^{34}S$ value of +17.7‰, which is very close to that of seawater sulphate ($\delta^{34}S$ +20.3‰). This suggests that instead of sulphide, this animal incorporates sulphate via symbiotic bacteria or by filter-feeding POM (generally $\delta^{34}S$ 17‰ to 21‰). Interestingly, this species was also shown to have the most negative $\delta^{15}N$ total SBOM values of all thiotrophs (-3.3‰ ±2.2, n=4, see Fig. 3.9), and $\delta^{13}C$ total SBOM values are as expected for thiotrophic chemosymbiosis ($\delta^{13}C$ -32.9‰ ±2.2, n=4). The precise nutritional strategy of this species therefore remains unclear.

Sulphur – comparison between families. Vesicomyidae have a wide range of $\delta^{34}S$ values (-24.3‰ to +4.6‰, and +17.7‰), whereas all lucinid specimens have $\delta^{34}S$ values of -10‰ or lower at the three localities (-18.1, ±6.4, n=12). Similar ^{34}S depleted values were found for a cold seep thyasirid (-19.1‰), and potentially cold seep solemyids (-6.7‰, resin obtained). *Bathymodiolus* $\delta^{34}S$ values are not depleted beyond -10‰ in our dataset. Although it is difficult to draw conclusions without known $\delta^{34}S$ values of local sulphide. The obvious difference between Vesicomyidae/Mytilidae and Lucinidae/Thyasiridae/Solemyidae is the infaunal lifestyle of the latter families, versus a (semi)epifaunal lifestyle of the other two families. Within the sediment the sulphide concentrations are higher, due to the sulphate-methane transition zone. At deep-sea cold seeps the sulphate-methane transition zone has a thickness of only a few centimetres (e.g. Fisher et al., 2012; Felden et al., 2014), and potentially there is less mixing between the various sulphur sources within this zone, which could lead to more depleted $\delta^{34}S$ values of sulphide in the sediment.

San Diego Trough. Compared to the rest of the dataset, the thiotrophic specimens/species from San Diego Trough are very different to other taxa, and are also different from each other (indicated as black circles in Fig. 3.9). Whilst the isotopic total SBOM values of a single *E. elongata* specimen ($\delta^{13}C$ -22.1‰, $\delta^{15}N$ +10.0‰, $\delta^{34}S$ 4.3‰ resin obtained) clearly suggest a heterotrophic lifestyle, the values for a solemyid specimen ($\delta^{13}C$ -26.7‰, $\delta^{15}N$ +13.9‰, $\delta^{34}S$ -6.7‰ resin obtained) are conflicting. The lucinid from this locality ($\delta^{13}C$ -29.1‰, $\delta^{34}S$ -25.3‰) appears to mainly rely on chemosynthesis-based nutrition. It is unclear what nutritional or environmental factors could produce these apparently conflicting isotopic values. Potentially the locality is limited in dissolved inorganic nitrogen, and the required filter-feeding to obtain sufficient nitrogen is also reflected in total SBOM carbon values. Due to the small number of specimens, it is unclear how much of the variation can be attributed to family specific differences.

3.4.1.3 Dual symbiosis

Dual symbiotic mussels harbour thiotrophic and methanotrophic bacteria, which means that they can use both CO_2 and methane as carbon sources, as well as retain the ability to filter feed POM. This can be beneficial when animals need to adapt to changes environmental conditions, and provides the possibility of partitioning and co-operation of resources between the different symbionts (Duperron et al., 2007). To be able to compare variation in SBOM to variation in

environmental sources, SBOM/soft tissues were predicted using local methane values and total SBOM values of thiotrophic bivalves from the same locality. Nitrogen and sulphur sources for chemosymbiotic bivalves are discussed in section 3.4.1.1.

Table 3.9 Dual symbiotic species: calculated and measured $\delta^{13}C$ values for total SBOM and shell carbonate values

Calculated $\delta^{13}C$ SBOM is based on 50% contribution of local methane sources (Table 3.3), and 50% fractionation of DIC, for which the average $\delta^{13}C$ value of thiotrophic specimens from the same locality (Table 3.8) was used. Calculations for shell carbonate are given at Table 3.7. Calculations using soft tissue values are between brackets in the table.

Specimen	**Calculated $\delta^{13}C$ SBOM**	**$\delta^{13}C$ SBOM**	**Remarks SBOM/ soft tissues**	**Calculated $\delta^{13}C$ shell**	**$\delta^{13}C$ shell** (% metabolic carbon)	**Remarks**
Cold seeps						
B. heckerae, adult (Florida Escarpment)	-62 to -46	**-60.2**	low end or mean of calculated range			
	-62 to -46	**-62.2**		-4.3	**-2.9** (7.5%)	enriched DIC or lower % metabolic C
	-62 to -46	**-54.6**		-3.6	**-2.0** (7%)	
	-62 to -46	**-58.0**				
	-70 to -54	[-69.2]				
	-70 to -54	[-65.8]				
B. heckerae, juvenile (Florida Escarpment)	-62 to -46 [-70 to -54]	**-35.6** [-65.3]	SBOM more enriched than calculated, soft tissues	-1.7 [-4.6]	**-1.0** (8%)	enriched DIC or lower % metabolic carbon
	-62 to -46 [-70 to -54]	**-42.9** [-66.0]		-2.4 [-4.7]	**-1.5** (8%)	
	-62 to -46 [-70 to -54]	**-30.2** [-66.9]		-1.1 [-4.8]	**-2.5** (15%)	depleted DIC or

	-62 to -46 [-70 to -54]	**-30.2** [-67.3]	at low end of the range	-1.1 [-4.8]	**-2.6** (15%)	higher % metabolic carbon
	-62 to -46 [-70 to -54]	**-37.7** [-65.9]		-1.9 [-4.7]	**-2.0** (10%)	as expected
B. heckerae (Blake Ridge)	-54.6 to -46.4	**-42.4**	SBOM more enriched than calculated, soft tissues more depleted	-2.2	**0.0** (4.5%)	enriched DIC or lower % metabolic carbon
	-54.6 to -46.4	**-36.4**		-1.6	**1.2** (2%)	
	[-54.7 to -49.4]	[-55.6]				
	[-54.7 to -49.4]	[-58.3]				
	[-54.7 to -49.4]	[-56.6]				
Bathymodiolus sp. (Barbados)	insufficient data available	**-64.4**	n/a	-4.4	**-3.4** (8.5%)	slightly depleted DIC or lower % metabolic C

Data for dual symbiotic *Bathymodiolus* could only be compared between Florida Escarpment and Blake Ridge, and statistical isotopic differences exist between them. Total SBOM of Florida Escarpment specimens is more depleted in carbon ($\delta^{13}C$: -58.7‰ ±3.3, n=4) than Blake Ridge (-39.4‰ ±4.3, n=2), as well as in nitrogen ($\delta^{15}N$: -7.7‰ ±0.3, n=3 vs. 2.6‰ ±0.9, n=3). Sulphur values are only known from soft tissues, and are slightly more positive for Florida Escarpment ($\delta^{34}S$ 10.7, n=1), than Blake Ridge (8.4 ±0.7, n=3). $\delta^{34}S$ values show that *B. heckerae* at neither locality are completely dominated by thiotrophic bacteria (> +5‰ threshold).

The significant depletion in carbon values for Florida Escarpment could be related to the more depleted methane values at this location (Table 3.3). For dual symbiotic species however, the relationship with environmental sources is

complicated because SBOM isotopic values can also be affected by the relative abundance of the two bacterial types. And their ratio has been suggested to vary according to availability of methane and/or sulphide (Trask and Van Dover, 1999; Salerno et al., 2005). In addition, there are complicated fractionation effects related to microbial-host interactions and translocation of nutrients. Relatively enriched $\delta^{13}C$ SBOM values could therefore also be explained to a higher abundance of thiotrophic bacteria. In addition, thiotrophic bacteria could incorporate CO_2 produced by the co-occurring methanotrophs, which will be isotopically lighter than seawater CO_2 (Fisher, 1996).

The relatively depleted $\delta^{13}C$ value (-64.4‰) of *Bathymodiolus* sp. with unknown strategy, suggests a very depleted methane source and/or a high abundance/reliance on methanotrophic bacteria. Nitrogen values ($\delta^{15}N$ 0.2‰ to 0.8‰, n=3) do not provide additional nutritional information. This species could therefore be either methanotrophic or dual symbiotic, and will only be further discussed when both nutritional groups are combined for statistical comparisons.

Ontogenetic effects. Specimens from a juvenile and an adult age group could be compared for *B. heckerae* from Florida Escarpment. The total SBOM $\delta^{13}C$ values of juvenile *B. heckerae* (-35.3‰ ±5.4, n=5) is very enriched compared to adult *B. heckerae* (-58.7‰ ±3.3, n=4), whilst soft tissues encompass similar isotopic ranges (-67.5‰ ±2.4, adult, n=2 and -66.3‰ ±0.8, juvenile, n=5). For nitrogen the same enrichment can be seen in total SBOM between adult ($\delta^{15}N$ -7.7‰ ±0.3, n=3) and juvenile (1.1‰, n=1), and not between soft tissues of the two age groups(adult: -10.1‰, n=1 / juvenile: -9.8‰ ±2.4, n=4). Soft tissue $\delta^{34}S$ data is also similar between the juvenile and adult specimens, unfortunately SBOM data cannot be compared.

In summary, the total SBOM isotopic values ($\delta^{13}C$, of juvenile specimens are significantly enriched compared to adult specimens, but

Is the difference between the age groups caused by a physiological difference in ΔSBOM-ST, or does the SBOM from the juvenile specimens reflect a previous nutritional strategy of filter feeding? The soft tissue values represent a shorter time period and have already undergone (partial) turn-over, which is known to occur within weeks or months (e.g. Hill et al., 2009), whilst metabolic inactive shells integrate the sources used throughout their entire lifespan when homogenized for SBOM extraction (Versteegh et al, 2011). However, study of post-larval and juvenile

species of *Bathymodiolus azoricus* and *Bathymodiolus heckeri* showed well-developed symbionts populations and no evidence of residual POC based tissues (Salerno et al., 2005). In addition, there are indications that for (very) small shells, soft tissues and SBOM are isotopically very different (section 3.4.2.3). In particular, collated *P. floridensis* limpets from this locality have the same isotopic values, as well as differences between soft tissues and SBOM, as the juvenile *B. heckerae* specimens.

3.4.1.4 Heterotrophy

Heterotrophic bivalves rely on suspended or particular organic matter (POM), derived from phytoplankton that fix seawater DIC photosynthetically. Because the RubisCO involved in this process has different characteristics than the RubisCO used by thiotrophic bacteria, there is less fractionation in carbon (see Ruby et al., 1987; Blumenberg, 2010) and the $\delta^{13}C$ of POM generally varies between -18.5‰ and - 22‰ (Hoefs et al., 2015). For heterotrophic species present at cold seeps and hydrothermal vents potential nutritional sources includes photosynthetically fixed POM that rains down to the deep sea from the surface waters (Hoefs et al., 2015). In addition, they can feed on organic carbon/matter synthesized from DIC by chemoautotrophic bacteria, or the bacteria themselves, which will be ^{13}C depleted. With increasing depth the reliance on chemosynthetically derived material is likely to become greater, and chemosynthetic production may be a significant source of nutrition to heterotrophs found there in an otherwise nutrient-poor deep ocean (Carney 1994). For $\delta^{13}C$ the threshold for local chemosynthethically produced carbon is usually placed at low $\delta^{13}C$ values (< −25‰). In contrast, fauna that depend on photosynthetically fixed carbon would have tissue $\delta^{13}C$ values that are enriched relative to these other sources (e.g., −25‰ to −15‰, (Fry and Sherr, 1984).

For nitrogen and sulphur a similar distinction between reducing and non-reducing environments is suggested. Heterotrophic species from non-reducing environments are expected to reflect POM ($\delta^{15}N$ 0‰ to 15‰, $\delta^{34}S$ +15‰ to +20‰), whereas heterotrophs at reducing environments (shallow reducing environments, cold seeps, hydrothermal vents) can also feed on locally produced organic matter or chemoautotrophic bacteria, and reflect the isotopically depleted values of those sources.

Table 3.10 Heterotrophic species: calculated and measured $\delta^{13}C$ values for total SBOM and shell carbonate values

(p. 137-139) Calculated $\delta^{13}C$ total SBOM values are based on the formula: [POM source value + 1% trophic enrichment] (these can be found in Table 3.3). Calculations for shell carbonate values are given at Table 3.7. Calculations using soft tissue values are between brackets in the table, underlined specimens are multiple specimens that have been collated.

Specimen	**Calculated $\delta^{13}C$ SBOM**	**$\delta^{13}C$ SBOM**	**Remarks SBOM/ soft tissues**	**Calculated $\delta^{13}C$ shell**	**$\delta^{13}C$ shell** (% metabolic carbon)	**Remarks**
Cold seeps						
P. floridensis	-66.9 to -24.3	**-36.8** [-66.1]	SBOM as expected, ST low end of the range	**-1.8** [-4.7]	**-8.3** (more similar to tissues) (28% / 15%)	depleted DIC or higher % metabolic C
Delectopecten (San Diego Trough)	-21.0 to -17.5	**-19.3**	as expected	0.1	**1.1** (4.5%)	enriched DIC or lower % metabolic C
Hydrothermal vents						
L. elevatus (East Wall)	-21.0 to -17.5	**-20.6** [-15.4]	SBOM as expected, ST enriched			
Shallow reducing environments						
A. alba (Gåsevik)	-21.0 to -17.5	**-24.6** [-18.8]	ST as expected, SBOM depleted	0.9 [1.5]	**-0.4** (15%)	depleted DIC or higher % metabolic C
E. tenuis (Gåsevik)	-21.0 to -17.5	**-21.5**	slightly depleted	1.2	**0.9** (11.5%)	
Shallow non-reducing environments						
T. sanguinea (Big Hope Bay)	-21.0 to -17.5	**-23.9** [-18.1]	SBOM and ST are largely within the expected range	1.0 [1.5]	**0.9** (10%)	as expected
	-21.0 to -17.5	**-21.2** [-17.4]		1.3 [1.6]	**1.4** (9.5%)	
	-21.0 to -17.5	**-20.4** [-19.0]		1.3 [1.4]	**0.4** (14%)	depleted DIC or higher % metabolic C
	-21.0 to -17.5	**-20.4** [-21.4]		1.3 [1.2]	**0.6** (14%)	

	-21.0 to -17.5	**-20.7**		1.3	**1.8** (8.5%)	slighty enriched DIC or lower % metabolic C
T. sanguinea (Tricky Cove)	-22.5	**-21.5** [-18.4]	SOM and ST generally more enriched than expected	1.2 [1.5]	**1.3** (9.5%)	as expected
	-22.5	**-23.9** [-18.1]		1.0 [1.5]	**1.2** (10.5%)	
	-22.5	**-17.5** [-17.5]		1.6 [1.6]	**1.2** (12%)	depleted DIC or higher % metabolic C
	-22.5	**-19.8**				
	-22.5	**-20.8** [-18.5]		1.3 [1.5]	**1.6** (8.5%)	ST as expected
	-22.5	**-20.8** [-19.4]		1.3 [1.4]	**1.6** (8.5%)	
	-22.5	**-20.4** [-18.5]		1.3 [1.5]	**1.7** (8%)	
N. nigricans (Tricky Cove)	-22.5	**-26.3**	SBOM around expected value, ST more enriched	0.7	**1.5** (7%)	slighty enriched DIC or lower % metabolic C
	-22.5	**-20.8** [-19.4]		1.3 [1.4]	**1.2** (10%)	as expected
	-22.5	**-19.2** [-19.0]		1.4 [1.5]	**1.4** (10%)	
	-22.5	**-25.0** [-19.1]		0.9 [1.4]	**1.6** (7%)	ST as expected
	-22.5	**-20.2** [-18.3]		1.2 [1.5]	**1.6** (8.5%)	
L. neozalanica (Tricky Cove)	-22.5	**-21.0**	SBOM around expected value, ST more enriched	1.3	**2.7** (3.5%)	enriched DIC or lower % metabolic C
	-22.5	**-21.7** [-16.9]		1.2 [1.7]	**2.9** (2.5%)	
	-22.5	**-21.4** [-16.7]		1.2 [1.7]	**2.8** (4%)	
	-22.5	**-22.8**		1.1	**2.4** (4.5%)	

	-22.5	**-22.0** [-14.4]		1.2 [1.9]	**2.4** (5%)	
	-22.5	**-20.2**				
	-22.5	**-21.6**				
L. uva (Tricky Cove)	-22.5	**-23.7**		1.0	**2.4** (4%)	enriched DIC or lower % metabolic C
	-22.5	**-22.9**		1.1	**1.4** (8.5%)	
	-22.5	**-21.9** [-17.7]		1.2 [1.6]	**2.2** (5.5%)	
C. edule (Dorset, UK)	-21.0 to -17.5	**-19.6**	low end of the range	1.4	**-0.5** (19%)	depleted DIC or higher % metabolic C
	-21.0 to -17.5	**-22.2**		1.1	**-1.1** (19.5%)	
R. decussatus (Wales)	-21.0 to -17.5	**-20.8**	low end of the range	1.4	**0.0** (16.5%)	
	-21.0 to -17.5	**-21.2**		1.2	**-1.4** (22%)	
M. edulis (Southern France)	-21.0 to -17.5	**-16.0**	high end of the range	1.8	**0.6** (16.5%)	
	-21.0 to -17.5	**-17.5**		1.6	**0.4** (16.5%)	

The large $\delta^{13}C$ difference between the cold seep limpet *Paralepetopsis* (-36.8‰ / soft tissues -66.1) and scallop *Delectopecten* (-19.3‰) from San Diego Trough is likely caused by the former species feeding on organic matter that was locally synthesized and based on depleted biogenic methane, which is in agreement with values from sedimentary organic matter (up to -67.9‰ depleted) from Florida Escarpment (Paull et al., 1992). Another source could be free-living bacteria themselves, known to be eaten by deep sea gastropods (references in Reid et al., 2013). *Delectopecten* has a value expected for animals feeding on POM, this can also be concluded for *Lepetodrilus elevatus*, a $\delta^{13}C$ total SBOM: –20.6‰, and soft tissues values of -15.4‰. Total SBOM $\delta^{15}N$ also confirms a reliance on locally produced nitrogen (< −6‰ $\delta^{15}N$) for *P. floridensis* (3.3‰), and soft tissue values are even more depleted (-10.1‰). Whereas *Delectopecten* sp. has a total SBOM $\delta^{15}N$ value of 16.1‰. Soft tissue $\delta^{34}S$ for *P. floridensis* has a value of $\delta^{34}S$ 4.6‰, is also in agreement with indirect incorporation of hydrogen sulphide via chemoautotrophic bacteria.

Unlike cold seeps and hydrothermal vents, shallow environments are not driven by chemosynthethic production. $\delta^{13}C$ values obtained from *A. alba* (total SBOM: -24.6, soft tissue: -18.8‰) and *E. tenuis* (total SBOM: -21.5‰) reflect values of photosynthetically derived POM, as do the positive nitrogen values. The negative $\delta^{34}S$ soft tissues value of *A. alba* (-4.7‰) is unexpected, and could be caused by a depleted sulphate source, e.g. when sulphide produced during AOM is oxidized back to sulphate (Aharon & Fu, 2003). This is plausible because the animal lives infaunally, where mixing of seawater sulphate is limited (Yamanaka et al., 2000).

As expected, the brachiopod taxa occupy very different ranges compared to the taxa from reducing environments (overview Figure): total SBOM carbon values are similar to shallow reducing environments ($\delta^{13}C$ -21.5‰ ±1.8, n=27), but sulphur (total SBOM: +13.3‰, n=1, and soft tissues 15.8‰ ±2.5, n=14) and nitrogen (8.6‰ ±1.0, n=18) are distinctly more positive, and not influenced by chemosynthesis.

3.4.2. What is the isotopic relationship between total SBOM and soft tissues?

3.4.2.1 Isotopic variation between soft tissues

The success of SBOM as a nutritional proxy is generally determined by its similarity to related soft tissues values. However, the variation between soft tissue values of individual specimens (intra-individual variation) is rarely taken into account, and this must be discussed before SBOM is compared to soft tissues as a single mean value. Box-and-whisker plots of the isotopic variation in SBOM and soft tissues of species are given in Figure. 3.6. These plots show that intra-specific and intra-individual soft tissue variation is generally less than 1‰ for $\delta^{13}C$ and $\delta^{15}N$, but that intra-individual variation is generally greater by ~ +0.5‰ than between intra-specific variation. For species for which both statistics were obtained, the intra-individual variation was greater for $\delta^{13}C$ in 10 out of 16 species for, and for $\delta^{15}N$ in 11 out of 13 species. It should also be noted that the highest intra-specific SBOM/soft tissue variation is shown for *B. manusensis*, and in this species an obvious outlier was observed (section 3.3.1.10). For sulphur both statistics show very large variation compared to carbon and nitrogen: half of the data has variability of 1‰ to 3‰ or higher, and the intra-individual variation can be as large as 6‰ in our dataset. Intra-individual variation was greater than intra-specific variation for sulphur in 6 out of 9 species. The maximum variation between soft tissues of an individual specimen can even be up to 6‰ for $\delta^{13}C$, up to 4‰ for $\delta^{15}N$, and up to 8‰ for $\delta^{34}S$. These

observations show that when comparing individual SBOM to individual mean soft tissues values, the latter underestimates the actual isotopic variation of soft tissues.

Figure 3.6 Box-and-whisker plots showing the intra-specific and intra-individual isotopic variation in SBOM and soft tissues

Isotopic variation is shown for the stable isotope composition of SBOM in the same species (S.D., "Intra-specific SBOM"), the mean soft tissue values of the same species (S.D., "Intra-specific ST"), the variation between different soft tissues in individuals of the same species (mean of individual S.D's, "Intra-individual ST"), and the maximum intra-individual variation per species: calculated as the Intra-individual ST + Intra-individual ST S.D. ("Max. Intra-indiv. ST"). In the plots, the horizontal line represents the median, and the limits of the box and whiskers contain 50% and 100% of the data, respectively, unless in the case of outliers. These are shown separately as asterisks, and fall outside the 1.5*inter-quartile range (which is then indicated by the length of the whiskers). SBOM data was only used from species with associated soft tissue data.

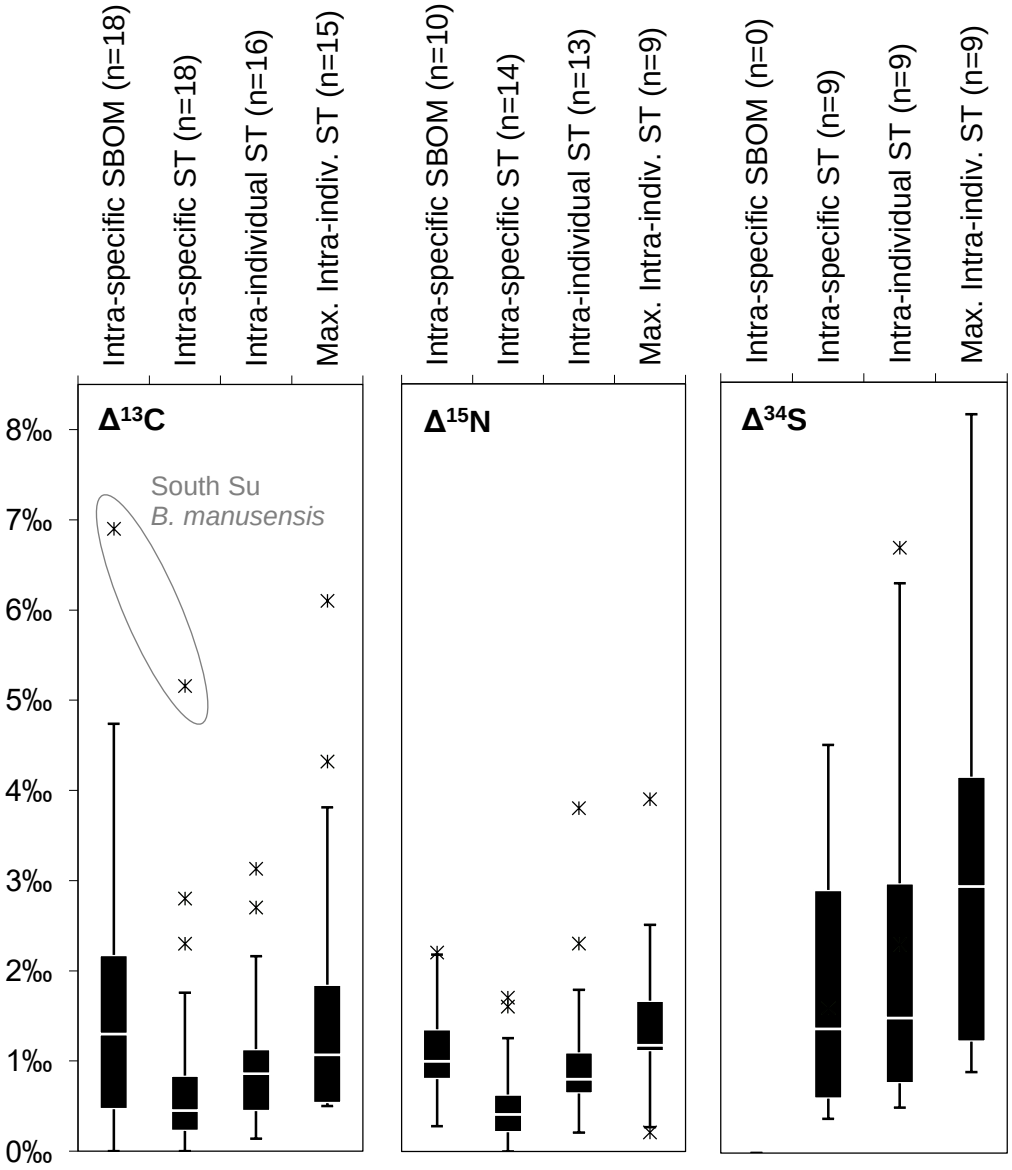

Table 3.6 shows the isotopic relationship between soft tissue of individual specimens. For the large majority of the species investigated there is an obvious order between gills vs. other tissues (mantle, foot, and/or muscle) for all specimens: either consistently enriched or consistently depleted for ^{13}C, $\delta^{15}N$, and $\delta^{34}S$. Of the chemosymbiotic taxa sufficient data (multiple tissues for a minimum of two specimens) was only available for thiotrophic species (excl. juveniles). For the large majority of these species gills have depleted values for $\delta^{13}C$ (8 out of 11) and $\delta^{15}N$ (9 out of 9), and are enriched in $\delta^{34}S$ (4 out of 6). 'Rest' has the same isotopic relationship compared to other soft tissues as 'gills', with the exception of enriched $\delta^{15}N$ values in *V. venusta*. Compared to the gills, muscle tissue is often on the opposite end of the range of values for all isotope systems. For all brachiopods species, the gills generally have depleted values for $\delta^{13}C$ (3 out of 3), and show an enrichment in $\delta^{15}N$ (3 out of 3). In general, these isotopic difference between soft tissues should be taken into account when comparing soft tissues to SBOM values, because the use of a single type of soft tissue can confound interpretations of the SBOM-soft tissue relationship. Our study shows that the most similar soft tissue depends on the order of depletion within individual specimens, as well as the relationship between SBOM and mean soft tissue (discussed in section 3.4.2.2)

The enriched $\delta^{15}N$ and $\delta^{13}C$ values of 'other tissues' in chemosymbiotic taxa are consistent with a trophic level enrichment ($\delta^{15}N$ +3.4‰, $\delta^{13}C$ +1‰, DeNiro & Epstein, 1878) of organic material derived from gill symbionts, and the 'rest' (visceral mass) mainly contains stomach contents (Fisher, 1990; Van Dover et al., 2003; Geist et al., 2005). It could be hypothesized that the species in which no trophic enrichment was found, the host relies on metabolic by-products instead of consuming the symbionts as true primary consumers. Trophic level differences are not associated with isotopic changes in sulphur (Michener et al., 2007) and do not explain the $\delta^{34}S$ enrichment of the gills/rest. The $\delta^{13}C$ in the gills could also be linked to the presence of the symbionts, as bacteria pellets were shown to have more depleted values than the gills that house them (Van der Geest et al., 2014). There are however several other explanations for isotopic variability between tissues in addition to trophic level differences. These possibilities are outlined in detail in Chapter 2, but cannot be investigated further within the scope of this study because detailed information about tissue composition and organism physiology is lacking.

3.4.2.2 The isotopic relationship between total SBOM and soft tissues

For carbon and nitrogen, the isotopic variation in SBOM is generally greater than for mean soft tissue values (Fig. 3.5), which is in part caused by averaging multiple soft tissues (as evident from the higher intra-individual variation). The different time periods represented by SBOM and soft tissues could also be of influence. If the nutritional sources used by bivalves change isotopically, this will be reflected in the soft tissues within months, whilst the shells integrate the sources used throughout their entire lifespan, which can be up to 15-30 years for the seep clam *C. kilmeri* (Barry et al., 2007) and at least several decades for *B. childressi* (Nix et al., 1995). Therefore, direct calculations between shell and soft tissue isotopic values are difficult (Versteegh et al., 2011).

The isotopic offset between SBOM and soft tissues ($\Delta_{SBOM-ST}$) is shown in Fig. 3.7. The plots for $\delta^{13}C$ and $\delta^{15}N$ appear to show an evolving relationship between total SBOM and $\Delta_{SBOM-ST}$, from total SBOM being more enriched than soft tissues for $\delta^{13}C$ < -25‰ / $\delta^{15}N$ < 5‰, and generally more depleted for values below that threshold.

Figure 3.7 Isotopic relationship between total SBOM and soft tissues for individual specimens

Isotopic differences between total SBOM and mean soft tissue values ($\Delta_{SBOM-ST}$) of individual specimens (per species) are plotted as the average difference (+ S.E.M.) for $\delta^{13}C$ and $\delta^{15}N$. For $\delta^{34}S$, individual specimens (10%HCl) are used: mean difference, and min. and max. difference between SBOM and various soft tissues. Key shown in Fig. 3.9, outlined symbols: Mae et al (2008, vent) and Dreier et al (2012, shallow) (both using EDTA), in addition heterotrophic bivalves from Chapter 2 are shown.

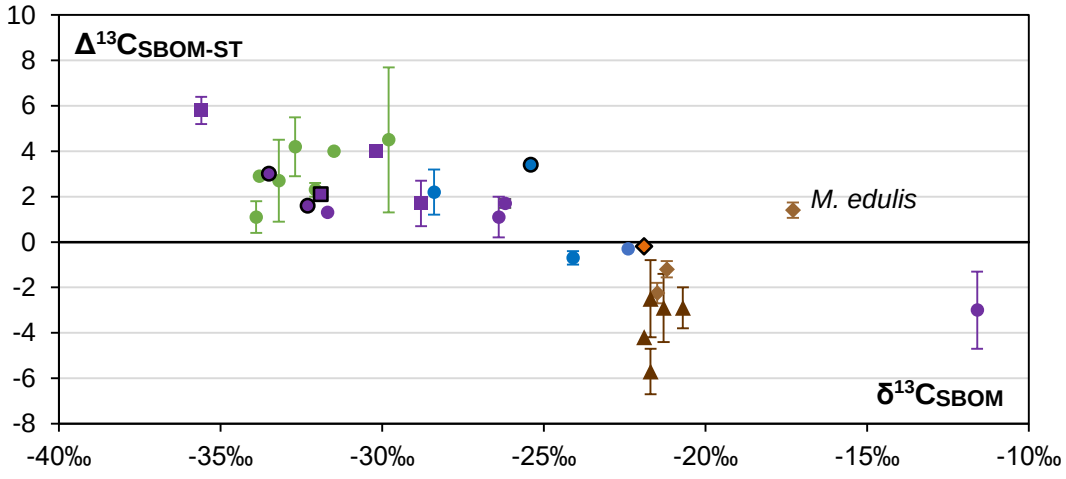

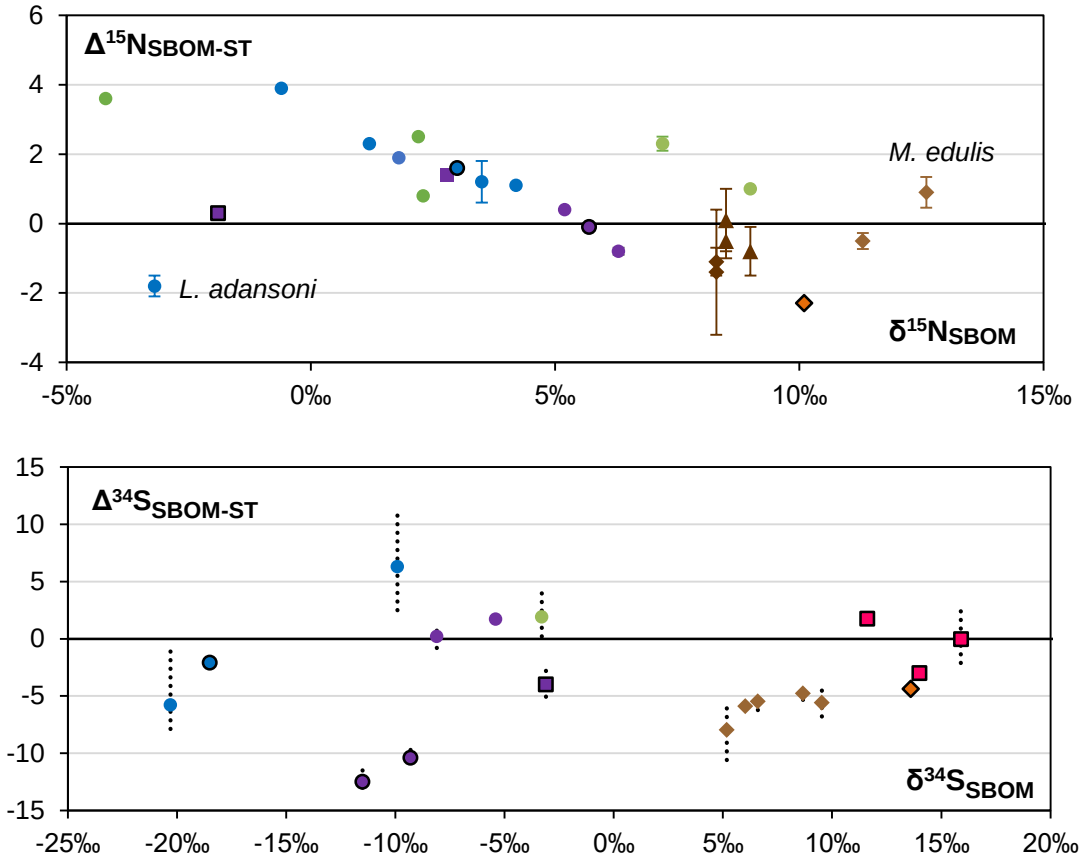

The plots have R-squared values of 0.61 for $\delta^{13}C$ (without *M. edulis*: 0.70), and 0.23 for $\delta^{15}N$ (excluding *L. adansoni*: 0.56), respectively. It is unlikely that this trend is caused by the isotopic effects of residual cation exchange resin, because the resin has a $\delta^{13}C$ value of -29.0‰ and it would be expected to find $\Delta_{SBOM–ST}$ = 0 around that value. In the case of nitrogen, the range of $\Delta_{SBOM–ST}$ encompasses a trophic level difference of $\delta^{15}N$ 3.4‰, and could potentially confound ecological interpretations. Published data is generally in agreement with our observations. In Chapter 2 a difference in $\delta^{13}C$ and $\delta^{15}N$ $\Delta_{SBOM–ST}$ was found between *M. edulis* (SBOM enriched compared to soft tissue values) vs. *R. decussatus* and *C. edule* (SBOM depleted compared to soft tissue values), and potentially related to the combined mineralogy of *M. edulis* shell (calcite and aragonite) compared to the aragonitic shells of the other two species. *Bathymodiolus* species from this study also belong to the Mytilidae family and share the shell mineralogy of *M. edulis*, but no obvious $\Delta_{SBOM–ST}$ enrichment is observed compared to the aragonitic shells of other chemosymbiotic taxa (*Bathymodiolus* does have the largest $\Delta_{SBOM–ST}$ of +5.8 ±0.6, n=2). Contrarily, for the completely calcitic shells of filter-feeding brachiopods SBOM can be more depleted for $\delta^{13}C$ and $\delta^{15}N$ than *R. decussatus* and *C. edule*.

Furthermore, it is interesting that a similar evolving relationship is observed for total SBOM versus intra-crystalline SBOM $\delta^{13}C$ and $\delta^{15}N$ data (Fig. 3.10). Potentially the presence of this small intra-crystalline pool could influence $\Delta_{SBOM–ST}$ towards the observed offsets, and hypothetically the inter-crystalline pool would be more similar to soft tissue values.

For $\delta^{34}S$ ΔSBOM–ST no obvious trend can be observed in relation to $\delta^{34}S$ of total SBOM, but very large (mostly negative) off-sets > 5 per mille are present. Moreover, this relationship can vary between different soft tissues by > 5 per mille, this is in agreement with the large intra-specific and intra-individual sulphur stable isotope variation (Fig. 3.6). Because of the unpredictable nature of $\Delta_{SBOM–ST}$, a likely scenario is that shell removal techniques influence the sulphur isotope composition of SBOM, as was also discussed in Chapter 2.

3.4.2.3 Isotopic relationship between total SBOM and soft tissues for collated specimens

For the very small species in our suite of samples it was necessary to collated multiple specimens (> 2) to obtain sufficient shell material (Table 3.1). SBOM and soft tissue data for these species was obtained for $\delta^{13}C$ and $\delta^{15}N$ (no $\delta^{34}S$ data available), and large isotopic differences were noted between the different organic pools, plotted in Fig. 3.8. This figure also includes the large $\Delta_{SBOM–ST}$ noted for juvenile *B. heckerae* individual specimens from Florida Escarpment.

One explanation for the extreme off-sets is that the SBOM of the species represents a different nutritional strategy than the soft tissues. Whilst SBOM (shell powder) of multiple specimens can be easily homogenized, it is much more difficult to homogenize soft tissues. This could be an explanation for e.g. *M. spinifera* and *V.* cf. *kaikoi* enrichment, where be the soft tissue reflect a chemosymbiotic ($\delta^{13}C$/ $\delta^{15}N$ depleted) lifestyle, and SBOM reflects a mixture of chemosymbiotic and filter feeding ($\delta^{13}C$/ $\delta^{15}N$ enriched). This would be in agreement with the limited offset for *T. sarsi*, because thyasirids are more reliant on symbionts and it is less likely that SBOM reflects filter-feeding values.

Figure 3.8 Isotopic relationship between collated total SBOM and soft tissues

Isotopic differences between total SBOM and mean soft tissue values (ΔSBOM–ST) are plotted as the average difference for $\delta^{13}C$ and $\delta^{15}N$. Key shown in Fig. 3.9.. Juvenile *B. heckerea* is also included, as well as values from Fig. 3.7 (in grey).

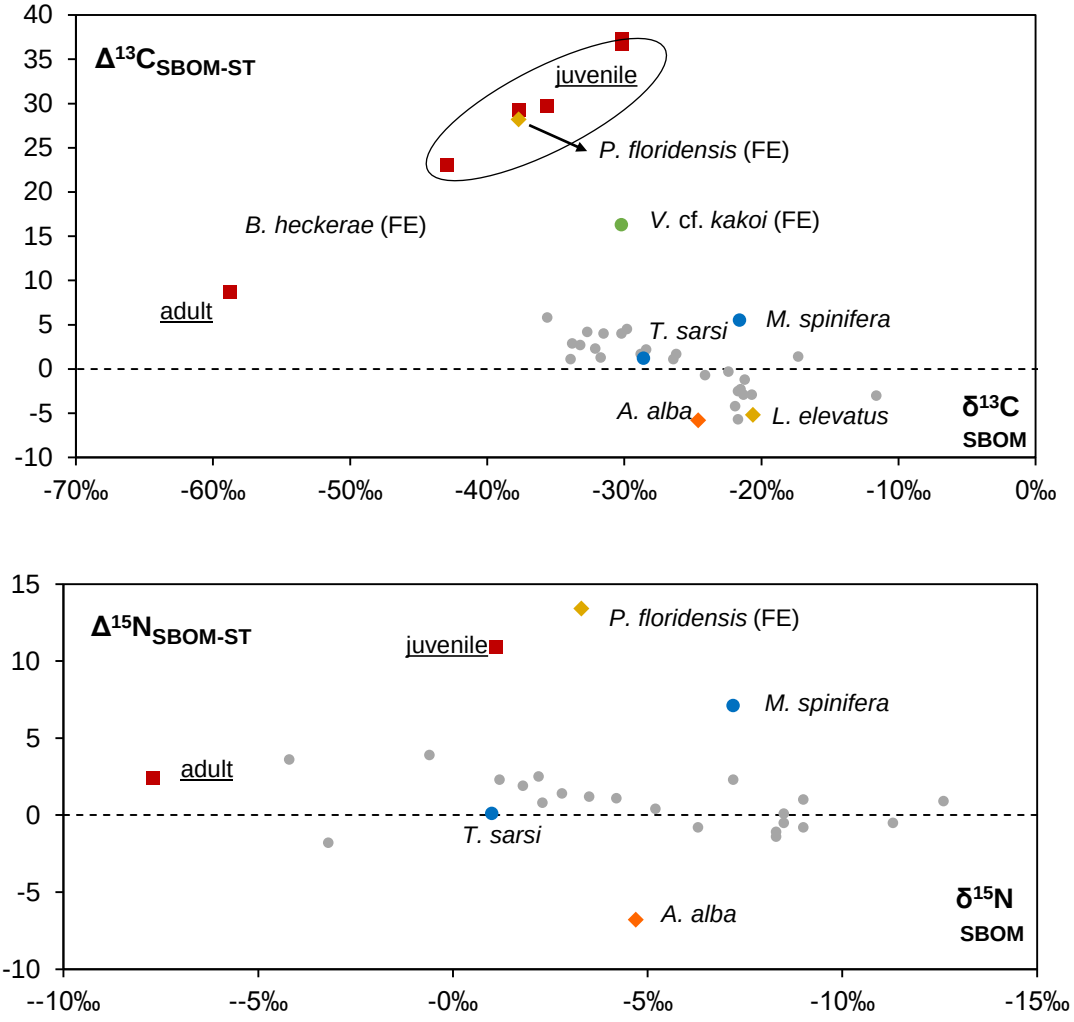

For juvenile *B. heckerae* the two different nutritional strategies appear to be reflected in the soft tissues (chemosymbiosis) and SBOM (filter-feeding) of the individual specimens (section 3.4.1.3). However, the same differences are observed for *P. floridensis*, and would mean a change from filter-feeding to active grazing/digesting bacteria. There is also no known lifestyle change for heterotrophic taxa (*A. alba* and *L. elevatus*), and the negative ΔSBOM–ST is most likely physiological. Therefore, SBOM of collated or juvenile specimens should be cautiously used.

3.4.3 Can different nutritional strategies be identified using total SBOM stable isotope values?

This study is based on the hypothesis that nutritional strategies will be reflected in the isotopic signature of SBOM, and moreover, that these signatures are distinct. An overview of all data from this study is shown in Figure 3.9.

3.4.3.1 Cold seeps

Mollusc species that live at cold seeps can use one of several nutritional strategies: methanotrophy, thiotrophy, dual symbiosis or heterotrophy. Our data shows that a thiotrophic lifestyle ($\delta^{13}C$ -31.6‰ ±2.7, n=51, localities=8), can be differentiate from dual symbiosis/methanotrophy ($\delta^{13}C$ -53.5‰ ±7.9, n=18, localities=4) at cold seeps ($p =< 0.0001$), because of the different carbon sources used by the different nutritional strategies. Due to the large variation in methane values between different cold seeps and the strong influence of methane on the total SBOM $\delta^{13}C$ values of dual symbiotic bivalves, methanotrophic bivalves (-51.9‰ ±5.8, n=9, localities=1) cannot be statistically differentiated from dual symbiotic bivalves (-59.6‰ ±3.7, n=7, localities=2).

It is unclear whether the statistically depleted nitrogen values of either dual symbiotic (-2.6 ±5.7, n=6) or methanotrophic (-12.5‰ ±1.9, n=10) can be used to differentiate these taxa from thiotrophic species, because the ranges between dual symbiosis (-8.8‰ to 3.6‰) and thiotrophy (-4.9‰ to 13.9‰) strongly overlap, and also *B. childressi* from a previous study can have positive $\delta^{15}N$ values (Riekenberg et al., 2016). Because only one thiotrophic species has a negative $\delta^{15}N$ value (*C. kilmeri*, -3.3‰ ±2.2, n=4), the presence of methanotrophic species could be linked to utilizing a more ^{15}N depleted nitrogen source, which would very likely be ammonium. The absence of depleted $\delta^{15}N$ depleted values does however not necessarily indicate thiotrophy.

The $\delta^{34}S$ values of thiotrophic cold seep specimens are for the large majority characteristically depleted (< 5‰) (2.3‰ ±4.6, n=36) compared to dual symbiotic/methanotrophic species (11.2‰ ±2.8, n=14) due to the incorporation of ^{34}S depleted hydrogen sulphide.

Figure 3.9 $\delta^{13}C$, $\delta^{15}N$, and $\delta^{34}S$ SBOM or soft tissue data from species analysed in this study

Values are given as mean + S.D., for several species $\delta^{15}N$ and $\delta^{34}S$ soft tissue data is used when SBOM data is not available. Arrow indicates SBOM $\delta^{34}S$ value obtained using cation exchange resin. Outlined specimens are from San Diego Through (discussed in 3.4.1.2). The different letters indicate the dominant nutritional strategies: A) Heterotrophy, B) Thiotrophy, C) Dual symbiosis/methanotrophy. *C. kilmeri* values are indicated with an asterisk.

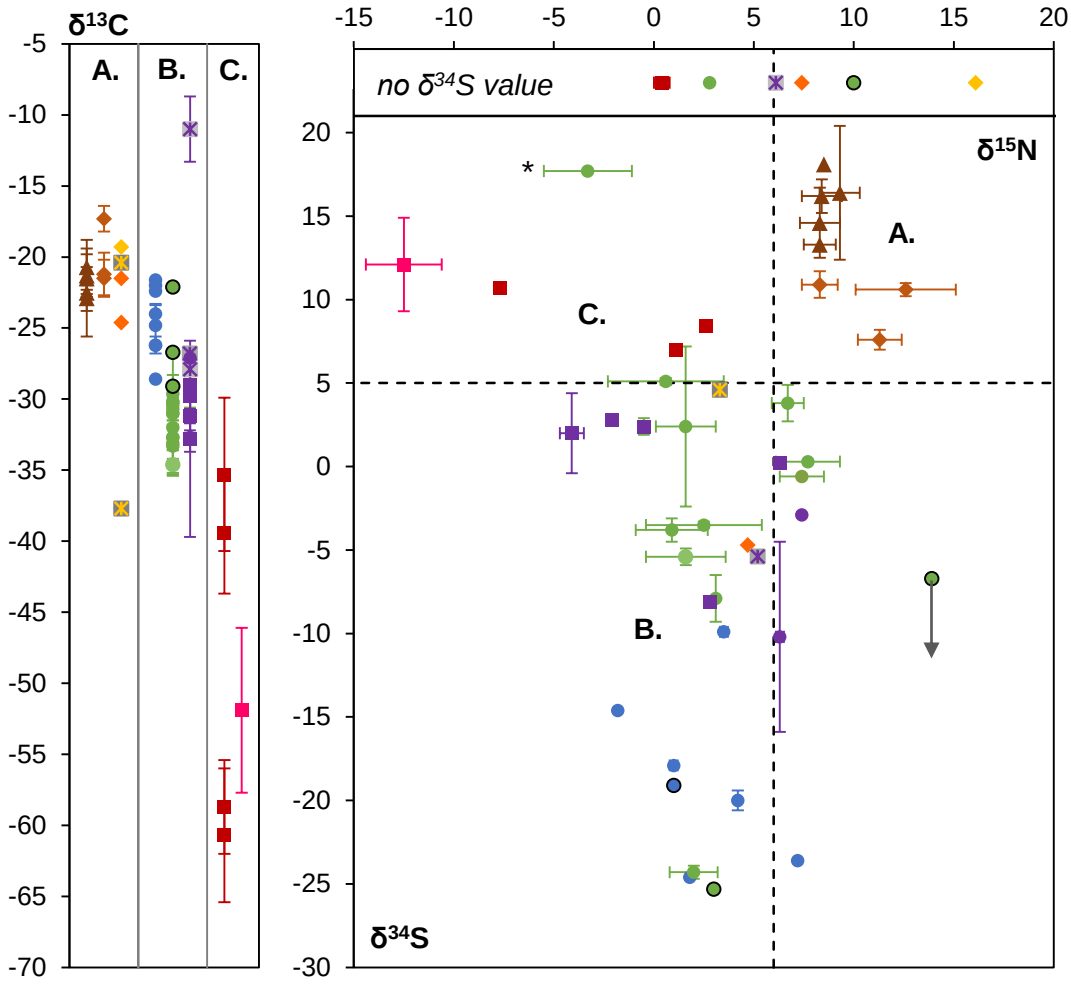

Heterotrophic species from deep sea chemosynthetic environments are not frequently collected, and were only represented by two cold seep specimens in our dataset. The nutrition of the limpet *P. floridensis* ($\delta^{13}C$ total SBOM: -36.8‰/soft tissue -66.1‰, $\delta^{15}N$ total SBOM: 3.3‰/soft tissue -10.1‰, soft tissue: 4.6‰) is strongly influenced by the local chemosynthethic sources and therefore has similar values to chemosymbiotic cold seep species. The scallop *Delectopecten* (total SBOM: -19.3‰, $\delta^{15}N$ 16.1‰) does rely on photosynthetically created organic matter, and falls therefore outside of the range of chemosymbiotic seep bivalves (-37.3 ±10.7, n=69, nutritional lifestyles=3). It is likely that *P. floridensis* can incorporate free-living methanotrophic and/or thiotrophic bacteria because of its grazing lifestyle, these values are therefore not expected for bivalves. Additional data on non-chemosymbiotic bivalves from cold seeps localities is necessary.

3.4.3.2 Hydrothermal vents

Specimens analysed from hydrothermal vents either used thiotrophy or heterotrophy as a nutritional strategy. Within the thiotrophic specimens a clear distinction can be made between species using RubisCO Form I (*Alviniconcha*, -11.6‰ ±2.3, n=3, localities=1) and Form II (-29.7 ±3.3, n=22, localities=7 - *Bathymodiolus*, Vesicomyidae, Lucinidae, *Ifremeria*) using $\delta^{13}C$ total SBOM (p=< 0.0001). The heterotrophic limpet *L. elevatus* (-20.6‰, East Wall) falls outside the range of thiotrophy using RubisCO Form I (-10.0‰ to -13.2‰) and Form II (-39.4‰ to -27.0‰), and can therefore be differentiated using total SBOM. No additional heterotrophic $\delta^{15}N$ or $\delta^{34}S$ data is available for further comparison.

3.4.3.3 Shallow reducing environments

Heterotrophic species ($\delta^{13}C$ -23.1‰ ±2.2, n=2, localities=1) cannot be differentiated from thiotrophic specimens ($\delta^{13}C$ -24.8‰ ±2.7, n=14, localitites=8) at shallow environments using $\delta^{13}C$ total SBOM. All heterotrophic total SBOM data was however obtained from collated specimens, that do not accurately reflect soft tissue values (section 3.4.2.3). Soft tissue measurements from *A. alba* ($\delta^{13}C$ -18.8‰, $\delta^{15}N$ 11.5‰, $\delta^{34}S$ -4.7‰) do not overlap with the thiotrophic ranges ($\delta^{15}N$: -3.8 to 4.3 / $\delta^{34}S$: -22.7‰ to -9.9‰). Additional total SBOM data from larger heterotrophic species is therefore required.

3.4.3.4 Comparison of nutritional strategies across environmental settings

The depleted $\delta^{13}C$ total SBOM values of dual symbiosis/ methanotrophy (-53.5‰ ±7.9, n=18, cold seeps) are statistically different from all thiotrophs in our dataset (-30.0 ±3.7, n=87, p=<0.0001), as well as all heterotrophs (-20.9‰ ±2.2, n=62, p=<0.0001). $\delta^{15}N$ values from thiotrophic bivalves from vents/shallow reducing environments however also show negative values (in addition to cold seep *C. kilmeri*) and restrict the potentially distinctive $\delta^{15}N$ values for dual symbiosis/methanotrophy to below $\delta^{15}N$ -5‰. The distinction in $\delta^{34}S$ values of dual symbiosis/methanotrophy (11.2‰ ±2.8, n=14) is however upheld in comparison to hydrothermal vents (-2.3‰ ±5.6, n=13) and shallow reducing environments (-19.6‰ ±2.7, 7,n=11). Whether it is possible to distinguish these chemosymbiotic species from heterotrophic taxa will be dependent on whether they incorporate locally produced, or photosynthetically produced organic matter (as discussed in the previous sections). In comparison to non-reducing environments, the chemosymbiotic species can clearly be identified and occupy completely different ranges (Figure 3.9). This includes the distinction between shallow reducing thiotrophic specimens ($\delta^{13}C$ -24.8‰ ±2.7, n=14, shallow reducing) and non-reducing heterotrophs ($\delta^{13}C$ -21.0‰ ±2.2, n=60) using total SBOM carbon values (p=<0.0001).

3.4.4 What is the isotopic relationship between intra-crystalline SBOM and total SBOM?

It has previously been noted that intra-crystalline SBOM stable isotope values are less closely related to the values of soft tissue/nutritional sources than total SBOM. Therefore the focus is placed on the relationship between intra-crystalline SBOM and total SBOM, instead of soft tissue values. Interestingly, Figure 3.10 shows an evolving relationship between the two SBOM pools for both $\delta^{13}C$ and $\delta^{15}N$. Compared to the depleted total SBOM values for seep bivalves, the intra-crystalline value is generally more enriched – particularly for the most depleted values of methanotrophic/dual symbiotic specimens. However, around $\delta^{13}C$ -27‰ / $\delta^{15}N$ +5‰ total SBOM this relationship changes, and intra-crystalline values become more depleted than total SBOM.

Figure 3.10 Isotopic relationship ($\delta^{13}C$, $\delta^{15}N$) between total SBOM and intra-crystalline SBOM for individual specimens

Specimens are ordered by total SBOM value, the key for nutritional strategies is given in Figure 3.9. Methane source values for methanotrophic bivalves are indicated with grey bars.

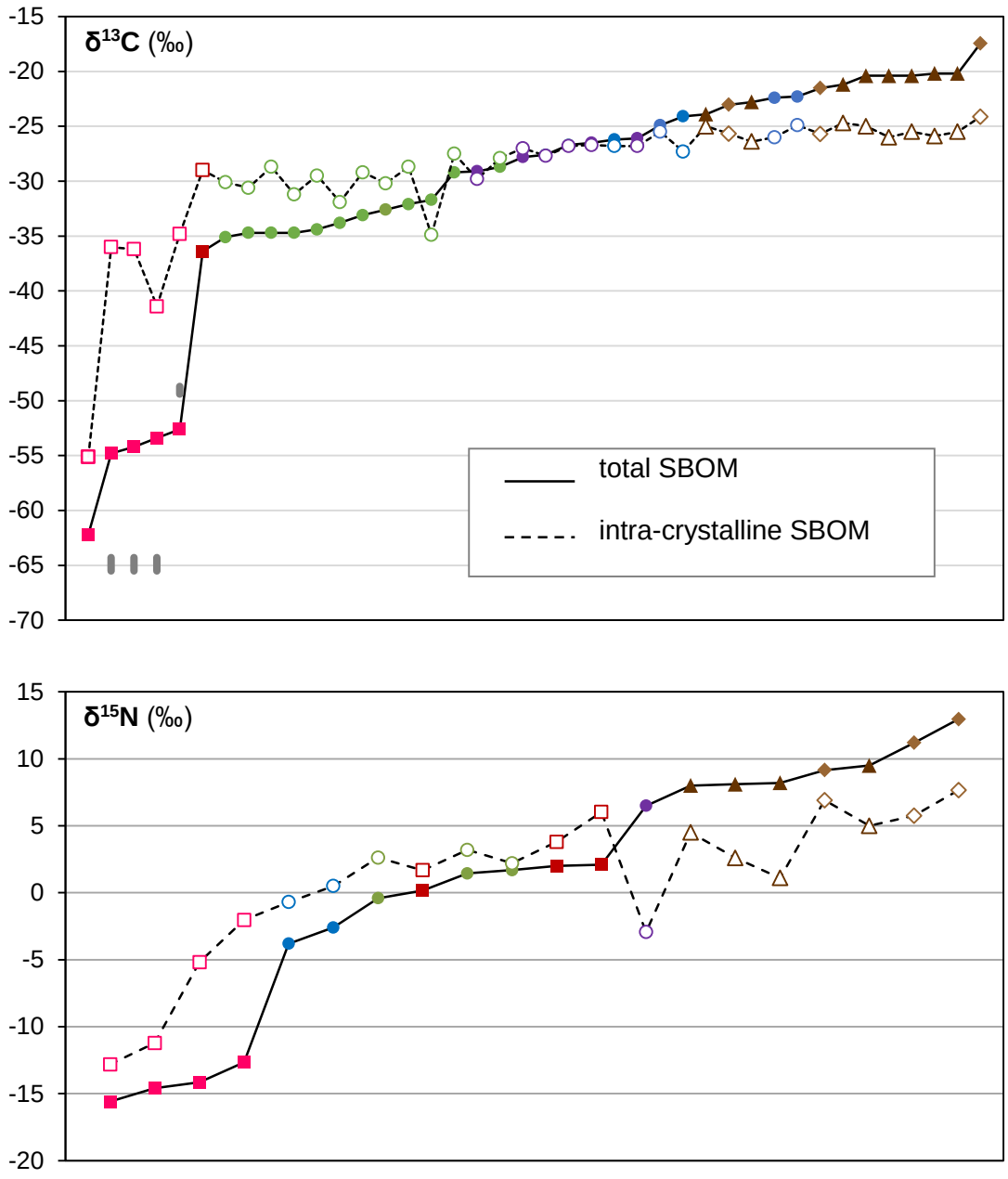

In Chapter 2 it was suggested that high lipid content could cause the depleted $\delta^{13}C$ values of heterotrophic bivalves (total SBOM $\delta^{13}C$ -25‰ to -15‰), because lipids are generally have depleted $\delta^{13}C$ values than other types of macromolecules. The high lipid content of intra-crystalline SBOM compared to total SBOM was also confirmed within this study for chemosymbiotic species, as shown for *C. ponderosa* from the Gulf of Mexico. However, the enriched intra-crystalline values in relation to

very depleted total SBOM $\delta^{13}C$ values, suggest a restricted range of $\delta^{13}C$ and $\delta^{15}N$ for intra-crystalline SBOM, instead of consistent depletion compared to total SBOM. Compared to total SBOM, the intra-crystalline SBOM composition is potentially more strongly controlled, and e.g. more important for the biomineralisation process, and similar between all bivalve taxa. Whereas the inter-crystalline SBOM pool would be less strongly controlled and more strongly influenced by nutritional sources.

Compound-specific $\delta^{13}C$ values of lipids in the gills of *Bathymodiolus* species have been shown to closely track nutritional carbon values (Duperron et al., 2007), but this study suggests that despite the high relative abundance of lipids in the intra-crystalline SBOM fraction, their contribution to the bulk $\delta^{13}C$ signal is limited.

Insufficient data could be obtained for intra-crystalline $\delta^{34}S$ values to investigate its relationship to total SBOM.

3.4.5 Can different nutritional strategies be identified using intra-crystalline SBOM stable isotope values?

The limited isotopic range of $\delta^{13}C$/ $\delta^{15}N$ of intra-crystalline SBOM compared to total SBOM means that isotopic differences between nutritional strategies will be much more difficult to detect, and the link between intra-crystalline SBOM and environmental sources is complex. In this section it is investigated whether it is possible to identify different nutritional strategies in a similar way as was shown for total SBOM in the previous sections. Direct comparisons will be made to the main conclusions about use of total SBOM as a proxy for nutritional strategies. Unfortunately no heterotrophic intra-crystalline values are available from deep-sea or shallow reducing environments.

1. Total SBOM $\delta^{13}C$ values at cold seeps and across environmental settings can differentiate between thiotrophy vs. dual symbiosis/methanotrophy

At cold seeps this distinction can also be made using intra-crystalline SBOM of thiotrophs (-30.5‰ ±1.7, n=16) and dual symbiotic/methanotrophic bivalves (-38.3 ±8.4, n=7) (p=0.0015). Similarly, this is possible compared to thiotrophs from shallow reducing environments (-26.0‰ ±1.2, n=5) and hydrothermal vents (-27.6 ±1.2, n=8).

2. Extremely depleted total SBOM $\delta^{15}N$ values are potentially restricted to methanotrophic/dual symbiotic species (total SBOM below $\delta^{15}N$ -5‰)

Intra-crystalline SBOM $\delta^{15}N$ from methanotrophic *B. childressi* (-8.3‰ ±4.5, n=5) are statistically depleted compared to dual symbiotic species (+4.9‰ ±1.6, n=2, p=0.0119) and thiotrophic species (+3.8‰ ±3.9, n=7, p=0.006) at cold seeps, and potentially compared to thiotrophic species from hydrothermal vents (-2.9, n=1) and shallow reducing environments (-0.7‰ and +0.5‰). Therefore it does appear that the most depleted $\delta^{15}N$ intra-crystalline SBOM values are also restricted to methanotrophic (and possibly dual symbiotic) taxa.

3. Total SBOM $\delta^{34}S$ values (below $\delta^{34}S$ +5‰) are distinctly depleted for thiotrophic taxa compared to methanotrophic/dual symbiotic species

Unfortunately no intra-crystalline SBOM $\delta^{34}S$ data is available for methanotrophic/dual symbiotic species, but for thiotrophic taxa the intra-crystalline SBOM reflects the general trends of total SBOM: total SBOM $\delta^{34}S$ values of *C. pacifica* are -4.3‰ and -3.3‰, and intra-crystalline SBOM also has a negative value of -2.4‰, similarly *C. kilmeri* (total SBOM: 17.7‰) has positive intra-crystalline values of $\delta^{34}S$ 2.5‰ and 9.2‰. Therefore it could be possible to distinguish thiotrophy from other nutritional strategies using intra-crystalline SBOM $\delta^{34}S$ values.

4. Total SBOM $\delta^{13}C$ values can differentiate between chemosymbiotic nutritional strategies vs. heterotrophy from non-reducing environments

Intra-crystalline $\delta^{13}C$ values of thiotrophs from shallow reducing environments (-26.0‰ ±1.2, n=5) are very similar (p=0.4358) to the heterotrophs (-25.5 ±1.3, n=24) from shallow non-reducing environments. Therefore it will also not be possible to differentiate thiotrophy from heterotrophy at shallowing reducing environments. It is however possible to differentiate heterotrophy from seep thiotrophs (-30.5‰ ±1.7, n=16, p=0.0001) and vent thiotrophs (p=0.0004), as well as from dual symbiotic/methanotrophic taxa (-38.3‰ ±8.4, n=7, p=0.0001).

3.4.6 Can different nutritional strategies be identified using shell carbonate $\delta^{13}C$ values?

3.4.6.1 Current understanding of shell carbonate $\delta^{13}C$ composition

Shell material could be a potential proxy for nutritional strategies, because $\delta^{13}C$ of shell carbonate indirectly incorporates nutritional sources via metabolic carbon (e.g. Lietard & Pierre, 2009). Whilst the large majority of the shell carbonate is derived from seawater DIC, a small proportion of the shell is made up of metabolic CO_2 (McConnaughey et al., 2008). The amount of nutritional carbon that is incorporated into the shell is still debated, and has been hypothesized at 10% or less for marine molluscs (McConnaughey, 1997; Gillikin et al., 2006; Beirne et al., 2012), although other studies suggest a higher contribution (e.g. Gillikin et al, 2007). In this study the $\delta^{13}C$ value of shell carbonate was determined on homogenized shell powder, thus representing a life-time average. To investigate how nutrition is reflected into the shell carbonate signal, the data will be compared to SBOM and soft tissue $\delta^{13}C$ values. In this context SBOM could potentially be a better proxy for metabolic carbon than soft tissue, because both shell carbonate and SBOM represent a life-time average.

It has been proposed that the amount of utilized metabolic carbon increases throughout ontogeny, as more metabolic carbon becomes available for calcification (Lorrain et al., 2004; Gillikin et al., 2007), but other researchers have observed no effect, or an age-related enrichment of ^{13}C in shell carbonate (Beirne et al., 2012 and references within). In addition to variation in the $\delta^{13}C$ value and contribution of metabolic carbon, much of the variability in the $\delta^{13}C$ signal of shell carbonate is expected to relate to DIC $\delta^{13}C$ differences between localities and environments. In general, the DIC at deep sea environments is more depleted because conversion into organic matter results in ^{13}C enrichment of the residual DIC (Hoefs, 2015). Of the deep sea ecosystems, bottom water DIC at cold seeps is known to have very variable and depleted $\delta^{13}C$ values (Joye et al., 2004; Joye et al., 2010). The ^{13}C depleted DIC is caused by methane oxidized into depleted CO_2 by the symbiotic bacteria present within the bivalve specimens, as well as by free-living methanotrophic bacteria at the seep sites ($CH_4 + 2O_2 \rightarrow CO_2 + 2H_2O$), or anaerobically in the subsurface during AOM ($CH_4 + SO_4^{2-} \rightarrow HCO_3^- + HS^- + H_2O$ (Brooks et al., 1984; Lartaud, 2010). At hydrothermal vents AOM also occurs (Holler et al., 2011) but methane values have less depleted $\delta^{13}C$ values because it primarly produced abiotically in water-rock interactions (review in McCollom and

Seewald, 2007). In addition, methane concentrations are much lower (µM to low mM) at vents than at cold seeps (higher mM) (Petersen & Dubilier, 2009) and therefore AOM is also likely to be less influential. Particularly because DIC $\delta^{13}C$ is likely to stay close to seawater values because of a large dilution rate of hydrothermal fluids (Le Bris and Duperron, 2010; Nedoncelle, 2014).

In addition to these environmental sources, vital or kinetic effects are well-known to effect $\delta^{13}C$ shell values of molluscs, because of their complicated biomineralisation pathway. Shells are secreted via the mantle and periostracum from extrapallial fluids, these fluids are isolated from the external environment and contain a complex mixture of organic and inorganic components (Immenhauser et al., 2016). During this biomineralisation process $\delta^{13}C$ depletion can occur because of preferential incorporation of ^{12}C during diffusion through cell membranes, and Rayleigh fractionation during secretion (Immenhauser et al., 2016). The kinetic isotope effects of membrane diffusion are minimal in marine molluscs because it is facilitated by activity of the enzyme carbonic anhydrase (Beirne et al., 2012 and references within). Rayleigh fractionation is expected because the biominerals are secreted in a (semi-)closed system, which causes the calcifying solution to become continuously depleted because of preferable incorporation into the minerals (Immenhauser et al., 2016). The major causes of ^{13}C enrichment are non-equilibrium precipitation of the shell compared to the parent fluid, and the existence of fluid pathways between the extrapallial fluids and ambient waters, decreasing the respired fraction of shell carbon (McConnaughey and Gillikin, 2008). Altogether these processes lead to a ^{13}C enrichment of around +2‰ in the biomineral (Immenhauser et al., 2016; Beirne et al., 2012). For the calculation of predicted mollusk shell carbonate $\delta^{13}C$ values in this chapter the formula [10% $\delta^{13}C$ SBOM + 90% $\delta^{13}C$ DIC + 2‰] will therefore be used. By comparing calculated shell carbonate $\delta^{13}C$ values to measured $\delta^{13}C$ shell carbonate data, it will be possible to identify broad scale differences in sources or synthesis between nutritional strategies and environmental settings. Brachiopods have a similar biomineralisation pathway to bivalves, but the precise sources and fractionation processes are poorly understood (Immenhauser et al., 2016). Therefore the predicted $\delta^{13}C$ of brachiopod shell carbonate is calculated similarly to mollusks.

Comparison between calculated and measured $\delta^{13}C$ shell carbonate values were presented in the total SBOM sections, in the Tables 3.7 (methanotrophic species), Table 3.8 (thiotrophic species), Table 3.9 (dual symbiotic species), and Table 3.10 (heterotrophic species).

3.4.6.2 Methanotrophy

Measured shell carbonate $\delta^{13}C$ values of methanotrophic *B. childressi* (-5.7‰ ±2.4, n=7, localities=1) were compared to calculated values (Table 3.7), to gain insights into the way nutritional carbon is incorporated into the shell carbonate $\delta^{13}C$ composition. Based on a 10% metabolic contribution and local DIC values, this comparison showed that measured $\delta^{13}C$ values are generally depleted by -2-4‰ compared to those predicted. This depletion could either be the result of higher amounts of metabolic carbon (calculated in Table 3.7 to be 13.5% to 18.5%, n=6), as well as ^{13}C depleted DIC values. It is challenging to distinguish between these scenarios, and they will have to be compared to other cold seep taxa. However, considering the consistent depletion across specimens, it seems unlikely that this can be attributed to the much more variable depleted ^{13}C DIC values at seeps. The incorporation of increased amounts of metabolic carbon, or internal DIC depletion are therefore considered more likely.

One of the specimens in this dataset was identified as potentially supplementing its diet with POM through filter-feeding, because of enriched total SBOM $\delta^{13}C$ (-37.0‰) compared to the other specimens ($\delta^{13}C$ -53.7‰ ±2.7, n=7). It is encouraging that this specimen also has an anomalously enriched shell carbonate value ($\delta^{13}C$ -0.5‰) compared to the other samples ($\delta^{13}C$ -6.5‰ ±0.8, n=7). The shell carbonate value appears to be disproportionally enriched compared to the specimens, requiring only 8% of metabolic carbon or enriched DIC of 2.4‰. It is unclear whether this additional enrichment is related to the hypothesized absence of methanotrophic bacteria. A less likely explanation would be the presence of ^{13}C enriched CO_2, which is known to very variably occur at other types of seeps (Etiope et al., 2009).

3.4.6.3 Thiotrophy

Shell carbonate $\delta^{13}C$ values for thiotrophic bivalves can be compared across various environments. Despite the possible differences in local DIC $\delta^{13}C$ values between cold seep localities and shallow reducing environments, the shell carbonate $\delta^{13}C$ values are very similar between thiotrophs from the two types of environmental settings. At cold seeps the $\delta^{13}C$ data spans a limited range from -2.8‰ to 2.2‰ (-0.2‰ ±1.3, n=22, localities=6), that is statistically similar to shell carbonate $\delta^{13}C$ values from shallow reducing settings (0.3‰ ±1.9, n=11, localities=7).

Both locality settings are however strikingly different from the shell carbonate $\delta^{13}C$ values from hydrothermal vents, that are statistically enriched and have a mean $\delta^{13}C$ value of 4.2‰ ±2.6 (n=22, localities=6). The potential environmental parameters that could contribute to the enriched $\delta^{13}C$ at hydrothermal vents are further discussed in section 3.4.6.6 below. Within the hydrothermal vent thiotrophy dataset, of particular interest are the extremely enriched $\delta^{13}C$ values of the South Su gastropod *Ifremeria* (9.2‰ ±0.2, n=3), even when compared to *Alviniconcha* (3.0‰ ±0.4, n=3) and *B. manusensis* (3.8‰ ±3.4, n=3, up to 6.4‰) from the same locality. Even though these three species inhabit different microhabitats at seeps, the $\delta^{13}C$ of DIC is unlikely to be consistently different by 6‰. Especially because hydrothermal vent DIC $\delta^{13}C$ values have been suggested to stay close to seawater values, as discussed above. Difference in (metabolic) activity could explain the difference, since *Ifremeria* is relatively inactive compared to *Alviniconcha* that is very active and in the venting water (Desbruyeres et al., 1994; Podowski et al., 2009). Slow metabolic rates and sluggish live modes can lead to more positive $\delta^{13}C$ shell carbonate values (Immenhauser et al., 2016; and references within). For those species with depleted $\delta^{13}C$ SBOM/soft tissue values, the small increase in metabolic carbon into the shell will have a much stronger effect, such as for Gulf of Mexico GC233 methanotrophs.

Another possible influence on the $\delta^{13}C$ of shell carbonate is shell mineralogy. Various studies have shown that biogenic aragonite is $\delta^{13}C$ enriched compared to calcite, this is however generally less than 1‰ per mille (Lecuyer et al., 2012) compared to calcite in the same specimen, although the difference has been suggested to be larger ($\delta^{13}C$ 1.7±0.4‰) based on synthetically precipitated minerals (Romanek et al, 1992). This difference is however minor, considering the overall variation in values for all three environmental settings, and between species of the same mineralogy.

3.4.6.4 Dual symbiosis

Bathymodiolus species with dual symbiotic nutrition have $\delta^{13}C$ shell carbonate values that are generally more enriched than calculated.

3.4.6.5 Heterotrophy

The depleted value of *Paraleptopsis* ($\delta^{13}C$ -8.3‰) is in agreement with the depleted SBOM/soft tissue values, although the depletion is larger than calculated. Shell carbonate values from brachiopods ($\delta^{13}C$ 1.6‰ ±0.7, n=26) are statistically

enriched compared to heterotrophic bivalves from non-reducing environments ($\delta^{13}C$ 0.3‰ ±0.8, n=6) (p=0.0004). This difference is interesting, because the it does not reflect the predicted enrichment of aragonitic bivalve shells compared to calcitic brachiopod shells, as discussed above. Instead, the difference between these animals is likely environmental or physiological.

3.4.6.6 Comparison between nutritional strategies and environments

At cold seeps shell carbonate $\delta^{13}C$ values of methanotrophic bivalves (-5.7‰ ±2.4, n=7, localities=1) are statistically depleted compared to dual symbiosis (-1.1‰ ±1.6, n=5, p=0.0040) and thiotrophy (-0.2‰ ±1.3, n=22, p=<0.0001), and strongly depleted compared to heterotrophic *Delectopecten* (1.1‰). There are no statistical differences between the latter three nutritional lifestyles. Similarly, no statistical difference (p=0.8542) exists between shell carbonate $\delta^{13}C$ values from thiotrophic bivalves (0.5 ±1.8, n=12) and the deposit feeders *A. alba* (-0.4‰) and *E. tenuis* (0.9‰) at shallow reducing environments. At the other environments no comparisons between strategies can be made.

All methanotrophic samples in our dataset belong to *B. childressi* from the Gulf of Mexico, primarily the brine seep GC233. In order to use $\delta^{13}C$ < -5‰ values of shell carbonate as a proxy for methanotrophy, this threshold should be upheld for other methanotrophic species and at different localities as well. In addition, it was noted that the $\delta^{13}C$ values of *B. childressi* were more depleted than calculated (Table 3.7), which contributes to the distinct values of the species. To investigate whether very depleted $\delta^{13}C$ values and/or the negative offset compared to calculated values are also present in methanotrophic species from other localities and environmental settings, the offset between measured and calculated values was calculated for published data on methanotrophic *Bathymodiolus* species (Fig. 3.11). By plotting this isotopic offset, the influence of differences in methane $\delta^{13}C$ values (reflected in SBOM) and DIC $\delta^{13}C$ values between specimens can be investigated.

Firstly, published data shows that *B. childressi* from a different Gulf of Mexico cold seep (GC185) does not generally have shell carbonate $\delta^{13}C$ values lighter than -5‰ (mean: -2.5‰ ±1.2, n=82; Riekenberg et al., 2016). Moreover, the range of $\delta^{13}C$ shell carbonate data falls around the expected value (off-set: -0.2‰ ±1.2, Fig. 3.11) calculated using soft tissue values. In addition to this study, published data for *B. childressi* from GC233 also confirms the depleted shell carbonate values (-9.0‰ ±2.5, n=90), and the large offset between calculated and measured values (-4.4‰ ±2.4, n=90) (Riekenberg et al., 2016; Lietard & Pierre, 2009).

Figure 3.11 Isotopic offset between calculated and measured shell carbonate $\delta^{13}C$ values for all samples

Data shown and calculated in Table 3.7-3.10. The dashed line separates the specimens that have an enrichment that cannot be explained by lower amounts of nutritional carbon (nutritional carbon 0%). Published data (*) references: Mae et al, 2008, Paull et al., 1989, Lietard & Pierre, 2009, Colaco et al, 1998; Riekenberg et al., 2016, were used to calculate off-sets. Different colours of *B. childressi* were collected in different years. Deviating values that were identified in the text to have anomalous total SBOM values are outlined. Open symbol for *P. floridensis* represents soft tissue off-set.

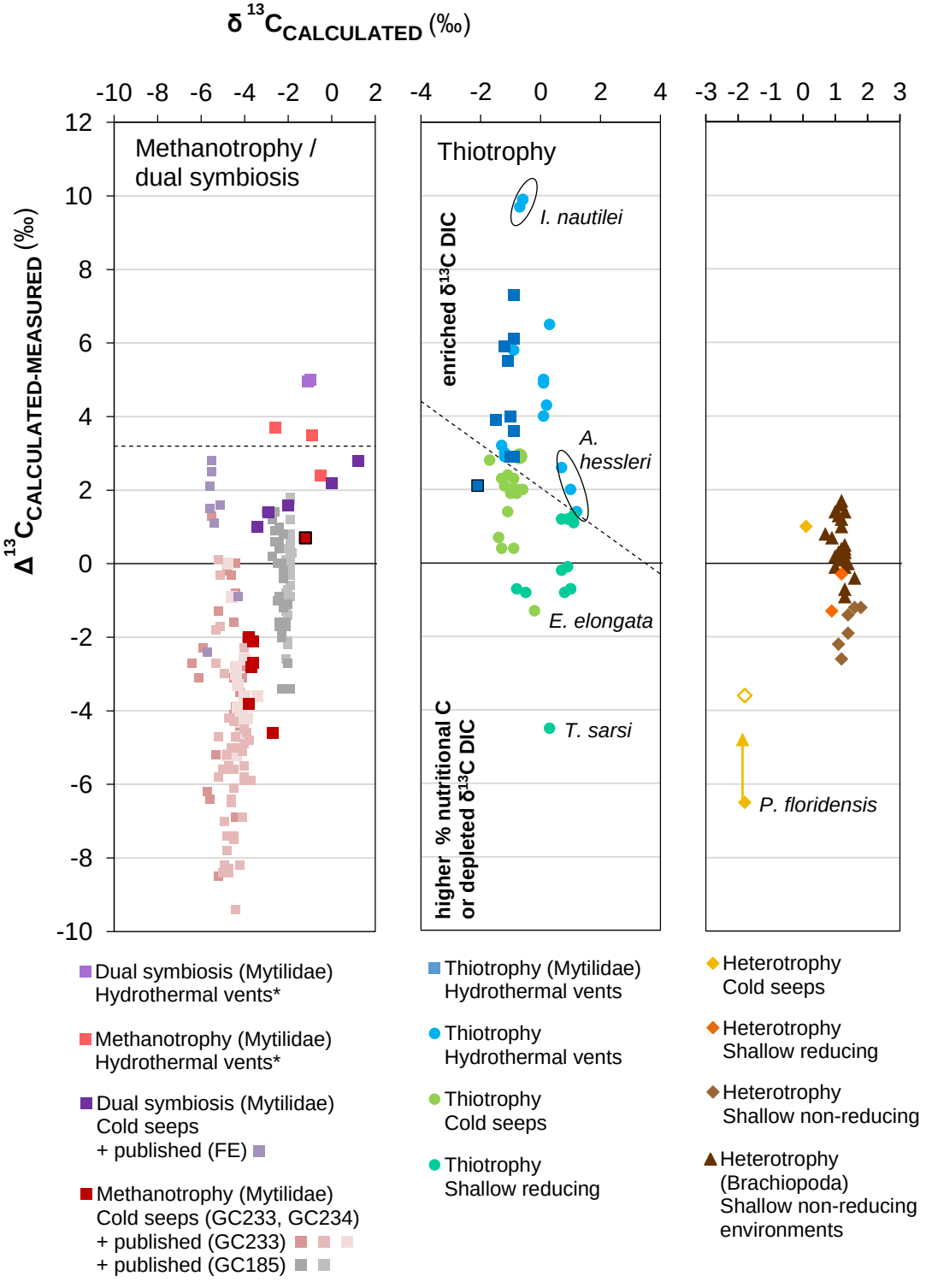

Riekenberg et al. (2016) explain the difference between the Gulf of Mexico localities, and the intra-locality variation, by increasing amounts of metabolic carbon being incorporated into shells with more negative $\delta^{13}C$ values, due to higher food availability at GC233.

The picture becomes more complicated when *B. childressi* results are compared to other nutritional strategies and localities: as increasingly positive offsets are shown in Figure 3.11 for (1) dual symbiotic *Bathymodiolus* at seeps, (2) methanotrophic *Bathymodiolus* at vents, (3) dual symbiotic *Bathymodiolus* at vents, and (4) thiotrophic *Bathymodiolus* at vents. Thiotrophic seep specimens in general are also more enriched than the methanotrophic seep specimens, and an even larger positive offset is observed for thiotrophic vent specimens. Therefore this data shows two notable observations: i) thiotrophic bacteria (in dual symbiotic and thiotrophic taxa) appear to cause enriched $\delta^{13}C$ shell carbonate values, ii) at vent localities $\delta^{13}C$ shell carbonate values are more enriched than at cold seeps and shallow reducing environments. Presence at vents is more influential than harbouring thiotrophic symbionts, since the enrichment of methanotrophic/dual symbiotic vent *Bathymodiolus* is similar to or higher than thiotrophic/dual symbiotic seep specimens. Moreover, for the majority of vent specimens their $\delta^{13}C$ shell carbonate values cannot be explained without environmental or internal ^{13}C enrichment. This has previously been explained through internal ^{13}C enrichment of the DIC, possibly due to thiotrophic bacteria using the dissolved inorganic carbon and preferentially incorporating $^{12}CO_2$ and concentrating ^{13}C in the extrapallial fluid (Rio et al., 1992; Lietard & Pierre 2009; Nedoncelle et al., 2014). Alternatively or additionally, the presence of methanotrophic bacteria could cause a depletion, by direct exposure to ^{13}C depleted CO^2 resulting from internal methane oxidation.

These suggestions could account for the differences between nutritional strategies, it does not explain the difference between ecosystems, that is likely underlain by difference in environmental parameters. The difference between hydrothermal vents and cold seeps could also be explained by known very depleted local DIC of seeps. This does however not explain the offset compared to shallow reducing environments. Alternatively, compared to cold seep settings the chemical fluids present at hydrothermal vents are lower in pH, which ensures DIC is primarily present as CO_2 (Tunnicliffe et al., 2003; Sibuet and Olu, 1998). There are multiple forms of DIC in the water, and it has previously been noted that using molecular CO^2 can cause negative value for the incorporation of metabolic carbon (McConnaughey et al., 2008). In ambient seawater DIC will largely reflect HCO3, as suggested experimentally by Beirne et al (2012).

In summary, the $\delta^{13}C$ values of shell carbonate are a complicated proxy, that is suggested to be strongly influenced by environmental settings and metabolic activity. Negative $\delta^{13}C$ values at cold seeps (below -2‰) are however restricted to some dual symbiotic specimens (-1.1‰ ±1.6, n=5), as well as methanotrophic specimens (-5.7‰ ±2.4, n=7), and could therefore be indicative of the presence of methanotrophic bacteria. Shell carbonate values below $\delta^{13}C$ -5‰ could be unique to methanotrophic species, but more enriched $\delta^{13}C$ values are also possible for methanotrophic specimens.

3.5 Conclusions

Both the $\delta^{13}C$ and $\delta^{34}S$ values of total SBOM allow for the differentiation between thiotrophy and dual symbiosis/methanotrophy, and a combination of both values is particularly conclusive. In addition, $\delta^{15}N$ SBOM values can potentially also be used to distinguish between bivalves harbouring methanotrophic bacteria (dual symbiosis and methanotrophy) and does that do not (thiotrophy and heterotrophy), if further study shows that extremely depleted nitrogen values are restricted to the presence of methanotrophic bacteria. Thus the isotopic signatures of the different nutritional strategies override environmental and biological heterogeneity. The possibility of differentiating chemosymbiotic species from local heterotrophs will depend on whether these specimens are utilizing chemosynthetically or photosynthetically derived organic matter. If the latter values are similar to heterotrophs from non-reducing environments, the differences are very large for all isotope systems.

Many of the identifications that can be made using total SBOM stable isotope values, can also be identified using intra-crystalline SBOM. This is particularly important for potential future work on ancient specimens, because the intra-crystalline SBOM is thought to preserve better because it is protected by the mineral (Sykes et al., 1995). This study confirmed the compositional difference between total SBOM and intra-crystalline SBOM, that is likely to underlay the isotopic differences. It could be concluded that the range of isotopic values of intra-crystalline SBOM is much more restricted than for total SBOM, and this strong control is potentially related to the function of intra-crystalline SBOM within the biomineralisation process.

Contrary to SBOM, the $\delta^{13}C$ shell carbonate values are strongly influenced by environment and biology. It is potentially only possible to identify the presence of methanotrophic bacteria in relation to ^{13}C depleted values.

Chapter 4

Potential preservation of stable isotopic signatures for chemosymbiosis in shell-bound organic matter from fossil cold seep invertebrates

Edine Pape[a], Fiona Gill[a], Robert J. Newton[a], Crispin T.S. Little[a], Kirsty Penkman[b], Geoffrey D. Abbott[c], and Adrian Boyce[d]

[a] School of Earth and Environment, University of Leeds, Leeds LS2 9JT, United Kingdom

[b] Department of Chemistry, University of York, York YO10 5DD, United Kingdom

[c] School of Civil Engineering and Geosciences, Newcastle University, Newcastle upon Tyne NE1 7RU, United Kingdom

[d] Scottish Universities Environmental Research Centre, East Kilbride, G75 0QF, United Kingdom

Author contribution

EP collected and prepared the fossil specimens, performed SBOM extractions and prepared SBOM for stable isotope analysis, helped with stable isotope/radiocarbon analysis, performed CL analysis, and wrote the paper. EP, FG, RJN and CTLS designed the research and commented on the manuscript. RJN carried out stable isotope analysis and supervised the contribution of EP therein. CTSL and EP carried out SEM analysis. CTSL contributed fossil specimens and helped with specimen identification. GDA generated Py-GC/MS results, that were interpreted by FG and GDA. AB contributed shell carbonate $\delta^{13}C$ data, and KP performed amino-acid racemization analysis.

Relevant research questions

The aim of the research presented in this thesis is to reconstruct the occurrence of chemosymbiosis through geological time using stable isotope analysis of shell-bound organic matter (SBOM), and to investigate the influence of chemosymbiosis on the evolution of deep sea fauna and ecosystems. In **Chapter 2** and **Chapter 3** we confirmed that carbon ($\delta^{13}C$), nitrogen ($\delta^{15}N$), and sulphur ($\delta^{34}S$) stable isotope analysis can be used to differentiate nutritional lifestyles, in particular chemosymbiosis. In this chapter we investigate the preservation of SBOM in the fossil record: **Research question 4: Are SBOM and its original stable isotopic composition preserved over geological time?**

4.1 Introduction

Stable isotope analysis of shell-bound organic matter (SBOM) is a powerful technique to identify the nutritional strategies and nutritional sources of animals in modern ecosystems (O'Donnell et al., 2003; Mae et al., 2008; Dreier et al., 2012 and 2014). Moreover, it has the potential to elucidate the palaeobiology of dead and (sub)fossil specimens that cannot be investigated using traditional stable isotope analysis of soft tissues. In Chapter 2 it was shown that chemosymbiosis can be identified using the carbon ($\delta^{13}C$), nitrogen ($\delta^{15}N$), and sulphur ($\delta^{34}S$) SBOM composition of bivalves and gastropods in deep sea ecosystems. These distinct values are the result of symbiotic bacteria that use either methane (methanotrophic) or hydrogen sulphide (thiotrophic) to generate energy for carbon fixation and provide host nutrition (Duperron et al., 2009). Because of these extreme and distinct values, the stable isotope analysis of SBOM from ancient suspected chemosymbiotic bivalves is an ideal test case to investigate fossil SBOM as a proxy for nutritional strategies. If chemosymbiotic biosignatures are preserved on geological timescales, the occurrence of chemosymbiosis in certain taxa and time periods can be identified, which will allow for a reconstruction of the evolution of chemosymbiosis. The presence of chemosymbiosis likely had a major influence on the evolution of cold seep fauna during the Phanerozoic, and SBOM stable isotope analysis provides a unique opportunity to obtain direct evidence for the timing of these evolutionary changes. In addition to analysing the complete SBOM fraction in the shell of a specimen (total SBOM), particular focus was placed on the isotopic signature of the intra-crystalline SBOM pool. Intra-crystalline SBOM is encased in the minerals, and therefore has greater potential for preservation over longer timescales (Sykes et al., 1995; Penkman et al., 2008). Data presented in Chapter 2 and Chapter 2 has shown that intra-crystalline SBOM also has a different isotopic signal compared to total SBOM, which is likely underlain by compositional differences between the intra-crystalline en inter-crystalline pools.

Chemosymbiotic lifestyles are primarily known from the deep sea, where the symbioses support high invertebrate biomass in extremely unfavourable living conditions (Van Dover, 2001). The reduced compounds required for bacterial carbon fixation are present at two types of deep sea ecosystems: the long-lived cold seeps where fluids are emitted slowly, and at hot hydrothermal vents with vigorous and highly unstable conditions. Both hydrothermal vents and cold seeps have been recognized in the fossil record (Kiel et al., 2010), but vent fossils are always preserved as moulds of pyrite and lack original shell material (Little et al.,

2002). Therefore only SBOM from ancient cold seep specimens can be analysed. Within this study effort was put into obtaining both suspected chemosymbiotic specimens as well as suspected heterotrophic specimens from the same locality, or from surrounding non-seep areas. In addition to bivalves, brachiopods from pre-Cretaceous cold seep localities were analysed. The very high abundance of the brachiopods has led some to suggest a chemosymbiotic lifestyle, even though modern brachiopods are suspension-feeders and generally absent from cold seeps (Sandy, 2010).

Modern SBOM stable isotope thresholds. The stable isotope SBOM composition of the fossil specimens was compared to modern thresholds for nutritional strategies determined in Chapter 3. At modern cold seeps, bivalves harbouring thiotrophic symbionts have total SBOM $\delta^{13}C$ values of -31.6‰ ±2.7 (n=51, species=13). These values are depleted compared to heterotrophic bivalves from cold seeps (-19.3‰, n=1), as well as bivalves (-20.4‰ ±2.4, n=31, species=3) and brachiopods (-21.5‰ ±1.8, n=27, species=4) from shallow non-reducing environments, because the symbionts fractionate dissolved inorganic carbon (DIC) to a greater degree than the photosynthetic organisms on which heterotrophic invertebrates generally feed. The $\delta^{13}C$ total SBOM value of bivalves living in symbiosis with methanotrophic bacteria, or both methanotrophic and thiotrophic bacteria (dual symbiosis), is even more depleted due to the incorporation of ^{13}C depleted methane. The variation in total SBOM $\delta^{13}C$ (-53.5‰ ±7.9, n=18, species=4). is large for these two lifestyles, because of the presence of thiotrophic bacteria (utilizing ^{13}C enriched DIC), and the $\delta^{13}C$ variation between local methane sources. The intra-crystalline SBOM $\delta^{13}C$ value of methanotrophic/dual symbiotic bivalves (-38.3 ±8.4, n=7, species=3) is also more depleted than in thiotrophic bivalves (-30.5‰ ±1.7, species=4). No intra-crystalline SBOM $\delta^{13}C$ values for heterotrophic cold seep bivalves are available, but the intra-crystalline SBOM of non-seep bivalves (-25.4‰ ±1.6, n=14, species=3) and brachiopods (-25.6‰ ±0.6, n=10, species=4), are more enriched than the chemosymbiotic taxa. Nutritional carbon reflected in SBOM is also incorporated into the shell carbonate of invertebrates. The amount of nutritional carbon has been suggested to lie around 10%, therefore the majority of the $\delta^{13}C$ signal of the shell carbonate reflects DIC. In Chapter 2 it was shown that shell carbonate $\delta^{13}C$ of heterotrophy (1.1‰, n=1), thiotrophy (-0.2‰ ±1.3, n=22, species=9), dual symbiosis (-1.1‰ ±1.6, n=5, species=3) overlap in values, but dual symbionts can generally be differentiated from the other two lifestyles by $\delta^{13}C$ more depleted than -1‰. Methanotrophic *Bathymodiolus childressi* (Gulf of Mexico, GC233) $\delta^{13}C$ shell carbonate values are

additional depleted (-5.7‰ ±2.4, n=7, generally lighter than $\delta^{13}C$ -5‰) and statistically different from the other nutritional strategies. However, it should be noted that *B. childressi* from other Gulf of Mexico localities has more enriched $\delta^{13}C$ values (-2.5 ±1.2, n=82, Riekenberg, 2015). Therefore shell carbonate $\delta^{13}C$ of -2‰ or lighter generally indicates the presence of methanotrophic (in addition to thiotrophic) bacteria, but all shell carbonate data should be interpreted with caution. In Chapter 2 it was shown that $\delta^{13}C$ ratios can be strongly influenced by the amount of incorporated metabolic carbon, local DIC $\delta^{13}C$ variation, local POM (particulate organic matter) $\delta^{13}C$ variation, and potentially by internal DIC ^{13}C enrichment by thiotrophic bacteria.

In addition to carbon, $\delta^{34}S$ values can be useful to identify the presence of thiotrophic bacteria because of the incorporation of ^{34}S depleted hydrogen sulphide (data given excludes SBOM obtained using cation exchange resin). Total SBOM data are generally negative ($\delta^{34}S$ -4.4‰ ±7.4, n=12, species=8) and ranges from $\delta^{34}S$ -25‰ to +5‰. Comparative total SBOM data from other nutritional strategies is limited (methanotrophic *B. childressi* +12.1‰ ±2.8, n=10) but, in combination with soft tissue data, suggests that other nutritional strategies at cold seeps are generally characterized by values ranging from $\delta^{34}S$ +5‰ to +15‰. The latter range is also observed for total SBOM of non-seep bivalves. Brachiopod soft tissue $\delta^{34}S$ values are however even more enriched, and range from +10‰ to +20‰. Unfortunately very limited intra-crystalline SBOM $\delta^{34}S$ data is available, but $\delta^{34}S$ values are generally also slightly negative.

Chemosymbiotic bivalves can assimilate various inorganic nitrogen sources that are not directly linked to the type of symbionts, and have a mean $\delta^{15}N$ total SBOM value of -0.5‰ ±6.8 (n=66, species=20), and mean intra-crystalline SBOM of -0.2‰ ±6.9 (n=15, species=7). The only seep heterotroph has a total SBOM $\delta^{15}N$ enriched value of 16.1‰, and shows higher reliance on photosynthetically derived nitrogen from POM. There are however indications that heterotrophs living at cold seeps could incorporate depleted $\delta^{15}N$ organic sources, produced by free-living chemoautotrophic bacteria. At non-reducing environments, bivalves and brachiopods have more enriched $\delta^{15}N$ ratios for total SBOM (10.0‰ ±2.3, n=48, species=7) and intra-crystalline SBOM (8.5‰ ±2.9, n=41, species=6). To apply modern thresholds on fossil SBOM, changing baseline values for DIC, methane, hydrogen sulphide and nitrogen sources should also be considered.

Methods to assess SBOM preservation. This study relies on the assumption that the isolated SBOM is indigenous, and therefore retains its original isotopic signal.

Loss or contamination of original SBOM could alter the isotopic signal, and potentially confound interpretations about the nutritional strategy and environmental sources used by the animal. Although previous studies assumed isotopic alteration of SBOM to be limited over time (O'Donnell et al., 2003; Mae et al., 2007), more recent work recognized gradual degradation and transformation, particularly of total SBOM (Dreier et al., 2012; Penkman et al., 2008). To evaluate the preservation and alteration of SBOM through time, several geochemical and visual analyses were performed in addition to stable isotope analysis.

- **Radiocarbon analysis of SBOM and shell carbonate**

Subfossil shells from our suite of samples were dated using radiocarbon analysis of shell carbonate. The age of the samples was unknown or poorly constrained, and specimens within this age range (10^2-10^4 years) are critical for understanding the effects of age on the fidelity of the isotopic SBOM signal. In addition radiocarbon dating of SBOM was attempted. Although the incorporation of ^{14}C into SBOM has not previously been investigated, theoretically the ^{14}C analysis of related total SBOM from dated shell samples should show whether the SBOM is original (similar ^{14}C age as the shell) or has become contaminated by the recent external environment (younger ^{14}C age than the shell). Although it might not be possible to detect diagenetic alteration that occurred shortly after the death of the animal.

In addition, radiocarbon analysis can potentially be used to identify the presence of methanotrophic symbionts. Because the methanotrophs incorporate geologically old, ^{14}C dead methane into the SBOM, the ^{14}C age of SBOM from methanotrophic or dual symbiotic bivalves will be older than the ^{14}C age of the shell. In combination with $\delta^{13}C$ total SBOM data, this can further constrain the dominant carbon sources contributing to SBOM.

- **Amino acid racemization (AAR)**

The originality of proteins within intra-crystalline SBOM was investigated using amino-acid racemization (AAR), a relative dating method using amino acids, the basic building blocks of proteins. The AAR technique uses the predictable post-mortem conversion of levo-rotaty (L-) amino acids into dextro-rotary (D-) amino acids over time (in combination with the age of the fossils), to establish whether the SBOM has remained unaffected by external factors (Penkman et al., 2008). Because proteins make up the majority of SBOM, and proteins are considered to be relatively susceptible to degradation (Marin et al., 2012), AAR results are assumed to be a good indicator of preservation for the complete intra-crystalline SBOM pool.

- **Pyrolysis gas chromatography mass spectrometry (Py-GC/MS)**

Changes to the bulk chemical composition of original SBOM can also be recognized using Py-GC/MS, an identification method for macromolecular constituents of insoluble organic matter. Thermal degradation of the organics produces low molecular weight products that are separated according to fragment mass by GC, and identified using MS (Schweitzer et al., 2008). In addition to break-down products of proteins, Py-GC/MS can identify other macromolecular components present in SBOM, such as polysaccharides and lipids. Py-GC/MS analysis has not previously been used on modern or fossil SBOM, and the main objectives within this study are (i) to chemically characterize SBOM in modern specimens (with various nutritional strategies), (ii) determine to what extent these chemical constituents can survive diagenesis and be detected in fossils of varying geological ages, and (iii) recognize diagenetic contaminants in fossil specimens. Potentially, diagnostic molecular components of nutritional strategies identified in modern samples can also contribute to the identification of these lifestyles in fossil specimens.

- **Scanning electron microscopy (SEM) and cathodoluminescence (CL) imaging**

In addition to direct biochemical analyses of SBOM, its preservation can indirectly be assessed by the diagenetic condition of the shell. Chemical or physical alterations can be identified using cathodoluminescence (CL) imaging and scanning electron microscopy (SEM), respectively. One of the main problems concerning shell preservation is recrystallization, this process is known to modify the primary isotopic composition of shell carbonate and is also assumed to indicate chemical alteration of the original SBOM signal (England et al., 2006). Recrystallisation is most common in aragonitic shells, that often transform to the more stable mineralogical calcite phase (Clarkson, 2009). SEM analysis can identify recrystallisation (erasing the microstructure of the shell) and other morphological changes by examining the shell ultrastructure using a very narrow electron beam.

Chemical preservation of the shell material can be evaluated using CL imaging, whereby visible radiation can be emitted under the impact of electrons. If luminescence of the shell is observed, this is considered indicative of diagenesis. Generally, luminescence is linked to elevated manganese concentrations due to manganese substitution in the calcium carbonate lattice. Luminescence can also be caused by structural defects (England et al., 2005; Barbin et al., 2013).

4.2 Material and Methods

4.2.1 Material

The suite of samples is shown in Table 4.1 and contains fossil shell material from both suspected chemosymbiotic and suspected heterotrophic species from a wide range of bivalve families, as well as other animal groups. Because fossil cold seep fossils are relatively rare, it is often not possible to analyse many specimens of the same species. By analysing a limited number of specimens from many specimens we still aim to establish a statistically reliable dataset to compare nutritional strategies. This particularly applies to heterotrophic animals in the absence of available bivalve specimens. In addition, the variety of samples makes it possible to also compare differences in shell mineralogy/structure (calcite vs. aragonite), as well as behavioural ecologies (infaunal vs. epifaunal), in addition to nutrition. Because this sample set include various shelled cephalopods, a modern *Nautilus* specimen was analysed for reference isotopic values (*Nautilus pompilius*, Phillippines).

Suspected nutritional strategies was assigned to all analysed specimens by analogy to modern taxa, and family specific information on suspected nutritional and behavioural strategies is given below. The variation in shell mineralogy is limited to either solely aragonite or calcite crystals, or a combination of the two forms. Within the chemosymbiotic bivalve families, aragonitic shells have been identified for Lucinidae (e.g. Lietard & Pierre, 2009), Thyasridiae (*Conchocele bisecta*, Nishida et al., 2011), Solemyidae (e.g. Sato et al., 2013) and Vesicomyidae (Kennish et al., 1998). The shells of deep sea mytilids, including *Bathymodiolus* and *Gigantidas* were reported by Genio et al (2012) to consist of both calcite and aragonite, similar to the general mytilid condition.

Within the heterotrophic bivalves several families have completely calcitic shells, these include the Ostreidae (*Ostrea*) and Gryphaeidae. Specimens of Pectinidae can have both mineral types, although modern *Mizuhopecten* has been identified as completely calcitic (Bouillon, 1958; Sarashina and Endo, 1998; Esteban-Delgado et al., 2008). These specimens all include at least a calcitic component, commonly an external calcitic shell layer. The combination of aragonite and calcite is furthermore known from Inoceramidae (Wright, 1987).

The shells of all other bivalves are aragonitic, and include species within the orders Arcoida, Veneroida and Nuculida (Esteban-Delgado et al., 2008; Taylor et al., 1969, for *Glycymeris* – Oliver & Holmes, 2006; for *Cucullaea* and *Lahillia* – Petersen et

al., 2016). Two fossil ostreid shells were excluded from this study because SBOM could not be isolated, using XRD it was confirmed that much of the original shell was replaced by silica.

The shells of most gastropods consist of aragonite layers, though many also have a calcitic outer layer (Clarkson, 2009; Taylor & Reid, 1990 and references within). For modern *Neptunea* both crystal forms have indeed been identified (e.g. Xiao-Fei et al., 2014). Turritulidae however precipitate aragonitic shells (Allmon, 1988).

Of the other taxa analysed, ammonoids (Cephalopoda) and *Nautilus* are characterized by an aragonitic shell (Clarkson et al., 2009), as is the shell from species of *Dentalium* within the Scaphopoda (Smith & Spender, 2015). All brachiopod species in our sample set belong to the rhynchonelliformeans, that are characterized by calcitic valves (Clarkson et al., 2009). Within the fossil *Rotularia* (Annelida) a calcite layer was identified, as well as possibly an aragonitic layer (Savazzi, 1995).

Table 4.1 Overview of samples from ancient cold seep localities

(p. 170-173) Species that are underlined were collated (> 2 specimens) to obtain sufficient shell material for SBOM isolation and analysis

Locality	**Age**	**Species (Family)**	**Suspected strategy**
Cold seep localities			
Congo Fan	1283 B.P.	*Laubiericoncha chuni* (Vesicomyidae)	Thiotrophic chemosymbiosis
Hikurangi Margin (NZ)	1227 B.P.	*Calyptogena tuerkayi* (Vesicomyidae)	Thiotrophic chemosymbiosis
Krishna-Godavari Basin (India)	42.5-40.0 ka	Vesicomyidae sp. (Vesicomyidae)	Thiotrophic chemosymbiosis
		Bathymodiolus sp. (Mytilidae)	Chemosymbiosis
Kakinokidai seep (Japan)	Locality I Middle Pleistocene	*Acharax* sp. (Solemyidae)	Thiotrophic chemosymbiosis
		Lucinoma aokii (Lucinidae)	Thiotrophic chemosymbiosis

	Locality II Middle Pleistocene (younger)	*Lucinoma aokii* (Lucinidae)	Thiotrophic chemosymbiosis
Koshiba Formation (Japan)	Early Pleistocene	*Lucinoma spectabilis* (Lucinidae)	Thiotrophic chemosymbiosis
		Conchocele bisecta (Thyasiridae)	Thiotrophic chemosymbiosis
		Solemya japonica (Solemyidae)	Thiotrophic chemosymbiosis
Kounandai seep, Locality I and II (Japan)	Early Pleistocene	*Lucinoma* sp. (Lucinidae)	Thiotrophic chemosymbiosis
Takanabe Formation (Japan)	Plio-Pleistocene	*Lucinoma* sp. (Lucinidae)	Thiotrophic chemosymbiosis
Shiramaza Formation (Japan)	Upper Pliocene	*Calyptogena* sp. (Vesicomyidae)	Thiotrophic chemosymbiosis
Rocky Knob (NZ)	Miocene	*Lucinoma* aff. *taylori* (Lucinidae)	Thiotrophic chemosymbiosis
		Bathymodiolus heretaunga (Mytilidae)	Chemosymbiosis
Moonlight North (NZ)	Miocene	*Gigantidas coseli* (Mytilidae)	Thiotrophic chemosymbiosis
		Lucinoma sp. (Lucinidae)	Thiotrophic chemosymbiosis
		Liothyrella sp. (Brachiopoda)	Heterotrophy
Hokkaido (Japan)	Miocene	*Calyptogena pacifica* (Vesicomyidae)	Thiotrophic chemosymbiosis
Izura seep,	Lower Miocene	*Lucinoma acutentilineatum* (Lucinidae) (I)	Thiotrophic chemosymbiosis

Locality I and II (Japan		*Mizuhopecten kobiyami* (Pectinidae) (I)	Heterotrophy
		Calyptogena sp. (Vesicomyidae) (II)	Thiotrophic chemosymbiosis
Lincoln Creek Formation (US)	Oligocene	*Conchocele bisecta* (Thyasiridae)	Thiotrophic chemosymbiosis
		Lucinoma sp. (Lucinidae)	Thiotrophic chemosymbiosis
		Solemyidae sp.	Thiotrophic chemosymbiosis
		Vesicomyidae sp.	Thiotrophic chemosymbiosis
		Mytilidae sp.	Unknown / heterotrophy
		Ennucula sp. (Nuculidae)	Heterotrophy
Tepee Buttes	Campanian	*Nymphalucina occidentalis* (Lucinidae)	Thiotrophic chemosymbiosis
		Inoceramus sp. (Inocermidae)	Unknown/ heterotrophy
		Baculites sp. (Ammonoidea)	Heterotrophy
Seymour Island	Maastrichtian	'*Thyasira*' *townsendi* (Thyasiridae)	Thiotrophic chemosymbiosis
		Solemya rossiana (Solemyidae)	Thiotrophic chemosymbiosis
		Maorites seymourianus (Ammonoidea)	Heterotrophy
Brachiopoda – cold seep localities			
Oregon/Colorado (US)	Jurassic	*Anarhynchia gabbi*	Unknown

(*suggested cold seep adaption*)			
Graylock (US)	Triassic	*Halorella* sp**.**	Unknown
Harz Mountains (Germany)	Carboniferous	*Ibergirhynchia contraria*	Unknown
Sidi Amar (Morroco)	Devonian	*Dzieduszyckia crassicostata*	Unknown
		Dzieduszyckia tenuicostata	Unknown
Middle Atlas (Morroco) (*suggested cold seep adaptation*)	Silurian	*Septatrypa*	Unknown

Table 4.2 Overview of samples from ancient non-seep localities

(p. 173-175) Species that are underlined were collated (> 2 specimens) to obtain sufficient shell material for SBOM isolation and analysis

Locality	**Age**	**Species (Family)**	**Suspected strategy**
Non-seep localities			
in proximity to Kakinokidai seep (Japan)	Middle Pleistocene	Gastropoda	
		Neptunea kuroshio (Buccinidae)	Heterotrophy
		Fulgoraria prevostiana (Volutidae)	Heterotrophy
		Scaphopoda	
		Dentalium sp. (Dentaliidae)	Heterotrophy
Koshiba Formation (Japan)	Early Pleistocene	Bivalvia	
		Ostrea musashiana (Ostreidae)	Heterotrophy
		Glycymeris sp. (Glycymerididae)	Heterotrophy

		Gastropoda	
		Fusitrition oregonensis (Ranellidae)	Heterotrophy
		Ranella galea (Ranellidae)	Heterotrophy
		Fulgoraria kamakuraensis (Volutidae)	Heterotrophy
		Scaphopoda	
		Dentalium sp. (Dentaliidae)	Heterotrophy
		Brachiopoda	
		Terebratulidae (Brachiopoda)	Heterotrophy
Seymour Island (*in proximity or associated with seep locality*)	Maastrichtian	Bivalvia	
		Lahillia larseni (Cardiidae)	Heterotrophy
		Cucullaea sp. (Cucullaeidae)	Heterotrophy
		Leionucula suboblonga (Nuculidae)	Heterotrophy
Seymour Island (*no noted proximity to seep locality*)	Maastrichtian	*Pycnodonte* (*Phygraea*) *vesicularis vesicularis*	Heterotrophy
		Gastropoda	
		Neogastropod n. gen.	Heterotrophy
		Vanikoropsis arktowskiana (Vanikoridae)	Heterotrophy
		Amberleya spinigera (Amberleyidae)	Heterotrophy
		Cephalopoda (Ammonoidea)	
		Maorites seymourianus	Heterotrophy
		Kitchinites sp.	Heterotrophy

		Pachydiscus (*Pachydiscus*) *riccardii*	Heterotrophy
		Diplomoceras cylindraceum	Heterotrophy
		Eutrephoceras dorbignyanum (Nautiloidea)	Heterotrophy
		Annelida	
		Rotularia ssp.	Heterotrophy
Owl Creek Formation	Maastrichtian	Bivalvia	
		Cucullaea capex (Cucullaeidae)	Heterotrophy
		Nucula percrassa (Nuculidae)	Heterotrophy
		Gastropoda	
		Turritella	Heterotrophy
		Drilluta	Heterotrophy
		Cephalopoda (Ammonoidea)	
		Baculites	Heterotrophy
		Eubaculites	Heterotrophy
		Discoscaphites	Heterotrophy

4.2.1.1 Bivalvia

Vesicomyidae

Vesicomyid clams are dominant species at modern cold seeps and hydrothermal vents, where they can grow to extremely large sizes and live shallowly buried in the sediment (Sibuet and Olu, 1998; Krylova and Sahling, 2010). All vesicomyids rely on thioautotrophic symbionts for nutrition, and they only have a rudimentary gut (Taylor and Glover, 2010). The oldest occurrence of Vesicomyidae is Eocene (Kiel and Goedert, 2006). The oldest samples in our samples in our data set are

Oligocene (Vesicomyidae), followed by specimens from two Miocene cold seep localities (*Calyptogena* sp. and *Calyptogena pacifica*). Preliminary study of the vesicomyid material from the Krishna-Godavari Basin (geological age of older than 50ka) revealed multiple species and results can therefore only be discussed at a family level. The two subfossil species, *Laubiericoncha chuni* and *Calyptogena tuerkayi*, are extant and the presence of thiotrophic bacteria has been confirmed for modern *L. chuni* (Decker et al., 2013).

Mytilidae

All mussels species found at modern cold seeps and hydrothermal vents belong to the class Bathymodiolinae within the family Mytilidae, that has its oldest fossil occurrence in the Eocene (Kiel and Amano, 2013). The mussels have an epifaunal lifestyle, and are generally attached to hard substrates via a byssus (Duperron, 2010). All modern investigated species have been shown to obtain nutrition via chemosymbiosis, and the mussels can house thiotrophic and/or methanotrophic bacteria in their gills. The ability to harbour methanotrophic bacteria is a very rare feature among bivalves (Taylor & Glover, 2010). In addition, for a few species up to six bacterial types have been identified in the gills (multiple symbiosis), although their effects on nutrition are not yet known (overview in Duperron et al., 2008 and 2013). For all mussel species it should be noted that filter feeding can still play a nutritional role, despite the presence of a reduced gut (Page et al., 1991; Von Cosel, 2002). Because different types of chemosymbiosis exist for bathymodiolid mussels, the various fossil species analysed in this study are discussed separately.

***Bathymodiolus* sp. (Krishna-Godavari Basin).** Broken mussel shells were obtained during a drilling and coring expedition of gas hydrate occurrences (Mazumdar et al., 2009), and examined for this study. The shell pieces have a modioliform shell shape and size, but could not be identified to species level. These specimens is therefore expected to harbour either thiotrophic, methanotrophic or dual symbiotic symbionts.

***Bathymodiolus heretaunga* (Rocky Knob).** Morphological features place this species in the *B. childressi* clade/group (Saether et al., 2010). The *B. childressi* clade consists of several *Bathymodiolus* species based on morphological and molecular phylogenetic analyses, and all modern species within that group have methanotrophic endosymbionts (Miyazaki et al., 2010). Methanotrophic chemosymbiosis could therefore perhaps also be expected for *B. heretaunga*.

Gigantidas coseli. Modern *Gigantidas* species are closely related to the *B. childressi* group (e.g. Miyzaki et al., 2010; Jones et al., 2006), and include the *Gigantidas gladius* (Cosel and Marshell, 2003) and *Gigantidas horikoshii* (Hashimoto and Yamane, 2005) that both live at hydrothermal vents. Despite phylogenetic similarity to the *B. childressi* group, both *Gigantidas* species harbour thiotrophic specimens (Miyzaki et al., 2010; Duperron et al., 2010). It should be noted that both *B. heretaunga* and *G. coseli* are small compared to modern species (Saether et al., 2010).

Mytilidae sp. A mussel specimen from the Lincoln Creek Formation was identified as modiolid. The specimen does not exhibit the bathymodiolin shell shape, and is therefore suspected to be heterotrophic.

Solemyidae (Protobranchia)

Solemyid clams are known from modern cold seeps and hydrothermal vents (Taylor and Glover, 2010), and date back to the Ordovician (Cope, 1996). In general the fossils have a similar morphology to living species (Taylor & Glover, 2010). All investigated Solemyidae harbour thiotrophic bacteria on which they are very dependent for their nutrition; in some species the digestive system is completely absent. They have an infaunal lifestyle and drill deep burrows in the sediment. (Duperron, 2013 and references within). Fossil specimens in our data have been assigned to (species within) the genera *Acharax* and *Solemya*, or have been identified only at a family level.

Lucinidae

The modern Lucinidae family contains the most chemosymbiotic bivalve species, and seep lucinids first emerged during the Jurassic period (Kiel et al., 2010). In our data set lucinids are represented by fossil specimens from 11 cold seep localities, ranging in age from the Pleistocene to the Cretaceous. All modern lucinids harbour thiotrophic symbionts within their gills (Taylor and Glover, 2000) and fossil specimens are therefore also suspected of having been chemosymbiotic. In addition to relying on symbionts for nutrition, lucinids retain the ability to filter feed (Duplessis et al., 2004). The large majority of our specimens belong to the genus *Lucinoma*, of which modern species are most widely reported from deep water habitats, including cold seeps. It has been observed that lucinid clams appear to be

more abundant at fossil cold seeps than at recent localities, which might be due to a sampling bias because of their burrowing lifestyle (Taylor & Glover, 2010).

Thyasiridae

Thyasiridae is represented in our suite of samples by specimens from the species *Conchocele bisecta*, from fossil cold seeps from the Early Pleistocene (Koshiba Formation) and the Oligocene (Lincoln Creek Formation), and '*Thyasira' townsendi* from cold seeps of Maastrichtian age from Seymour Island. *C. bisecta* is the largest living thyasirid and known from modern hydrocarbon seeps, where it obtains nutrition via thiotrophic chemosymbiosis (Kamenev et al., 2001). The majority of Thyasiridae are not chemosymbiotic, but because the larger thyasirid species, like *C. bisecta*, do harbour thiotrophic bacteria and it is therefore assumed that *T. townsendi* was also chemosymbiotic (Little et al., 2015). The chemosymbiotic species burrow deep into the sediment using their super-extensile foot, particularly at cold seeps, hydrothermal vents and oxygen minimum zones (Dufour and Felbeck, 2003). It has been suggested that symbioses have evolved several times during the evolution of this family, that first appeared in the Early Cretaceous (e.g. Duperron et al., 2013). The earliest association of thyasirids with seep deposits is Ryazanian (Hryniewicz et al., 2014).

Within the Thyasiridae dependence on symbiont-based nutrition can vary widely within chemosymbiotic thyasirids, and large species such as *C. bisecta* and can derive parts of their nutrition from filter feeding (Dando & Spiro, 1993; Dufour & Felbeck, 2006). In addition, there is evidence for bacterial sequences other than thiotrophs in the gills of thyasirids, but these have not yet been shown to be important symbionts (Rodrigues and Duperron, 2011).

Non-chemosymbiotic bivalve families

Ostreida. The Ostreidae (true oysters), Pectinidae (scallops) and Gryphaeidae (honeycomb oysters) families belong to the order Ostreida. The genus *Ostrea* within Ostreidae (represented by *Ostrea mushiana* in our suite of samples) contains sedentary filter feeders, that live epifaunally (Clarkson, 2009). Modern pectinid scallops from the *Mizuhopecten* genus (related to the fossil specimen *Mizuphopecten kobiyami*) also have an epifaunal and heterotrophic lifestyle, feeding on phytoplankton and detritus (e.g. Aya and Kudo, 2010). Lastly, *Pycnodonte* (*Phygraea*) *vesicularis vesicularis* from the Gryphaeidae was analysed,

this species is also expected to have obtained nutrition via filter-feeding on the sediment surface.

Praecardioida. Inoceramids (Inoceramidae) are an extinct group of large pteriomorph bivalves that became extinct at the end of the Mesozoic. Their common presence in low-oxygen environments and cold seeps has led some to suggest a chemosymbiotic lifestyle (MacLeod and Hoppe, 1992; Kauffmann, 1996). Alternatively, they could have been filter feeding on suspended food particles. Their unusually large gills would have been capable of processing large volumes of water quickly, which would have been beneficial in low oxygen ecosystems (Kiel et al., 2010; Knight et al., 2014). Inoceramids in our suite of samples were obtained from the Cretaceous Tepee Buttes seeps, and have been identified as *Inoceramus* sp.

Arcoida. The order Arcoida is represented in our material firstly by the filter-feeding family Glycymerididae (*Glycymeris* sp), that are expected to have been shallow burrowers similar to modern glycymerids (Tunnell et al., 2010). In addition, the order Arcoida is represented by the family Cucullaeidae, with fossil specimens from *Cucullaea* sp. and *Cucullaea capex*. Presently only one modern cucullaeid genus (including four *Cucullaea* species) still exists, and the animals are shallow burrowers that obtain nutrition via suspension feeding (Morton, 1981).

Veneroida. The species *Lahillia larensi* from Seymour Island belongs to the family Cardiidae. The species has an infaunal morphology, and is therefore suspected to have been a suspension feeder.

Nuculida (Protobanchia). The order Nuculida belongs to the Protobranchia, whereas all other orders in this section (with the exception of Solemyidae) belong to the autolamellibranchs with large leaf-like gills generally modified for food gathering and respiration. In general, protobranchs have simple protobranch gills, and are adapted to deposit feeding in soft muds (Stanley, 1986). Our suite of material contains three fossil taxa from the family Nuculidae within this order: *Ennucula* sp., *Nucula percrassa* and *Leionucula suboblonga*. Modern nuculids are infaunal and use extensible palp proboscides to collect sediment deposits (Yonge, 1939).

4.2.1.2 Gastropoda

All fossil gastropod specimens in our data set are suspected heterotrophs, that rely on photosynthetically produced carbon for their nutrition.

Caenogastropoda (excl. Neogastropoda). Ceanogastropoda are the largest and most diverse group of living snails, and taxa occupy a range of habitats and feeding

strategies (Colgan et al., 2007). Fossil material belonging to the clade Caenogastropoda contains a fossil representative of the modern predatory snail *Fusitrition oregonensis* that belongs to the family Ranellidae. *Ranella galea* also belongs to the ranellids, and modern species of this genus have been observed to 'graze' on sessile prey (Booth, 2014). In addition *Vanikoropsis arktowskiana* from the family Vanikoridae was analysed, which is suspected to be predatory and have obtained nutrition through boring other bivalves and gastropods (pers. comm. J. Witts). The final family of the ceanogastropods that was analysed are the Turritellidae (*Turritella* sp.). Living turritellids are mainly sessile, semi-faunal suspension feeders (Allmon, 2011).

Neogastropoda. Several of specimens belong to the clade Neogastropoda within the Caenogastropoda, modern species within this clade are generally carnivorous with varying degrees of predatory activity (applies to Neogastropod n.gen. from this study). This clade includes the family Buccinidae (with the fossil species *Neptunea kuroshio* of the carnivorous genus *Neptunea* from this study) that includes many generalist species that feed on a variety of dead and living organisms. The Volutidae family (includes the fossil species *Fulgoraria prevostiana* and *Fulgorira kamakuraensis*) also belongs to the neogastropods, and modern volutids are known to feed on other gastropods and bivalves, among other invertebrates (Smith et al., 2011 – *Neptunea*; Modica & Halford, 2010 and references within). A similar feeding strategy has been suggested for the family Fasciolariidae, to which the genus *Drilluta* belongs (Modica & Halford, 2010).

Vetigastropoda. *Amberleya spinigera* from Seymour Island belongs to the extinct family Amberleyidae, and it's palaeoecology is currently unknown, but a heterotroph lifestyle is suggested.

4.2.1.4 Cephalopoda

In our suite of samples cephalopods are primarily represented by the ammonoids, an extinct group characterized by an external aragonitic shell with complex sutures. Most fossil ammonoids show no morphological resemblance to recent cephalopods, which has hampered investigation into the palaeoecology of this group. It is however evident that ammonoids evolved a buoyancy mechanism and were capable of swimming, and their habitat is suggested to be epipelagic, mesopelagic or epibenthic. But in addition to nektic carnivores, they have also been suggested to

be demersal herbivores or scavangers, and various modes of life (in relation to the water column – nektonic / planktonic / bentic) have been suggested (Ritterbush et al., 2014 and references therein). In addition to ammonoids from non-seep environments, our data set includes fossil ammonoid specimens that were obtained from ancient colds seep settings: the heteromorph *Baculites* sp. (Tepee Buttes) and the coiled *Maorites seymourianus* (Seymour Island). It has been suggested that seep ammonoids were feeding on the phytoplankton and zooplankton attracted to the methanotrophic and thiotrophic bacteria (Landman et al., 2012). Non-seep ammonoids include a variety of species from Owl Creek Formation and Seymour Island. The latter locality also provided the species *Eutrephoceras dorbignyanum*, that belongs to the subclass Nautiloidea (characterized by simple sutures of the shell) and their palaeobiology is similarly obscure. However, this subclass contains the living genus *Nautilus*. The extant species *Nautilus pompilius* (Phillippines) was therefore also analysed.

4.2.1.3 Scaphopoda

Our suite of samples contains *Dentalium* sp. from two Japanese fossil seep localities. The genus belongs to the family Dentallidae within the tusk shells. Modern tusk shells are infaunal predators (Shimek, 1990).

4.2.1.5 Phylum: Brachiopoda

In addition to molluscan groups, fossil specimens from the phylum Brachiopoda were analysed. Modern brachiopods are heterotrophic, and filter feed food particles out of the water using the lophophore organ whilst attached to the seafloor (Clarkson, book). A heterotrophic lifestyle is therefore also postulated for specimens of the family Terebratulidae (Koshiba Formation, non-seep locality) and *Liothyrella* sp. (Moonlight North), that also belongs to the terebratulid family. At the latter Miocene seep locality brachiopods are considered as background fauna, because they are not found in seep environments at the present day. However, at many Palaeozoic and Mesozoic seeps brachiopods were common components, in particular species belonging to the superfamily Dimerelloidea, within the order Rhynchonellida. Their mass abundance has led some to propose a chemosymbiotic lifestyle for ancient seep brachiopods, in particular the larger species (Sandy et al., 2010 and references within). Our suite of samples includes the seep-dwelling dimerelloid genera: *Halorella*, *Ibergirhynchia* and *Dzieduszyckia.* An adaptation to

seeps has also been suggested for dimerelloid *Anarhynchia*, and for *Septatrypa* belonging to the order Atrypida (Sandy et al., 1995; Sandy et al., 2010).

4.2.1.5 Phylum: Annelida

The annelids are represented in our sample set by the extinct genus *Rotularia*, that belongs to the family Serpulidae. *Rotularia* are tubeworms with spirally coiled calcareous shells. Unlike most serpulids, *Rotularia* lived unattached, instead of (partially) cemented to the substrate (Vinn and Furrer, 2008). Suggestions about their palaeoecology vary, and they have been described as both epifaunal and as burrowers, as grazers as well as sessile filter/suspension feeders (Savazzi, 1995).

4.2.2 Methods

4.2.2.1 SBOM isolation, stable isotope analyses and elemental concentration

SBOM was isolated using cation exchange resin, as well as 10%HCl. For SBOM isolation using resin, SBOM is isolated from shell powder placed in a dialysis bag that is surrounded by deionised water with cation exchange resin, the resin binds calcium ions whilst releasing carbon dioxide. For SBOM isolation using acidification, 10%HCl was added to shell powder in a glass vial, expelling inorganic carbon as CO_2. Intra-crystalline SBOM was be analysed by treating the shell powder with 12% NaOCl (bleach) prior to SBOM isolation, which removes the inter-crystalline SBOM fraction. Carbonate-associated sulphate (CAS) was precipitated from the deionised water containing the cation exchange resin, as well as from 10%HCl solutions. Detailed descriptions of the methodologies concerning SBOM/CAS isolation and isotopic and elemental analyses are given in Chapter 2. The analysis of most fossil specimens required additional preparation, whereby shell material had to be removed from the sediment using a hammer and chisel, as well as a scalpel.

Effect of SBOM isolation on the isotopic signal of SBOM and CAS

Cation exchange resin was initially used on all samples because of known limitations of alternative shell removal techniques. However, method comparison in a related study (Chapter 2) showed that residual resin compounds influence the sulphur signatures of SBOM samples, with $\delta^{34}S$ moving closer to the resin value ($\delta^{34}S$ -1.5‰) with increasing elemental sulphur concentrations. Therefore SBOM

was also isolated using 10%HCl for samples with sufficient remaining shell powder after extraction using cation exchange resin. In addition, it was shown in Chapter 2 that resin-obtained total SBOM samples still allow differentiation between sulphur sources with positive $\delta^{34}S$ (SBOM > +3‰, representing soft tissue values up to +20‰), and sources with negative $\delta^{34}S$ values (SBOM < -3‰, values below < -5‰ represent soft tissue values up to -25‰). For intra-crystalline SBOM the thresholds are $\delta^{34}S$ +2‰ and -2‰, respectively. SBOM obtained using cation exchange resin with $\delta^{34}S$ values within the described thresholds are also included in Figure 4.19. $\delta^{34}S$ values of CAS obtained using cation exchange resin are similarly affected by residual resin, and do not reflect modern seawater sulphate values ($\delta^{34}S$ +20.3‰) (as discussed in Chapter 2). However, for several fossil samples very negative $\delta^{34}S$ values were obtained, that cannot explained by the presence of residual resin and are therefore reported in this study.

Because for multiple specimens in this study SBOM was obtained from homogenized shell powder using both cation exchange resin and 10%HCl, the effects of both methods on $\delta^{13}C$ SBOM values could be compared. Differences in carbon composition are generally less than 1‰ between the two methods ($\delta^{13}C$ 0.0‰ ±2.6, n=27, total SBOM and intra-crystalline SBOM), and no obvious trend can be observed in relation to total SBOM $\delta^{13}C$ values. Insufficient data (n=2) was available for $\delta^{15}N$ comparison.

4.2.2.2 Shell carbonate $\delta^{13}C$ analysis

Aliquots of the homogenized shell powder used for SBOM isolation were analysed for $\delta^{13}C$ values of the mineral phase, which was performed at the Scottish Universities Environmental Research Centre (East Kilbride). CO_2 was quantitatively released by standard in vacuo digestion with 100% phosphoric acid at 25°C. The produced gases were analysed on a VG SIRA 10 mass spectrometer, minotoring mass to charge ratios of 44, 45 and 46. Analytical raw data were corrected using standard procedures (Craig, 1957). The error of reproducibility, based on complete analysis of internal standards (including acid digestion) was ±0.1‰.

4.2.2.3 Radiocarbon dating of subfossil shell and SBOM samples

Shell fragments and SBOM were converted into graphite at the NERC Radiocarbon Facility-East Kilbride, and subsequent ^{14}C analysis was performed at the SUERC AMS Laboratory. The dating of the subfossil samples was unknown or poorly

constrained: Congo Fan (45.5-3.0ka BP, Feng et al., 2010), Hikurangi Margin (unknown), and Krishna-Godavari Basin (nearby core site, similar depth: 42.5-40 ka BP, Mazumdar et al., 2009). Shell fragments from these localities were prepared by removing the outer 20% by weight of the sample by controlled hydrolysis with dilute HCl. The samples were subsequently rinsed in deionised water, dried and homogenised. A known weight of the pre-treated sample was hydrolysed to CO_2 using 85% orthophosphoric acid at room temperature. The CO_2 was converted to graphite by Fe/Zn reduction.

From the same suite of shell fragments, SBOM was obtained for ^{14}C analysis using cation exchange resin. Because SBOM had not previously been used for ^{14}C analysis, test materials with known ^{14}C enrichment were prepared following the cation exchange resin method to constrain the effect of SBOM extraction. These test materials include SBOM from *Mytilus edulis* (modern) and Cretaceous *Nymphalucina occidentalis* (radiocarbon dead), as well as the standard materials TIRI barleymash (modern) and anthracite (radiocarbon dead) that were both isolated in milligram quantities from a mixture with Iceland spar calcite (< 0.5 grams) to simulate SBOM isolation from the shell minerals. All the test materials were quantitatively transferred into pre-cleaned quartz inserts. The total carbon in this weight was recovered as CO_2 by heating with CuO in a sealed quartz tube. The gas was converted to graphite by Fe/Zn reduction. In addition the $\delta^{13}C$ values and carbon content (% by wt.) of the test material were measured on a dual inlet stable isotope mass spectrometer (Thermo Fisher Delta V). Any effect on the test materials will be incorporated into the final radiocarbon results by using the test materials to calculate an SBOM specific process background correction.

4.2.2.4 Amino acid racemization analysis

Amino acid racemization analyses were performed on fifteen samples from varying geological ages, ranging from subfossil to the Devonian (Table 4.3). Chiral amino acid analyses of subsamples from the homogenized shell powders were undertaken to assess the originality of protein, and were performed at the University of York. All samples were prepared using the procedures of Penkman et al. (2008) to isolate the intra-crystalline protein by bleaching. Two subsamples were then taken from each shell; one fraction was directly demineralised using 2M HCl and the free amino acids analysed (referred to as the 'free' amino acids, FAA, F), and the second was treated to release the peptide-bound amino acids by demineralisation using 7M HCl and heating in a 110° oven for 24h, thus yielding the 'total' amino acid concentration,

referred to as the ‘total hydrolysable amino acid fraction (THAA, H*). Samples were then dried by centrifugal evaporator and rehydrated for RP-HPLC analysis with 0.01 mM L-homo-arginine as an internal standard. The amino acid compositions of the samples were analysed in duplicate by RP-HPLC using fluorescence detection following a modified method of Kaufman and Manley (1998). During preparative hydrolysis both asparagine and glutamine undergo rapid irreversible deamidation to aspartic acid and glutamic acid respectively (Hill, 1965). It is therefore not possible to distinguish between the acidic amino acids and their derivatives and they are reported together as Asx and Glx respectively.

4.2.2.5 Scanning Electron Microscopy and Cathodoluminescence imaging

Shell pieces from a subset of the samples (Table 4.3) were embedded in epoxy and sectioned using a speed saw. The cut surfaces were ground and polished, and before SEM analysis the polished blocks were coated with iridium to prevent charging. For the subsequent CL analysis of the sectioned blocks were re-polished to completely remove the iridium coating.

SEM analysis was performed at the University of Leeds using a FEI Quanta 650 FEMSEM with 5 micron resolution. CL analysis was conducted at the University of Edinburgh using a cold cathode, CITL 8200 Mk 3A mounted on a Nikon Optiphot petrological microscope and a Lumenera Infinity 3 digital camera. For the analysis 30Kv and 1000uA electron gun current were used.

Analytical approach

The various analyses of SBOM and shell fragments are summarised in Table 4.3, and the species and localities on which these were performed (excl. stable isotope analysis) are listed.

Table 4.3 Overview of analyses

Species (Family)	Age / Locality	Radio carbon	AAR	Py-GC/MS	SEM and CL
L. chuni (Vesicomyidae)	1283 B.P. Congo Fan	X	X		
C. tuerkayi (Vesicomyidae)	1227 B.P. Hikurangi Margin	X			X
Vesicomyidae	42.5-40 ka Krishna-Godavari Basin	X	X	X	X
Bathymodiolus sp. (Mytilidae)		X		X	
Acharax sp. (Solemyidae)	Middle Pleistocene Kakinokidai seep				X
L. aokii (Lucinidae)			X	X	X
L. spectabilis (Lucinidae)	Early Pleistocene Koshiba Formation		X		
C. bisecta (Thyasiridae)					X
Terebratulidae			X		
Lucinoma sp. (Lucinidae)	Early Pleistocene Kounandai seep				X
Lucinoma sp. (Lucinidae)	Plio-Pleistocene Takanabe Formation				X
Calyptogena sp. (Vesicomyidae)	Upper Pliocene Shiramaza Formation		X		X
G. coseli (Mytilidae)	Miocene Moonlight North				X
Lucinoma sp. (Lucinidae)			X		
Liothyrella sp. (Brachiopoda)			X		X
C. pacifica (Vesicomyidae)	Miocene Hokkaido		X		X
L. acutentilineatum (Lucinidae)	Lower Miocene Izura seep				X
Lucinoma sp. (Lucinidae)	Oligocene Lincoln Creek Formation		X		X
N. occidentalis (Lucinidae)	Cretaceous Tepee Buttes	X	X	X	X
Inoceramus sp. (Inocermidae)					X

Anarhynchia (Brachiopoda)	Jurassic Oregon, US		X		X
Halorella (Brachiopoda)	Triassic Oregon, US		X	X	X
I. contraria (Brachiopoda)	Carboniferous Harz Mountains				X
D. crassicostata (Brachiopoda)	Devonian Sidi Amar		X		X

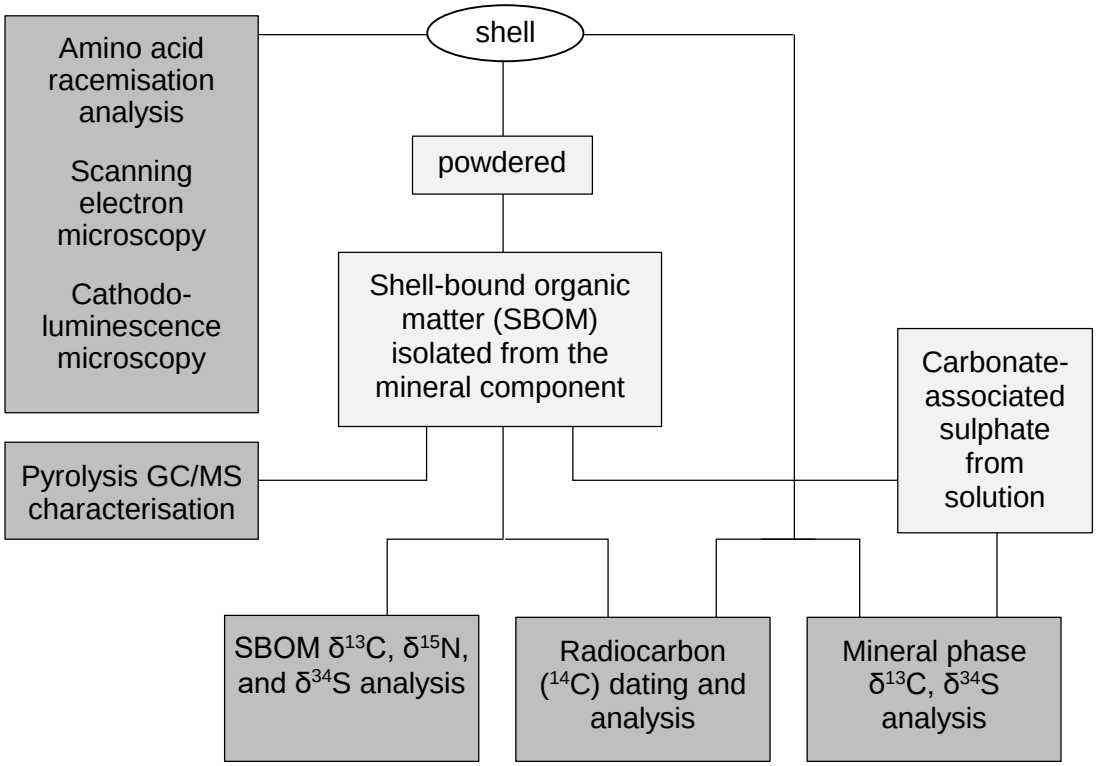

4.3 Results

In this section the results from methods assessing the preservation of SBOM are presented first, followed by stable isotope results of SBOM and shell carbonate.

4.3.1 Radiocarbon analysis

Radiocarbon ages (± 1σ) were obtained from shell fragments of *L. chuni* from Congo Fan (1299 ±37, 1298 ±35, 1250 ±35, and 1283 ±36 years BP), and *C.*

tuerkayi from Hikurangi Margin (1227 ±35 years BP). For the samples of Vesicomyidae sp. and *Bathymodiolus* sp. from the Krishna-Godavari Basin the results were indistinguishable from the background, meaning that net sample activity is < 1σ of the process background of 51,227 ±2,835 years BP.

^{14}C analysis of subfossil SBOM from the same sample set was not performed because it was not possible to obtain reliable ^{14}C values for test materials. Both radiocarbon dead test samples are enriched in ^{14}C, with radiocarbon ages of 9,966 (±42) years BP for *N. occidentalis* SBOM, and 24,876 (±181) years BP for the anthracite sample. A modern age was measured for SBOM for *M. edulis*, but the calculated age of the TIRI barleymash sample (419 ±37 years BP) suggests incorporation of anthropologically derived ^{14}C. Because of the variable and significant sources of contamination of the ^{14}C values from the test materials, it was not attempted to analyse the SBOM from subfossil samples. Quantification of this contamination would require further, extensive testing of each stage of the cation exchange resin method, which is outside the scope of this project.

4.3.1 Amino acid racemisation analysis

AAR is used to determine whether intra-crystalline protein components of SBOM have remained unaffected by external diagenetic influences. The criteria to determine whether organic degradation products are original include: (i) correlation between free (FAA) amino acids and total hydrolysable amino acids (THAA), that indicates a closed system because free amino acids are the most easily leached amino compounds, (ii) D/L ratios consistent with age, based on expected racemisation speed over time of the different amino acids, (iii) amino acid concentrations consistent with a decrease over time, and (iv) consistency in composition amongst the samples (THAA composition shown in Fig. 4.1) (pers. comm. K. Penkman; Mitterner, 1993). By reviewing the data using these criteria it was concluded that amino acids isolated from Vesicomyidae sp. (Krishna-Godvari basin), *Laubiericoncha chuni* (Congo Fan), *Lucinoma aokii* (Kakinokidai seep), *Lucinoma spectabilis* and Terebratulidae sp. (Koshiba Formation), *Calyptogena* sp. (Shiramaza Formation), *Calyptogena pacifica* (Hokkaido), and *Nymphalucina occidentalis* (Tepee Buttes) are consistent with the presence of original protein.

Figure 4.1 THAA composition of intra-crystalline SBOM for selected samples

Samples shown: original amino acids were found in species from the Krishna-Godavari Basin (KGB, subfossil), Shiramaza Formation (SF, Upper Pliocene), Hokkaido (H, Miocene), and Tepee Buttes (TB, Cretaceous). Samples from Moonlight North (MLN, Miocene) and Lincoln Creek (LC, Oligocene) show evidence for modern contamination, in particular for the D/L ratio of serine (indicated by the arrow).

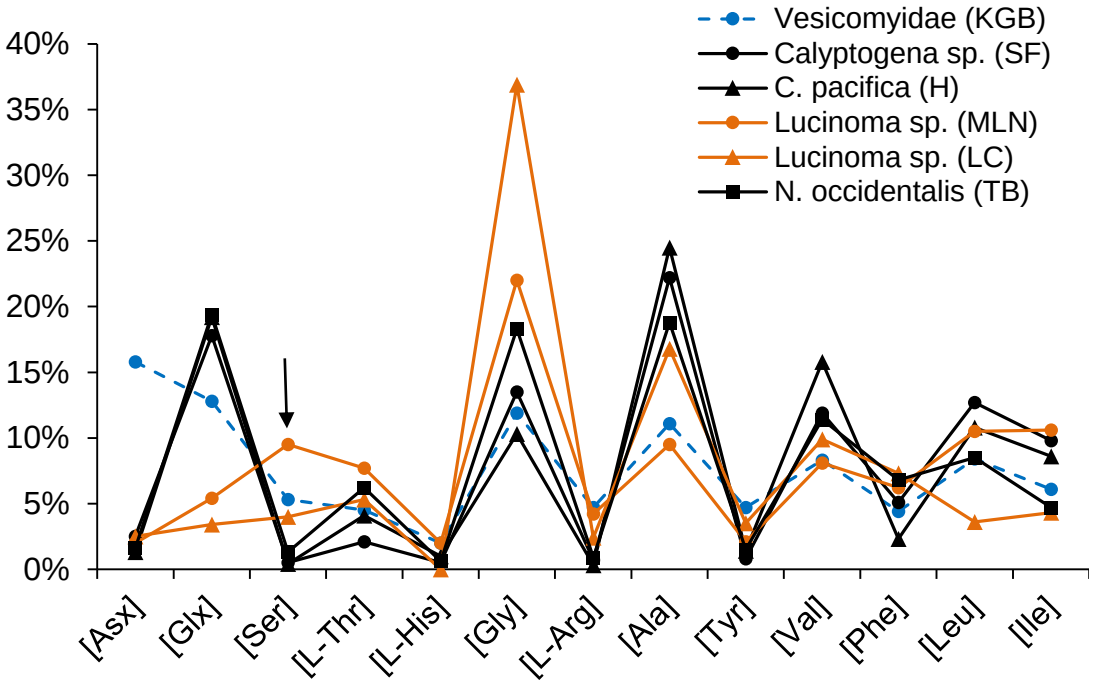

Three samples were low in concentration and inconsistent in composition: *Liothyrella* sp. and *Lucinoma* sp. (Moonlight North), and *Lucinoma* sp. (Lincoln Creek)**.** In particular should be noted the high L-serine (Ser, Fig. 4.1) value, which is a major by-product of metabolic processes (Hamilton, 1965; Hare, 19655), and indicates modern contamination instead of original amino acids (e.g. Preece & Penkman, 2005). The serine ratio is therefore also relatively high in the subfossil Vesicomyidae sp. sample (Krishna-Godavari Basin). In the intra-crystalline SBOM from the Palaeozoic seep brachiopod samples *Anarhyncha*, *Halorella* and *Dzieduszyckia crassicostata* no amino acids were detectable (limit of detection: ~picomoles/mg).

These results suggest that original intra-crystalline protein (cf. intra-crystalline SBOM) has to be potential to be preserved unaltered in Cretaceous specimens (*N. occidentalis*) and possibly older fossils, but can also become contaminated in geological younger specimens (Miocene, Oligocene). This suggests that the presence of original protein/SBOM is strongly linked to local preservation

conditions. All analysed Palaeozoic brachiopod samples have yielded (total) SBOM, and the absence of amino acids in these samples indicates that the original protein has converted into a non-hydrolysable kerogen-like substance as a result of condensation reactions. This condensed substance can also contain contaminants from the surrounding environment, in addition other compounds (e.g. small free amino acids) could have leached out of the shell. Kerogen is more stable than the original labile biochemicals, and can be expected in ancient remains (Mittinger, 1993).

4.3.2 Pyrolysis gas chromatography mass spectrometry (Py-GC/MS)

The selected results from Py-GC/MS analysis are shown in Fig. 4.2, in which a comparison is made between modern *Calyptogena ponderosa* (Vesicomyidae) from the Gulf of Mexico seeps, and two extremes of our fossil dataset: subfossil Vesicomyidae sp. (Krishna-Godavari Basin), and Cretaceous *N. occidentalis* (Tepee Buttes). Identification and distribution of the major peaks can be compared between the samples. The most striking difference between the modern and fossil samples, is the absence/low intensity of the akyl lipids in Vesicomyidae sp. and *N. occidentalis*. The pyrogram Vesicomyidae sp. is much more similar to the modern sample than *N. occidentalis*, though both species do not show the variety of protein-compounds (compounds 7-11). Moreover, additional major peaks are present in *N. occidentalis* that have not been identified in the modern and subfossil sample. The observation of a sugar (compound 16) is very interesting.

Figure 4.2 Total ion chromatograms from pyrolysis GC/MS for total SBOM from suspected thiotrophic cold seep fossils

Vesicomyidae sp. and *N. occidentalis* total SBOM samples were isolated using cation exchange resin. The results are compared to total SBOM from thiotrophic *Calyptogena ponderosa* (presented in Chapter 3).

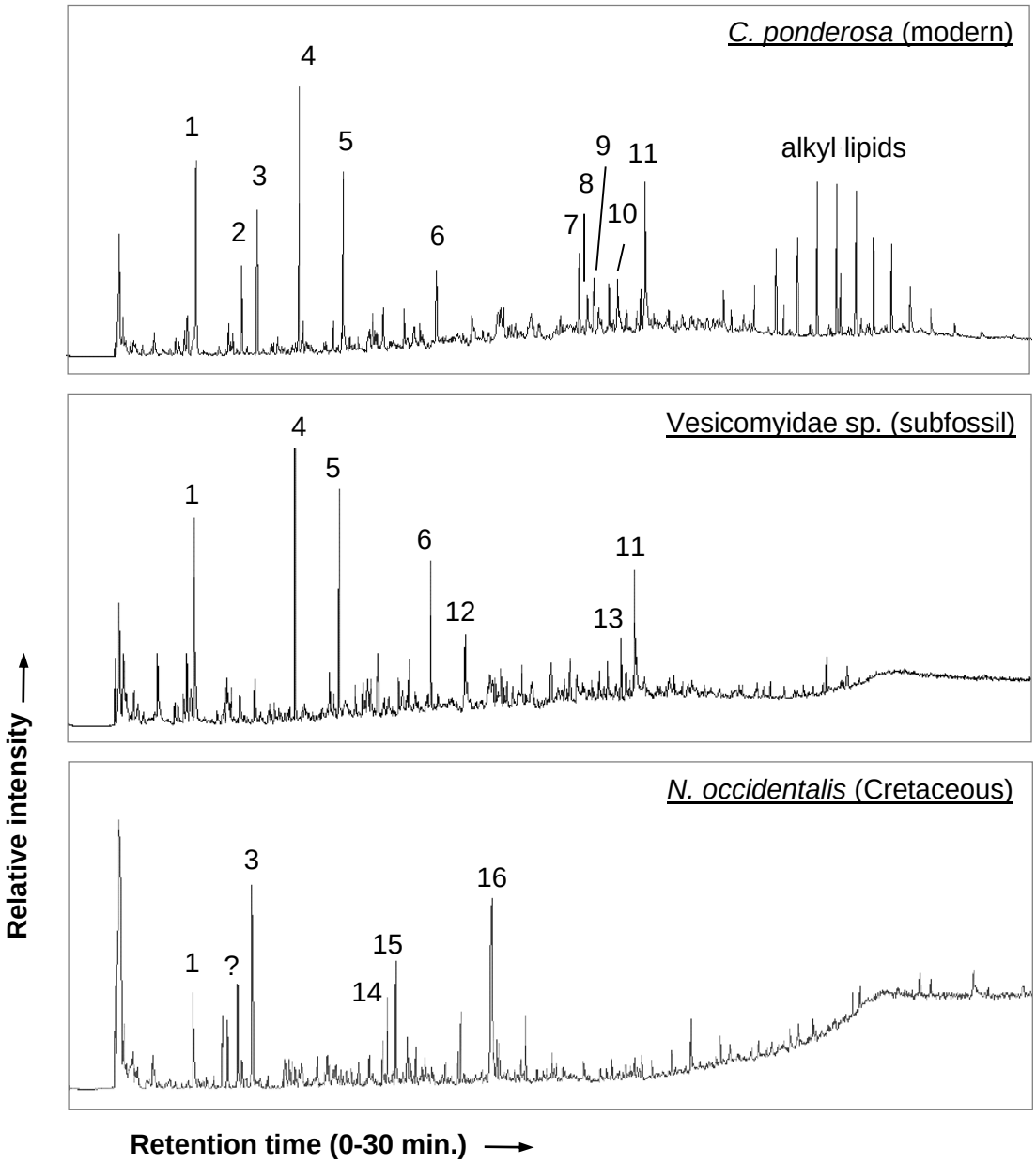

1	Toluene	**9**	Glycyl-L-proline
2	Ethyl Benzene	**10**	Pyrrolo[1,2-a]pyrazine-1,4-dione, hexahydro-3-(2-methylpropyl)-
3	Styrene	**11**	5,10-Diethoxy-2,3,7,8-tetrahydro-1H,6H-dipyrrolo[1,2-a;1',2'-d]pyrazine
4	Phenol	**12**	1H-Indole, 2-methyl
5	Methyl Phenol	**13**	Heptadecanenitrile
6	5H-1-Pyrindine	**14**	Decane, 2,3,5,8-tetramethyl-
7	Uric Acid	**15**	Benzaldehyde, 3,4-dimethyl-
8	1H-Pyrazole-1-carboxaldehyde, 4-ethyl-4,5-dihydro-5-propyl-	**16**	à-D-Glucopyranose, 4-O-á-D-galactopyranosyl-

4.3.3 Scanning Electron Microscopy (SEM) and Cathodoluminescence Imaging (CL)

The focus of SEM and CL analyses in this study is placed on identifying possible preservational issues and diagenetic indicators in the shell material. Many bivalves and brachiopods possess multi-layered shells with a variety of microstructures, and to be able to effectively identify potential changes to the shell material over time, the shell structures are compared to modern (pristine) shells. These comparisons are made per family/species, because the ultrastructure of shells is often linked to phylogenetic classification. The two screening techniques are discussed together per specimens. For the large majority of samples younger than the Cretaceous, no luminescence was observed and these specimens are assumed to have retained their primary minerology. For these specimens CL results are not explicitly mentioned and no CL images are included.

4.3.3.1 Vesicomyidae

Modern *Calyptogena* shells have a two-layered structure: an outer homogenous/granular layer, and an inner nacreous layer (Gale et al., 2004; Sato-Okoshi et al., 2005). In other vesicomyid species, irregular fibrous prisms, and diffuse (complex) crossed lamellar (appearing homogenous at higher magnification), and spherulitic structures have also been identified (Signorelli et al., 2015; Kennish et al., 1996 and 1998).

Calyptogena tuerkayi (Hikurangi Margin, subfossil). In *C. tuerkayi* the inner layer appears the be absent, and the complete shell structure is homogenous (Fig. 4.3A). The primary mineralogy of the shell is confirmed by the presence of several myostracal layers (Fig. 4.3C), these have been laid down underneath muscle attachment areas (Taylor et al., 1969) and would have been obliterated during recrystallization. Only the presence of several thin cracks points to possible preservational issues of the main areas of the shell material. However, the inner and outer margin of the section are amorphous in appearance (Fig. 4.3B,D,E), which could be caused by marine microorganisms. Potentially these areas are obscuring additional shell layers of *C. tuerkayi*.

Vesicomyidae sp. (Krishna-Godavari Basin, subfossil). The vesicomyid specimens from the Krishna-Godavari Basin have a similar single-layer structure to the previous specimens (Fig. 4.3F), but in this specimen faint chevron patterning was observed, indicating the presence of a type of cross-lamellar microstructure (Cuif et al, 2011 and refs within; no nice picture to show). Further evidence for the originality

of the shell structure is presence of myostracal layers (Fig. 4.3F). At the bottom of the section there is some dissolution and merging of shell crystals (Fig. 4.3G).

For both subfossil specimens it is very likely that the diagenetically altered outer layers of the shell were removed during cleaning. Because of the geologically recent age of the specimens a potential nacreous inner layer is assumed to be obscured by these diagenetic effects, or to not have been present.

***Calyptogena* sp.** (Shiramaza Formation, Upper Pliocene). Four specimens from this species were analysed and preservation differs between them. The large majority of each shell section consists of small homogenous crystals, and in some a complex crossed lamellar structure can clearly be identified (Fig. 4.4B). In the most pristine specimen several different microstructures known from modern vesicomyids can be seen throughout the section, in particular towards the top and edges of the section. These include a spherulitic structure underlain by a fibrous prismatic area (Fig. 4.4A), and horizontally orientated plywood-structure (Fig. 4.4D),. None of the specimens showed luminescence, but diagenetic alterations of the specimens includes: a poorly preserved, recrystallized area along the top of the section (~500µm thickness) and the presence of sulphide crystals near this front (Fig 4.4C), merging of crystals and upper and lower margin, as well as (small) patches within the better preserved areas (Fig. 4.4D, in addition to the dark patches of recrystallization), and dissolution of shell material on the edges and in the centre (~500µm width)

Calyptogena pacifica (Hokkaido, Miocene). The Hokkaido specimens all display a homogenous structure with myostraca and the absence of a nacreous layer, with hints of a crossed lamellar structure in one specimen. In the same sample a quarter of the shell is strongly diagenetically altered and shows microborings (Fig 4.4E), in general similar dark patches of recrystallization as in *Calyptogena* sp. are present, as well as the marginal amorphous diagenesis seen in *C. tuerkayi* (Fig. 4.4F). One of the specimens is very poorly preserved and, contrary to the other specimens, primary shell structure is largely absent and the original crystal shape is lost (Fig. 4.4G).

Figure 4.3 SEM images of cross-sections from subfossil *C. tuerkayi* and Vesicomyidae sp. shell fragments

C. tuerkayi: (a) area overview, (b) upper area, (c) middle area, (d) lower area, (e) detail of the lower area, with an amorphous appearance. Vesicomyidae sp.: (f) single layer structure with myostracal layers, (g) dissolution and merging of crystals. Scale bars: white=100µm, black=10µm

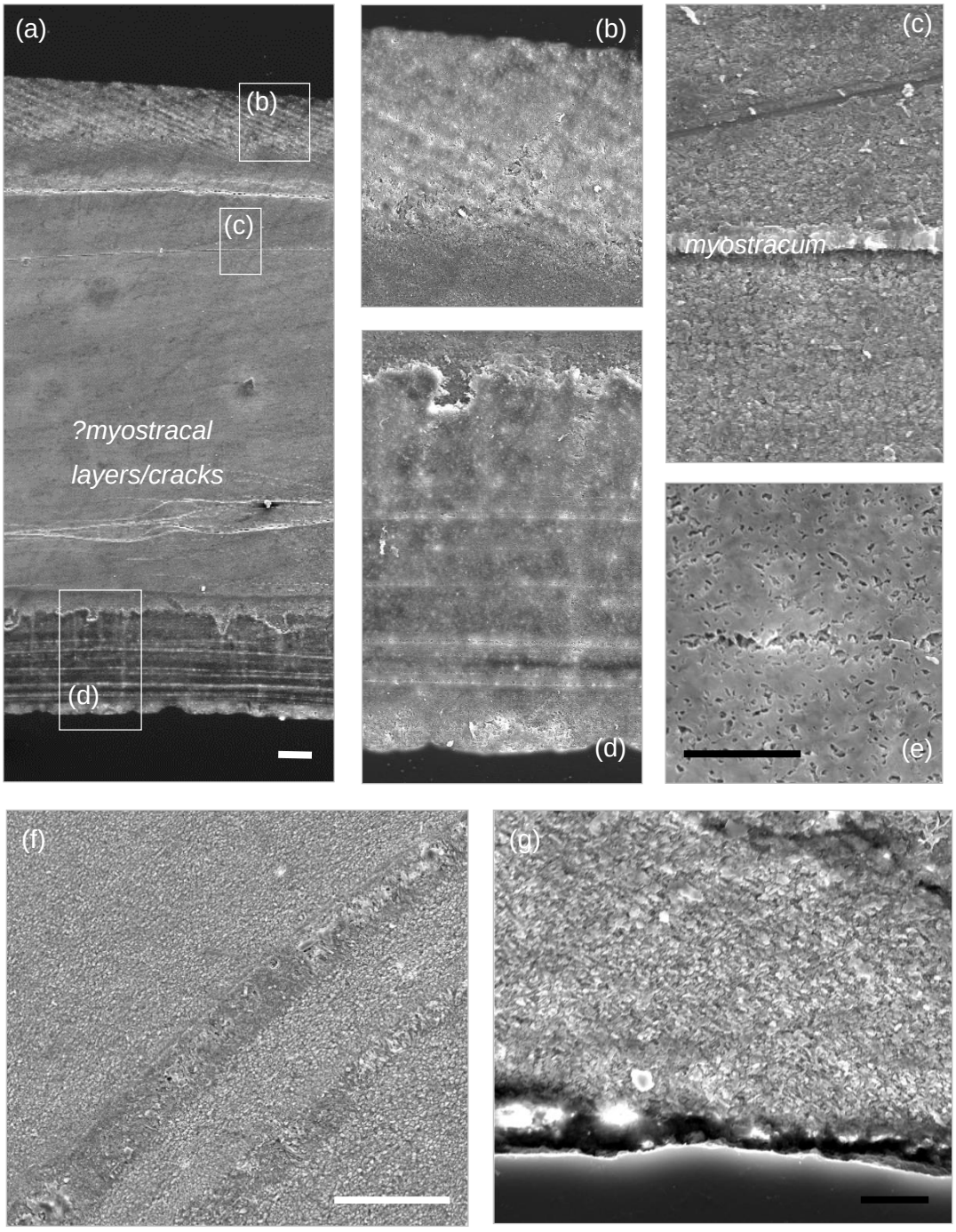

Figure 4.4 SEM images of cross-sections from *Calyptogena* sp. and *C. pacifica* shell fragments

Calyptogena sp.: (a) top of the section with spherulitic and prismatic structures, (b) complex crossed lamellar structure, (c) recrystallisation and sulphide crystals, (d) bottom of the section with plywood structure, with recrystallisation patch. *C. pacifica*: (e) microborings, (f) recrystallisation, (g) poor preservation with absence of shell structure. Scale bars: white=100µm, black=10µm

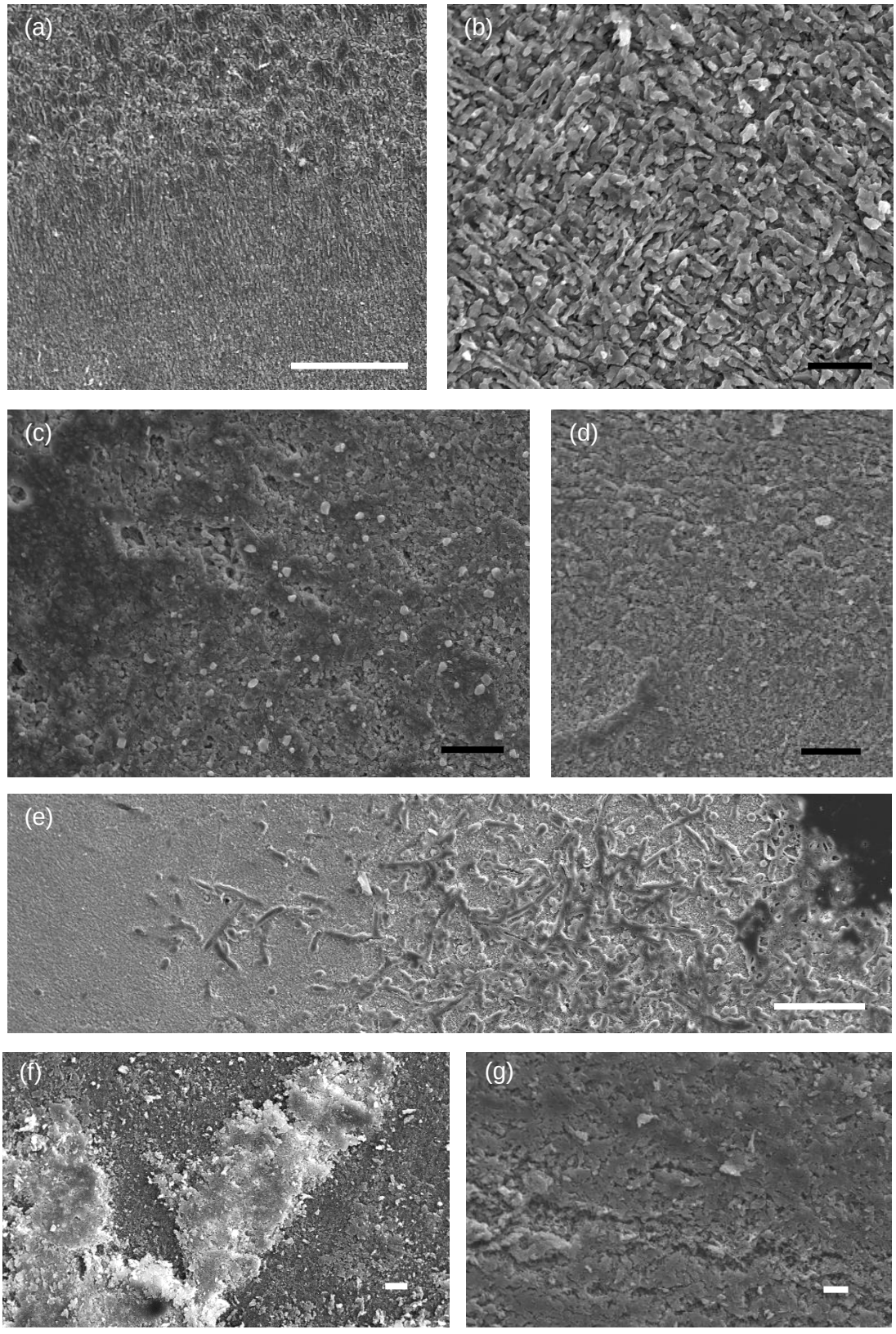

4.3.2.2 Lucinidae

In the modern lucinid shell usually three shell layers can be recognized: and outer irregular spherulitic layer, and middle layer of crossed-lamellar structure, and an inner complex crossed lamellar layer together with thin prismatic sheets (Taylor, Kennedy & Hall, 1973).

Lucinoma aokii (Kakinokidai seep, Middle Pleistocene). Two pristine specimens were examined and clearly show three distinct layers (Fig. 4.5A), with an upper spherulitic layer similar to modern specimens (Fig. 4.5C), but the middle and inner layer differ. Instead of a crossed lamellar structure the middle layers consists of very small tabular crystals, intertwined with vertical lines of organic matter (Fig. 4.5B), it is unclear if the latter is a diagenetic artefact, considering the otherwise pristine preservation of the specimens. The inner layer consists of broad, irregular prismatic fibres instead of sheets (Fig. 4.5A).

Figure 4.5 SEM images of cross-sections from *L. aokii* shell fragments
(a) three layered structure, (b) middle tabular layer with vertical “organic” lines (c) upper spherulitic layer. Scale bars: white=100µm, black=10µm

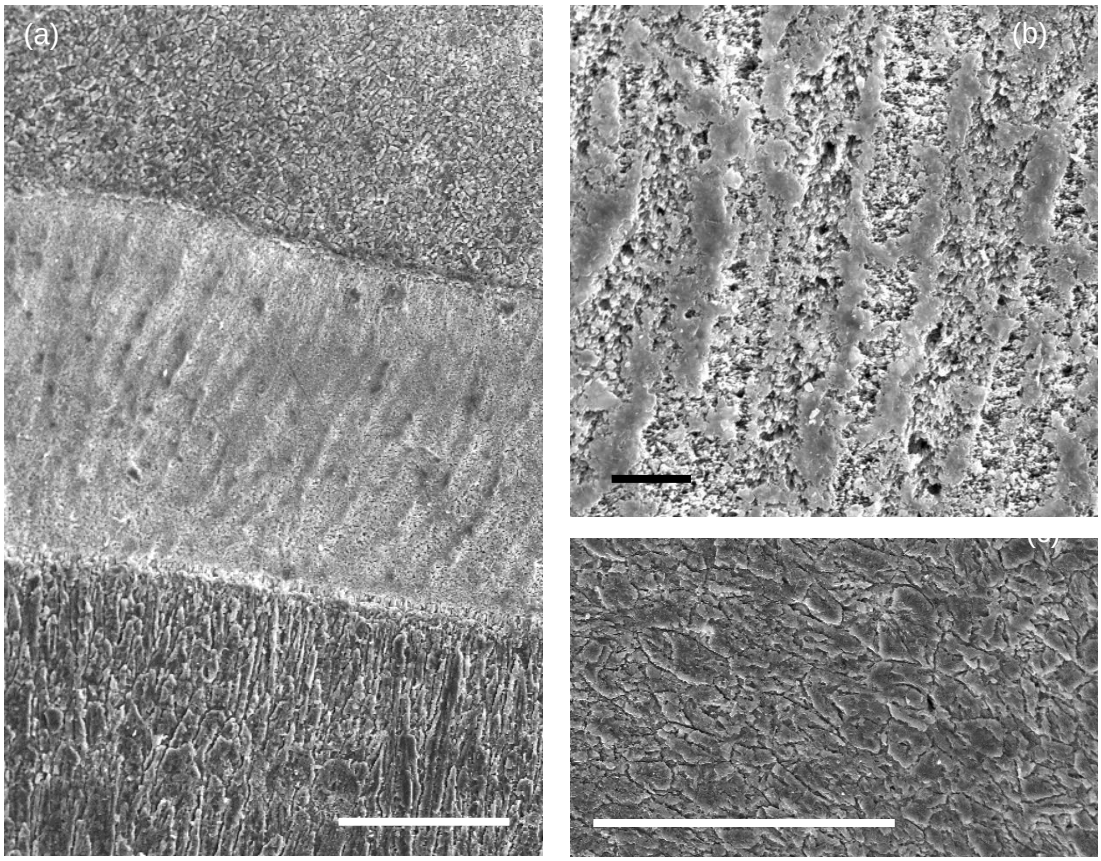

***Lucinoma* sp.** (Kounandai seep, Early Pleistocene). The specimens show the same three-layered structure as the *L. aokii* specimens described above (Fig. 4.6A), including the vertical rows of merged 'organics' in the middle layer. However, in one of the specimens the crossed-lamellar structure is visible in the middle layer (Fig. 4.6C). In this layer diagenetic alteration is visible and becomes more severe towards the upper margin, ranging from the merging of crystals to heterogeneous/unorientated crystals showing a relic chevron structure. Additionally, in this specimen a strongly diagenetically altered 'front' is present (<100µm thickness), that is present continuously above a (?recrystallized) inner layer with uncoordinated crystal structure (Fig. 4.6D).

Figure 4.6 SEM images of cross-sections from *Lucinoma* sp. shell fragments (a) middle and inner layer, (b) myostracal layer, (c) crossed-lamellar structure in middle layer, (d) diagenetic front. Scale bars: white=100µm, black=10µm

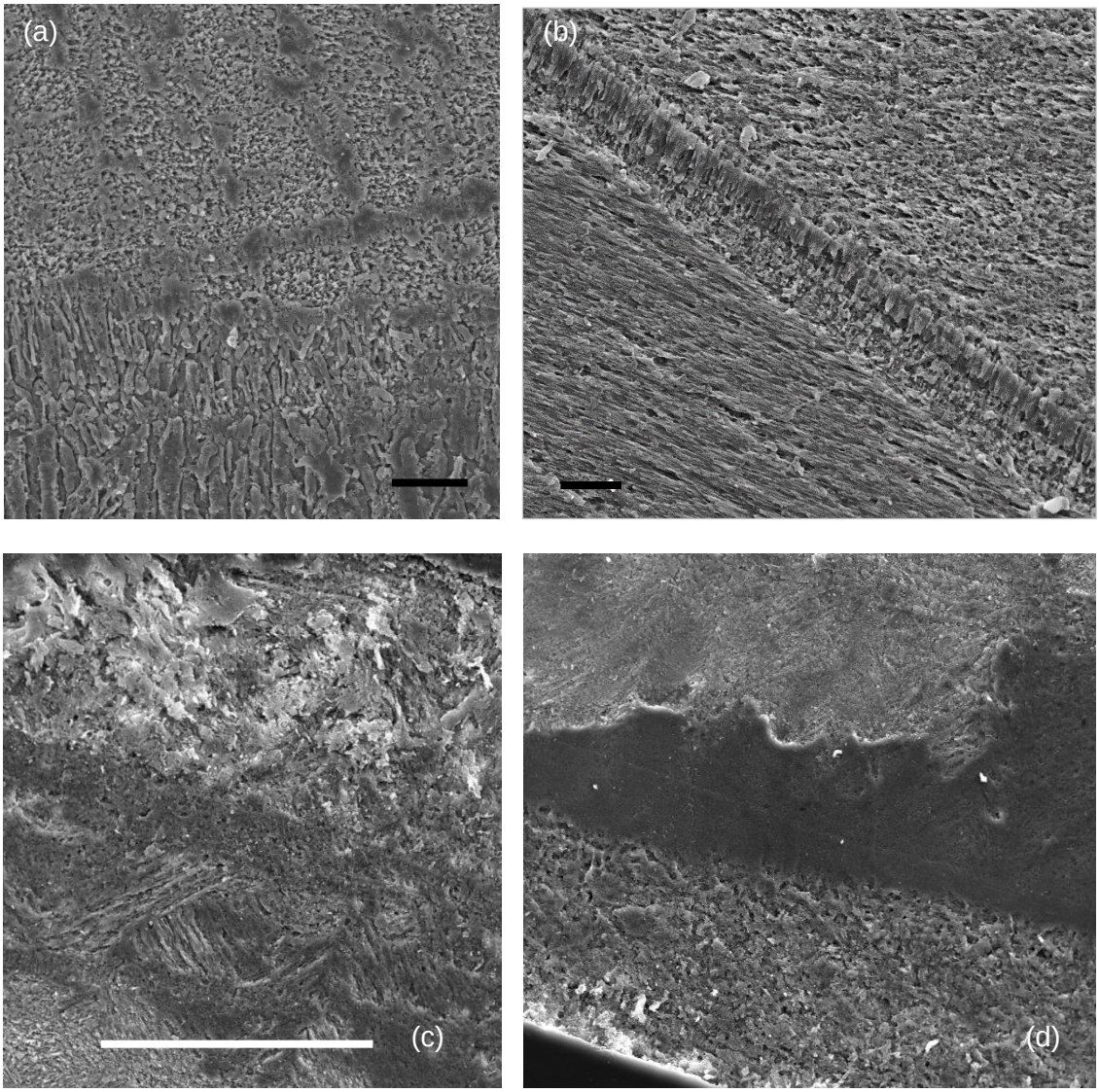

***Lucinoma* sp.** (Takanabe Formation, Plio-Pleistocene). The specimen (Fig. 4.7A) shows the same three-layer structure as *L. aokii*, and the majority of lucinid specimens from the Kounandai seep, and is in pristine conditions. In the middle layers the vertical organic pillars are however much less distinct, and it is unclear if this is due to better preservation, or a different angle at which the shell was cut. In addition, crystals with an oblique orientation are present in areas of the middle layer, commonly associated with growth lines (Fig. 4.7B).

Lucinoma acutentilineatum (Izura seep, Miocene). Within the specimen a thin vertical crack is visible on the SEM image, that was very faintly luminescent during CL analysis. This specimen is similar to the majority of the lucinid specimens, although the organic vertical pillars of the middle layer are completely absent. The preservation of the shell becomes less pristine towards the inner margin of the section, but still clearly retains original mineralogy as evident from the clear distinction between different layers and myostracal bands. However, compared to the previous species, the crystals are less clearly defined.

Figure 4.7 SEM images of cross-sections from *Lucinoma* sp. shell fragments (a) three layered structure, (b) middle layer. Scale bars: (a) 1mm, (b) 100μm

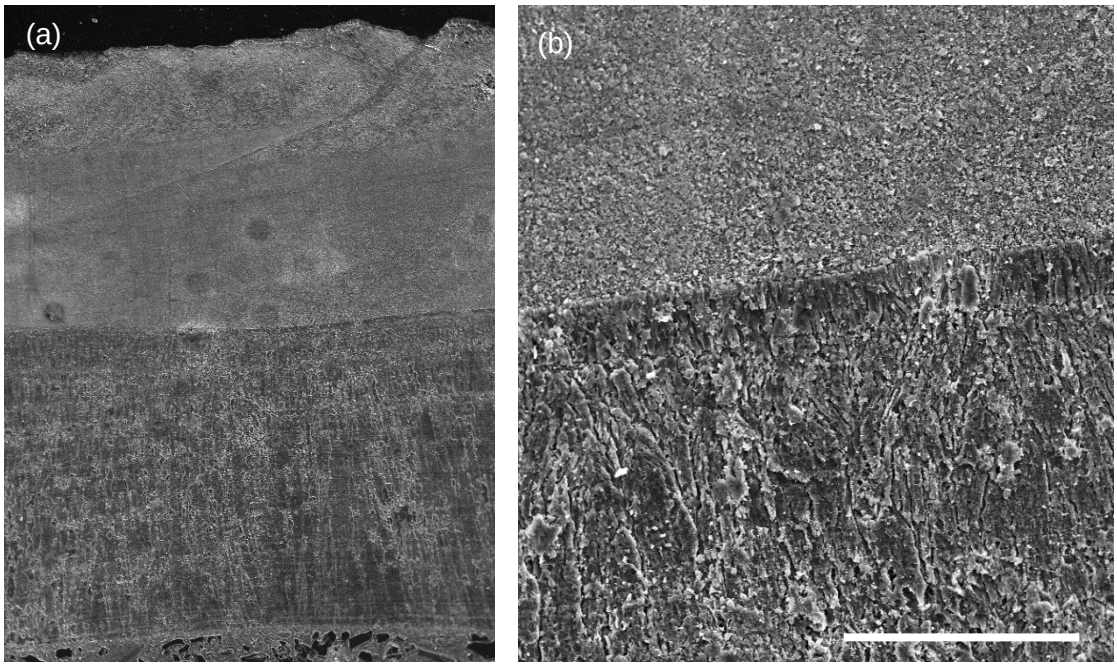

***Lucinoma* sp.** (Lincoln Creek, Oligocene). SEM images show that the broken shell fragments are embedded within matrix, and the shell fragments show high intensity luminescence (Fig. 4.8). It was however noted that luminescence is concentrated in

the middle layer, and luminescence of the inner layer is only very faint. In addition, there is a potential presence of an upper layer. The inner layer shows irregular prisms fibres reminiscent of the lowest layer in the younger fossil specimens (Fig. 4.8A). The highly luminescent middle consists has a very uncoordinated structure, that confirms it is highly diagenetically altered (Fig. 4.8B).

The other specimens from the same locality were in visually better condition, and it is unclear if the poor preservation of this specimen is representative of all specimens from the Lincoln Creek locality.

Figure 4.8 SEM and CL images of cross-sections from *Lucinoma* sp. (a) inner layer, (b) middle layer. Scale bars: white=1mm, (a/b) 100µm.

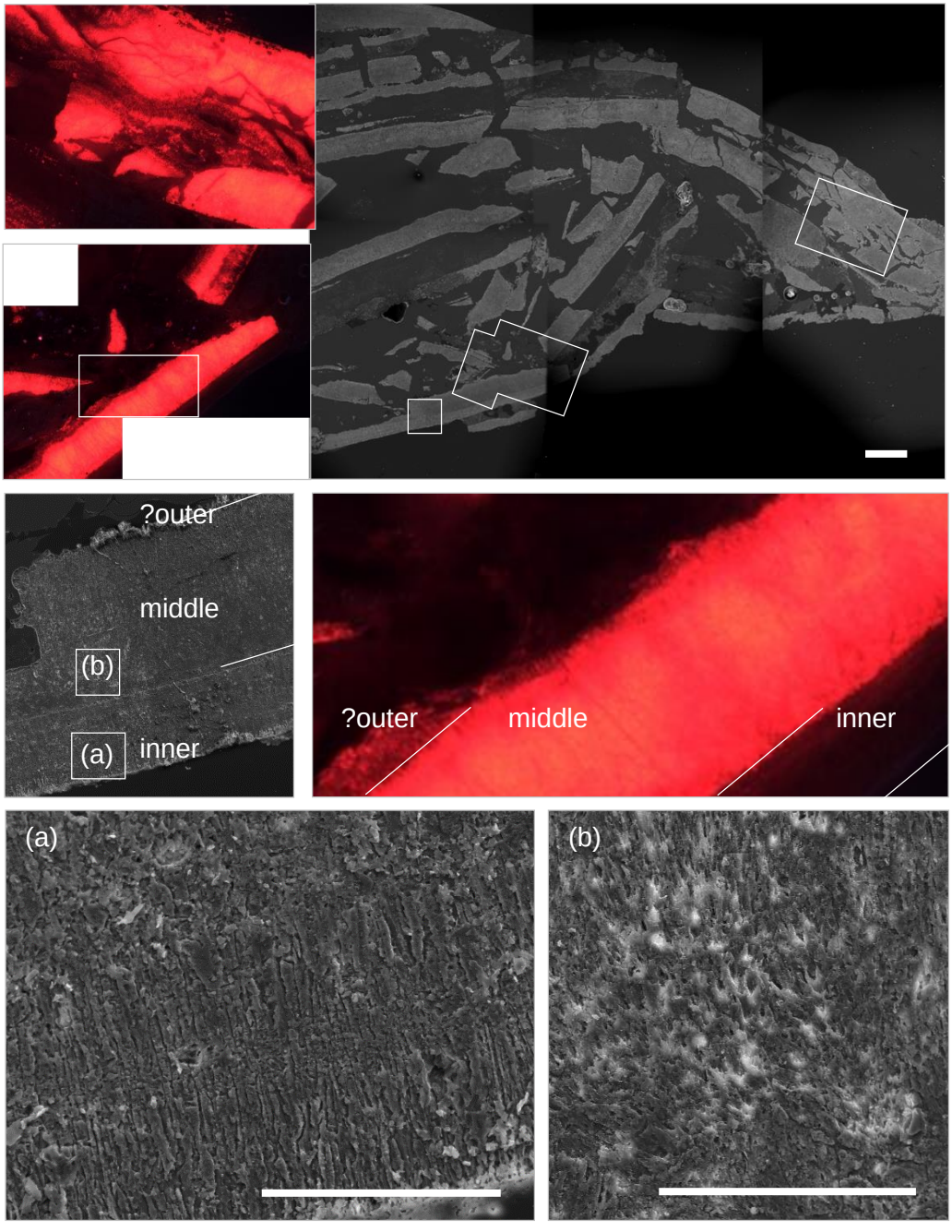

Nymphalucina occidentalis (Tepee Buttes, Cretaceous). In all four analysed specimens faint blue/purple luminescence is visible, and in one specimens high intensity red luminescence is visible (Fig. 4.9A, related to a darker area of the shell), in another specimen additional green banding is present (Fig. 4.9B), that appears to be related to less well preserved bands of the shell material. Green to yellow luminescence is usually related to the presence of aragonite in modern luminescent specimens. The only relic structure recognizable in the specimens appears cross-lamellar (Fig. 4.9C). Preservation within specimens ranges from lamellae that can still be individually recognized with only small recrystallized patches on top, to an amorphous blend without any recognizable crystals (e.g. Fig. 4.9D). In the Fig. 4.9D potentially a different relic structure is present.

Figure 4.9 SEM and CL images of cross-sections from *N. occidentalis* shell fragments

(a) CL image with high intensity red, (b) CL image with green banding, (c) cross-lamellar relic structure, (d) amorphous diagenesis. Scale bars: (a/b) 500µm, (c) 10µm, (d) 20µm.

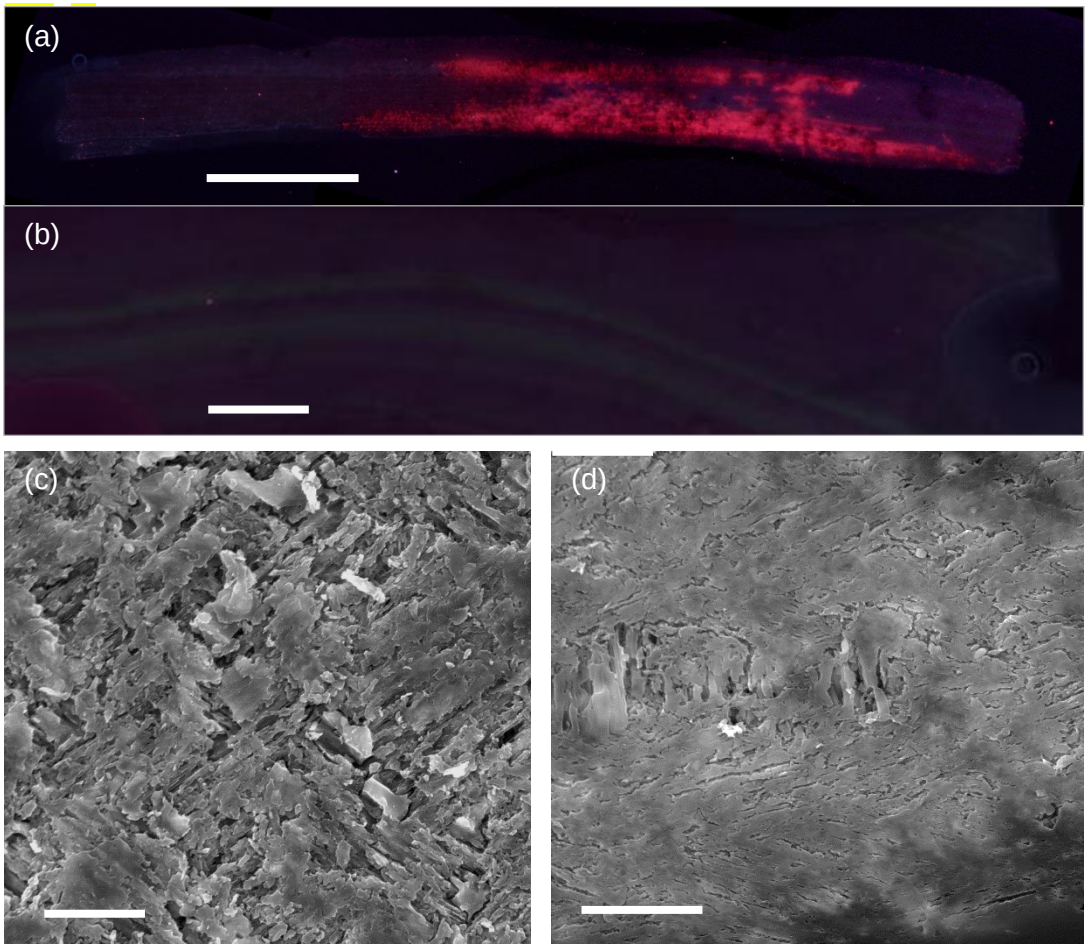

4.3.2.3 Solemyidae

Of our suite of solemyid samples only *Acharax* sp. (Kakinokidai seep) was analysed using CL and SEM, and no luminescence was observed. The structure of the sample is similar to that of *Acharax johnsoni* (Sato et al, 2013). This specific grouping of outer and inner micro structures was not observed in other solemyids, and potentially identifies this fossil specimen as the same species. Throughout the shell two shell layers are visible (Fig. 4.10A): (i) outer shell layer with a reticulate structure, that consists of blocky nested unit, pattern is structured by SBOM (ii) the inner layer identified as a “cone complex crossed lamellar structure” (c-CCL, Fig. 4.10B); stacks of chevrons indicative of the CCL are clearly visible.

Figure 4.10 SEM images of cross-sections from *Acharax* sp. shell fragment (a) CL image with high intensity red, (b) CL image with green banding, (c) cross-lamellar relic structure, (d) amorphous diagenesis. Scale bars: 100µm

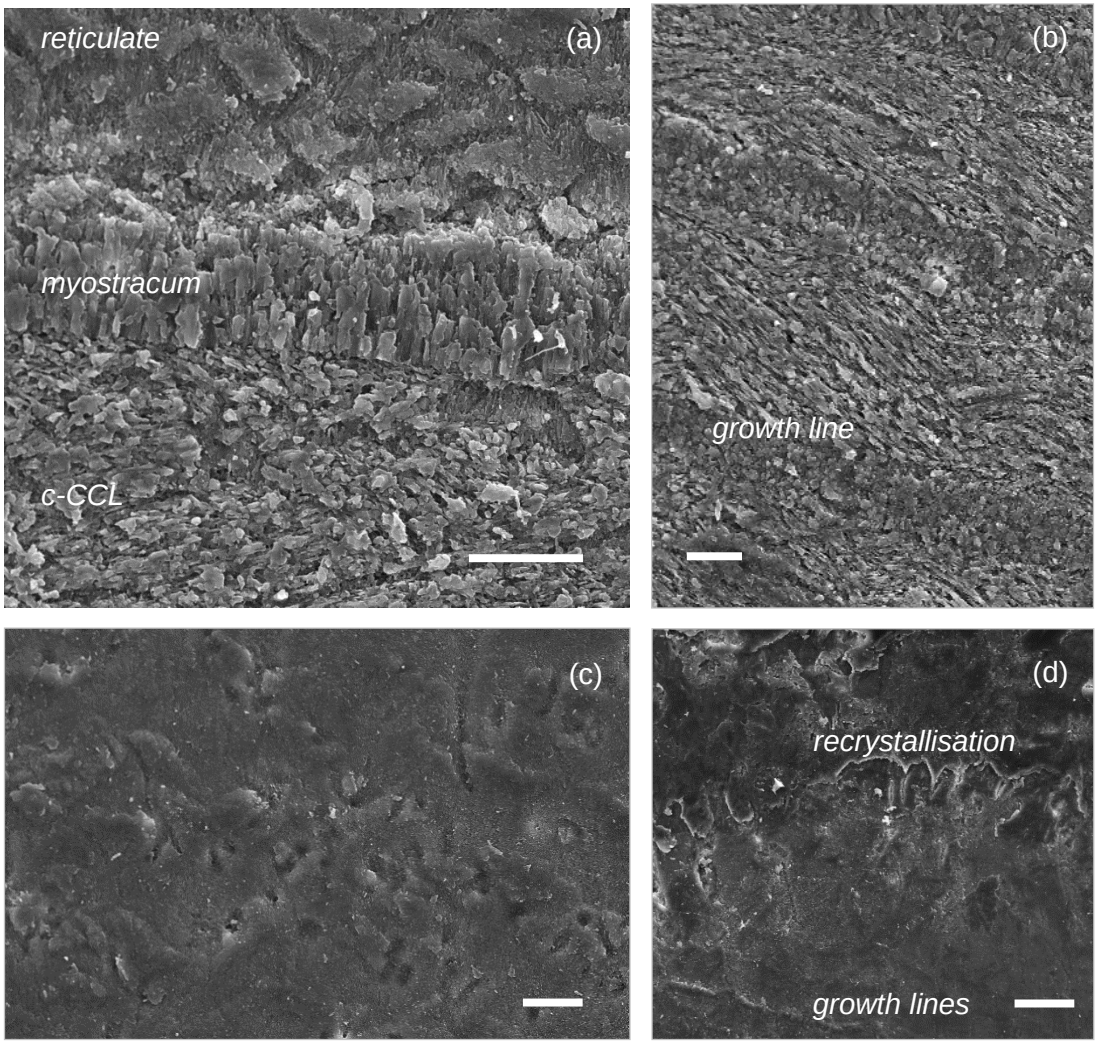

Compared to the modern specimen, evidence of diagenetic alteration includes: the individual granules of reticulate units can no longer be identified, and the outlines of the units are blurred. Towards the section edge, the reticulate pattern can almost no longer be recognized. The outer margin (approx.. 50um) is strongly affected and no longer shows any structure, this amorphous area also ‘seeps’ into the shell where cracks are present. At the bottom the structureless area has a thickness of around 20µm.

4.3.2.4 Thyasiridae

The fossil *Conchocele bisecta* specimen (Koshiba Formation, Pleistocene) can directly be compared to modern specimens of that species (Nishida et al., 2011). Of the three shell layers in modern specimens, the most inner layer appears to be missing and our section ends with a myostracal layer (Fig. 4.11C). The middle layer has crossed lamellar structures similar to the modern specimen, and shows very good preservation (Fig. 4.11A and B). The upper layer shows no defined microstructures (as known from the modern specimen) but instead contains areas that are not very structured (Fig. 4.11C), as well as amorphous sections.

Figure 4.11 SEM images of a cross-section from *C. bisecta* shell fragment (a/b) crossed lamellar structures, (c) unstructured upper layer, (d) two layered structure. Scale bars: white=100µm, black=10µm

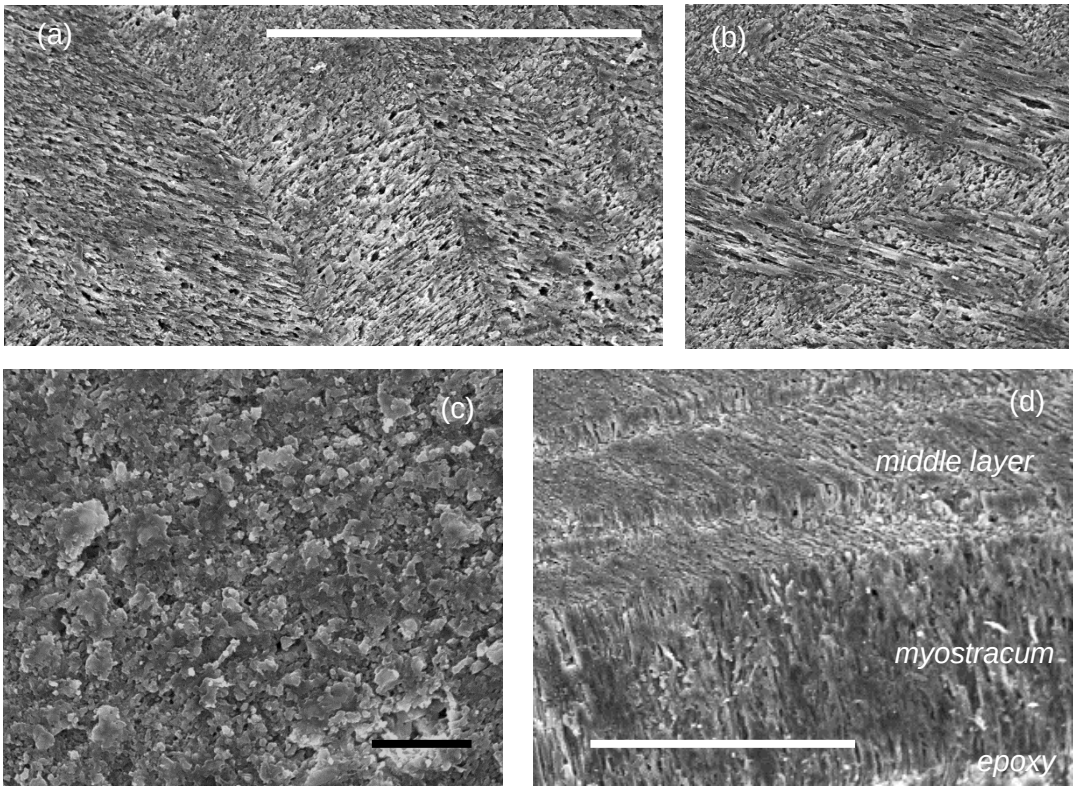

4.3.2.5 Mytilidae

G. coseli (Moonlight North, Miocene) was the only mytilid specimen of which sufficient shell material was available for SEM and CL analysis. Luminescence is observed from several cracks, that are clearly visible with SEM (Fig. 4.12D). The large majority of the shell has an granular, unstructured appearance that is unlikely to be original (Fig. 4.12B). Patches of original shell mineralogy are potentially visible, including parts of an outer prismatic layer (Fig. 4.12A) and brick-like nacre layers (Fig. 4.12B and C), both known from modern mytilids (Taylor et al., 1969) and *Gigantidas gladius* in particular (Genio et al., 2012).

Figure 4.12 SEM and CL images of a cross-section from *G. coseli* shell fragment (a) amorphous with potential prismatic structure, (b) nacre structure, (c) nacre structure, (d) overview image. Scale bars: white=200µm, black=20µm

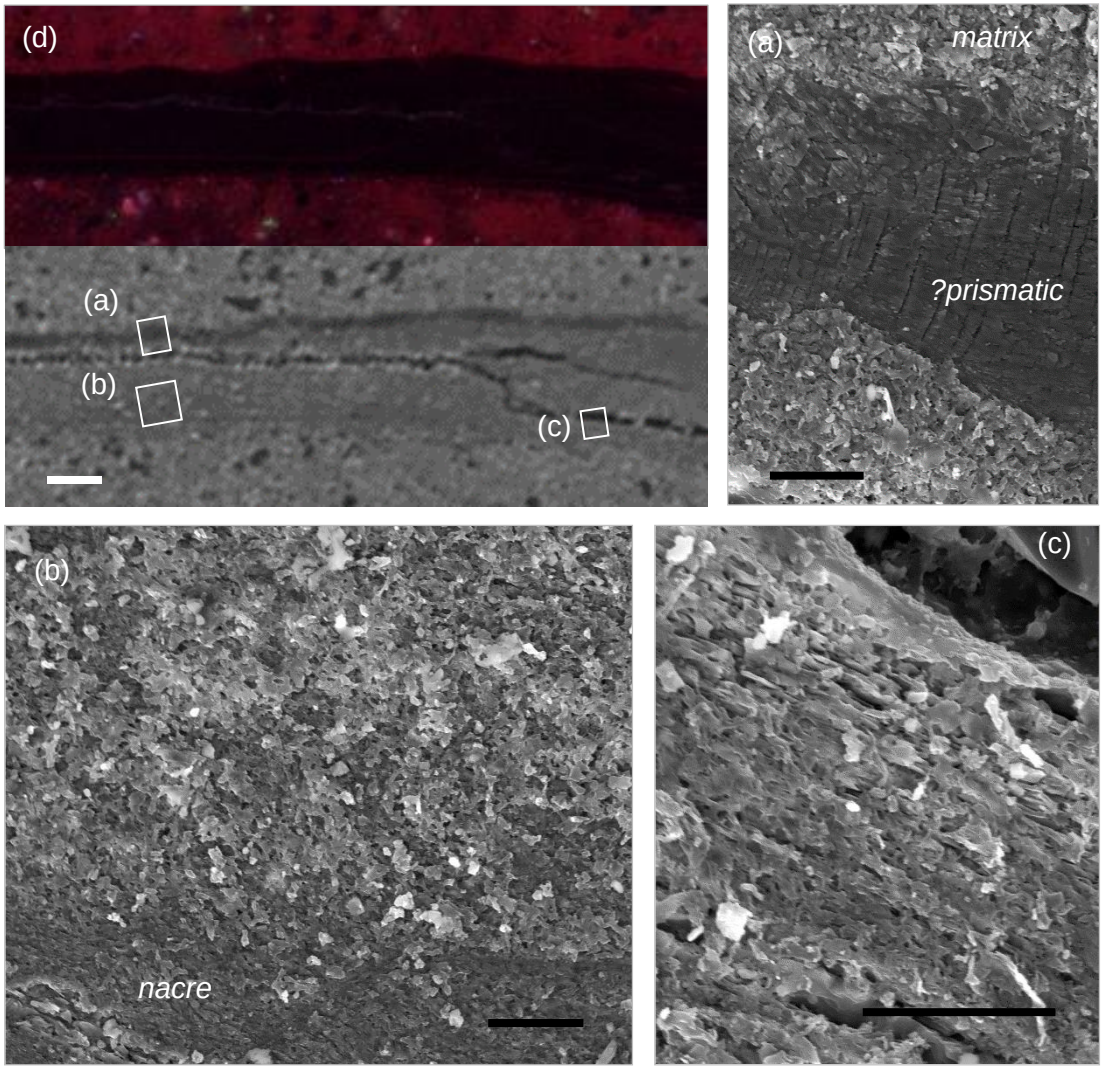

4.3.2.5 Inoceramidae

Inceramid shells are usually composed of two layers: an inner aragonitic layer of nacre, and a thick outer prismatic layer of calcite (e.g. Wright, 1987). In our specimen of *Inoceramus* sp. (Tepee Buttes, Cretaceous) only the nacreous layer is present. The shell layer is nicely preserved with only small patches is accumulated crystals on top of pristine nacre (Fig. 4.13).

Figure 4.13 SEM images of a cross-section from *Inoceramus* sp. shell fragment Well-preserved nacreous structure is visible. Scale bar: white=10µm

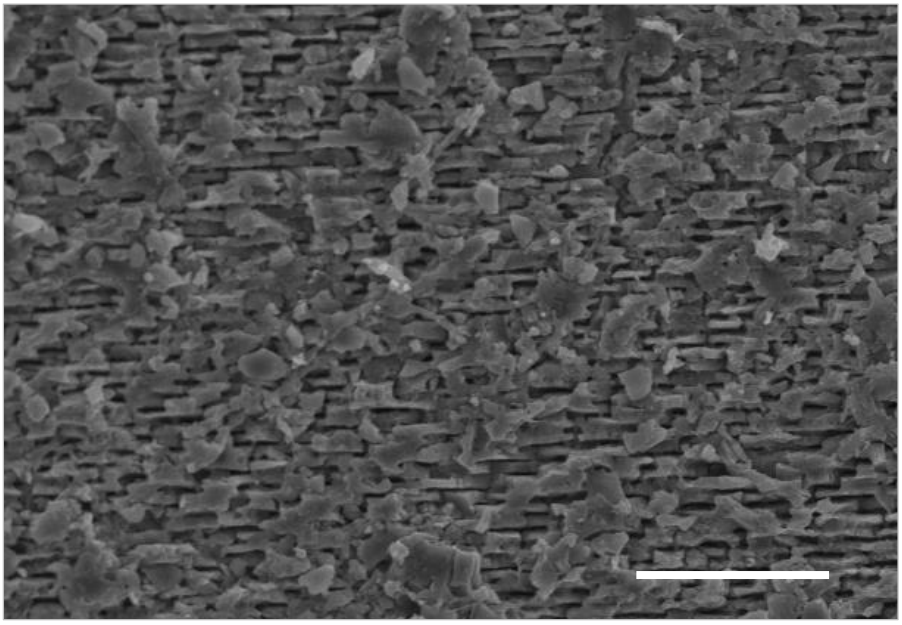

4.3.2.5 Brachiopoda

***Liothyrella* sp.** (Moonlight North, Miocene). CL imaging shows no luminescence of the shell material, with the exception of faint blue in a visible crack, likely the result of sediment compaction. A comparison can be made with modern *Liothyrella* species, and both *Liothyrella uva* and *Liothyrella neozelanica* have a three-layered structure with prismatic, fibrous and homogenous structures (Parkinson et al., 2005; Goetz et al., 2009). In the fossil specimen two layers are visible (Fig. 4.14A), an upper layer of thin fibrous layers, and broad pillar-shaped columnar crystals. Either the inner or outer layer could be missing. Punctae are visible within the section (Fig. 4.14C), that also point to the presence of primary mineralogy, because recrystallisation is expected to obliterate these. Some amalgamating diagenesis of the fibres is visible, and possibly the pristine structure of the columnar lower layer is only visible in several patches within the layer (Fig. 4.14B).

Figure 4.14 SEM images of a cross-section from *Liothyrella* sp. shell fragment (a) two layered structure, (b) potential pristine columnar shells structure, (c) punctae. Scale bars are 10μm.

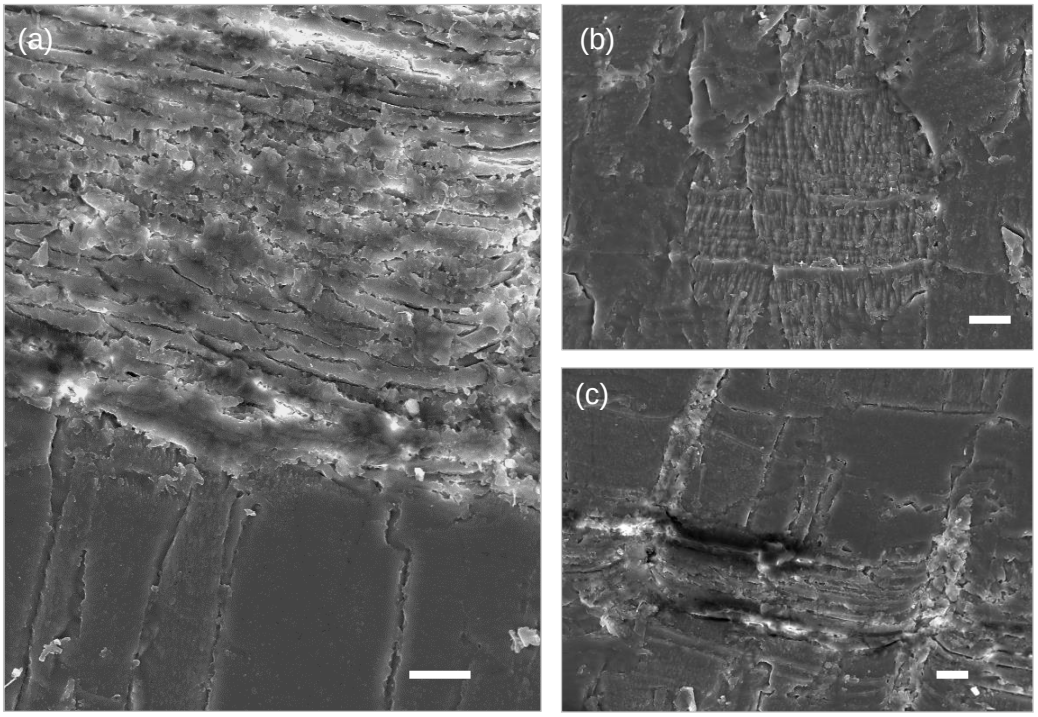

Rhynchonellid brachiopods

In modern rhynchonellid brachiopods the tertiary layer is absent, and the secondary layer consist of fibrous calcite (Voigt, 2000). Voigt (2000) noted that the primary layer is mostly not preserved in fossil specimens, which appears to also be the case for our specimens of *Anarhynchia*, *Dzieduszyckia* and *Halorella*.

Anarhynchia (Jurassic). The specimen is luminescent with variable intensity throughout the shell (Fig. 4.15B). The fibrous layer of the shell is not well preserved (Fig. 4.15C), and can be completely smoothed out in certain areas (Fig. 4.15D).

Dzieduszyckia crassicostata (Devonian). In this specimen luminescence is also present throughout the shell, and particularly intense in vertical cracks (Fig. 4.16A). The fibrous layers appear better preserved than for *Anarhynchia* specimen, with more clearly defined individual fibres (Fig. 4.16B).

Figure 4.15 SEM and CL images of a cross-section *Anarhynchia* shell fragment (p. 205) (a) SEM overview, (b) CL overview, (c) fibrous layer, (d) poorly preserved fibrous layer. Scale bars: white=1mm, black=10μm.

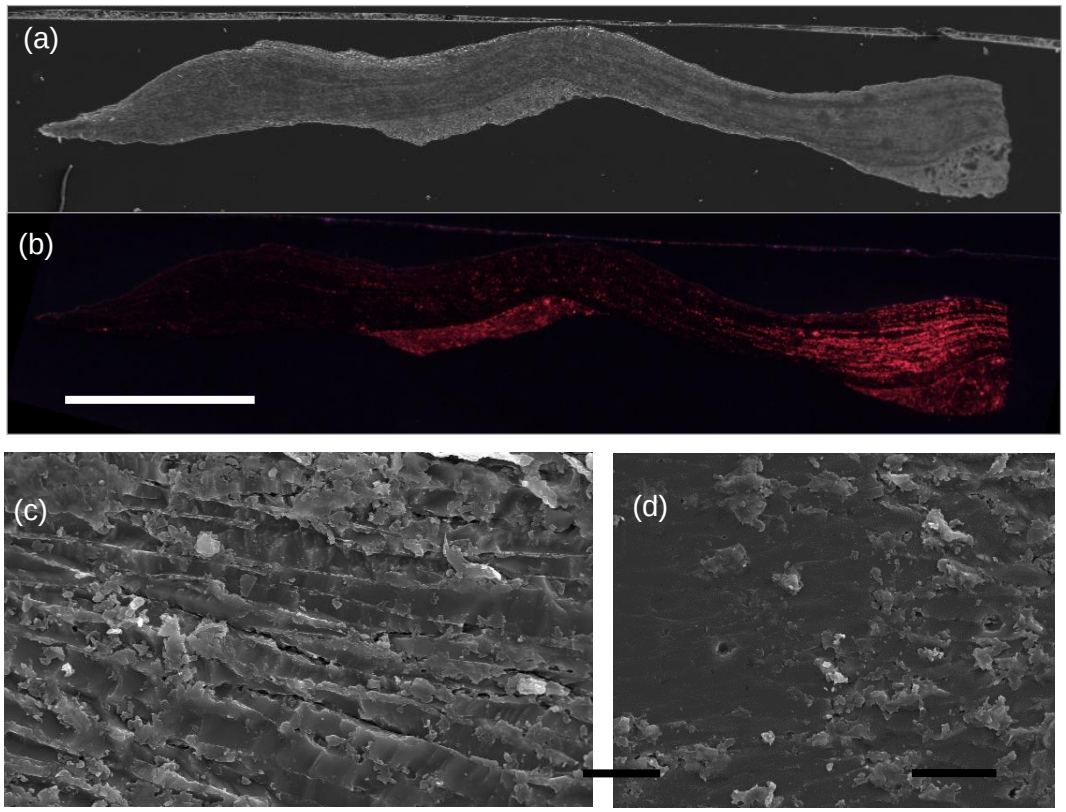

Figure 4.16 SEM and CL images of a cross-section from *D. crassicostata* shell fragment

(a) SEM overview, (b) CL overview, (c) fibrous layer. Scale bars: (a/b)=1mm, (c)=50µm.

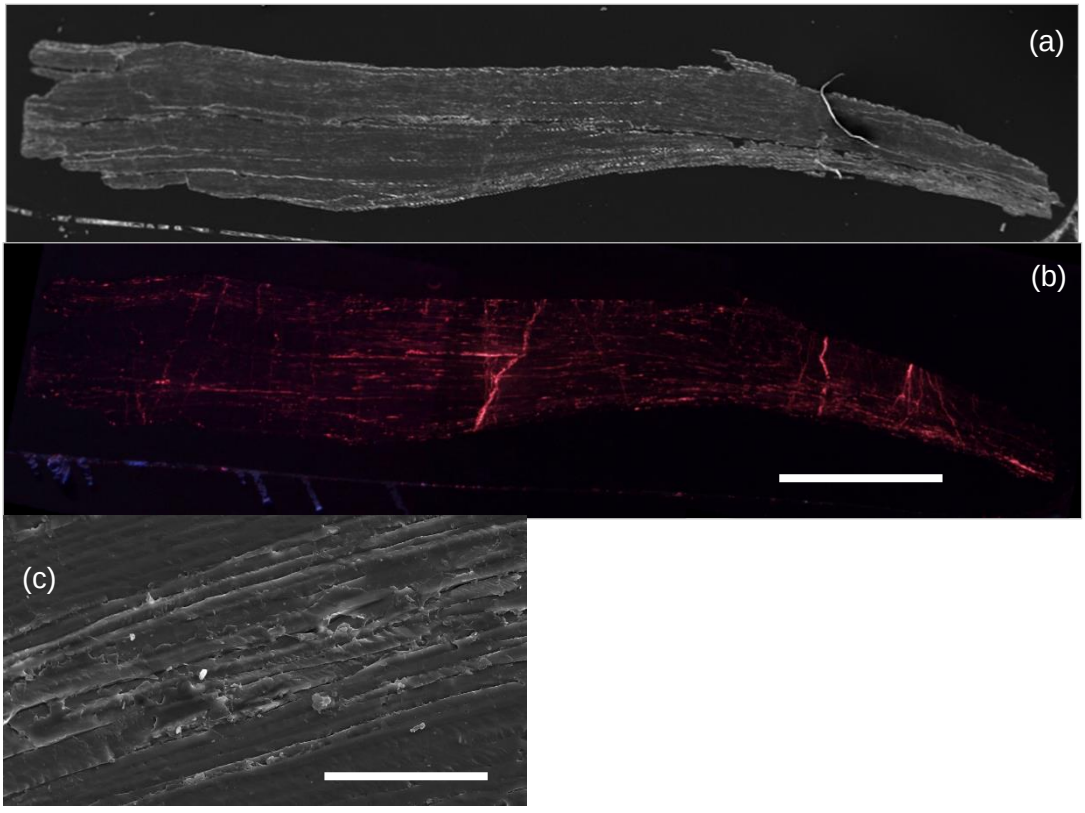

Halorella (Triassic). The specimens show similar CL intensity to *Anarhynchia* (Fig. 4.17), as well as similar preservation of the fibres in SEM images (not shown).

Ibergirhynchia (Carboniferous). Visually the preservation of *Ibergirhynchia* appears to be poor compared to *Dzieduszyckia*, although this cannot be inferred from the CL images, in which luminescence is absent (Fig. 4.18).

Figure 4.17 CL images of *Halorella* shell fragments.
Scale bar = 1mm.

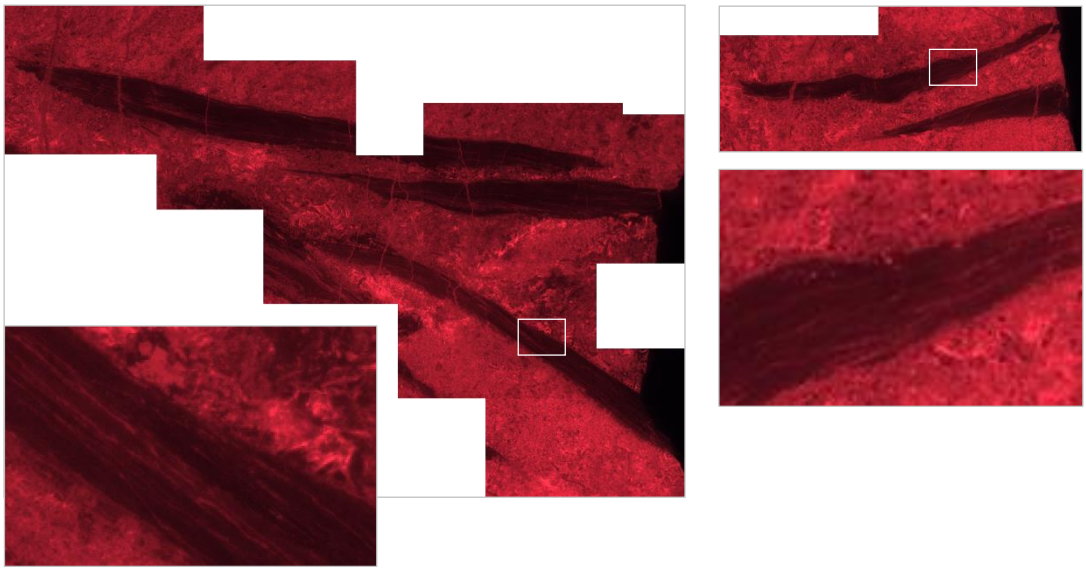

Figure 4.18 SEM and CL image of *Ibergirhynchia*
Shell material is present in a small section of the specimen. Scale bar = 1mm.

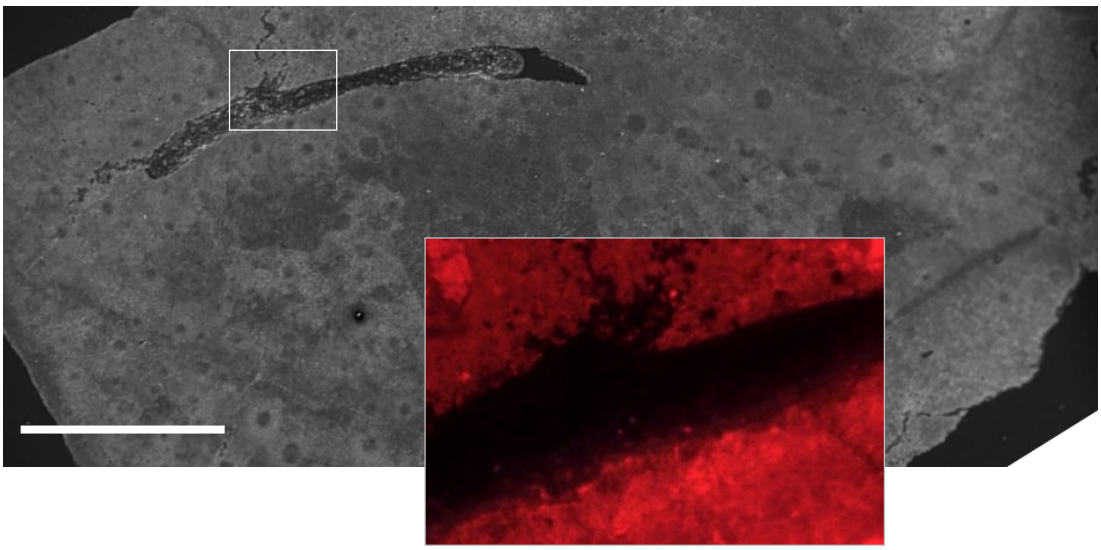

4.3.4 Stable isotope analysis of SBOM, shell carbonate and CAS

For SBOM from fossil specimens the stable isotope results are discussed per locality, to investigate potential differences between nutritional strategies that are location-specific. The values given for each specimen are mean values of multiple measurements, for sulphur only values obtained using 10%HCl are given, unless explicitly stated.

4.3.4.1 Modern *Nautilus pompilius*

Because our suit of samples contains multiple specimens of shelled cephalopods, the extraction of SBOM and its relationship to soft tissues was investigated for modern *Nautilus pompilius*. Total SBOM was obtained from five positions throughout the shell (1 gram minimum weight), and shows mean values of $\delta^{13}C$ -14.3‰ ±0.7 (n=5), and $\delta^{15}N$ 11.6‰ ±0.3 (n=5). It was only possible to obtain isotope measurments from the organic siphuncle of the specimen, which was on average -2.1‰ depleted for carbon ($\delta^{13}C$ -17.4‰), and more depleted for nitrogen (7.2‰ and 10.1‰). This data suggests the SBOM of shelled cephalopods reflects soft tissue values within several per mille. The siphuncle has stable isotope sulphur values of $\delta^{34}S$ 13.2‰ and 15.5‰. Shell carbonate values range from -0.2‰ to 1.0‰, and a combination with SBOM carbon values shows a clear relation between the two carbon pools (Fig. 4.19). In Chapter 3 it was shown that the $\delta^{13}C$ value of metabolic carbon in part determines shell carbonate $\delta^{13}C$ values.

Figure 4.19 Modern *Nautilus* SBOM and shell carbonate $\delta^{13}C$ values

Specimen was sampled throughout the shell, SBOM is shown as a solid line (left axis) and shell carbonate as a dashed line (right axis).

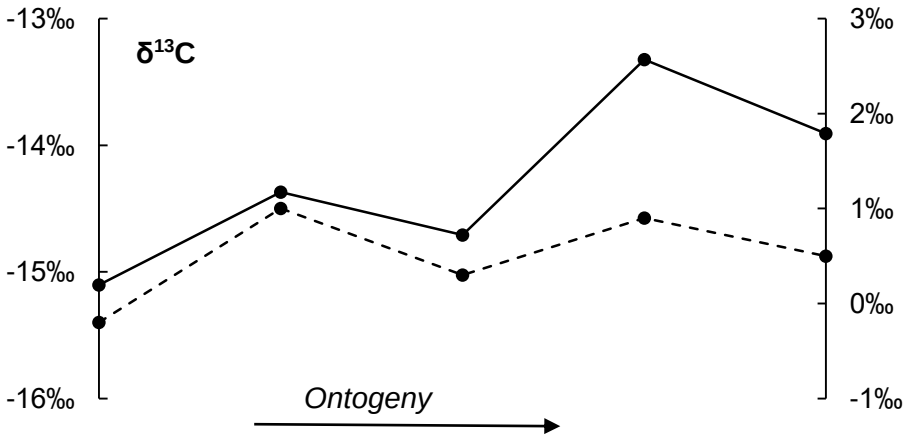

Figure 4.20 $\delta^{13}C$, $\delta^{15}N$ and $\delta^{34}S$ values of SBOM from analysed specimens

Overview of the species and localities is given in Table 4.1 and Table 4.2. Symbol key is presented below, and each column represents an individual specimen (collated specimens are indicated in Table 3.1). $\delta^{34}S$ values obtained from SBOM samples isolated using cation exchange resin are only shown when these are can be used to differentiate between positive and negative sulphur sources (as discussed in section 4.2.2.1).

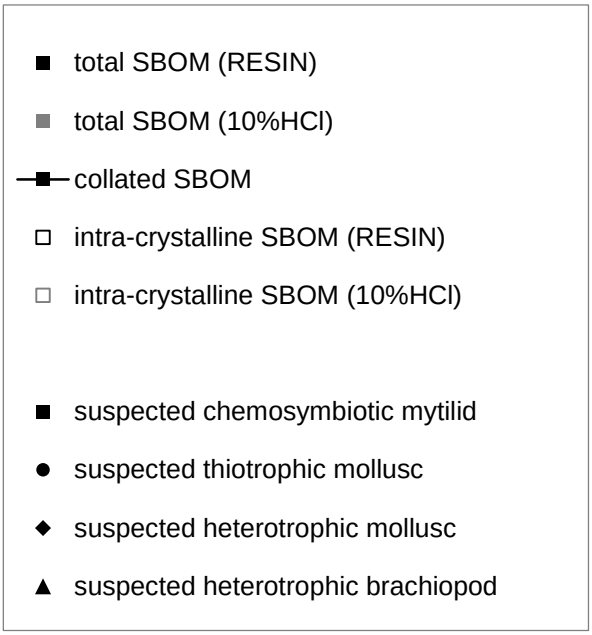

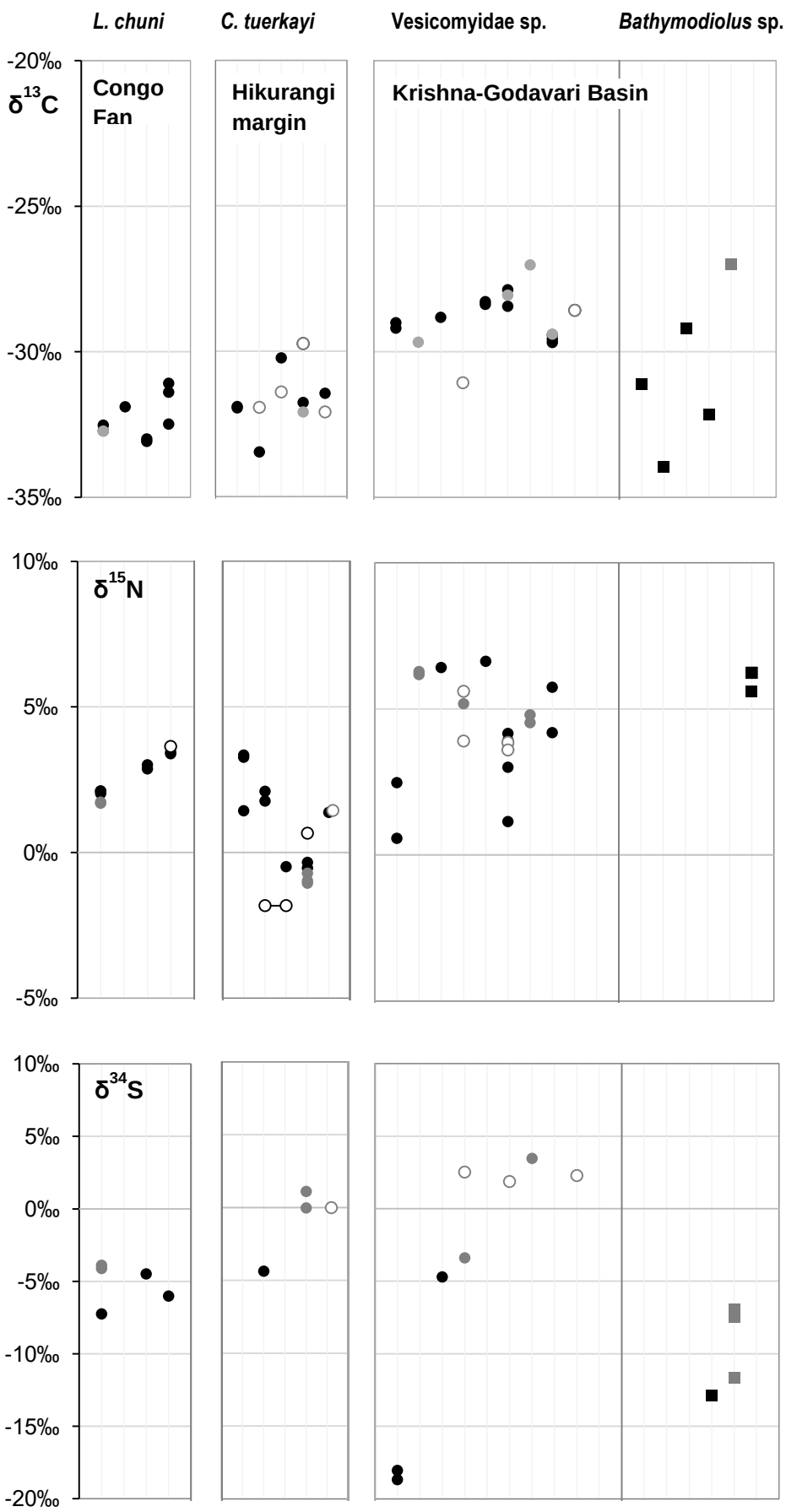
L. chuni
C. tuerkayi
Vesicomyidae sp.
Bathymodiolus sp.
δ13C
Congo Fan
Hikurangi margin
Krishna-Godavari Basin
-20‰
-25‰
-30‰
-35‰
δ15N
10‰
5‰
0‰
-5‰
δ34S
10‰
5‰
0‰
-5‰
-10‰
-15‰
-20‰

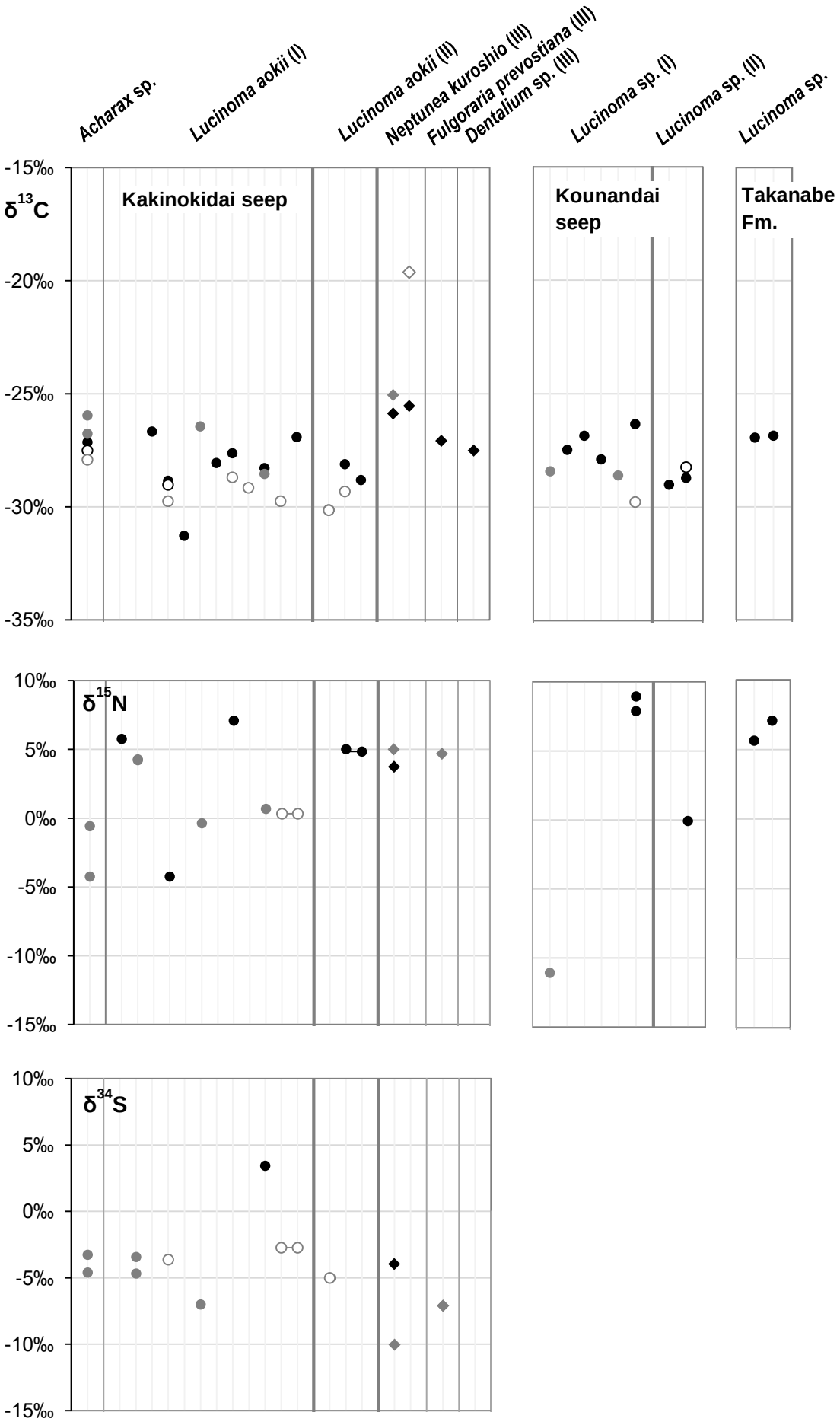
Acharax sp.
Lucinoma aokii (I)
Lucinoma aokii (II)
Neptunea kuroshio (III)
Fulgoraria prevostiana (III)
Dentalium sp. (III)
Lucinoma sp. (I)
Lucinoma sp. (II)
Lucinoma sp.
Kakinokidai seep
Kounandai seep
Takanabe Fm.
δ13C
-15‰
-20‰
-25‰
-30‰
-35‰
δ15N
10‰
5‰
0‰
-5‰
-10‰
-15‰
δ34S
10‰
5‰
0‰
-5‰
-10‰
-15‰

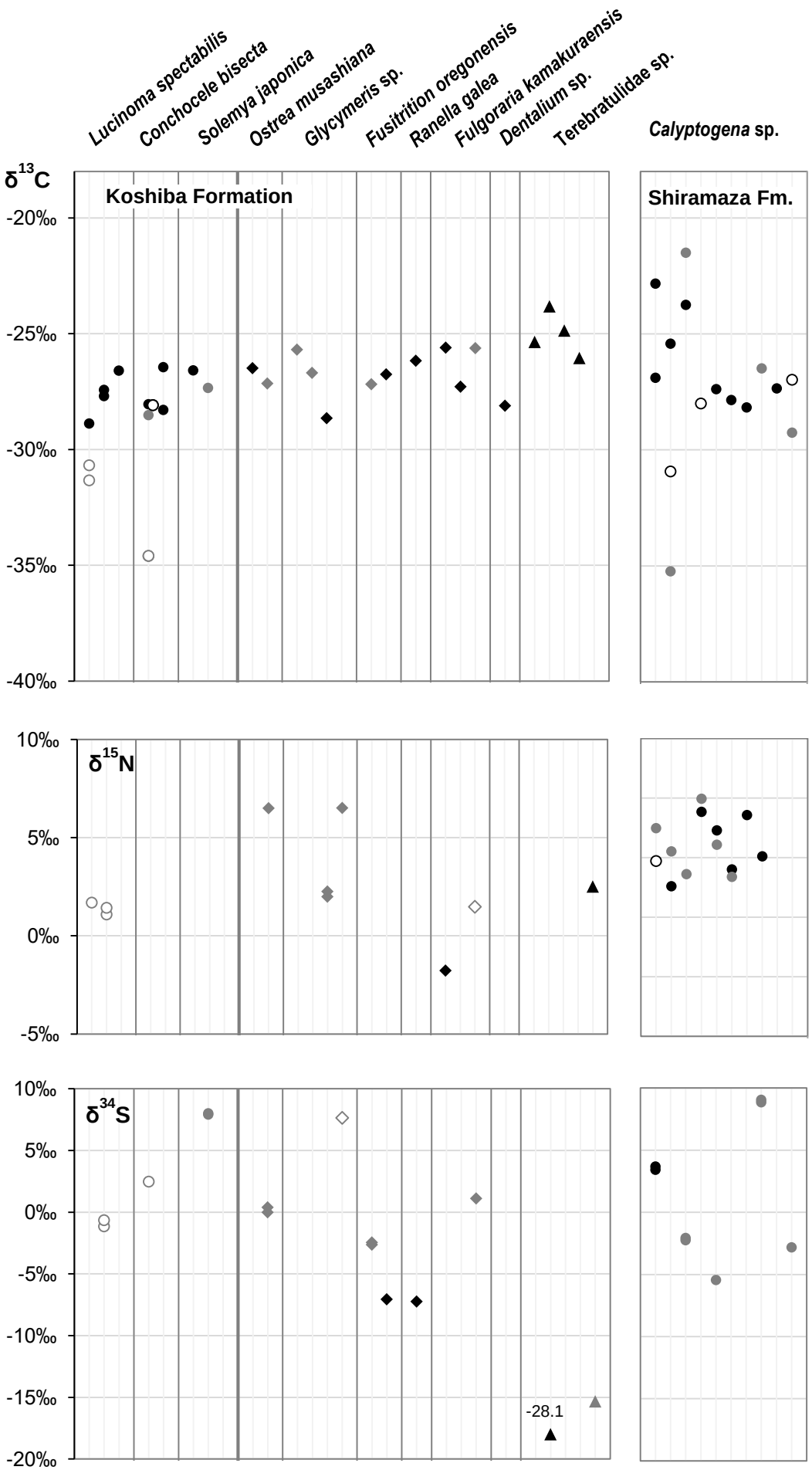
Lucinoma spectabilis
Conchocele bisecta
Solemya japonica
Ostrea musashiana
Glycymeris sp.
Fusitrition oregonensis
Ranella galea
Fulgoraria kamakuraensis
Dentalium sp.
Terebratulidae sp.
Calyptogena sp.
δ13C
Koshiba Formation
Shiramaza Fm.
-20‰
-25‰
-30‰
-35‰
-40‰
δ15N
10‰
5‰
0‰
-5‰
δ34S
10‰
5‰
0‰
-5‰
-10‰
-15‰
-20‰
-28.1

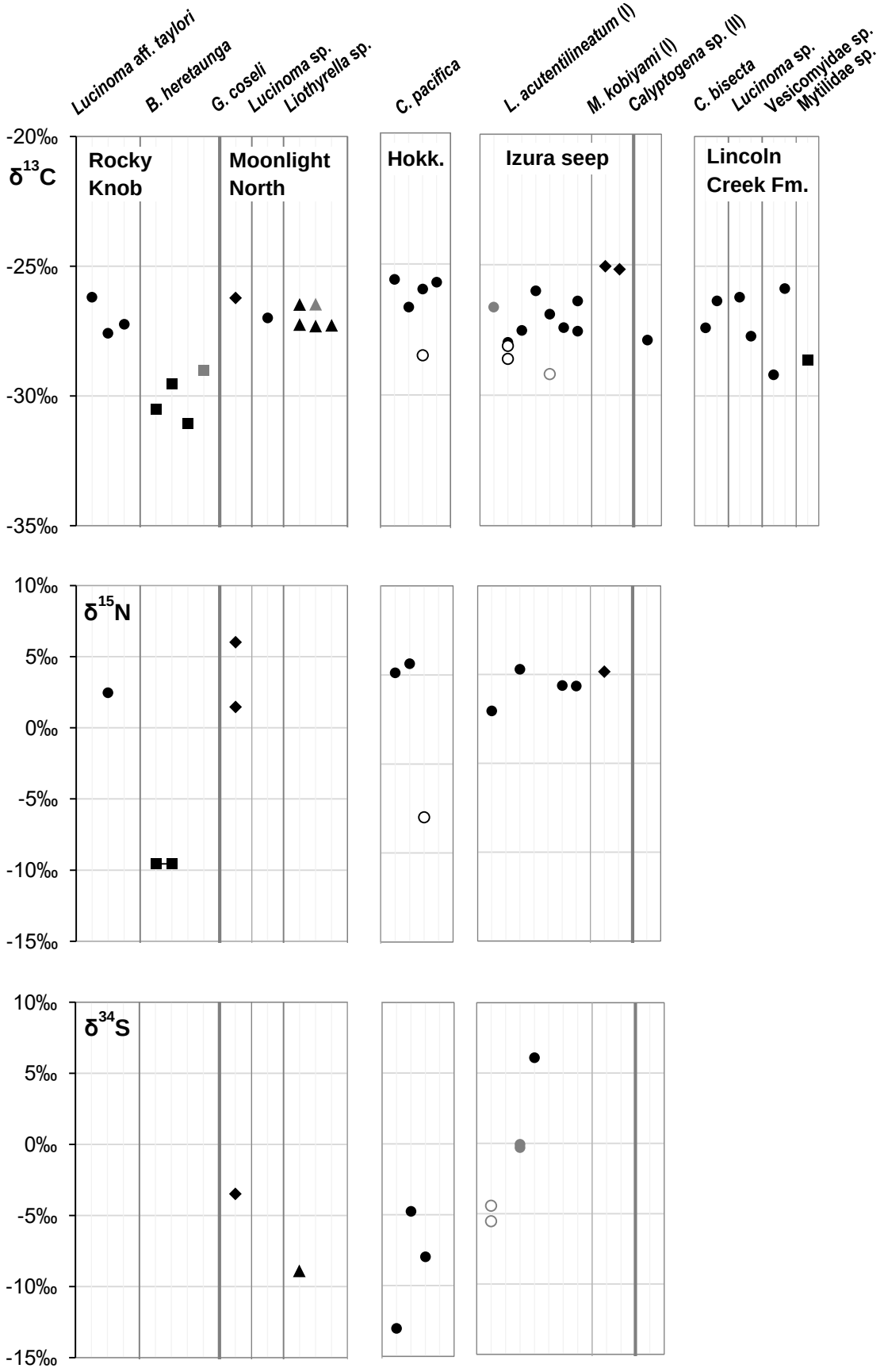
Lucinoma aff. taylori
B. heretaunga
G. coseli
Lucinoma sp.
Liothyrella sp.
C. pacifica
L. acutentilineatum (I)
M. kobiyami (I)
Calyptogena sp. (II)
C. bisecta
Lucinoma sp.
Vesicomyidae sp.
Mytilidae sp.
δ13C
-20‰
-25‰
-30‰
-35‰
Rocky Knob
Moonlight North
Hokk.
Izura seep
Lincoln Creek Fm.
δ15N
10‰
5‰
0‰
-5‰
-10‰
-15‰
δ34S
10‰
5‰
0‰
-5‰
-10‰
-15‰

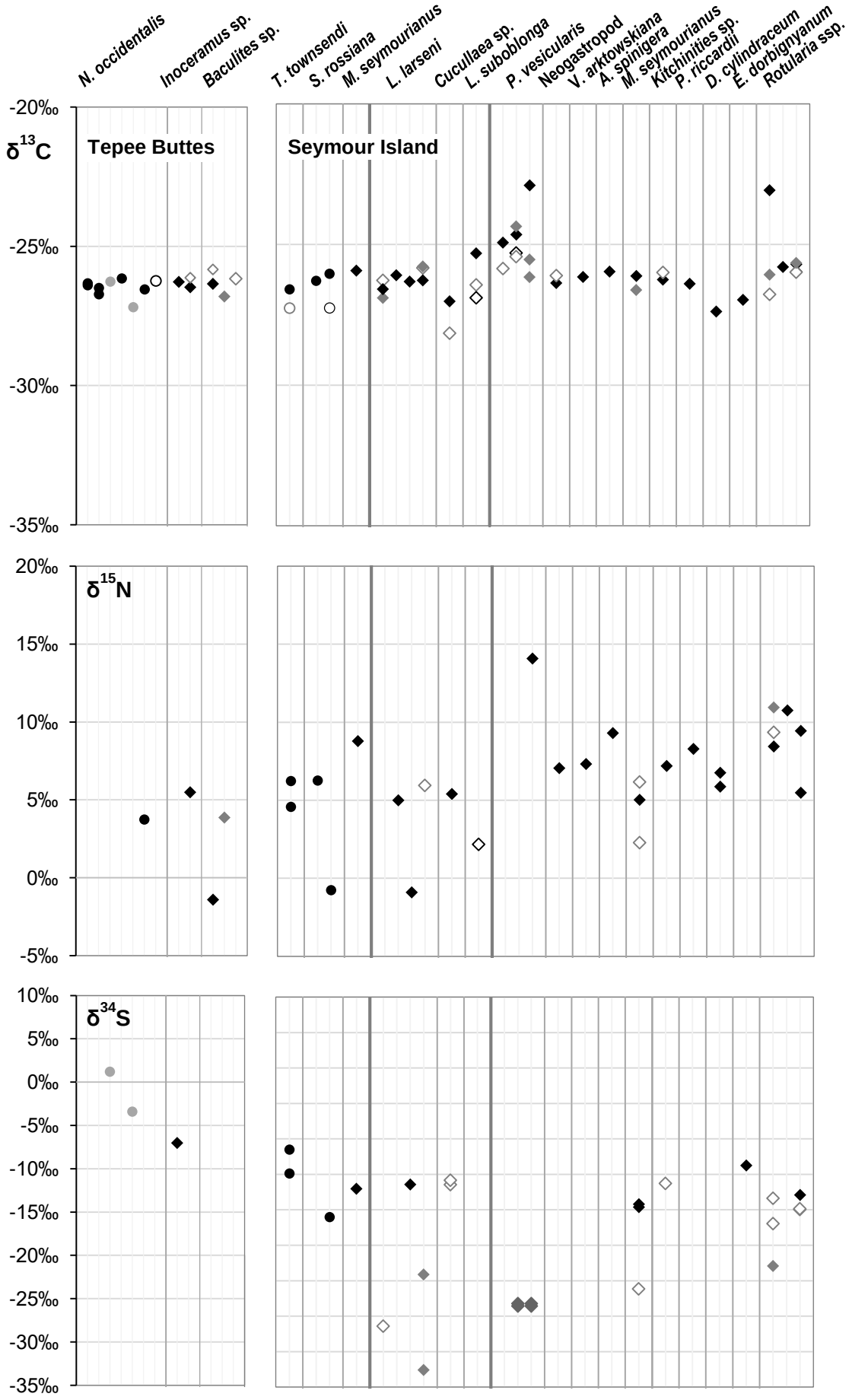
N. occidentalis
Inoceramus sp.
Baculites sp.
T. townsendi
S. rossiana
M. seymourianus
L. larseni
Cucullaea sp.
L. suboblonga
P. vesicularis
Neogastropod
V. arktowskiana
A. spinigera
M. seymourianus
Kitchinities sp.
P. riccardii
D. cylindraceum
E. dorbignyanum
Rotularia ssp.
δ13C
Tepee Buttes
Seymour Island
-20‰
-25‰
-30‰
-35‰
δ15N
20‰
15‰
10‰
5‰
0‰
-5‰
δ34S
10‰
5‰
0‰
-5‰
-10‰
-15‰
-20‰
-25‰
-30‰
-35‰

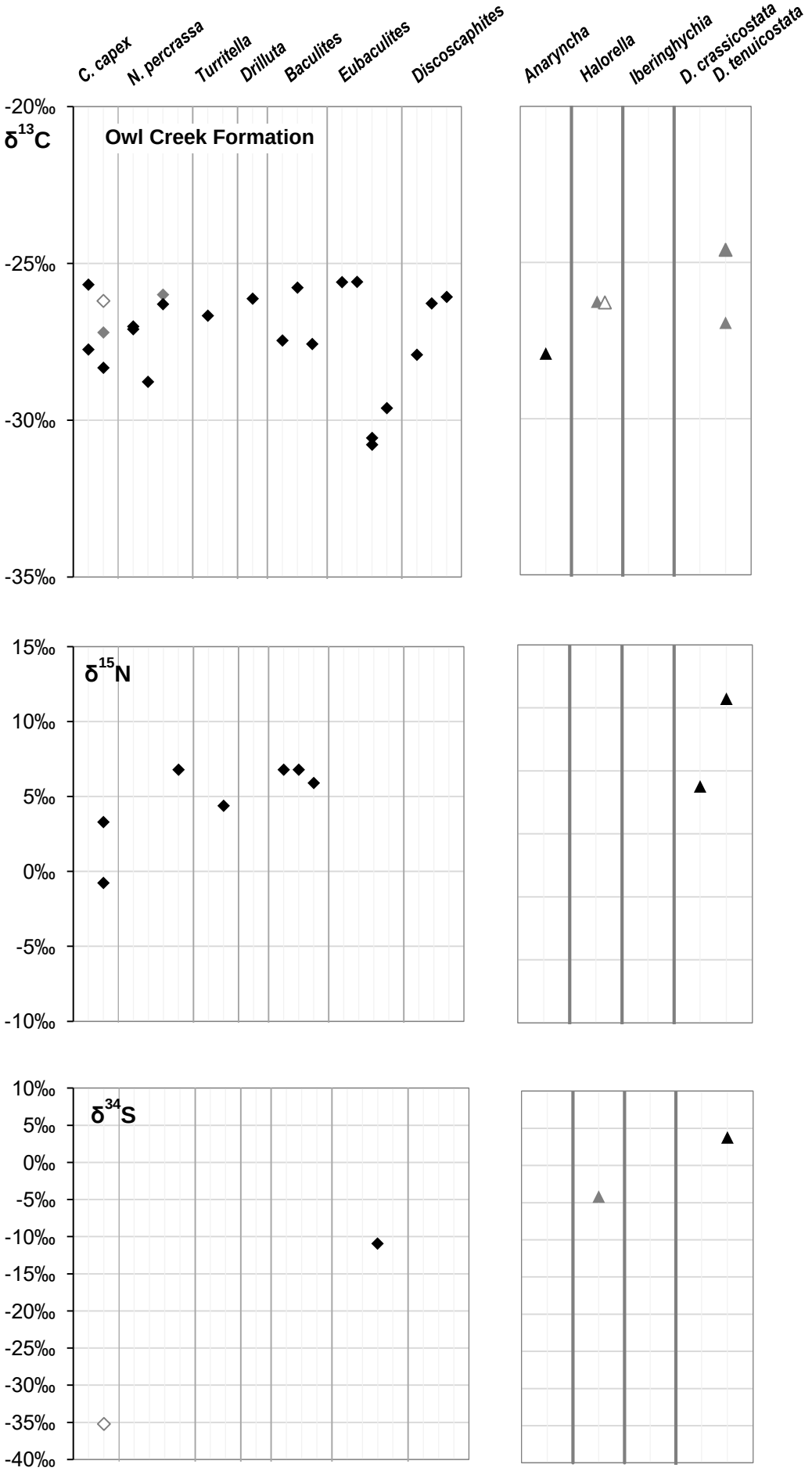
C. capex
N. percrassa
Turritella
Drilluta
Baculites
Eubaculites
Discoscaphites
Anaryncha
Halorella
Iberinghychia
D. crassicostata
D. tenuicostata
Owl Creek Formation
δ13C
-20‰
-25‰
-30‰
-35‰
δ15N
15‰
10‰
5‰
0‰
-5‰
-10‰
δ34S
10‰
5‰
0‰
-5‰
-10‰
-15‰
-20‰
-25‰
-30‰
-35‰
-40‰

4.3.4.2 Subfossil localities

Congo Fan

Total SBOM of the vesicomyid *Laubiericoncha chuni* has $\delta^{13}C$ values ranging from -33.0‰ to -31.7‰ (n=4), $\delta^{15}N$ between 1.9‰ and 3.4‰ (n=3, 2.8 +/- 0.8, n=3; intra-crystalline SBOM = 3.6‰), and $\delta^{34}S$ is -4.0‰. Resin isolated using cation exchange resin shows even more depleted $\delta^{34}S$ values, up to -7.2‰ (n=3).

L. chuni shell carbonate values are between 0.4‰ and 1.1‰ (n=4; 1.0 +/- 0.5)

Hikurangi margin

Calyptogena tuerkayi total SBOM $\delta^{13}C$ values fall between -33.5‰ and - 30.2‰ (n=5), intra-crystalline SBOM $\delta^{13}C$ is on average +0.8‰ enriched (±1.8, n=3) for individual specimens, and has a mean $\delta^{13}C$ value of -30.7 +/-1.1 (n=4) which is statistically different (P=0.0001) from the total SBOM pool. Shell carbonate values ($\delta^{13}C$ -2.4‰ to -0.1‰, n=3) include a depleted outlier of -11.8‰, that does not have deviating total SBOM value.

$\delta^{15}N$ total SBOM ranges from -0.7‰ to 2.7‰ (n=5), intra-crystalline SBOM from -1.8 to 1.4 (n=3). A single $\delta^{34}S$ total SBOM value is: -1.3‰, as expected for intermediate values the resin data is inconclusive.

Krishna-Godavari Basin

***Bathymodiolus* sp.** Total SBOM from *Bathymodiolus* sp. has $\delta^{13}C$ values ranging from -33.9‰ to -27.0‰ (n=5), $\delta^{15}N$ value is 5.9‰, and $\delta^{34}S$ is -8.7‰ (resin value of -12.9‰ is also very depleted). Shell carbonate is a mean $\delta^{13}C$ value of -5.6‰ ±3.7 (n=3).

***Vesicomyidae*.** The vesicomyids from this locality have a narrow range of $\delta^{13}C$ total SBOM: -29.7‰ to -27.0‰ (n=7), intra-crystalline $\delta^{13}C$ from -31.1‰ to -28.5‰ (n=4), for individual specimens the intra-crystalline pool is both more enriched (+0.5‰) and depleted (-1.5‰). The same isotopic pattern between the two SBOM pools is found for $\delta^{15}N$, with the total SBOM showing mean values of 4.9‰ ±1.8 (n=8), and the inter-crystalline values of 4.2‰ ±0.5 (n=3). Sulphur values of the total SBOM are variable: $\delta^{34}S$ -3.4‰ and 3.5‰, intra-crystalline SBOM always have positive $\delta^{34}S$ values, ranging from 1.9‰ to 3.5‰ (n=4). For one individual specimen, the intra-crystalline SBOM was $\delta^{34}S$ +5.9‰ more enriched compared to total SBOM. Shell carbonate values range from -2.2‰ to 1.5‰ (n=5).

Comparison between species and suspected nutritional strategies. The $\delta^{13}C$ total SBOM values from the two families are not statistically different (p=0.0938), but $\delta^{13}C$ shell carbonate of *Bathymodiolus* are significantly depleted by (p=0.0211, difference between means: -5.4‰) compared to those of Vesicomyidae. Nitrogen values of both families are similar ($\delta^{15}N$ 5.9‰ vs. 4.9‰ ±1.8, n=8), but sulphur values appear to be more depleted for *Bathymodiolus*, and are below $\delta^{34}S$ -5‰.

4.3.4.3 Pleistocene and Pliocene localities

Kakinokidai seeps and associated non-seep locality

***Acharax* sp. (Locality I)** Total SBOM has a mean $\delta^{13}C$ value of -26.6‰, $\delta^{15}N$ of -2.4‰, and $\delta^{34}S$ of -3.9‰ (resin samples inconclusive). Intra-crystalline SBOM shows a value of $\delta^{13}C$ -27.7‰, and shell carbonate of $\delta^{13}C$ -2.9‰.

***Lucinoma aokii*.** At Locality I $\delta^{13}C$ values of total SBOM range from **-**31.3‰ to -26.7‰ (n=7), and of intra-crystalline SBOM from -29.8‰ to -28.7‰ (n=4). Locality II specimens have similar total SBOM values of $\delta^{13}C$ -28.1‰ and -28.8‰, and intra-crystalline of -30.1‰ and -29.3‰. For both localities the two different SBOM pools are not statistically different for carbon. $\delta^{15}N$ values of total SBOM are very variable, and range from -4.2‰ to 7.1‰ (n=6) for Locality I (intra-crystalline value: 0.3‰), and 4.8‰ for Locality II. Sulphur values are negative for both localities: total SBOM $\delta^{34}S$ (I) -7.0‰ and -4.1‰, (II) -3.6‰, and for intra-crystalline SBOM: (I) -2.7‰, and (II) -5.0‰ (resin values are inconclusive). Shell carbonate values are for Locality I $\delta^{13}C$ –0.7 ±0.3 (n=3) and for Locality II $\delta^{13}C$ -1.2‰ ±2.0 (n=2). There are no statistical differences between the two cold seep localities for any of the measured isotopes.

At a non-seep locality located between the two cold seeps, several gastropod specimens were collected for comparison.

Neptunea kuroshio. Total SBOM values are $\delta^{13}C$ -25.5‰ and -25.9‰ (n=2, -25.7 ±0.3), $\delta^{15}N$: 4.4‰, and $\delta^{34}S$: -10.0‰ (in agreement with resin value of -4.0‰). Intra-crystalline SBOM shows a carbon value of $\delta^{13}C$ -19.6, and is +5.9‰ enriched compared to the total SBOM value of the same specimen. Shell carbonate has a value of $\delta^{13}C$ -0.5‰.

***Fulgoraria prevostiana*.** $\delta^{13}C$ total SBOM is -27.1‰, $\delta^{15}N$: 4.7‰, and $\delta^{34}S$: -7.1‰. Shell carbonate $\delta^{13}C$ is 0.6‰.

***Dentalium* sp**. For *Dentalium* only carbon values are available, for total SBOM: -27.5‰, and shell carbonate: $\delta^{13}C$ 2.1‰.

Comparison between species and suspected nutritional strategies. Due to the limited amount of specimens, it is not possible to statistically compare the results between species of the same suspected nutritional strategy for the suspected thiotrophic bivalves (*Acharax* sp., *L. aokii*) and the suspected heterotrophic gastropods and scaphopod (*N. kuroshio*, *F. prevostiana*, *Dentalium* sp.).

The $\delta^{13}C$ total SBOM of thiotrophs (-28.2‰ ±1.4, n=10, species=3) is are statistically depleted (p=0.0489) by 1-2‰ compared to the heterotrophs (-26.5‰ ±1.0, n=4, species=3), and the difference between $\delta^{13}C$ intra-crystalline SBOM between suspected thiotrophs (-29.2‰ ±0.8, n=7, species=3) and a heterotrophic value (-19.6‰) is even greater.

Based on modern SBOM thresholds the $\delta^{13}C$ total SBOM is expected to be more depleted compared to thiotrophy. Modern intra-crystalline SBOM is however more depleted for heterotrophs/enriched values above roughly 25 per mille total SBOM. The range of fossil thiotrophic values (-31.3‰ to -26.6‰) does only not overlap with the heterotrophic values of *N. kuroshio* (25.5‰ and -25.9‰), for the other species no threshold for heterotrophy is evident. Thiotrophy can potentially be assigned for values below -27.5‰.

A comparison between nitrogen values of total SBOM shows no statistical difference between suspected thiotrophs (2.3‰ ±4.1, n=8, species=3) and suspected heterotrophs (4.6‰ ±0.2, n=2, species=2), and the relatively depleted values for the heterotrophs in non-reducing environments are unexpected. Similarly unexpected are the depleted sulphur values for the heterotrophs (-8.6‰ ±2.1, n=2, species=2) (even compared to the suspected thiotrophs: -4.7‰ ±1.6, n=4, species=3) which is usually associated with using hydrogen sulphide as a sulphur source, instead of heterotrophic feeding. No further intra-crystalline values are available for heterotrophs except carbon.

A comparison of shell carbonate $\delta^{13}C$ values between the two species shows that the thiotrophs (0.3‰ ±2.0, n=9, species=3) and heterotrophs (0.7‰ ±2.0, n=3, species=3) are not statistically different.

Koshiba Formation: cold seep and non-seep specimens

***Lucinoma spectabilis*.** The total SBOM obtained from *L. spectabilis* has $\delta^{13}C$ values ranging from -28.9 to -26.6 (-27.7‰ ±1.1, n=3), and a $\delta^{15}N$ value of 1.7‰. Intra-crystalline SBOM is slightly more depleted for $\delta^{13}C$ (-31.0‰), as well as $\delta^{15}N$ (1.3‰), and has a sulphur value of $\delta^{34}S$ -0.9‰. Shell carbonate values fall between -5.3‰ and 0.5‰ (n=3, -1.8 ±3.1)

Conchocele bisecta. Specimens of *C. bisecta* yielded total SBOM with values of $\delta^{13}C$: -28.3‰ and -27.4‰ (n=2, -27.8 ±0.6) Intra-crystalline SBOM has a mean value of $\delta^{13}C$ -31.3‰, $\delta^{15}N$ -0.5‰, and $\delta^{34}S$ 2.5‰. Carbon values of shell carbonate are very variable, ranging from -13.9‰ to 1.3‰ (n=3).

Solemya japonica. Total SBOM was obtained from one specimen, with a carbon value of $\delta^{13}C$ -27.0‰, and a sulphur value of $\delta^{34}S$ 8.0‰. For shell carbonate, $\delta^{13}C$ values very variable: -0.3‰ and -8.1‰ (n=2).

***Ostrea musashiana*.** Total SBOM obtained from the oyster *O. musashiana* shows carbon values of -26.5‰ and -27.1‰ (n=2, -26.8 ±0.5), a nitrogen value of 6.5‰, and a sulphur value of 0.2‰. Shell carbonate has values of 0.4‰ and 1.2‰.

***Glycymeris* sp.** $\delta^{13}C$ of total SBOM ranges from -28.6‰ to -25.7‰ (n=3, -27.0 ±1.5), For both nitrogen and sulphur, the intra-crystalline SBOM values ($\delta^{15}N$: 6.5‰, and $\delta^{34}S$: 7.6‰) are more enriched than the total SBOM values ($\delta^{15}N$: 2.1‰, and $\delta^{34}S$: -1.2‰). The shell carbonate of *Glycymeris* (1.3‰ and 1.4‰) shows little variation between the two specimens.

Fusitrition oregonensis. Total SBOM obtained from specimens of the gastropod *F. oregonensis* has $\delta^{13}C$ values -27.2‰ and -26.8‰ (-27.0‰ ±0.3, n=2). In addition a value for sulphur ($\delta^{34}S$: -2.5‰) was obtained, a sulphur value obtained using resin of -7.1‰ is even more depleted. $\delta^{13}C$ of shell carbonate is 1.0‰.

***Ranella galea*.** A single specimen of *Ranella* was analysed, with a total SBOM $\delta^{13}C$ value of -26.2‰. For this resin obtained sample the sulphur value is conclusively depleted ($\delta^{34}S$ -7.3‰)

***Fulgoraria kamakuraensis*.** Total SBOM carbon values range from -27.3‰ to -25.6 (n=3), a sulphur value of $\delta^{34}S$ 1.1‰ was obtained. Shell carbonate values ($\delta^{13}C$ -0.3‰ and 1.0‰, n=2) have little variation.

***Dentalium* sp.** A single specimen shows a total SBOM value of $\delta^{13}C$ -28.1‰, and a shell carbonate value of $\delta^{13}C$ 0.2‰.

Terebratulidae. Terebratulid brachiopods total SBOM ranges from $\delta^{13}C$ -26.1‰ to -23.8‰ (n=4). A nitrogen value of $\delta^{15}N$ 2.5‰ was also obtained, as well as a sulphur value of $\delta^{34}S$ -15.3‰ (total SBOM obtained using resin showed an even more depleted value of -28.1‰). Shell carbonate values ranged from -0.3‰ to 1.5‰ (n=3).

Comparison between species and suspected nutritional strategies. Between the suspected thiotrophic bivalves (*L. spectabilis, C. bisecta*, *S. japonica*) there are no statistical differences in $\delta^{13}C$ of total SBOM, and the three species have a

combined value of $\delta^{13}C$ -27.6 ±0.8 (n=10). Amongst the different heterotrophic animals (all other species), only the terebratulid brachiopod is statistically enriched (-25.0 ±0.9, n=4) compared to several of the other species. The heterotrophic species have a combined value of total SBOM $\delta^{13}C$: -26.3‰ ±1.1 (n=16, species=7), which is statistically enriched compared to the thiotrophic species (also when removing the brachiopod data). However, the range of chemosymbiotic values (-28.9‰ to -26.6‰) does only not overlap with the brachiopods (26.1‰ to -23.8‰), and no heterotrophy threshold can be estimated for the other species.; thiotrophy can be assigned below -28.6‰ at this locality.

The intra-crystalline SBOM $\delta^{13}C$ values of thiotrophs (-31.2‰ ±0.2, n=2, species=2) could unfortunately not be compared to heterotrophic intra-crystalline SBOM. But for thiotrophs intra-crystalline SBOM is statistically depleted compared to total SBOM, and depleted beyond the threshold of total SBOM thiotrophy.

Very limited nitrogen data is available, and obtained values for thiotrophs ($\delta^{15}N$ 1.7‰) and heterotrophs ($\delta^{15}N$ 3.7‰ ±2.4, n=3, species=3) do not overlap in range. Intra-crystalline SBOM differences are even more pronounced: $\delta^{15}N$ 0.4‰ ±1.3 (n=2, species=2) versus 6.5‰, respectively.

Surprisingly, sulphur values of total SBOM show an enriched value for suspected thiotrophs ($\delta^{34}S$ 8.0‰) compared to the heterotrophic values (-3.8‰ ±7.6, ranging down to -15.3‰). Intra-crystalline values however show the opposite relationship between the two nutritional strategies, whereby the depleted thiotrophic values (0.8‰ ±2.4, n=2, species=2) compared to the heterotrophic specimen (7.6‰, n=1) can be explained through the use of depleted hydrogen sulphide by thiotrophic bacteria.

Shell carbonate values are very variable for all three suspected thiotrophic species, due to several very depleted values (below $\delta^{13}C$ -5‰), and have a combined value of: $\delta^{13}C$ -4.6‰ ±5.6 (n=7, species=3). Heterotrophic species shell carbonate values have a combined value of $\delta^{13}C$ 0.8‰ ±0.7 (n=11, species=6), which is statistically enriched (p=0.0054) compared to the suspected thiotrophs. However, when the extremely depleted values are removed ($\delta^{13}C$ 0.3‰ ±0.8 (n=4, species=3), there is no statistical difference.

Kounandai seep

***Lucinoma* sp.** At Kounandai seep *Lucinoma* (Lucinidae) specimens from two adjacent cold seep localities were analysed. The data for these localities are

combined because no further environmental data is available to investigate potential isotopic differences. For total SBOM values range from $\delta^{13}C$ -29.0‰ to -26.3‰ (n=8), intra-crystalline SBOM $\delta^{13}C$ values are -29.8‰ and -28.2‰. The nitrogen values are very variable, ranging from $\delta^{15}N$ -11.1‰ to 8.4‰ (n=3). A single sulphur measurment shows a very depleted value for total SBOM: $\delta^{34}S$ -8.2‰.

Shell carbonate $\delta^{13}C$ values are all negative, ranging from -8.9‰ to -4.0‰ (n=3).

Takanabe Formation

***Lucinoma* sp.** *Lucinoma* total SBOM values are $\delta^{13}C$ -26.9‰ and -26.9‰, and $\delta^{15}N$ 5.6‰ and 7.1‰. Two out of three shell carbonate $\delta^{13}C$ values are extremely depleted (-20.2‰ and -27.8‰), compared to the other sample of 0.5‰.

Shiramaza Formation

***Calyptogena* sp.** From a Shiramaza Formation cold seep the suspected thiotroph *Calyptogena* sp. was analysed. Total SBOM carbon values are variable, and mean values range from $\delta^{13}C$ -30.3‰ to -22.6‰ (-27.1‰ ±2.3, n=9), intra-crystalline SBOM $\delta^{13}C$ values are equally variable (-30.9‰ to -27.0‰, n=3), and slightly more depleted. $\delta^{13}C$ values of shell carbonate range from -1.1‰ to 1.0‰ (n=4)

Nitrogen values of total SBOM range from $\delta^{15}N$ -1.6‰ to 4.9‰ (n=10, 1.5‰ ±2.3), a single intra-crystalline value is more depleted than this range (-2.5‰). The total SBOM sulphur values are extremely variable, ranging from $\delta^{34}S$ -5.4‰ to 9.0‰ (n=4) a single resin value is also positive, other measurements are inconclusive.

4.3.4.4 Miocene and Oligocene localities

Rocky Knob

***Lucinoma* aff. *taylori*.** Total SBOM ranges from $\delta^{13}C$ -27.6‰ to -26.2‰ (n=3, -27.0‰ ±0.7), and has a nitrogen value of $\delta^{15}N$ 2.5‰. Two $\delta^{13}C$ shell carbonate values are extremely depleted ($\delta^{13}C$ -27.4‰ and -24.6‰) compared to a much less extreme sample ($\delta^{13}C$ 0.2‰).

***Bathymodiolus heretaunga*.** Carbon values for total SBOM fall between -31.1‰ and -29.5‰ (n=4, -30.0‰ ±0.9). A nitrogen value of -9.6‰ is reported. Shell carbonate values are -3.3‰ and -3.5‰, as well as a more depleted outlier of -21.3‰.

Comparison between species and nutritional strategies. Statistical comparison confirms that *B. heretaunga* total SBOM carbon values are significantly depleted (on average by $\delta^{13}C$ -3.0‰) compared to *Lucinoma*. The nitrogen value of *B. heretaunga* is also more depleted. Shell carbonate values are difficult to compare because both include extremely depleted values.

Moonlight North

***Gigantidas coseli*.** Total SBOM obtained from a single *G. coseli* specimen has a $\delta^{13}C$ value of -26.2‰, and $\delta^{15}N$ of 3.7‰. Resin obtained total SBOM points towards negative sulphur values ($\delta^{34}S$ -3.5‰). For this specimen the shell carbonate value is -13.8‰.

***Lucinoma* sp.** A single specimen was analysed and has a total SBOM $\delta^{13}C$ value of -27.0‰, and a shell carbonate $\delta^{13}C$ value of -13.6‰.

***Liothyrella* sp.** Carbon values of total SBOM have a narrow range, from $\delta^{13}C$ -27.3‰ to -26.9‰ (n=3). Total SBOM obtained using resin has a value of $\delta^{34}S$ -8.9‰.

Comparison between species and nutritional strategies. The total SBOM $\delta^{13}C$ range of suspected heterotroph *Liothyrella* (-27.3‰ to -26.9‰) overlaps or is more depleted than the suspected thiotrophic species *G. coseli* (-26.2‰) and *Lucinoma* (-27.0‰), were the latter two species are expected to be more depleted. Similarly, the depleted sulphur value for the brachiopod species is unexpected, as comparable results are associated with the presence of thiotrophic symbionts.

Hokkaido

***Calyptogena pacifica*.** Carbon values for total SBOM range from $\delta^{13}C$ -26.7‰ to -25.6‰ (n=4), an intra-crystalline SBOM carbon value is more depleted: $\delta^{13}C$ -28.5‰. Similarly, the intra-crystalline nitrogen value ($\delta^{15}N$ -3.0‰) is more depleted than total SBOM ($\delta^{15}N$ 4.3‰ and 5.3‰). Sulphur values of total SBOM obtained using resin indicate very negative sulphur values (-13.0‰ to -4.8‰ to n=3). Shell carbonate of *C. pacifica* has a narrow range of $\delta^{13}C$ values, from -1.6‰ to -0.7‰ (n=4).

Izura seep

Lucinoma acutentilineatum. Total SBOM was obtained from eight specimens, and $\delta^{13}C$ values range from -27.5‰ to -26.0‰ (n=8, -27.0‰ ±0.7). Nitrogen values range from $\delta^{15}N$ 3.0‰ to 5.2‰ (n=5), and sulphur of total SBOM shows a value of $\delta^{34}S$ -0.2‰. Intra-crystalline SBOM shows more depleted value for both carbon

($\delta^{13}C$ -29.2‰ and -28.4‰; n=2 -28.8±0.6; statistically different, p=0.0107) and sulphur ($\delta^{34}S$: -5.0‰). Total SBOM obtained using resin contains a conclusively positive value ($\delta^{34}S$: 6.1‰). Shell carbonate values have a narrow range, from 0.7‰ to 1.4‰ (n=4).

Mizuhopecten kobiyami. Two specimens of the oyster M. kobiyami were available for analysis. Total SBOM values are $\delta^{13}C$ -25.1‰ and -25.2‰, and $\delta^{15}N$ 2.9‰ and 5.7‰. Sulphur values are not available. Shell carbonate values are: 1.3‰ and -2.2‰ (n=2, -0.5‰ ±2.5)

***Calyptogena* sp.** Total SBOM was obtained from collated *Calyptogena* specimens, showing a carbon value of $\delta^{13}C$ -27.9‰. The specimens have a shell carbonate value of $\delta^{13}C$ -5.4‰.

Comparison between species and nutritional strategies. The total SBOM carbon values of suspected thiotroph *L. acutentilineatum* (n=8, -27.0‰ ±0.7). are statistically depleted compared to the suspected heterotroph *M. kobiyami* (-25.1‰ ±0.1, n=2; p=0.0064), the value of *Calyptogena* (-27.9‰) is also depleted compared to *M. kobiyami*. Total SBOM nitrogen values of the first two species are statistically similar, sulphur results could not be compared. A comparison between shell carbonate $\delta^{13}C$ values shows that *Calyptogena* (-5.4‰) is depleted compared to the other two species, that are not statistically different from each other.

Lincoln Creek Formation

For several specimens of *Lucinoma*, as well as for the vesicomyid specimen, it was not possible to obtain reliable carbon data, probably due to the very low elemental concentration of carbon. In addition, one *Lucinoma* specimen could not be dissolved potentially due to silicification.

Conchocele bisecta. Total SBOM obtained from *C. bisecta* has carbon values of $\delta^{13}C$ -27.4‰ and -26.3‰, and shell carbonate shows carbon value of $\delta^{13}C$ -2.8‰ and -1.0‰. A sulphur value of resin obtained SBOM is conclusively negative: -5.2‰.

***Lucinoma* sp.** Carbon values of *Lucinoma* are $\delta^{13}C$ -29.2‰ and -25.9‰ for total SBOM, and fall between $\delta^{13}C$ -2.5‰ and 0.0‰ for shell carbonate. Resin obtained SBOM has depleted sulphur values of -4.8‰ and -4.3‰.

Solemyidae sp. Total SBOM $\delta^{13}C$ values are -27.7‰ and -26.3‰, shell carbonate is $\delta^{13}C$ 0.8‰ and 1.6‰.

Vesicomyidae sp. Shell carbonate value of $\delta^{13}C$ 0.6‰.

Mytilidae sp. (modiolid). Carbon value of total SBOM was shown to be -28.6‰, and the carbon value of shell carbonate is -0.2‰.

***Ennucula* sp.** Shell carbonate value of $\delta^{13}C$ 2.2‰.

Comparison between species and nutritional strategies. The total SBOM carbon values of all suspected thiotrophic species overlap (*C. bisecta*, *Lucinoma*, solemyid) and range from ^{13}C -29.2‰ to -25.9‰. Modiolid total SBOM (^{13}C -28.6‰) is amongst the most depleted values. The heterotrophic specimen *Ennucula* (^{13}C 2.2‰) has a more enriched shell carbonate value compared to the suspected chemosymbiotic species (^{13}C -2.5‰ to 1.6‰).

4.3.4.5 Cretaceous localities

Tepee Buttes

***Nymphalucina occidentalis*.** Total SBOM carbon values range from $\delta^{13}C$ -27.2‰ to -26.2‰ (n=8, -26.5‰ ±0.4), intra-crystalline SBOM has a carbon value of -26.2‰. In addition, nitrogen ($\delta^{15}N$ 3.7‰) and sulphur (-3.4‰ and 1.2‰) values of total SBOM were also obtained. Shell carbonate values from $\delta^{13}C$ -2.2 to -0.5 (n=3), as well as a more depleted value of $\delta^{13}C$ -12.6‰.

***Inoceramus* sp.** Carbon values for SBOM are $\delta^{13}C$ -26.8 and -26.3 (-26.6±0.3, n=3) for total SBOM, and $\delta^{13}C$ -26.2‰ and -25.8‰ for intra-crystalline SBOM (-26.0 ±0.2, n=2). These two pools are not statistically different. Nitrogen values for total SBOM are $\delta^{15}N$ -1.4‰ and 3.9‰ (n=2, 1.2 ±3.7). Carbon values of shell carbonate range from 0.0‰ to 2.6‰ (n=3; 1.6‰ ±1.4, n=3).

***Baculites* sp.** Total SBOM shows carbon values of $\delta^{13}C$ -26.5‰ and -26.3‰ (n=2, -26.4‰ ±0.1, n=2), and an intra-crystalline carbon value of -26.1‰. In addition, for total SBOM a nitrogen value ($\delta^{15}N$ 5.5‰) was obtained, as well as a depleted sulphur value for total SBOM obtained using cation exchange resin ($\delta^{34}S$ -7.1‰). Shell carbonate values range from -4.8‰ to -1.3‰ (n=3; -3.2 ±1.8).

Comparison between species and nutritional strategies. Total SBOM carbon values have a very narrow range for all three species, and are statistically similar (total range: -27.2‰ to -26.3‰). Similarly, the values for intra-crystalline are very similar, and range from -26.2‰ to -25.8‰. *Inoceramis* shell carbonate is statistically enriched, compared to the other two species.

***Seymour Island*.**

***Thyasira townsendi*.** Total SBOM shows isotopic values of: $\delta^{13}C$ -26.3‰, $\delta^{15}N$ 5.4‰, and a depleted $\delta^{34}S$ value (-4.9‰). Intra-crystalline SBOM values are slightly

more depleted for carbon ($\delta^{13}C$ -27.3‰) and more enriched for sulphur ($\delta^{34}S$ -1.5‰). The specimen has a shell carbonate of - $\delta^{13}C$ -3.5‰.

Solemya rossiana. Carbon values for *S. rossiana* specimens are: $\delta^{13}C$ -26.3‰ and -26.0‰ (-26.2‰ ±0.2, n=2) for total SBOM, $\delta^{13}C$ -27.3‰ for intra-crystalline SBOM, and $\delta^{13}C$ -9.9‰ and -2.9‰ for shell carbonate (n=2, -6.4‰ ±4.9). In addition nitrogen values of $\delta^{15}N$ -0.8‰ and 6.3‰ were obtained (2.8‰ ±4.9, n=2) for total SBOM.

***Maorities seymourianus*.** Total SBOM has a $\delta^{13}C$ value of -25.9‰, and a $\delta^{15}N$ value of 8.8‰. Shell carbonate of this specimen shows a carbon value of -13.0‰ (because of presence at seep after death).

Lahillia larseni. Carbon values for total SBOM range from $\delta^{13}C$ -26.7‰ to -26.0‰ (=-26.3‰ ±0.3, n=4), for intra-crystalline SBOM from $\delta^{13}C$ -28.2‰ to -25.8‰ (n=3; -26.8‰ ±1.2). Nitrogen values for total SBOM are $\delta^{15}N$ -0.9‰ and 5.4‰ (2.3‰ ±4.6, n=2) , for intra-crystalline SBOM nitrogen has a value is $\delta^{15}N$ 5.9‰. A sulphur value for total SBOM is $\delta^{34}S$ -32.6‰ (resin values are also negative, up to -19.1‰), for intra-crystalline SBOM values are: $\delta^{34}S$ -26.4‰ and -6.2‰ (=2, -16.4‰ ±14.3).

***Cucullaea* sp.** Isotopic values of $\delta^{13}C$ -27.0‰ and $\delta^{15}N$ 5.0‰ were obtained for total SBOM.

Leionucula suboblonga. Both total and intra-crystalline SBOM were analysed for a single specimen. The carbon value of total SBOM is $\delta^{13}C$ -25.3‰, intra-crystalline SBOM values are $\delta^{13}C$ -26.7‰ and $\delta^{15}N$ 2.2‰. The carbon value for shell carbonate is 1.9‰.

Pycnodonte* (*Phygraea*) *vesicularis vesicularis. Total SBOM carbon values are $\delta^{13}C$ -24.8‰ (±0.2, n=3), intra-crystalline values are $\delta^{13}C$ -25.6‰ (±0.3, n=2). For total SBOM a single depleted sulphur value was obtained: $\delta^{34}S$ -23.4‰, as well as an enriched nitrogen value of $\delta^{15}N$ 14.1‰. Shell carbonate values are $\delta^{13}C$ 0.8‰ and 1.8‰ (1.3‰ ±0.7, n=2) .

***Neogastropod* n. gen.** Total SBOM obtained from a single specimen has values of $\delta^{13}C$ -26.4‰, and $\delta^{15}N$ 7.1‰, intra-crystalline SBOM of -26.1‰. Shell carbonate has a value of 1.6‰.

Vanikoropsis arktowskiana. Carbon values are $\delta^{13}C$ -26.1‰ for total SBOM, and $\delta^{13}C$ 2.7‰ for shell carbonate. In addition a nitrogen value of $\delta^{15}N$ 7.3‰ was obtained.

Amberleya spinigera. Total SBOM values are $\delta^{13}C$ -26.0‰ and $\delta^{15}N$ 7.3‰, shell carbonate has a value of $\delta^{13}C$ 3.8‰.

Maorites seymourianus. The carbon value for total SBOM is $\delta^{13}C$ -26.4‰, nitrogen is $\delta^{15}N$ 5.0‰ for total SBOM and 4.2‰ for intra-crystalline SBOM. Sulphur

results were also obtained for intra-crystalline SBOM: $\delta^{34}S$ -21.2‰, for total SBOM obtained using resin sulphur values are also strongly depleted ($\delta^{34}S$ -9.4‰). The *M. seymourianus* specimen has a shell carbonate value of 3.5‰.

***Kitchinites* sp.** Stable isotope values are $\delta^{13}C$ -26.2‰, and $\delta^{15}N$ 7.2‰ for total SBOM, and $\delta^{13}C$ -26.0‰ and $\delta^{34}S$ -6.3‰ for intra-crystalline SBOM. In addition a shell carbonate value of $\delta^{13}C$ -1.0‰ was obtained.

***Pachydiscus* (*Pachydiscus*) *riccardii*.** Total SBOM values are $\delta^{13}C$ -26.4‰ and $\delta^{15}N$ 8.3‰. The carbon value of shell carbonate is -0.8‰.

***Diplomoceras cylindraceum*.** Total SBOM values are $\delta^{13}C$ -27.4‰ and $\delta^{15}N$ 6.3‰. The shell carbonate value of this species is very depleted ($\delta^{13}C$ -21.1‰).

***Eutrephoceras dorbignyanum*.** Stable isotope results for total SBOM were obtained for carbon ($\delta^{13}C$ -27.0‰) and sulphur (-3.7‰, obtained using cation exchange resin). The carbon value of shell carbonate is $\delta^{13}C$ -3.6‰.

***Rotularia* ssp.** Carbon values range from $\delta^{13}C$ -25.8‰ to -24.6‰ (-25.4‰ ±0.2, n=3) for total SBOM, and are $\delta^{13}C$ -26.8‰ and -25.8‰ for intra-crystalline SBOM (-25.7‰ ±1.5, n=2). Nitrogen values range from $\delta^{15}N$ 7.5‰ to 10.8‰ (n=3, 9.3‰ ±1.7) for total SBOM, and are $\delta^{15}N$ 9.3‰ for intra-crystalline SBOM. Intra-crystalline SBOM sulphur values are $\delta^{34}S$ -9.9‰ and -8.4‰ (n=2, -9.9‰ ±1.1), the total SBOM sample shows a value of $\delta^{34}S$ -18.0‰ (this is in agreement with very depleted resin values of -12.0 and -7.9). Shell carbonate values of *Rotularia* specimens are $\delta^{13}C$ 2.7‰ and 4.2‰ (mean: 3.5‰ ±1.1, n=2).

Comparison between species and nutritional strategies.

A total SBOM comparison between bivalves that are suspected to obtain nutrition via symbionts ($\delta^{13}C$: -26.3‰ ±0.2, n=3, species=2) does not differ from suspected heterotrophic bivalves ($\delta^{13}C$: -25.7‰ ±0.8, n=8, species=4) for carbon. Similarly, intra-crystalline values ($\delta^{13}C$: -27.3‰ ±0.0, n=2, species=2; versus; -26.4‰ ±1.0, n=6, species=3) are similar. The range of nitrogen values for suspected chemosymbionts ($\delta^{15}N$ total: -0.8‰ to 6.3‰ (n=3, species=2) completely overlaps with the range of heterotrophs (-0.9‰ to 14.4‰) (intra-crystalline SBOM could not be compared). Similarly for sulphur, both suspected nutritional strategies are strongly depleted, for thiotrophs (total: -4.9‰, intra: -1.5‰) and heterotrophs (total: -28.0‰ ±6.5, n=2, species=2; intra: -16.4‰ ±14.3, n=2, species=1). Difference in shell carbonate values between the chemosymbiotic bivalves (-5.4‰ ±3.8, n=3, species=2) and the heterotrophic bivalves (1.5‰ ±0.6, n=3, species=2).

Owl Creek Formation

Cucullaea capex. Carbon total SBOM values range from -27.7‰ to -25.7‰ (n=3; -27.1 ±1.2), for intra-crystalline a value of -26.2‰ was obtained. In addition, a nitrogen value of $\delta^{15}N$ 1.3‰ for total SBOM, and a sulphur value of $\delta^{34}S$ -35.2‰ for intra-crystalline SBOM are shown.

Nucula percrassa. Total SBOM values fall between $\delta^{13}C$ -28.8‰ and -26.1‰ for carbon (n=3; -27.3‰ ±1.3), and has a nitrogen value of $\delta^{15}N$ 6.8‰.

***Turritella*.** The carbon value of total SBOM is $\delta^{13}C$ -26.7‰, the nitrogen value is 4.4‰.

Drilluta. Combined specimens belonging to the genus *Drilluta* have a total SBOM value of $\delta^{13}C$ -26.1‰.

Baculites. Total SBOM carbon values range from -27.6‰ to -25.8‰ (n=3; -26.9‰ ±1.00; nitrogen for total SBOM has values of 5.9‰ and 6.8‰ (n=2; 6.4‰ ±0.6), no sulphur values are available.

Eubaculites. Carbon values range from $\delta^{13}C$ -30.7‰ to -25.6‰ (n=4; -27.9‰ ±2.7) for total SBOM. In addition a nitrogen value ($\delta^{15}N$ 4.0‰) and sulphur value ($\delta^{34}S$ -11.0, via cation exchange resin) were obtained.

Discoscaphites. Total SBOM values have a carbon range of -27.9‰ to -26.1‰ (n=3; -26.8‰ ±1.0), and a nitrogen value of $\delta^{15}N$ 4.6‰.

4.3.4.6 Palaeozoic and Mesozoic seep brachiopods

Anarhyncha. Total SBOM has a carbon value of $\delta^{13}C$ -27.9‰, and shell carbonate of $\delta^{13}C$ -2.9‰.

Halorella. Carbon isotope values are $\delta^{13}C$ -26.3‰ for total SBOM, $\delta^{13}C$ -26.3‰ for intra-crystalline SBOM, and $\delta^{13}C$ -1.4‰ for shell carbonate. In addition a sulphur value of $\delta^{34}S$ -4.2‰ was obtained.

Iberinghychia contraria. Total SBOM values of $\delta^{13}C$ -23.9‰ and $\delta^{15}N$ -12.0‰.

Dzieduszyckia. Two species of this genus were analysed for total SBOM, showing values of $\delta^{13}C$ -24.6‰, $\delta^{15}N$ 3.8‰ and $\delta^{34}S$ 3.8‰ (resin) for *D. crassicostata*, and $\delta^{13}C$ -26.9‰ and $\delta^{15}N$ 10.7‰ for *D. tenuicostata*. In addition an intra-crystalline SBOM value of $\delta^{13}C$ -26.3‰ was obtained. Shell carbonate values of the two species are -0.6 (*D. crassicostata*) and 0.3 (*D. tenuicostata*).

Septatrypa. Insufficient shell material was available, shell carbonate $\delta^{13}C$ -0.8‰.

Figure 4.21 SBOM stable isotope results summarized per time period

Range of $\delta^{13}C$, $\delta^{15}N$ and $\delta^{34}S$ values for total SBOM and intra-crystalline SBOM are shown per nutritional strategy, for multiple localities per geological time period

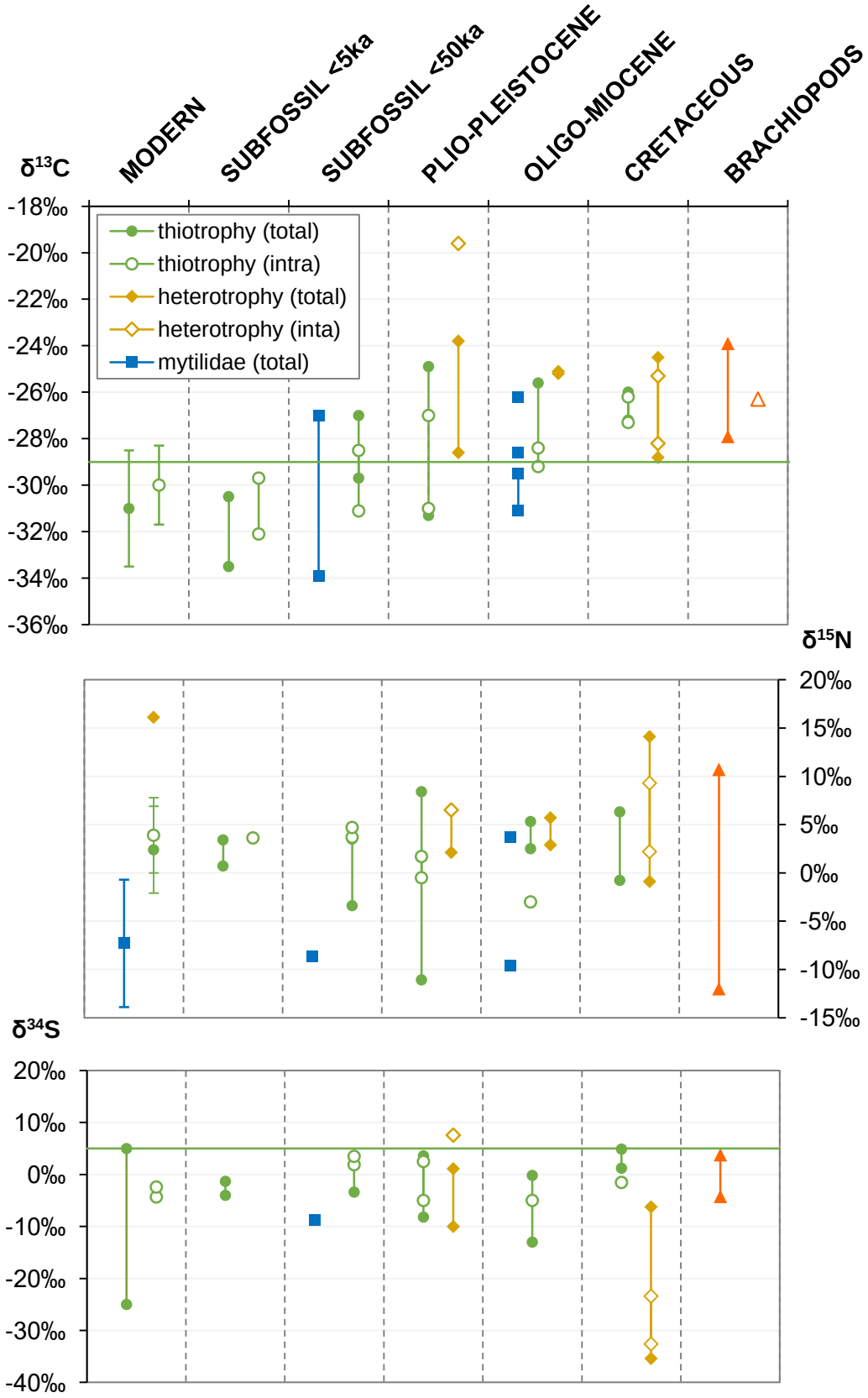

Figure 4.22 $\delta^{13}C$ shell carbonate values per time period
Results are shown per nutritional strategy, heterotrophs outlined in black were obtained from seep localities

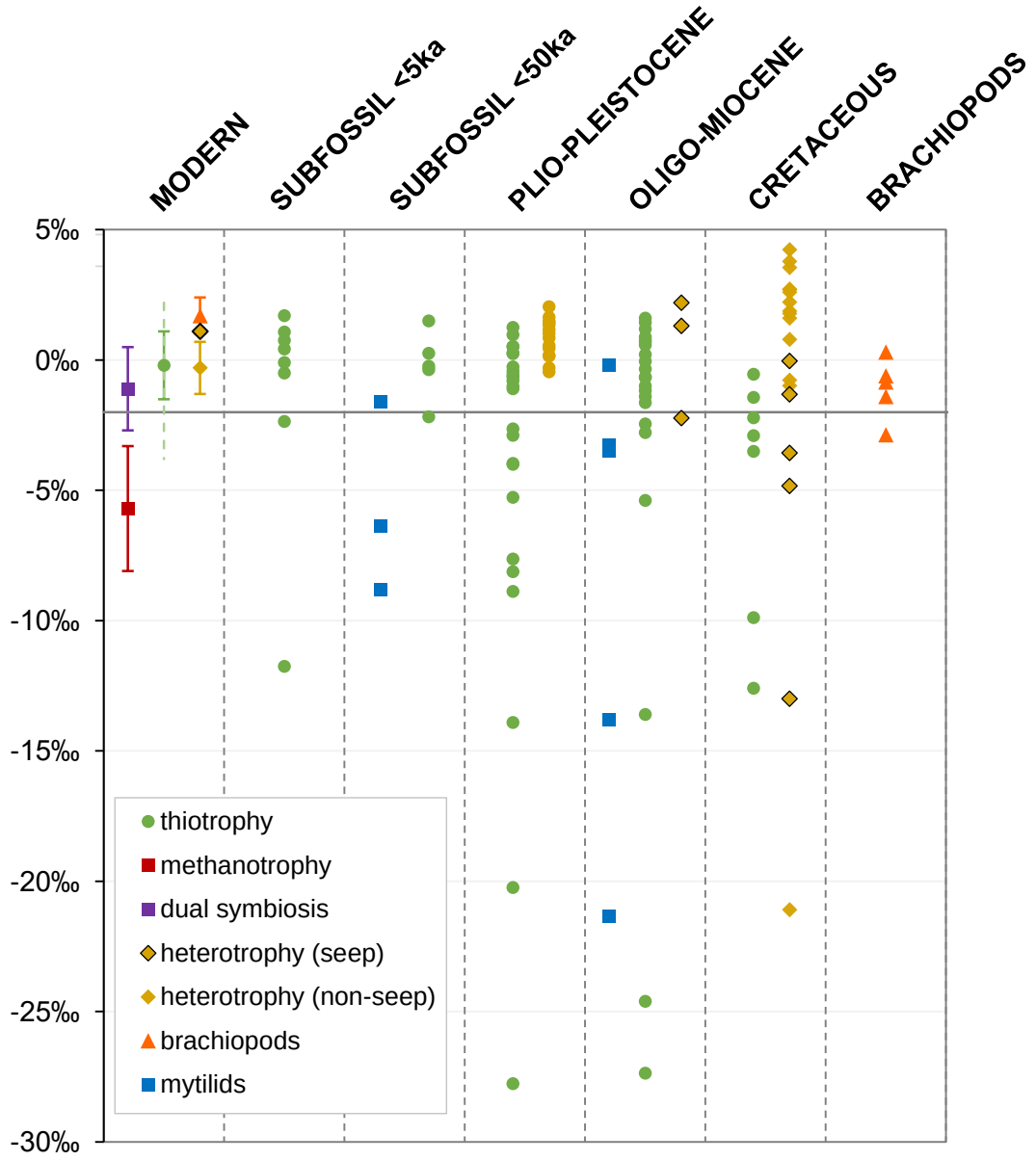

4.3.4.7 $\delta^{34}S$ values of carbonate-associated sulphate

In the Methodology chapter it was explained that $\delta^{34}S$ values of carbonate-associated values (CAS) obtained using the cation exchange method do not reflect modern seawater sulphate values ($\delta^{34}S$ +20.3‰) but are depleted because of the presumed incorporation of residual resin. However, several of the CAS values (total SBOM) obtained from the Cretaceous fossil specimens are lower than the value of

resin (+1.5‰). These include CAS obtained from the Seymour Island non-seep taxa *Rotularia* ($\delta^{34}S$ -4.4‰ and -4.8‰) and the seep specimen *Maorites seymourianus* ($\delta^{34}S$ -8.2‰), as well as *Inoceramus* (-4.7‰) and *Baculites* (-4.7‰) from the Tepee Buttes. CAS obtained from bleached shell powder from these specimens are even more depleted: -12.9‰ for *Baculites*, and -11.3‰ for the lucinid *Nymphalucina occidentalis*. $\delta^{34}S$ CAS obtained using HCl on unbleached shell powder from the latter specimen has a value of 7.5‰.

4.3.4.8 SBOM wt.% and elemental concentrations

SBOM preservation based on weight percent. Contaminant material can replace or be added through diagenesis, e.g. bacterial contamination. Calculating the weight percent (wt.%) SBOM of the shell potentially makes it possible to determine added contaminants, when comparing wt% to known modern ranges. Modern wt.% SBOM ranges were previously determined to be < 1% for total SBOM, and < 0.2% for the intracrystalline pool (Chapter 3). Based on this data, fossil specimens for which the wt.% SBOM was determined were classified in three categories for both SBOM pools, with increased weight % classified between 1.0-2.0% for total SBOM, and 0.2-0.5% for intra-crystalline SBOM. Specimens excluded from this analysis are Mytilidae, that were previously shown to contain relatively large amounts of SBOM relative to shell weight. Similarly the shelled cephalopods were excluded, based on analysis of *Nautilus* in this study, with a weight% of 2.6%. Fig. 4.23 shows an increase with time in specimens falling into the questionable/poor wt.% SBOM categories.

Elemental concentrations. Generally the C/N ratio is used as an indicator of preservation for organic matter (e.g. O'Donnell et al., 2003), but with the chosen methodology it is not possible to determine the elemental concentration of carbon. Therefore the concentrations of nitrogen (resin and HCl) and sulphur (HCl) of the SBOM from fossil specimens are shown, grouped per time period. Of these two elements sulphur concentration is least informative about possible contamination, because sulphur can be added as well as lost, e.g. external sulphide can bind to the organics.

Figure 4.23 SBOM wt% of the shell, and elemental concentrations of SBOM per time period

Number of analysed specimens are shown for each time bin.

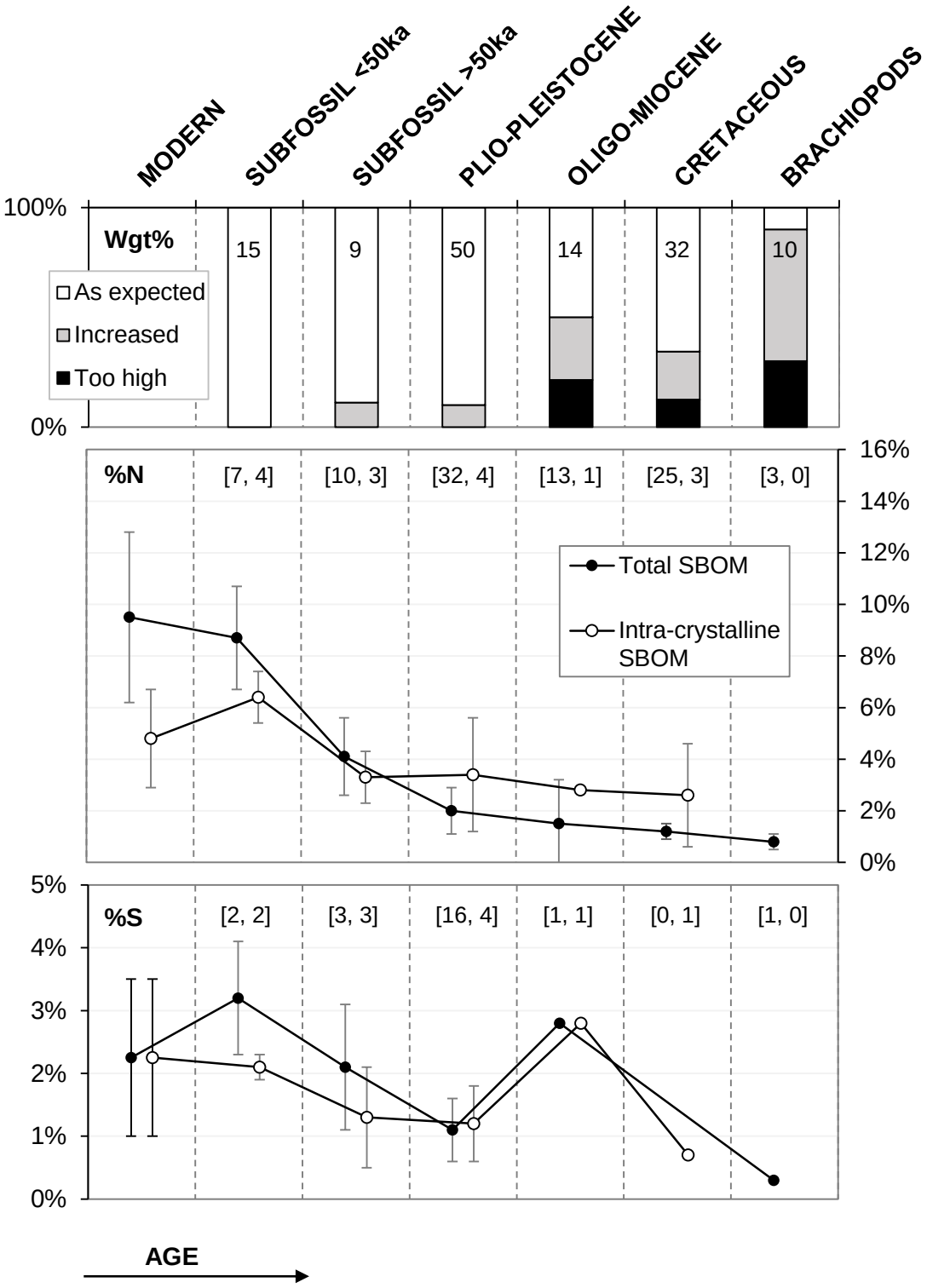

4.4 Discussion

The results for the different analytical techniques will be discussed per geological period, with the various localities divided into: subfossil <5ka (Congo Fan, Hikurangi Margin), subfossil <50ka (Krishna-Godavari Basin), Pleistocene/Pliocene (Kakinokidai seep, Koshiba Formation, Kounandai seep, Takanabe Formation, Shiramaza Formation), Miocene/Oligocene (Rocky Knob, Moonlight North, Hokkaido, Izura seep, Lincoln Creek Formation), Cretaceous (Tepee Buttes, Seymour Island, Owl Creek Formation), and Palaeozoic brachiopods (*Halorella*, *Ibergirhynchia*, *Dzieduszyckia*, *Septatrypa*). By summarizing the results in these geological periods, it will be possible to gain a broader perspective on isotopic changes of SBOM through geological time.

4.4.1 Subfossil localities

Carbon. The isotopic $\delta^{13}C$ values obtained from subfossil SBOM can be compared to modern ranges reported in Chapter 3. In modern specimens $\delta^{13}C$ SBOM values have been shown to be very indicative of the different chemosymbiotic nutritional strategies. Thiotrophic bacteria use dissolved inorganic carbon (DIC) as a carbon source, which is strongly fractionationed when utilized by the symbiotic bacteria via the Calvin-Benson-Bassham cycle (Dubilier et al., 2008). For modern thiotrophic vesicomyids this process results in total SBOM values with a relatively narrow $\delta^{13}C$ range (-31.9‰ ±2.2, n=48), with the very large majority of specimens showing values between -35‰ and -30‰. The suspected thiotrophic vesicomyids from the Congo Fan (*L. chuni*, -32.3‰ ±0.6, n=4) and Hikurangi Margin (*C. tuerkayi*, 31.8‰ ±1.2, n=5) fall within this range, but the vesicomyids from Krishna-Godavari Basin have $\delta^{13}C$ values more enriched than -30‰ ($\delta^{13}C$ -28.7‰ ±0.9, n=7).

The intra-crystalline SBOM $\delta^{13}C$ values of modern thiotrophic species are generally more enriched than the total SBOM $\delta^{13}C$ values (30.5‰ ±1.7, n=16 for vesicomyids). The same relationship and $\delta^{13}C$ values were found for the younger subfossil samples. However, for the Krishna-Godavari Basin specimens intra-crystalline SBOM ($\delta^{13}C$ -29.4 ±1.2, n=4) are similar to the modern values, but have a similar range to total SBOM $\delta^{13}C$ values of the same specimens.

If the total SBOM ^{12}C enrichment of the Krishna-Godavari vesicomyids would be the result of very enriched $\delta^{13}C$ DIC, it is considered unlikely that this would not affect the intra-crystalline fraction. Moreover, the Krishna-Godavari shell carbonate $\delta^{13}C$ values ($\delta^{13}C$ -0.2‰ ±1.3, n=5) are similar to modern species and do not support

extremely enriched local DIC $\delta^{13}C$ values. This suggests a diagenetic ^{13}C enrichment of total SBOM, that is not present in the intra-crystalline fraction. This is in agreement with the expected superior preservation of intra-crystalline SBOM, that is present in a closed system and therefore not subjected to the wide range of diagenetic pathways that can affect inter-crystalline SBOM (Penkman et al., 2008). AAR confirmed the presence of original organics in the intra-crystalline SBOM of both *L. chuni* (Congo Fan) and Vesicomyidae sp. (Krishna-Godavari Basin), and therefore the presence of an original isotopic signal.

The suggested ^{13}C enrichment of total SBOM could be the result of contamination from the surrounding sediment or nearby organisms (with enriched $\delta^{13}C$ values), or the non-random loss of ^{13}C depleted compounds during post-mortem processes. The decrease in elemental nitrogen concentration (Fig. 4.23) confirms the interaction of total SBOM with the external environment.

In addition to Vesicomyidae sp. from the Krishna-Godavari Basin, *Bathymodiolus* sp. specimens from the same locality were analysed. These specimens are suspected of having relied on one of multiple types of symbiosis: thiotrophy, dual symbiosis or methanotrophy. The samples have a mean total SBOM value of $\delta^{13}C$ -30.7‰ ±2.7 (n=5), which is in agreement with a thiotrophic lifestyle, and contains several $\delta^{13}C$ values that are considerably depleted compared to the Vesicomyidae specimens (up to -34‰). Shell carbonate values of *Bathymodiolus* are considerably depleted ($\delta^{13}C$ -5.6‰ ±3.7, n=3) compared to modern thiotrophic bivalves ($\delta^{13}C$ -0.2‰ ±1.3, n=22) and this range of light values is very similar to that of modern methanotrophic *B. childressi* ($\delta^{13}C$ 5.7‰ ±2.4, n=7, Chapter 2). In Chapter 2 it was shown that all shell carbonate $\delta^{13}C$ values below -2‰ are associated with the incorporation of depleted methane via nutrition, and are not related to $\delta^{13}C$ depleted DIC derived from methane oxidation (Chapter 2), which is also confirmed by the shell carbonate data from the Vesicomyidae of this locality ($\delta^{13}C$ -0.2‰ ±1.3,n=5).

If the shell carbonate $\delta^{13}C$ values are taken as evidence of a methanotrophic/dual symbiotic lifestyle, total SBOM is expected to originally have been more ^{13}C depleted, as has been observed for modern species (total SBOM: δ13C -53.5‰ ±7.9, n=18). This diagenetic alteration is in agreement with the suggested diagenetic ^{12}C enrichment of Vesicomyidae sp. from the same locality, as well as several ‘residual’ more depleted $\delta^{13}C$ SBOM values outside the range of Vesicomyidae values.

Alternatively, instead of incorporation of depleted carbon via nutrition, ^{13}C depleted values can result from incorporation of environmental methane into the shell (after death). This explanation is supported by a very depleted outlier value of $\delta^{13}C$ -11.8‰ amongst the specimens from the Hikurangi margin, with the other specimens reporting a value of $\delta^{13}C$ 1.0‰ ±1.2 (n=3). In addition to our own modern dataset, no negative values are present in the overview of Rio et al., (1992), and in an extensive shell carbonate study of seep specimens by Lietard & Pierre (2009) only one very negative value is reported for a lucinid specimen ($\delta^{13}C$ -10.2‰), whilst all other specimens are not more negative than ~ $\delta^{13}C$ -3‰, and vesicomyids in general below approximately $\delta^{13}C$ -1‰. Therefore, the common occurrence of very negative shell carbonate $\delta^{13}C$ in (sub)fossil shells suggests a diagenetic effect. This possibility was previously investigated by Paull et al. (2008), and could be caused by the deposition of authigenic calcite derived from methane deposited on shell surfaces. This leads to the conclusion that the use of shell carbonate for the identification of methanotrophy can become compromised even for geologically young fossil specimens.

Sulphur. Very indicative of thiotrophy are depleted sulphur values, usually inferred from soft tissues below $\delta^{34}S$ 5‰, and this was also confirmed for total SBOM (Chapter 3). All subfossil species analysed in this study have values depleted beyond this threshold, and are generally negative. This includes total SBOM $\delta^{34}S$ values of *Bathymodiolus* sp. ($\delta^{34}S$ -8.7‰ / -12.7 for resin), that appear to confirm thiotrophy. However, Dreier et al. (2012) showed that SBOM of empty and subfossil shells in shallow reducing environments can become very strongly depleted in $\delta^{34}S$, even for heterotrophic specimens (up to $\delta^{34}S$ -30.8‰, Dreier et al., 2012; Dreier et al., 2014). Whilst nitrogen and carbon can have multiple macromolecular sources, sulphur is only present in two out of the 20 common amino acids: cysteine and methionine. The ^{32}S decrease in subfossil SBOM samples was attributed to instability of the sulphur-containing amino acids (Dreier et al., 2012). Additional sulphur from the surrounding environment could also cause a possible shift towards the sulphur isotope ratio of the burial environment, and no longer represent the original isotope signal (Nehlich and Richards, 2009).

Nitrogen. Chemosymbiotic bivalves primarily utilize inorganic nitrogen sources, but the exact sources, their $\delta^{15}N$ values, and the extent of fractionation during incorporation by the host/symbionts are poorly understood (Chapter 3). The $\delta^{15}N$ values of modern thiotrophic species generally fall between -5‰ to 10‰ for total SBOM, and the obtained $\delta^{15}N$ values from subfossil specimens in this study fall within that range (Figure 4.21), and are thus in agreement with thiotrophic

chemosymbiosis as a nutritional strategy. However, the elemental nitrogen concentration of these subfossil samples shows a ~50% decrease between modern/young subfossil localities and the samples from the Krishna-Godavari Basin. This decrease over time indicates interaction of total SBOM with the external environment, and the apparent loss of organic material. Nitrogen within SBOM is primarily present within protein, and the elemental concentration of nitrogen can therefore act as a proxy for protein yield. Proteins are thought to degrade preferentially and are therefore commonly used as an indicator of diagenesis. $\delta^{15}N$ values of SBOM could be strongly influenced by the effects of hydrolysis which, together with racemisation, are the main chemical reactions occurring during early diagenesis. During hydrolysis the peptide bonds of proteins are broken, and therefore ultimately converted into a mixture of only free amino acids. These smaller molecules are more readily leachable from the shell (Mitterer, 1993).

It is possible that leaching (without contamination) would not strongly affect the isotopic nitrogen value of SBOM, because nitrogen in animal protein is supplied almost entirely by dietary proteins and most proteins have similar $\delta^{15}N$ values (Koch et al., 2007). The %N for intra-crystalline SBOM from Krishna-Godavari Basin overlaps with the range of modern values, and suggests limited leaching of amino acids.

Discussion summary. The discussed data from the three subfossil localities suggests that total SBOM of ancient shells of a certain geological age (between 2ka and 40ka years BP) comes into contact with the external environment, causing leaching of amino acids and likely incorporation of extraneous compounds. Dreier et al (2012) have suggested that gradual degradation and transformation could be caused by heterotrophic microbial composers, which would be in agreement with the observed ^{13}C enrichment. The diagenetic alteration of total SBOM could not be inferred from SEM/CL analyses, that showed that the large majority of the shell material is original and unaltered. The pyrolysis GC/MS analysis of Vesicomyidae sp. from the Krishna-Godavari Basin also generally reflects the chemical composition of the modern vesicomyid, although the much lower concentration of alkyl lipids could be indicative of the diagenetic changes.

The nutritional strategy of *Bathymodiolus* sp. from Krishna-Godavari remains unresolved, but there are strong indications for the presence of methanotrophic symbionts, which could be confirmed using stable isotope analysis of intra-crystalline SBOM.

Comparison to published data. The stable isotope data from subfossil localities obtained in this study can be directly compared to total SBOM stable isotope values obtained from Vesicomyidae samples (*Phreagena* s.l. and *Isorropodon* sp.) from Vestanesa Ridge and Western Svalbard, dated to 17,500 years B.P (Ambrose et al., 2015). Firstly it was noted that several depleted shell carbonate values are reported, the most depleted value being $\delta^{13}C$ -13.2‰ (*Isorropodon*). Carbon values of total SBOM range from: *Phreagena* -28.6‰ to -21.3‰; and *Isorropodon* from -29.3‰ to -25.6‰. The lowest $\delta^{13}C$ SBOM values are in agreement with our observations about carbon enrichment of total SBOM for the Krishna-Godavari Basin, but the most enriched values of these ranges are unexpected – and suggest either very poor preservation of these specimens, or higher contribution of filter-feeding on $\delta^{13}C$ enriched particulate organic matter.

Additional total SBOM values of subfossil suspected thiotrophic species were obtained for species from shallow environments by Dreier et al. (2012), no exact age is given. The strongly depleted $\delta^{34}S$ values of total SBOM for a heterotrophic specimen were discussed above, the $\delta^{15}N$ value of this specimen (+5.5‰) shows that depleted nitrogen values are not necessarily indicative of chemosymbiosis. The subfossil carbon data obtained by Dreier et al. (2012, thiotrophic *Loripes lacteus*: -27.8‰ / heterotrophic *Venerupis* sp.: -24.1‰) cannot be directly compared to our data, because in modern thiotrophs from shallow-reducing environments are > +5‰ enriched compared to those from cold seep settings. Interestingly, Dreier et al (2012) observed a depletion in $\delta^{13}C$ values after death for both nutritional strategies: around -3‰ for *Loripes lacteus*, and -5‰ for *Venerupis*, and $\delta^{13}C$ total SBOM values for these specimens are therefore moving towards the carbon values observed in our specimens. This suggests the non-random leaching of compounds obtained from dietary compounds (with $\delta^{13}C$ values characteristic of the nutritional strategies), or the incorporation of a similar contaminant source.

4.4.2 Pleistocene and Pliocene localities

In shell samples of Pleistocene age and older, the isolated SBOM morphologically changes from voluminous/openly structured and a variety of colours (related to shell colour), to dark brown compressed material. A similar transition was noted by Dreier et al (2014).

Carbon. The observations made about total SBOM ^{13}C enrichment of subfossil thiotrophic specimens, are also seen in geologically older specimens: as the upper $\delta^{13}C$ boundary for suspected thiotrophy is extended to $\delta^{13}C$ -24.9‰ and, moreover,

the range of heterotrophic specimens spans from -23.8‰ to -28.5‰. In modern heterotrophic (non-seep) $\delta^{13}C$ total SBOM values are -20.4‰ ±2.4 (n=31, species=3, Chapter 2). The ^{13}C depletion of heterotrophic specimens is argued to be caused by a similar contaminant source. The overlap in $\delta^{13}C$ total SBOM values between heterotrophic and thiotrophic samples means that thiotrophy can only be confirmed for specimens with total SBOM $\delta^{13}C$ values more depleted than -29‰ (as indicated in the graph). This diagenetic effect on total SBOM $\delta^{13}C$ is in agreement with a continued decrease in elemental nitrogen concentration of total SBOM (Fig. 4.23). This figure also shows that for this time period, intra-crystalline SBOM %N can be higher than the %N of total SBOM (in modern specimens this is very clearly not the case), and is similar to the Krishna-Godavari Basin specimens.

The suggested superior preservation of intra-crystalline SBOM is confirmed by the $\delta^{13}C$ values of that SBOM pool, showing a very clear distinction between thiotrophy (-31.0‰ to -27.0‰, n=13) and heterotrophy (-19.6‰, n=1) in the limited data available. This shows that nutritional strategies can potentially still be differentiated using intra-crystalline stable isotope values.

For specimens of this time period it was noted that data from the oldest locality, the upper Pliocene Shiramaza Formation, extended the upper range from $\delta^{13}C$ -26.3‰ for total SBOM from to -24.9‰, and from $\delta^{13}C$ -27.7‰ for intra-crystalline SBOM to $\delta^{13}C$ -27.0‰. The vesicomyid specimens from that locality showed strong variation in their preservational state using SEM/CL, which is in accordance with the variety of $\delta^{13}C$ total SBOM values obtained ($\delta^{13}C$ -30.3‰ to -24.9‰, n=9) (although no obvious correlation between the SEM results and isotopic values exists).

The heterotrophic total SBOM range was extended upwards from $\delta^{13}C$ -25.5‰ to -23.8‰, when including brachiopods, because the range of brachiopod total SBOM values ($\delta^{13}C$ -26.1‰ to -23.8‰) being generally enriched compared to other heterotrophic species. This difference could be caused by the increased preservation potential of calcitic shells.

The shell carbonate values for suspected thiotrophic specimens can be extremely depleted ($\delta^{13}C$ -27.8‰ to 1.3‰, n=20) compared to suspected heterotrophs ($\delta^{13}C$ -0.5‰ to 2.1‰, n=11) and we attribute this depletion due to the presence of the shells at methane seep localities, instead of reflecting $\delta^{13}C$ depleted metabolic carbon indicative of a chemosymbiotic lifestyle. Fig. 4.22 shows that the ranges of shell carbonate values of the two nutritional strategies largely overlap, which was also observed for the modern data in Chapter 2.

Sulphur. As discussed above, diagenesis can cause significant ^{32}S depletion of total SBOM, and is suggested to cause the total SBOM $\delta^{34}S$ range of suspected heterotrophs (δ34S -10.0‰ to 1.1‰, n=6) to overlap, or even to become more the depleted, than for suspected thiotrophs (δ34S -8.2‰ to 3.6‰, n=5). This difference cannot be explained by changing baseline $\delta^{34}S$ values of nutritional sulphate, that is incorporated indirectly from photosynthetically derived organic matter, since $\delta^{34}S$ values have not been below +10‰ in any time during Earth history (Gill et al., 2007). Sulphur values for intra-crystalline values are limited, but show a significantly more positive value for a heterotrophic specimen (δ34S 7.6‰) than thiotrophic specimens (δ34S -5.0‰ to 2.5‰, n=4). This is in agreement with the presence of original compounds in the intra-crystalline SBOM pool.

Nitrogen. The total SBOM nitrogen range of heterotrophic values ($\delta^{15}N$ 2.1‰ to 6.5‰, n=4) completely overlaps with the values obtained for suspected thiotrophs ($\delta^{15}N$ -11.1‰ to 8.4‰). It should be noted that in our modern dataset, negative nitrogen values are relatively rare for thiotrophic specimens, and the observed $\delta^{15}N$ values could indicate contamination of a terrestrial source, that are commonly depleted in ^{15}N (cf. O'Donnell, 2003). Similar to carbon and sulphur values, the intra-crystalline SBOM does show a clear distinction between positive heterotrophic values ($\delta^{15}N$ 6.5‰) and thiotrophic specimens ($\delta^{15}N$ -0.5‰ to 1.7‰, n=3). Although the data for nitrogen and sulphur are limited, these results are in agreement with the AAR results for *L. aokii* (Middle Pleistocene), *L. spectabilis* and Terebratulidae (Early Pleistocene), and *Calyptogena* sp. (Upper Pliocene) showing that original proteins are present in the intra-crystalline SBOM. This confirms that the isotopic diagenesis of total SBOM is caused by external contamination or leaching of the original SBOM, instead of chemical transformation of the SBOM itself.

Comparison to published data. Interestingly, Dreier et al. (2014) could not obtain sufficient SBOM from a Pleistocene *Tridacna maxima* specimen for isotope analysis. Whilst the amount of shell powder from which SBOM was isolated (8-12 grams) was around 5x times more than the amount used in our methodology, which made it possible to at least obtain carbon values for all samples.

Stable isotopic SBOM values where obtained by Mae et al. (2007) for a Pliocene vesicomyid specimen, the values of $\delta^{13}C$ -28.5‰ and $\delta^{15}N$ -1.4‰ are in agreement with our data and interpretations for ^{13}C enrichment and ^{15}N depletion due to contamination. O'Donnell et al. (2003) analysed total SBOM from heterotrophic *Mercenaria mercenaria* from the Holocene to the Mid-Pleistocene at multiple

localities: $\delta^{13}C$ -27.5‰ to -13.1‰, and $\delta^{15}N$ +2.4‰ to +9.8‰. Although this wide range of values was attributed to changes in diet sources by authors, the very depleted values for both isotopic elements are likely the result of a strong diagenetic influences. Particularly because modern SBOM from adult *M. mercenaria* had stable isotope values of $\delta^{13}C$ -18.4‰ to -14.8‰, and $\delta^{15}N$ of +10.3‰ to +12.4‰ (and one outlier of 0.5‰). The more enriched stable isotope values could therefore retain a mostly original isotopic signal of total SBOM.

4.4.3 Miocene to Oligocene

For this time period the diagenetic influence on the isotopic signal of SBOM becomes strong enough to also affect intra-crystalline SBOM, in at least some of the specimens. AAR shows that the intra-crystalline SBOM is not original for Miocene *Liothyrella* sp. and *Lucinoma* sp. (Moonlight North) and *Lucinoma* sp. from the Oligocene (Lincoln Creek). The poor preservation of the Lincoln Creek lucinid was confirmed with SEM/CL, and other preservational issues for this locality were noted in the results section. However, *Liothyrella* sp. was interpreted to be reasonably well preserved and showing original shell structure. It should also be noted that other Miocene specimens showed very well preserved microstructures, such as specimens from the Izura seep. For *Calyptogena* specimens from Hokkaido no relationship between the preservation of the shell material and $\delta^{13}C$ total SBOM values was found.

The lowest $\delta^{13}C$ values for suspected thiotrophic specimens continue to become enriched, particularly for intra-crystalline values ($\delta^{13}C$ -29.2‰ to -28.4‰), which is agreement with the discussed AAR data. Because the mytilid specimens can potentially have chemosymbiotic strategies other than thiotrophy, they are shown separately in Fig. 4.21. Whilst the values from *G. coseli* ($\delta^{13}C$ -26.2‰) and the modiolid ($\delta^{13}C$ -28.6‰) from Lincoln Creek, fall within the range of fossil thiotrophic total SBOM values ($\delta^{13}C$ -29.2‰ to -25.6‰, n=26), the *B. heretaunga* specimens fall outside of this range ($\delta^{13}C$ -31.1‰ and -29.5‰). An interpretation of these values is hampered by the fact that it is unknown how the more depleted carbon total SBOM signatures of dual symbiosis and methanotrophy would be preserved. The potentially original shell carbonate values of $\delta^{13}C$ -3.5‰ and -3.3‰ in agreement with a methanotrophic or dual symbiotic lifestyle (Chapter 2). The very depleted nitrogen value (-9.6‰) would also be indicative of a methanotrophic/dual symbiotic lifestyle, if original. Due to limited data, no further isotopic differences in (intra-crystalline) SBOM can be identified between different nutritional strategies.

Similar to the other time periods, the shells presented at cold seeps have a very depleted shell carbonate $\delta^{13}C$ range ($\delta^{13}C$ -27.4‰ to 1.4‰), compared to heterotrophic specimens ($\delta^{13}C$ -2.2‰ to 2.2‰).

Comparison to published data. Total SBOM obtained from a Miocene mytilid specimen suspected of chemosymbiosis (Mae et al., 2007), has a nitrogen value of $\delta^{15}N$ 4.2‰ that is comparable to our dataset, however the total SBOM carbon value of $\delta^{13}C$ -23.1‰ is more enriched than any of our specimens, particularly the mytilids. The enriched values reported for the Mid-Miocene heterotrophic gastropod genus *Ecphora* ($\delta^{13}C$ -16.7‰ ±1.3 / $\delta^{15}N$ 7.3‰ ±2.2, n=17) are surprisingly positive (Nance et al., 2015), and are thought to indicate very good preservation of these specimens, or may be caused by a contaminant source with more positive $\delta^{13}C$ and $\delta^{15}N$ values than those present at the localities investigated in this study.

4.4.4 Cretaceous

AAR analysis of a *N. occidentalis* sample confirmed the preservation of original intra-crystalline SBOM proteins. However, the range of total SBOM carbon values for suspected thiotrophic specimens has become even more limited, only ranging from $\delta^{13}C$ -27.2‰ to -26.0‰ (n=11) and is, moreover, similar to the range of intra-crystalline values $\delta^{13}C$ -27.3‰ to -26.2‰ (n=3). The heterotrophic specimens report both more depleted, and more enriched values for total SBOM (n=22) and intra-crystalline SBOM (n=9). Also the pyrolysis GC/MS data for *N. occidentalis* shows large difference in comparison to the modern and subfossil sample, confirming diagenetic alteration of total SBOM.

In addition, very depleted sulphur values are also present in the intra-crystalline SBOM fraction of suspected heterotrophic specimens ($\delta^{34}S$ -35.4‰ to -6.2‰, n=5). These very depleted $\delta^{34}S$ values could be related to negative $\delta^{34}S$ CAS values from this time period.

Calcite vs. aragonite. Within the heterotrophic isotope ranges, both the enriched carbon values ($\delta^{13}C$ -24.9‰ to -25.5‰, n=3) and the enriched nitrogen value ($\delta^{15}N$ 14.1‰) were obtained from *P. vesicularis* (Seymour Island), that has a calcitic shell. It is unclear if the enriched $\delta^{13}C$ total SBOM value of this species, as well as younger *Liothyrella* sp. discussed above, is inherent to calcite itself, or superior preservation of a heterotrophic nutritional signal. Potentially the presence of calcite in *Bathymodiolus* shells could then also contribute to better preservation.

Shell carbonate. Fig. 4.22 shows that both suspected thiotrophs and suspected heterotrophs can have $\delta^{13}C$ shell carbonate values lower than -2‰. The majority of negative $\delta^{13}C$ values are reported for heterotrophs living at cold seep localities, and suggest ^{13}C depletion due to the deposition of methane-derived authigenic calcite. The most depleted value of suspected heterotrophs ($\delta^{13}C$ -21.1‰) was obtained from a heteromorphy ammonite, this mobile animal could potentially have been present at cold seeps earlier in life. The difference in shell carbonate $\delta^{13}C$ values in relation to environmental settings is also confirmed by the difference in shell carbonate values of seep (-13.7 to ~0‰) and non-seep ammonites (-1.8 to 3.4‰) observed by Landman et al (2012), although they attribute this to the incorporation of methane into the shell during life, instead of post-mortem.

Inoceramus. The very limited range of SBOM $\delta^{13}C$ values between species with different suspected nutritional strategies (thiotrophic *N. occidentalis* and heterotrophic *Baculites* sp.) at Tepee Buttes suggests that the original isotopic signal has been completely replaced by contaminant sources, and unfortunately do not allow for the identification of a nutritional strategies in *Inoceramus* sp. The ^{13}C enriched shell carbonate values of Tepee Buttes *Inoceramus* (1.6‰ ±1.4, n=3) compared to negative values of *Baculites* sp. (n=3; -3.2 ±1.8) and *N. occidentalis* (-1.4‰ ±0.8, n=3) have previously been attributed to a chemosymbiotic lifestyle (MacLeod and Hoppe, 1992), because of the potential ^{13}C enrichment of modern shell carbonate related to the activity of thiotrophic bacteria (Rio et al., 1992). In Chapter 3 it was also shown that the majority of thiotrophic and dual symbiotic bivalves are ~+2‰ enriched compared to calculated shell carbonate $\delta^{13}C$ values, which could be attributed to the preferential uptake of ^{12}C by the thiotrophic bacteria. However, the $\delta^{13}C$ values of the other two taxa are not in agreement with a heterotrophic lifestyle, but instead suggest ^{13}C depleted original soft tissue/SBOM values. This difference could not be attributed to mineralogical differences, because the presence of calcite in combination with aragonite in *Inoceramus* should cause a depletion compared to the completely aragonitic shells of the other two taxa (Immenhauser et al., 2016 and refs within). The most likely explanation therefore is that post-mortem methane incorporation has a greater effect on the $\delta^{13}C$ values of *N. occidentalis* and even more on very thin-shelled *Baculites* sp., compared to the very thick and layered shell structure of *Inoceramus*.

Comparison to other data. Ullmann et al., (2014) bases conclusions about changing seawater chemistry on total SBOM $\delta^{13}C$ values of Early Toarcian belemnites. Based on the age of these samples, and the range of the carbon values (-30‰ to -25‰), this data is unlikely to represent an original isotopic signal, and

more likely reflects changing $\delta^{13}C$ values of sedimentary organics or other contaminant. In addition, compared to modern ranges the $\delta^{13}C$ values are not in agreement with heterotrophic nutrition.

4.4.6 Palaeozoic and Mesozoic seep brachiopods

In the AAR results section (4.3.1) it was discussed that the absence of amino acids in the Palaeozoic brachiopods (*Anarhyncha*, *Halorella* and *Dzieduszyckia crassicostata*) is the result of SBOM becoming a kerogen-like substance. This observation, the very high weight percent SBOM of these shells, as well as a very low elemental nitrogen/sulphur concentrations, suggest that contaminants are incorporated into this kerogen-like substance, and the majority of original protein has been removed from the shell. The variation between the different species/localities in total SBOM $\delta^{13}C$ (-27.9‰ to -23.9‰, n=5), $\delta^{15}N$ (-12.0‰ to 10.7‰), and $\delta^{34}S$ (-4.2‰ to 3.8‰) is most likely the result of differences isotopic values of the contaminants at the various seep localities. The composition and type of kerogen depends on the nature of the biological input, the environment of deposition and the diagenetic pathway (De Leeuw and Largeau, 1993). The general absence of luminescence for the Palaeozoic brachiopod specimens can be explained by problems with CL imaging of calcite brachiopod shells, and published studies have shown that the chemical and isotopic composition of shell carbonate can be modified without the shell becoming luminescent (England et al., 2006 and references within).

4.4 Conclusions

Total SBOM stable isotope values are affected by contamination or leaching within several thousand years after death, and this diagenesis cannot be identified using SEM or CL imaging. However, a very encouraging outcome from this study is the retention of original isotopic signals from intra-crystalline SBOM for much longer periods of time. AAR analysis of the intra-crystalline fraction shows that this could be pristine at least up to the Cretaceous for well-preserved specimens.

The preservation of distinct isotopic signals within the intra-crystalline pool confirms that the isotopic changes to total SBOM are the result of diagenetic alteration, instead of changing baseline conditions related to environmental sources used by the different nutritional strategies.

Concerning shell carbonate $\delta^{13}C$ values, it is challenging to differentiate the environmental versus the nutritional signal from fossil seep specimens because of the apparent unpredictable post-mortem incorporation of methane.

Chapter 5
Summary and future work

In this thesis the isotopic value ($\delta^{13}C$, $\delta^{15}N$, $\delta^{34}S$) of shell-bound organic matter (SBOM) as a proxy for nutritional strategies was investigated, with the aim of reconstructing the evolution of chemosymbiosis through geological time. In particular, a distinction was made between the total SBOM of the shell, and the intra-crystalline SBOM pool that is protected within the mineral. Based on the information presented in the three manuscripts, the original research questions can be mostly answered.

- **Research question 1**: Is the stable isotopic composition of SBOM influenced by chemical extraction from shell carbonate? (Chapter 2)
- **Research question 2**: Does the stable isotopic composition of SBOM relate in a predictable way to that of soft tissues? (Chapter 2 and 3)
- **Research question 3**: Can different nutritional strategies be identified in SBOM (and soft tissues) by their distinct isotopic compositions? (Chapter 3)
- **Research question 4**: Are SBOM and its original stable isotopic composition preserved over geological time? (Chapter 4)

Research Question 1 and 2. Compared to soft tissues, the incorporation of nutritional sources into the isotopic signal of total SBOM is more complex. For total SBOM $\delta^{13}C$ and $\delta^{15}N$ this is evident from species-specific isotopic off-sets between SBOM and soft tissues, and an evolving relationship between soft tissues and total SBOM in general. Total SBOM $\delta^{34}S$ values are more unpredictable and appear to be strongly influenced by shell removal techniques, whereas the effects of SBOM isolation are generally small for $\delta^{13}C$ and $\delta^{15}N$. For intra-crystalline SBOM the link with nutritional sources is further complicated by a limited range of isotopic values ($\delta^{13}C$, $\delta^{15}N$) that is potentially related to compositional differences between the total and intra-crystalline SBOM pools, and their roles in the biomineralisation process.

Research Question 3. Despite these complications, distinct isotopic total SBOM and intra-crystalline SBOM ranges exist for different nutritional strategies (methanotrophy, dual symbiosis, thiotrophy, and heterotrophy), that can hypothetically be used as thresholds to identify nutrition in ancient shells.

Research Question 4. Subsequent SBOM analysis of ancient shells, including suspected thiotrophs and suspected heterotrophs, showed that the original isotopic signal of SBOM disappears or becomes altered within several thousand years after

death. It is however conclusively shown that intra-crystalline SBOM retains its original signal much longer, and can likely be used to differentiate nutritional strategies up to the Cretaceous and possible in older well-preserved specimens.

Future work

Because the main focus of this project was the analysis of total SBOM, the number of analyses of intra-crystalline SBOM from fossil specimens was relatively limited. Future stable isotope analysis of this protected SBOM pool has the potential to trace the occurrence of chemosymbiosis deep into geological time. In particular the study of intra-crystalline SBOM of ancient *Bathymodiolus* taxa can provide valuable insights into the evolution of the different chemosymbiotic strategies, as modern species can harbour multiple types of bacteria. Because lipids are present within intra-crystalline SBOM, it is potentially also possible to do compound-specific $\delta^{13}C$ analysis of lipids that more closely track the $\delta^{13}C$ of nutritional sources/soft tissues, that appear to only have a limited contribution to the bulk $\delta^{13}C$ signal.

In addition, further development of radiocarbon analysis would be an interesting avenue to pursue. Although it was not possible to obtain positive results for total SBOM test materials (isolated using cation exchange resin) in this study, the methodology can be improved by using intra-crystalline SBOM, and a shorter SBOM isolation time using acidification to limit modern ^{14}C contamination. As suggested, radiocarbon analysis can potentially be used to identify the presence of methanotrophic symbionts due to the incorporation of ^{14}C dead methane into the (intra-crystalline) SBOM. This would however be limited to samples younger than 50ka. Similarly, study of ancient DNA in the intra-crystalline SBOM would be possible on samples of this age.

The long-term preservation of intra-crystalline SBOM also provides opportunities to look for biomarkers of chemosymbiosis. In the gills of modern chemosymbiotic bivalves unique compounds have been identified that can unambiguously be assigned to methanotrophic symbionts (Jahnke et al., 1995), and potentially these also exist for thiotrophic symbionts. However, whilst the presence of these biomarkers in the gills is expected, it is unknown whether they are incorporated into SBOM, and particularly intra-crystalline SBOM. It would therefore first have to be investigated whether biomarkers are present in the SBOM of modern specimens.

References

- Aharon, P., E. R. Graber, and H.H. Roberts. 1991. Detection of hydrocarbon venting on the Gulf of Mexico sea floor from determinations of dissolved inorganic carbon and ^{13}C of the water column overlying seeps. *Gulf Coast Association of Geological Societies Transactions* 41: 2-9.

- Aharon, P., and B. Fu. 2003. Sulfur and oxygen isotopes of coeval sulfate–sulfide in pore fluids of cold seep sediments with sharp redox gradients. *Chemical Geology* 195: 201-218.

- Albeck, S., L. Addadi, and S. Weiner. 1996. Regulation of calcite crystal morphology by intracrystalline acidic proteins and glycoproteins. *Connective tissue research* 35: 365-370.

- Allmon, W.D. 1988. Ecology of recent turritelline gastropods (Prosobranchia, Turritellidae): current knowledge and paleontological implications. *Palaios* 3: 259–284.

- Allmon, W.D. 2011. Natural history of turritelline Gastropods (Cerithiodea: Turritellidae): a status report. *Malacologia* 54: 159-202.

- Aloisi, G., K. Wallmann, S.M. Bollwerk, A. Derkachev, G. Bohrmann, and E. Suess. 2004. The effect of dissolved barium on biogeochemical processes at cold seeps. *Geochimica et Cosmochimica Acta* 68: 1735-1748.

- Ambrose, W.G., G. Panieri, A. Schneider, A. Plaza-Faverola, M.L. Carroll, E.K.L. Astrom, W.L. Locke, and J. Carroll. 2015. Bivalve shell horizons in seafloor pockmarks of the last glacial-interglacial transition: a thousand years of methane emissions in the Arctic Ocean. *Geochemistry, Geophysics, Geosystems* 16: 4108-4129.

- Anderson, T.F., and M.A. Arthur. 1983. Stable isotopes of oxygen and carbon and their application to sedimentologic and paleoenvironmental problems. In: M.A. Arthur et al. (eds.), *Stable isotopes in sedimentary geology*, Society of Economic Paleontologists and Mineralogists Short Course Series 10: 1-15.

- Ava, F.A., and I. Kudo. 2010. Isotopic shifts with size, culture habitat, and enrichment between the diet and tissues of the Japanese scallop *Mizuhopecten yessoensis* (Jay, 1857). *Marine biology* 157: 2157-2167.

- Baker, D.M., C.J. Freeman, N. Knowlton, R.W. Thacker, K. Kim, and M.L. Fogel. 2015. Productivity links morphology, symbiont specificity and bleaching in the evolution of Caribbean octocoral symbioses. *The ISME journal: Multidisciplinary Journal of Microbial Ecology* 9: 2620-2629.

- Barbieri, R., G.G. Ori, B. Cavalazzi. 2004. A Silurian cold-seep ecosystem from the Middle Atlas, Morocco. *Palaios* 19: 527-542.

- Barbin, V. 2013. Application of cathodoluminescence microscopy to recent and past biological materials: a decade of progress. *Mineralogy and Petrology* 107: 353-362.

- Barry, J.P., K.R. Buck, R.K. Kochevar, D.C. Nelson, Y. Fujiwara, S.K. Goffredi, and J. Hashimoto. 2002. Methane-based symbiosis in a mussel, *Bathymodiolus platifrons*, from cold seeps in Sagami Bay, Japan. *Invertebrate Biology* 121: 47-54.

- Barry, J.P., P.J. Whaling, and R.K. Kochevar. 2007. Growth, production, and mortality of the chemosynthetic vesicomyid bivalve, *Calyptogena kilmeri* from cold seeps off central California. *Marine Ecology* 28: 169-182.

- Becker, E.L., R.W. Lee, S.A. Macko, B.M. Faure, and C.R. Fisher. 2010. Stable carbon and nitrogen isotope compositions of hydrocarbon-seep bivalves on the Gulf of Mexico lower continental slope. *Deep Sea Research Part II: Topical Studies in Oceanography* 57: 1957-1964.

- Beinart, R.A., A. Gartman, J.G. Sanders, G.W. Luthers, and P.R. Girguis. 2015. The uptake and excretion of partially oxidized sulfur expands the repertoire of energy resources metabolized by hydrothermal vent symbioses. *Proceedings of the Royal Society B* 282: 20142811.

- Beirne, E.C., A.D. Wanamaker, and S.C. Feindel. 2012. Experimental validation of environmental controls on the δ13C of *Arctica islandica* (ocean quahog) shell carbonate. *Geochimica et Cosmochimica Acta* 84: 395-409.

- Blumenberg, M. 2010. Microbial chemofossils in specific marine hydrothermal and cold methane cold seep settings. In*:* S. Kiel (ed.), *The Vent and Seep Biota Aspects from Microbes to Ecosystems*, Topics in Geobiology 33, Springer*,* Heidelberg, p. 73–106.

- Booth, D. 2014. Ecology of Australian Temperate Reefs. *Frontiers of Biogeography* 6.

- Bottrell, S.H., and R. Raiswell. 2000. Sulphur isotopes and microbial sulphur cycling in sediments. In: R.E. Riding and S.M. Awramik (eds.), *Microbial Sediments*, Springer, Berlin/Heidelberg, p. 96-104.

- Bouillon, J. 1958. Quelques observations sur la nature de la coquille chez les Mollusques. *Annales de la Société royale zoologique de Belgique* 89: 229-237.

- Bourgoin, B.P. 1988. A rapid and inexpensive technique to separate the calcite and nacreous layers in *Mytilus edulis* shells. *Marine environmental research* 25: 125-129.

- Boetius, A**.,** K. Ravenschlag, C. Schubert, D. Rickert, F. Widdel, A. Gieseke, R. Amann, B. B. Jørgensen, U. Witte, and O. Pfannkuche. 2000. A marine microbial consortium apparently mediating anaerobic oxidation of methane. *Nature* 207: 623-626.

- Bradley, A.S., W.D. Leavitt, M. Schmidt, A.H. Knoll, P.R. Girguis, and D.T. Johnston. 2016. Patterns of sulfur isotope fractionation during microbial sulfate reduction. *Geobiology*, 14: 91-101.

- Brooks, J.M., M.C. Kennicutt, R.R. Fay, T.J. McDonald, and R. Sassen. 1984. Thermogenic gas hydrates in the Gulf of Mexico. *Science* 226: 965-967.

- Campbell, K.A. 2006. Hydrocarbon seep and hydrothermal vent paleoenvironments and paleontology: past developments and future research directions. *Palaeogeography, Palaeoclimatology, Palaeoecology* 232: 362-407.

- Canfield, D.E. 2001. Isotope fractionation by natural populations of sulfate-reducing bacteria. *Geochimica et Cosmochimica Acta* 65: 1117-1124.

- Carabel, S., P. Verisimo, and J. Freire. 2009. Effects of preservatives on stable isotope analyses of four marine species. *Estuarine, Coastal and Shelf Science* 82: 348-350.

- Carmichael, R.H., T.K. Hattenruth, I. Valiela, and R.H. Michener. 2008. Nitrogen stable isotopes in the shell of *Mercenaria mercenaria* trace wastewater inputs from watersheds to estuarine ecosystems. *Aquatic Biology* 4: 99-111.

- Carney, R.S. 1994. Consideration of the oasis analogy for chemosynthetic communities at Gulf of Mexico hydrocarbon vents. *Geo-Marine Letters* 14: 149-159.

- Cavanaugh, C.M., C.O. Wirsen, and H.W. Jannasch. 1992. Evidence for methylotropic symbionts in a hydrothermal vent mussel (Bivalvia: Mytilidae) from the mid-Atlantic Ridge. *Applied Environmental Microbiology* 58: 3799–3803.

- Checa, A.G., F.J. Esteban-Delgado, and A.B. Rodríguez-Navarro. 2007. Crystallographic structure of the foliated calcite of bivalves. *Journal of structural biology* 157: 393-402.

- Childress, J.J., C.R. Fisher, J.M. Brooks, M.C. Kennicutt, R. Bidigare, and A. Anderson. 1986. A methanotrophic marine molluscan (Bivalvia, Mytilidae) symbiosis: Mussels fueled by gas. *Science* 233: 1306-1308.

- Childress, J.J., and P.R. Girguis. 2011. The metabolic demands of endosymbiotic chemoautotrophic metabolism on host physiological capacities. *Journal of Experimental Biology* 214: 312-325.

- Childress, J.J., and C.R. Fisher. 1992. The biology of hydrothermal vent animals: physiology, biochemistry, and autotrophic symbiosis. *Oceanography Marine Biology Annual Reviews* 30: 337-441.

- Clarkson, E. 2009. *Invertebrate palaeontology and evolution*. Blackwell Publishing, Oxford, United Kingdom.

- Cline, J.D., and I.R. Kaplan. 1975. Isotopic fractionation of dissolved nitrate during denitrification in the eastern tropical North Pacific Ocean. *Marine Chemistry* 3: 271-299.

- CoBabe, E.A., and L.M. Pratt. 1995. Molecular and isotopic compositions of lipids in bivalve shells: a new prospect for molecular paleontology. *Geochimica et Cosmochimica Acta* 59: 87-95.

- Colgan, D.J., W.F. Ponder, E. Beacham, and J. Macaranas. 2007. Molecular phylogenetics of Caenogastropoda (Gastropoda: Mollusca). *Molecular phylogenetics and evolution* 42: 717-737.

- Conway, N.M., M.C. Kennicutt, and C.L. Van Dover. 1994. Stable isotopes in the study of marine chemosynthethic based ecosystems. In: K.Lajtha and R.H. Michener (eds.), *Stable isotopes in Ecology and Environmental Sciences*, Blackwell Publishing, Oxford, p. 158-186.

- Cope, J.C.W. 1996. Early Ordovician (Arenig) bivalves from the Llangynog Inlier, South Wales*. Palaeontology* 39: 979-1025.

- Corliss, J.B., J. Dymond, L.I. Gordon, J.M. Edmond, R.P. von Herzen, R.D. Ballard, K. Green, D. Williams, A. Bainbridge, K. Crane, and T.H. van Andel. 1979. Submarine Thermal Springs on the Galápagos Rift. *Science* 203: 1073-1083.

- Craig, H. 1957. Isotopic standards for carbon and oxygen and correction factors for mass-spectrometric analysis of carbon dioxide. *Geochimica et cosmochimica acta* 12: 133-149.

- Crenshaw, M.A. 1972. The soluble matrix from *Mercenaria mercenaria* shell. *Biomineralization* 6: 6-11.

- Curry, G.B., M. Cusack, D. Walton, K. Endo, H. Clegg, G. Abbott, H. Armstrong, J.L. Bada, and M.H. Engel. 1991. Biogeochemistry of brachiopod intracrystalline molecules [and discussion]. *Philosophical Transactions of the Royal Society of London Series B: Biological Sciences* 333: 359-366.

- Dando, P.R., and A.J. Southward. 1986. Chemoautotrophy in bivalve molluscs of the genus *Thyasira*. *Journal of the Marine Biological Association of the United Kingdom* 66: 915-929.

- Dando, P.R. and B. Spiro. 1993. Varying nutritional dependence of the thyasirid bivalves *Thyasira sarsi* and *T. equalis* on chemoautotrophic symbiotic bacteria, demonstrated by isotope ratios of tissue carbon and shell carbonate. *Marine Ecology-Progress Series* 92: 151-158.

- Dattagupta, S., D.C. Bergquist, E.B. Szalai, S.A. Macko, and C.R. Fisher. 2004. Tissue carbon, nitrogen, and sulfur stable isotope turnover in transplanted *Bathymodiolus childressi* mussels: relation to growth and physiological condition. *Limnology and Oceanography* 49: 1144-1151.

- De Leeuw, J.W., and C. Largeau. 1993. A review of macromolecular organic compounds that comprise living organisms and their role in kerogen, coal, and petroleum formation. In: M.H. Engel and S.A. Macko (eds.), *Organic Geochemistry*, Plenum Publishing Group, New York, p. 23-72.

- Decker, C., K. Olu, S. Arnaud-Haond, and S. Duperron. 2013. Physical proximity may promote lateral acquisition of bacterial symbionts in vesicomyid clams. *PloS One* 8: e64830.

- DeLong, M.D, and J.H. Thorp. 2009. Mollusc shell periostracum as an alternative to tissue in isotopic studies. *Limnology and Oceanography: Methods* 7: 436-441.

- Demarchi, B., K. Rogers, D.A. Fa, C.J. Finlayson, N. Milener, and K.E.H. Penkman. 2013. Intra-crystalline protein diagenesis (IcPD) in *Patella vulgata*. Part I: Isolation and testing of the closed system. *Quaternary Geochronology* 16: 144-157.

- Demirbas, A. 2010. Methane hydrates as potential energy resource: Part 2 – Methane production processes from gas hydrates. *Energy Conversion and Management* 51: 1562-1571.

- Demopoulos, A.W., D. Gualtieri, and K. Kovacs. 2010. Food-web structure of seep sediment macrobenthos from the Gulf of Mexico. *Deep sea research part II: topical studies in oceanography* 57: 1972-1981.

- DeNiro, M.J., and S. Epstein. 1976. You are what you eat (plus a few ‰): the carbon isotope cycle in food chains. *Geological Society of America Abstracts with Programs* 8: 834-835.

- De Ronde, C.E.J., E.T. Baker, G.J. Massoth, J.E. Lupton, I.C. Wrigt, R.J. Sparks, S.C. Bannister, M.E. Reyners, S.L. Walker, R.R. Greene, and J. Ishibashi. 2007. Submarine hydrothermal activity along the mid-Kermadec arc, New Zealand: Large-scale effects on venting. *Geochemistry, Geophysics, Geosystems* 8: Q07007.

- Desbruyères, D., A.M. Alayse-Danet, and S. Ohta. 1994. Deep-sea hydrothermal communities in Southwestern Pacific back-arc basins (the North Fiji and Lau Basins): composition, microdistribution and food web. *Marine Geology* 116: 227-242.

- Dreier, A., L. Stannek, M. Blumenberg, M. Taviana, M. Sigovini, C. Wrede, V. Thiel, and M. Hoppert. 2012. The fingerprint of chemosymbiosis: origin and preservation of isotopic biosignatures in the nonseep bivalve *Loripes lacteus* compared with *Venerupis aurea*. *FEMS microbiology ecology* 81: 480-493.

- Dreier, A., W. Loh, M. Blumenberg, V. Thiel, D. Hause-Reitner, and M. Hoppert. 2014. The isotopic biosignatures of photo-vs. thiotrophic bivalves: are they preserved in fossil shells? *Geobiology* 12: 406-423.

- Dubilier, N., C. Bergin, and C. Lott. 2008. Symbiotic diversity in marine animals: the art of harnessing chemosynthesis. *Nature Reviews Microbiology* 6: 725-740.

- Dufour, S.C., and H. Felbeck. 2003. Sulphide mining by the superextensile foot of symbiotic thyasirid bivalves. *Nature* 46: 65-67.

- Dufour, S.C., and H. Felbeck. 2006. Symbiont abundance in thyasirids (Bivalvia) is related to particulate food and sulphide availability. *Marine Ecology Progress Series* 320: 185-194.

- Duperron, S. 2010. The diversity of deep-sea mussels and their bacterial symbioses*.* In*:* S. Kiel (ed.), *The Vent and Seep Biota Aspects from Microbes to Ecosystems*, Topics in Geobiology 33, Springer*,* Heidelberg, p. 137-167.

- Duperron S., M. Sibuet, B.J. MacGregor, M.M. Kuypers, C.R. Fisher, and N. Dubilier. 2007. Diversity, relative abundance and metabolic potential of bacterial endosymbionts in three *Bathymodiolus* mussel species from cold seeps in the Gulf of Mexico. *Environmental Microbiology* 9: 1423-1438.

- Duperron, S., A. Fiala-Medioni, J.C. Caprais, K. Olu, and M. Sibuet. 2007. Evidence for chemoautotrophic symbiosis in a Mediterranean cold seep clam (Bivalvia: Lucinidae): comparative sequence analysis of bacterial 16S rRNA, APS reductase and RubisCO genes. *FEMS microbiology ecology* 59: 64-70.

- Duperron, S., S.M. Gaudron, C.F. Rodrigues, M.R. Cunha, C. Decker, and K. Olu. 2013. An overview of chemosynthethic symbioses in bivalves from the North Atlantic and Mediterranean Sea. *Biogeosciences* 10, 3241-3267.

- Duplessis, M.R., S.C. Dufour, L.E. Blankenship, H. Felbeck, and A.A. Yayanos. 2004. Anatomical and experimental evidence for particulate feeding in *Lucinoma aequizonata* and *Parvilucina tenuisculpta* (Bivalvia: Lucinidae) from the Santa Barbara Basin. *Marine Biology* 145: 551-561.

- England, J. M. Cusack, N.W. Paterson, P. Edwards, M.R. Lee, and R. Marin. 2006. Hyperspectral cathodoluminescence imaging of modern and fossil carbonate shells. *Journal of Geophysical Research: Biogeosciences* 111: G3.

- Esteban-Delgado, F.J., E.M. Harper, A.G. CHeca, and A.B. Rodríguez-Navarro. 2008. Origin and expansion of foliated microstructure in pteriomorph bivalves. *The Biological Bulletin* 214: 153-165.

- Etiope, G., A. Feyzullayev, and C.L. Baciu. 2009. Terrestrial methane seeps and mud volcanoes: a global perspective of gas origin. *Marine and Petroleum Geology* 26: 333-344.

- Farre, B., and Y. Dauphin. Lipids from the nacreous and prismatic layers of two Pteriomorpha mollusc shells. 2009. *Comparative Biochemistry and Physiology Part B: Biochemistry and Molecular Biology* 152: 103-109.

- Felden, J. S.E. Ruff, T. Ertefai, F. Inagaki, K.U. Hinrichs, and F. Wenzhofer. 2014. Anaerobic methanotrophic community of a 5346-m-deep vesicomyid clam colony in the Japan Trench. *Geobiology* 12: 183-199.

- Feng, D., C. Doufo, and H.H. Roberts. 2009. Petrographic and geochemical characterization of seep carbonate from Bush Hill (GC 185) gas vent and hydrate site of the Gulf of Mexico. *Marine and Petroleum Geology* 26: 1190-1198.

- Feng, D., M. Cheng, S. Kiel, J.W. Qiu, Q. Yang, H. Zou, Y. Peng, and D. Chen. 2015. Using *Bathymodiolus* tissue stable carbon, nitrogen and sulfur isotopes to infer biogeochemical process at a cold seep in the South China Sea. *Deep Sea Research Part I: Oceanographic Research Papers* 104: 52-59.

- Feng, D., D. Chen, J. Peckmann, and G. Bohrmann. 2010. Authigenic carbonates from methane seeps of the northern Congo fan: microbial formation mechanism. *Marine and Petroleum Geology* 27: 748-756.

- Fertig, B., T.J.B. Carruthers, W.C. Dennison, E.J. Ferig, and M.A. Altabet. 2010. Eastern oyster (*Crassostrea virginica*) $\delta^{15}N$ as a bioindicator of nitrogen sources: observations and modelling. *Marine pollution bulletin* 60(8), 1288-1298.

- Fisher, C.R. 1990. Chemoautotrophic and methanotrophic symbioses in marine-invertebrates. *Reviews in Aquatic Sciences* 2: 399-436.

- Fisher, C.R. 1996. Ecophysiology of primary production at deep-sea vents and seeps. In: R. Uiblein, J. Ott, and M. Stachowtish (eds.), *Deep-sea and extreme shallow water habitats: affinities and adaptations*, Biosystematics and Ecology Series 11: 311-334.

- Fisher, D., H. Sahling, K. Nothen, G. Bohrmann, M. Zabel, and S. Kasten. 2012. Interaction between hydrocarbon seepage, chemosynthetic communities, and bottom water redox at cold seeps of the Makran accretionary prism: insights from habitat-specific pore water sampling and modeling. *Biogeosciences* 9: 2013–2031.

- Formolo, M.J., and T.W. Lyons. 2013. Sulfur biogeochemistry of cold seeps in the Green Canyon region of the Gulf of Mexico. *Geochimica et Cosmochimica Acta* 119: 264-285.

- Freeman, C.J., and R.W. Thacker. 2011. Complex interactions between marine sponges and their symbiotic microbial communities. *Limnology and Oceanography* 56: 1577-1586.

- Fry, B., and C. Arnold. 1982. Rapid $^{13}C/^{12}C$ turnover during growth of brown shrimp (*Penaeus aztecus*). *Oecologia* 54: 200-204.

- Fry, B., and E.B. Sherr. 1984. $\delta^{13}C$ measurements as indicators of carbon flow in marine and freshwater ecosystems. *Contributions in Marine Science* 27: 13-47.

- Geist, J. K. Auerswald, and A. Boom. 2005. Stable carbon isotopes in freshwater mussel shells: environmental record or marker for metabolic activity? *Geochim Cosmochim Acta* 69:3545–3554.

- Genio, L., S. Kiel, M.R. Cuhna, J. Grahame, and C.T. Little. 2012. Shell microstructures of mussels (Bivalvia: Mytilidae: Bathymodiolinae) from deep-sea chemosynthetic sites: Do they have a phylogenetic significance?. *Deep Sea Research Part I: Oceanographic Research Papers* 64: 86-103.

- Gilikin, D.P., A. Lorrain, S. Bouillon, P. Willenz, and F. Dehairs. 2006. Stable carbon isotopic composition of *Mytilus edulis* shells: relation to metabolism, salinity, $\delta^{13}C$ DIC and phytoplankton. *Organic Geochemistry* 37: 1371-1382.

- Gilikin, D.P., A. Lorrain, L. Meng, and F. Dehairs. 2007. A large metabolic carbon contribution to the δ 13 C record in marine aragonitic bivalve shells. *Geochimica et Cosmochimica Acta* 71: 2936-2946.

- Gill, B.C., T.W. Lyons, and M.R. Saltzman. 2007. Parallel, high-resolution carbon and sulfur isotope records of the evolving Paleozoic marine sulfur reservoir. *Palaeogeography, Palaeoclimatology, Palaeoecology* 256: 156-173.

- Goni, M.A., K.C. Ruttenberg, and T.I. Eglinton. 1998. A reassessment of the sources and importance of land-derived organic matter in surface sediments from the Gulf of Mexico. *Geochimica et Cosmochimica Acta* 62: 3055-3075.

- Goulletquer, P., and M. Wolowicz. 1989. The shell of *Cardium edule*, *Cardium glaucum* and *Ruditapes philippinarum*: organic content,

composition and energy value, as determined by different methods. *Journal of the Marine Biological Association of the United Kingdom* 69: 563-572.

- Gotliv. B.-A., L. Addadi, and S. Weiner. 2003. Mollusk shell acidic proteins: in search of individual functions. *ChemBioChem* 4: 522-529.

- Gunstone, F.D., and J.L. Harwood. 2007. Occurrence and characterization of oils and fats. In: F.D. Gunstone and A.J. Dijkstra (eds.), *The lipid handbook*, CRC Press, Boca Raton, p. 37-141.

- Gupta, N.S., and D.E.G. Briggs. 2011. Taphonomy of animal organic skeletons through time. In: P.A. Allison and David J. Bottjer (eds.), *Taphonomy Process and Bias Through Time*, Topics in Geobiology 32, Springer, Amsterdam, p. 199-221.

- Habicht, K.S., and D.E. Canfield. 2001. Isotope fractionation by sulfate-reducing natural populations and the isotopic composition of sulfide in marine sediments. *Geology* 29: 555-558.

- Hare, P.E., M.L. Fogel., T.W. Stafford, A.D. Mitchell, and T.C. Hoering. 1991. The isotopic composition of carbon and nitrogen in individual amino acids isolated from modern and fossil proteins. *Journal of Archaeological Science* 18: 277-292.

- Hashimoto, J., and T. Yamane. 2005. A new species of *Gigantidas* (Bivalvia: Mytilidae) from a vent site on the Kaikata Seamount southwest of the Ogasawara (Bonin) Islands, southern Japan. *Venus* 64: 1-10.

- Hentschel, U., S.C. Carey, and H. Felbeck. 1993. Nitrate respiration in chemoautotrophic symbionts of the bivalve *Lucinoma aequizonata*. *Marine Ecology Progress Series* 94: 35-41.

- Heyl, T.P, W.P. Gilhooly, R.M. Chambers, G.W. Gilchrist, S.A. Macko, C.D. Ruppel, and C.L. Van Dover. 2007. Characteristics of vesicomyid clams and their environment at the Blake Ridge cold seep, South Carolina, USA. *Marine Ecology Progress Series* 339: 169-184.

- Hill, R.L. 1965. Hydrolysis of proteins. *Advances in protein chemistry* 20: 37-107.

- Hill, J.M., and C.D. McQuaid. 2009. Effects of food quality on tissue-specific isotope ratios in the mussel *Perna perna*. *Hydrobiologia* 635: 81-94.

- Hobson, K.A., and H.E. Welch. 1992. Determination of trophic relationships within high arctic marine food web using $\delta^{13}C$ and $\delta^{15}N$ analysis. *Marine Ecology Progress Series* 84: 9-18.

- Hobson, K.A., M.L. GLoutney, and H. Lisle Gibbs. 1997. Preservation of blood and tissue samples for stable-carbon and stable-nitrogen isotope analysis. *Canadian Journal of Zoology* 75: 1720-1723.

- Hoefs, J. 2015. Isotope fractionation processes of selected elements. In: J. Hoefs (ed.), *Stable Isotope Geochemistry*. Springer International Publishing, Berlin/Heidelberg, p. 47-190.

- Holler, T., F. Widdel, K. Knittel, R. Amann, M.Y. Kellermann, K-U. Hinrichs, A. Teske, A. Boetius, and G. Wegener. 2011. Thermophilic anaerobic oxidation of methane by marine microbial consortia. *The ISME journal*: *Multidisciplinary Journal of Microbial Ecology* 5: 1946-1956.

- Hu, L., S.A. Yvon-Lewis, Y. Liu, J.E. Salisbury, and J.E. O'Hern. 2010. Coastal emissions of methyl bromide and methyl chloride along the eastern Gulf of Mexico and the east coast of the United States. *Global biogeochemical cycles* 24: GB1007.

- Hügler, M., and S.M. Sievert. 2011. Beyond the Calvin cycle: autotrophic carbon fixation in the ocean. *Marine Science* 3: 261-289.

- Hryniewicz, K., C.T.S. Little, and H.A. Nakrem. 2014. Bivalves from the latest Jurassic-earliest Cretaceous hydrocarbon seep carbonates from central Spitsbergen, Svalbard. *Zootaxa* 3859: 1-66.

- Immenhauser, A., B.R. Schöne, R. Hoffmann, and A. Niedermayr. 2016. Mollusc and brachiopod skeletal hard parts: Intricate archives of their marine environment. *Sedimentology* 63: 1-59.

- Jannasch, H.W., and M.J. Mottl. 1985. Geomicrobiology of deep-sea hydrothermal vents. *Science* 229: 717-725.

- Jim, S., V. Jones, S.H. Ambrose, and R.P. Evershed. 2006. Quantifying dietary macronutrient sources of carbon for bone collagen biosynthesis using natural abundance stable carbon isotope analysis. *British Journal of Nutrition* 95: 1055-1062.

- Jones, W.J., Y.J. Won, P.A.Y. Maas, P.J. Smith, R.A. Lutz, and R.C. Vrijenhoek. 2006. Evolution of habitat use by deep-sea mussels. *Marine Biology* 148: 841-851.

- Johnson, S.B., A. Warén, V. Tunnicliffe, C. Van Dover, C.G. What, T.F. Schultz, and R.C. Vrijenhoek. 2015. Molecular taxonomy and naming of five cryptic species of *Alviniconcha* snails (Gastropoda: Abyssochrysoidea) from hydrothermal vents. *Systematics and Biodiversity* 13: 278-295.

- Johnstone, M.B., N.V. Gohad, E.P. Falwell, D.C. Hansen, K.M. Hansen, and A.S. Mount. 2015. Cellular orchestrated biomineralization of crystalline composites on implant surfaces by the eastern oyster, *Crassostrea virginica*

(Gmelin, 1791). *Journal of Experimental Marine Biology and Ecology* 463: 8-16.

- Jope, M. 1967. The protein of brachiopod shell-II, shell protein from fossil articulates: amino acid composition. *Comparative Biochemistry and Physiology* 20: 601-605.

- Jorgensen, B.B., and J.R. Postgate. 1982. Ecology of the bacteria of the sulphur cycle with special reference to anoxic-oxic interface environments [and discussion]. *Philosophical Transactions of the Royal Society of London B: Biological Sciences* 298: 543-561.

- Joye, S.B., A. Boetius, B.N. Orcutt, J.P. Montoya, H.N. Schulz, M.J. Erickson, and S.K. Lugo. 2004. The anaerobic oxidation of methane and sulfate reduction in sediments from Gulf of Mexico cold seeps. *Chemical Geology* 205: 219-238.

- Joye, S.B., I.R. MacDonald, J.P. Montoya, and M. Peccini. 2010. Geophysical and geochemical signatures of Gulf of Mexico seafloor brines. *Biogeosciences* 2: 295-309.

- Kaehler, S., and E.A. Pakhomov. 2001. Effects of storage and preservation on the $\delta^{13}C$ and $\delta^{15}N$ signatures of selected marine organisms. *Marine Ecology Progress Series* 219: 299-304.

- Kamenev, G.M., V.A. Nadtochy, and A.P. Kuznetsov. 2001. *Conchocele bisecta* (Conrad, 1849) (Bivalvia: Thyasiridae) from cold-water methane-rich areas of the Sea of Okhotsk. *The Veliger* 44: 84-94.

- Kampschulte, A., and H. Strauss. The sulfur isotopic evolution of Phanerozoic sweater based on the analysis of structurally substituted sulfate in carbonates. *Chemical Geology* 204: 255-286.

- Kaufman, D.S., and W.F. Manely. 1998. A new procedure for determining DL amino acid ratios in fossils using reverse phase liquid chromatography. *Quaternary Science Reviews* 17: 987-1000.

- Kaufmann, E.G., M.A. Arthur, B. Howe, and P.A. Scholle. 1996. Widespread venting of methane-rich fluids in Late Cretaceous (Campanian) submarine springs (Tepee Buttes), Western Interior seaway, USA. *Geology* 24: 799-802.

- Kennicutt, M.C., R.A. Burke, I.R. MacDonald, J.M. Brooks, G.J. Denoux, and S.A. Macko. 1992. Stable isotope partitioning in seep and vent organisms: chemical and ecological significance. *Chemical Geology: Isotope Geoscience section* 101: 293-310.

- Kennish, M.J., R.A. Lutz, and A.S. Tan. 1998. Deep-sea vesicomyid clams from hydrothermal vent and cold seep environments: analysis of shell microstructure. *The Veliger* 41: 195–200.

- Kiel, S., and J.L. Goedert. 2006. A wood-fall association from Late Eocene deep-water sediments of Washington State, USA. *Palaios* 21: 548-556.

- Kiel, S. 2010. The fossil record of vent and seep mollusks. In*:* S. Kiel (ed.), *The Vent and Seep Biota Aspects from Microbes to Ecosystems*, Topics in Geobiology 33, Springer*,* Heidelberg, p. 255-277.

- Kiel, S., and K. Amano. 2013. The earliest bathymodiolin mussels: an evaluation of Eocene and Oligocene taxa from deep-sea methane seep deposits in western Washington State, USA. *Journal of Paleontology* 87: 589-602.

- Knight, R.I., N.J. Morris, J.A. Todd, L.E. Howards, and A.D. Ball. 2014. Exceptional preservation of a novel gill grade in large Cretaceous inoceramids: systematic and palaeobiological implications. *Palaeontology* 57: 37-54.

- Knittel, K., and A. Boetius. 2009. Anaerobic oxidation of methane: progress with an unknown process. *Annual review of microbiology* 63: 311-334.

- Koch, P.L. 2007. Isotopic study of the biology of modern and fossil vertebrates. *Stable isotopes in ecology and environmental science* 2: 99-154.

- Kovacs, C.J., J.H. Daskin, H. Patterson, and R.H. Carmichael. 2010. *Crassostrea virginica* shells record local variation in wastewater inputs to a coastal estuary. *Aquatic Biology* 9, 77-84.

- Krylova, E.M., and H. Sahling. 2010. Vesicomyidae (Bivalvia): current taxonomy and distribution. *PLoS One* 5: e9957.

- Landman, N.H., J.K. Cochran, N.L. Larson, J. Brezina, M.P. Garb, and P.J. Harries. 2012. Methane seeps as ammonite habitats in the US Western Interior Seaway revealed by isotopic analyses of well-preserved shell material. *Geology* 40: 507-510.

- Lartaud, F., M. de Rafelis, G. Oliver, E. Krylova, J. Dyment, B. Ildefonse, R. Thibaud, P. Gente, E. Hoise, A.L. Meisterzheim, and Y. Fouquet. 2010. Fossil clams from a serpentinite-hosted sedimented vent field near the active smoker complex Rainbow, MAR, 36° 13′ N: Insight into the biogeography of vent fauna. *Geochemistry, Geophysics, Geosystems* 11: Q0AE01.

- LeBlanc, C. 1989. Terrestrial input to estuarine bivalves as measured by multiple stable isotope tracers, Ph.D. Thesis, McMaster University, Ontario.

- Le Bris, N., and S. Dupperon. 2010. Chemosynthethic communities and biogeochemical energy pathways along the Mid-Atlantic Ridge: The case of

Bathymodiolus azoricus. *Diversity of Hydrothermal Systems on Slow Spreading Ocean Ridges*: 409-429.

- Lecuyer, C. A. Hutzler, R. Amoit, V. Dauz, D. Grosheny, O. Otero, F. Martineau, F. Fourel, V. Balter, and B. Reynard. 2012. Carbon and oxygen isotope fractionations between aragonite and calcite of shells from modern molluscs. *Chemical geology* 332: 92-101.

- Lee, R.W., E.V. Thuesen, and J. J. Childress. 1992. Ammonium and free amino acids as nitrogen sources for the chemoautotrophic symbiosis *Solemya reidi* Bernard (Bivalvia: Protobranchia). *Journal of Experimental Marine Biology and Ecology* 158: 75-91.

- Lee, R.W., and J.J. Childress. 1994. Assimilation of inorganic nitrogen by marine invertebrates and their chemoautotrophic and methanotrophic symbionts. *Applied and Environmental Microbiology* 60: 1852-1858.

- Lee, R.W., J.J. Robinson, and C.M. Cavanaugh. 1999. Pathways of inorganic nitrogen assimilation in chemoautotrophic bacteria-marine invertebrate symbioses: expression of host and symbiont glutamine synthetase. *Journal of Experimental Biology* 202: 289-300.

- Liao, Z., L.F. Bao, M.H. Fan, P. Gao, X.X. Wang, C.L. Qin, and X.M. Li. 2015. In-depth proteomic analysis of nacre, prism, and myostracum of *Mytilus* shell. *Journal of proteomics* 122: 26-40.

- Lietard, C., and C. Pierre. 2009. Isotopic signatures ($\delta^{18}O$ and $\delta^{13}C$) of bivalve shells from cold seeps and hydrothermal vents. *Geobios* 42: 209-219.

- Little, C.T.S. 2002. The fossil record of hydrothermal vent communities. *Cahiers de Biologie Marine* 43: 313-316.

- Little, C.T.S, D. Birgel, A.J. Byce, J.A. Crame, J.E. Francis, S. Kiel, J. Peckmann, D. Pirrie, G.K. Rollinson, and J.D. Witts. 2015. Late Cretaceous (Maastrichtian) shallow water hydrocarbon seeps from Snow Hill and Seymour Islands, James Ross Basin, Antarctica. *Palaeogeography, Palaeoclimatology, Palaeoecology* 418: 213-228.

- Little, C.T.S., T. Danelian, R.J. Herrington, and R.M. Haymon. 2004. Early Jurassic hydrothermal vent community from the Franciscan Complex, California. *Journal of Paleontology* 78: 542-559.

- Lombardi, S.A., G.D. Chon, J.J. Lee, H.A. Lane, and K.T. Paynter. 2013. Shell hardness and compressive strength of the eastern oyster, *Crassostrea virginica*, and the Asian oyster, *Crassostrea ariakensis*. *The Biological Bulletin* 225: 175-183.

- Lorens, R.B., and M.L. Bender. 1980. The impact of solution chemistry on *Mytilus edulis* calcite and aragonite. *Geochimica et Cosmochimica Acta* 44: 1265-1278.

- Lorrain, A. Y-M. Paulet, L. Chavaud, R. Dunbar, D. Mucciarone, and M. Fontuge. 2004. $\delta^{13}C$ variation in scallop shells: increasing metabolic carbon contribution with body size?. *Geochimica et Cosmochimica Acta* 68: 3509-3519.

- Lowenstam, H.A., and S. Weiner. *On biomineralization*. 1989. Oxford University Press, Oxford.

- Liu, B., Y. Liu, Y. Li, H. Wang, and J. Xu. 2013. An assessment of sample preservation methods for the determination of stable carbon and nitrogen isotope ratios in mollusks. *Analytical Letters* 46: 2620-2634.

- MacAvoy, S.E., R.S. Carney, E. Morgan, and S.A. Macko. 2008. Stable isotope variation among the mussel *Bathymodiolus childressi* and associated heterotrophic fauna at four cold-seep communities in the Gulf of Mexico. *Journal of Shellfish Research* 27: 147-151.

- MacLeod, K.G., and K.A. Hoppe. 1992. Evidence that inoceramid bivalves were benthic and harbored chemosynthetic symbionts. *Geology* 20: 117-120.

- Mae, A., T. Yamanaka, and S. Shimoyama. 2007. Stable isotope evidence for identification of chemosynthesis-based fossil bivalves associated with cold-seepages. *Palaeogeography, Palaeoclimatology, Palaeoecology* 245: 411-420.

- Marin, F., N. LeRoy, and B. Marie. 2012. The formation and mineralization of mollusk shell. *Frontiers of Bioscience* 4: 1099-1125.

- Marin, F., I. Bundeleva, T. Takeuchi, F. Immel, and D. Medakovic. 2016. Organic matrices in metazoan calcium carbonate skeletons: Composition, functions, evolution. *Journal of Structural Biology* (in press.).

- Martens, C.S., J.P. Chanton, and C.K. Paull. 1991. Biogenic methane from abyssal brine seeps at the base of the Florida escarpment. *Geology* 19: 851-854.

- Martin, J.B., S.A. Day, A.E. Rathburn, M.E. Perez, C. Mahn, and J. Gieskes. 2004. Relationships between the stable isotopic signature of living and fossil foraminifera in Monterey Bay, California. *Geochemistry, Geophysics, Geosystems* 5: Q04004.

- Mateo, M.A., O. Serrano, L. Serrano, and R.H. Michener. 2008. Effects of sample preparation on stable isotope ratios of carbon and nitrogen in marine invertebrates: implications for food web studies using stable isotopes. *Oecologia* 157: 105-115.

- McCollom, T.M., and J.S. Seewald. 2007. Abiotic synthesis of organic compounds in deep-sea hydrothermal environments. *Chemical Reviews* 107: 382-401.

- McConnaughey, T.A., J. Burdett, J.F. Whelan, and C.K. Paull. 1997. Carbon isotopes in biological carbonates: respiration and photosynthesis. *Geochimica et Cosmochimica Acta* 61: 611-622.

- McConnaughey, T.A., and D.P. Gillikin. 2008. Carbon isotopes in mollusk shell carbonates. *Geo-Marine Letters* 28: 287-299.

- McCutchan, J.H., W. Lewis, C. Kendell, C.C. McGrath. 2003. Variation in trophic shift for stable isotope ratios of carbon, nitrogen and sulfur. *Oikos* 102: 378-390.

- McCullagh, J.S.O., J.A. Tripp, and R.E.M. Hedge. 2005. Carbon isotope analysis of bulk keratin and single amino acids from British and North American hair. *Rapid Communications in Mass Spectrometry* 19: 3227-3231.

- Meenanski, V.R., P.E. Hare, and K.M. Wilbure. 1971. Amino acids of the organic matrix of neogastropod shells. *Comparative Biochemistry and Physiology Part B: Comparative Biochemistry* 40: 1037-1043.

- Meyer, E., B. Nilkerd, E.A. Glover, and J.D. Taylor. 2008. Ecological importance of chemoautotrophic lucinid bivalves in a peri-mangrove community in eastern Thailand. *Raffles Bulletin of Zoology, Supplement* 18: 41-55.

- Michener, R. H., L. Kaufman, R. Michener, and K. Lajtha. 2007. Stable isotope ratios as tracers in marine food webs: an update. *Stable isotopes in ecology and environmental science* 2: 238-282.

- Milkov, A.V. 2005. Molecular and stable isotope compositions of natural gas hydrates: A revised global dataset and basic interpretations in the context of geological settings. *Organic Geochemistry* 36: 681-702.

- Mitterer, R.M. 1993. The diagenesis of proteins and amino acids in fossil shells. In: M.H. Engel and S.A. Macko, *Organic Geochemistry*, Plenum Press, New York, p. 739-753.

- Miyazaki, J-I., L. de Oliveira Martins, Y. Fujita, H. Matsumoto, and Y. Fujiwara. 2010. Evolutionary process of deep-sea *Bathymodiolus* mussels. *PLoS One* 5: e10363.

- Modica, M.V., and M. Holford. 2010. The Neogastropoda: evolutionary innovations of predatory marine snails with remarkable pharmacological

potential. In: P. Pontarotti (ed.), *Evolutionary Biology – Concepts, Molecular and Morphological Evolution*, Springer, Berlin/Heidelberg, p. 249-270.

- Moldoveanu, S.C. 1998. *Analytical pyrolysis of natural organic polymers* (Vol. 20), Elsevier, Amsterdam.

- Morton, B. 1981. The mode of life and function of the shell buttress in *Cucullaea concamerata* (Martini) (Bivalvia: Arccea*). Journal of Conchology* 30: 295–301.

- Muzamdar, A., P. Dewangen, H.M. Joao, A. Peketi, V.R. Khosla, M. Kocherla, F.K. Badesab, R.K. Joshi, P. Roxanne, P.B. Ramamurty, and S.M. Karisddaiah. 2009. Evidence of paleo–cold seep activity from the Bay of Bengal, offshore India. *Geochemistry, Geophysics, Geosystems* 10: 1-15.

- Myers, J.M., M.B. Johnstone, A.S. Mount, H. Silverman, and A.P. Wheelers. 2007. TEM immunocytochemistry of a 48kDa MW organic matrix phosphoprotein produced in the mantle epithelial cells of the Eastern oyster (*Crassostrea virginica*). *Tissue and Cell* 39: 247-256.

- Nakagawa, S., and K. Takai. 2008. Deep-sea vent chemoautotrophs: diversity, biochemistry and ecological significance. *FEMS microbiology ecology* 65: 1-14.

- Nance, J.R., J.T. Armstrong, G.D. Cody, M.L. Fogel, and R.M. Hazen. 2015. Preserved macroscopic polymeric sheets of shell-binding protein in the Middle Miocene (8 to 18Ma) gastropod *Ecphora*. *Geochemical Perspectives Letters* 1: 1-9.

- Nedoncelle, K., N. Le Bris, M. de Rafélis, N. Labourdette, and F. Lartaud. 2014. Non-equilibrium fractionation of stable carbon isotopes in chemosynthetic mussels. *Chemical Geology* 387: 35-46.

- Nehlich, O. 2015. The application of sulphur isotope analyses in archaeological research: a review. *Earth-Science Reviews* 142: 1-17.

- Nelson, D.C., and C.R. Fisher. 1995. Chemoautotrophic and methanoautotrophic endosymbiotic bacteria at deep-sea vents and seep. In: D.M. Karl (ed.), *The Microbiology of Deep-sea Hydrothermal Vents*, CRC Press, Boca Raton, p. 125-167.

- Nishida, K., R. Nakashima, R. Majima, and Y. Hikida. 2011. Ontogenetic changes in shell microstructures in the cold seep-associated bivalve, *Conchocele bisecta* (Bivalvia: Thyasiridae). *Paleontological Research* 15: 193-212.

- Nix, E., C.R. Fisher, K.M. Scott, and J. Vodenichar. 1995. Physiological ecology of a mussel with methanotrophic symbionts at three hydrocarbon seep sites in the Gulf of Mexico. *Marine Biology* 122: 605–617.

- O'Donnell, T.H., S.A. Macko, J. Chou, K.L. Davis-Hartten, and J.F. Wehmiller. 2003. Analysis of $\delta^{13}C$, $\delta^{15}N$, and $\delta^{34}S$ in organic matter from the biominerals of modern and fossil Mercenaria spp. *Organic Geochemistry* 34: 165-183.

- Okumara, T., M. Suzuki, H. Nagasawa, and T. Kongure. 2013. Microstructural control of calcite via incorporation of intracrystalline organic molecules in shells. *Journal of Crystal Growth* 381: 114-120.

- Oliver, P.G, and A.M. Holmes. 2006. The Arcoidea (Mollusca: Bivalvia): a review of the current phenetic-based systematics. *Zoological Journal of the Linnean Society* 148: 237-251.

- Olu-Le Roy, K., M. SIbuet, A. Fiala-Médioni, S. Gofas, C. Salas, A. Mariotti, J-P. Foucher, and J. Woodside. 2004. Cold seep communities in the deep eastern Mediterranean Sea: composition, symbiosis and spatial distribution on mud volcanoes. *Deep Sea Research Part I: Oceanographic Research Papers* 51: 1915-1936.

- Page, H.M., C.R. Fisher, and J.J. Childress. 1990. Role of filter-feeding in the nutritional biology of a deep-sea mussel with methanotrophic symbionts. *Marine Biology* 104: 251-257.

- Page, H.M., A. Fialmedioni, C.R. Fisher, and J.J. Childress. 1991. Experimental-evidence for filter-feeding by the hydrothermal vent mussel, *Bathymodiolus thermophilus*. *Deep-Sea Research Part I: Oceanographic Research Papers* 38: 1455–1461

- Paull, C.K., B. Hecker, R. Commeau, R. P. Freeman-Lynde, C. Neumann, W.P. Corso, S. Golubic, J.E. Hook, E. Sikes, and J. Curray. 1984. Biological communities at the Florida Escarpment resemble hydrothermal vent taxa. *Science* 226: 965-967.

- Paull, C.K., C.S. Martens, J.P. Chanton, A.C. Neumann, J. Coston, A.T. Jull, and L.J. Toolin. 1989. Old carbon in living organisms and young $CaCO_3$ cements from abyssal brine seeps. *Nature* 342: 166-168.

- Paull, C.K., J.P. Chanton, A.C. Neumann, J.A. Coston, C.S. Martens, and W. Showers. 1992. Indicators of methane-derived carbonates and chemosynthetic organic carbon deposits: examples from the Florida Escarpment. *Palaios* 7: 361-375.

- Paull, C.K., A.C. Neumann, B.A. Am Ende, W. Ussler III, and N.M. Rodriguez. 2000. Lithoherms on the Florida–Hatteras slope. *Marine Geology* 166: 83-101.

- Penkman, K.E.H., D.S. Kaufman, D. Maddy, and M.J. Collins. 2008. Closed-system behaviour of the intra-crystalline fraction of amino acids in mollusc shells. *Quaternary Geochronology* 3: 2-25.

- Petersen, J.M., and N. Dubilier. 2009. Methanotrophic symbioses in marine invertebrates. *Environmental Microbiology Reports* 1: 319-335.

- Petersen, J.M., F.U. Zielinski, T. Pape, R. Seifert, C. Moraru, R. Amann, S. Hourdez, P.R. Girguis, S.D. Wankel, V. Barbe, and E. Pelletier. 2011. Hydrogen is an energy source for hydrothermal vent symbiosis. *Nature* 476: 176-180.

- Petersen, S.V., A. Dutton, and K.C. Lohmann. 2016. End-Cretaceous extinction in Antarctica linked to both Deccan volcanism and meteorite impact via climate change. *Nature Communications* 7: 12079.

- Peterson, B.J., and B. Fry. 1987. Stable isotopes in ecosystem studies. *Annual review of ecology and systematics* 18: 293-320.

- Pile, A.J., and C.M. Young. 1999. Plankton availability and retention efficiencies of cold-seep symbiotic mussels. *Limnology and Oceanography* 44: 1833-1839.

- Podowski, E.L., T.S. Moore, K.A. Zelnio, G.W. Luther, and C.R. Fisher. 2009. Distribution of diffuse flow megafauna in two sites on the Eastern Lau Spreading Center, Tonga. *Deep Sea Research Part I: Oceanographic Research Papers* 56: 2041-2056.

- Pohlman, J.W. E.A. Canuel, N.R. Chapman, G.D. Spence, M.J. Whiticar, and R.B. Coffin. 2005. The origin of thermogenic gas hydrates on the northern Cascadia Margin as inferred from isotopic (^{13}C/12C and D/H) and molecular composition of hydrate and vent gas. *Organic Geochemistry* 36: 703-716.

- Rau, G.H., R.E. Sweeney, and I.R. Kaplan. 1982. Plankton ^{13}C:^{12}C ratio changes with latitude: differences between northern and southern oceans. *Deep Sea Research Part I: Oceanographic Research Papers* 29: 1035-1039.

- Rees, C.E., W. Jenkins, and J. Monster. 1978. The sulphur isotopic composition of ocean water sulphate. *Geochimica et Cosmochimica Acta* 42: 377-381.

- Reid, W.D.K., C.J. Sweeting, B.D. Wigham, K. Zwirglmaier, J.A. Hawkes, R.A.R. McGill, K. Linse, and N.V.C. Polunin. 2013. Spatial differences in East Scotia Ridge hydrothermal vent food webs: influences of chemistry, microbiology and predation on trophodynamics. *PLoS One* 8: e65553.

- Riekenberg, P. 2012. Biomass and Mass Balance Isotope Content of Mussel Seep Populations. Ph.D. Thesis, University of Texas.

- Riekenberg, P.M., R.S. Carney, and B. Fry. 2016. Trophic plasticity of the methanotrophic mussel *Bathymodiolus childressi* in the Gulf of Mexico. *Marine Ecology Progress Series* 547: 91-106.

- Rio, M., M. Roux, M. Renard, and E. Schein. 19992. Chemical and isotopic features of present day bivalve shells from hydrothermal vents or cold seeps. *Palaios* 7: 351-360.

- Ritterbush, K.A, R. Hoffmann, A. Lukender, and K. De Baets. 2014. Pelagic palaeoecology: the importance of recent constraints on ammonoid palaeobiology and life history. *Journal of Zoology* 292: 229-241.

- Robinson, J.J., and C.M. Cavanaugh. 1995. Expression of form I and form II Rubisco in chemoautotrophic symbioses: implications for the interpretation of stable carbon isotope values. *Limnology and Oceanography* 40: 1496-1502.

- Robinson, J.J., K.M. Scott, S.T. Swanson, M.H. O'Leary, K. Horken, F.R. Tabita, and C.M. Cavanaugh. Kinetic isotope effect and characterization of form II RubisCO from the chemoautotrophic endosymbionts of the hydrothermal vent tubeworm *Riftia pachyptila*. *Limnology and oceanography* 48: 48-54.

- Rodrigues, C.F., A. Hilário, and M.R. Cunha. 2013. Chemosymbiotic species from the Gulf of Cadiz (NE Atlantic): distribution, life styles and nutritional patterns. *Biogeosciences* 10: 2569-2581.

- Rodrigues, C.F., and S. Duperron. 2011. Distinct symbiont lineages in three thyasirid species (Bivalvia: Thyasiridae) from the eastern Atlantic and Mediterranean Sea. *Naturwissenschaften* 98: 281-287.

- Roeselers, G., and I.L.G. Newton. 2012. On the evolutionary ecology of symbioses between chemosynthethic bacteria and bivalves. *Applied microbiology and biotechnology* 94: 1-10.

- Romanek, C.S., E. L. Grossman, and J.W. Morse. 1992. Carbon isotopic fractionation in synthetic aragonite and calcite: effects of temperature and precipitation rate. *Geochimica et Cosmochimica Acta* 56: 419-430.

- Rooker, J.R., J.P. Turner, and S.A. Holt. 2006. Trophic ecology of *Sargassum*-associated fishes in the Gulf of Mexico determined from stable isotopes and fatty acids. *Marine Ecology Progress Series* 313: 249-259.

- Ruby, E.G., H.W. Jannasch, and W.G. Deuser. 1987. Fraction of stable carbon isotopes during chemoautotrophic growth of sulfur-oxidizing bacteria. *Applied and Environmental Microbiology* 53: 1940-1943.

- Ruiz-Cooley, R.I., K.Y. Garcia, and E.D. Hetherington. 2011. Effects of lipid removal and preservatives on carbon and nitrogen stable isotope ratios of squid tissues: Implications for ecological studies. *Journal of Experimental Marine Biology and Ecology* 407: 101-107.

- Ryther, J.H., and W.M. Dunstan. 1971. Nitrogen, phosphorus, and eutrophication in the coastal marine environment. *Science* 171: 1008-1013.

- Saether, K.P., C.T.S. Little, K.A. Capbell, B.A. Marshall, M. Collins, and A.C. Alfaro. 2010. New fossil mussels (Bivalvia: Mytilidae) from Miocene hydrocarbon seep deposits, North Island, New Zealand, with general remarks on vent and seep mussels. *Zootaxa* 2577: 1-45.

- Salerno, J.L., S.A. Macko, S.J. Hallam, M. Brights, Y.J. Won, Z. McKiness, and C.L. Van Dover. 2005. Characterization of symbiont populations in life-history stages of mussels from chemosynthetic environments. *The Biological Bulletin* 208: 145-155.

- Sandy, M.R. 1995. A review of some Palaeozoic and Mesozoic brachiopods as members of cold seep chemosynthetic communities: “unusual” palaeoecology and anomalous palaeobiogeographic patterns explained. *Földtani Közlöny* 125: 241-258.

- Sandy, M.R. 2010. Brachiopods from ancient hydrocarbon seeps and hydrothermal vents. In*:* S. Kiel (ed.), *The Vent and Seep Biota Aspects from Microbes to Ecosystems*, Topics in Geobiology 33, Springer*,* Heidelberg, p. 279–314.

- Sarakinos, H.C., M.L. Johnson, and M.J. Vander Zanden. 2002. A synthesis of tissue-preservation effects on carbon and nitrogen stable isotope signatures. *Canadian Journal of Zoology* 80: 381-387.

- Sarashina, I., and K. Endo. 1998. Primary structure of a soluble matrix protein of scallop shell: implications for calcium carbonate biomineralization. *American Mineralogist* 83: 1510-1515.

- Sassen, R., S. Joye, S.T. Sweets, D.A. DeFreitas, A.V. Milkov, and I.R. MacDonald. 1999. Thermogenic gas hydrates and hydrocarbon gases in complex chemosynthetic communities, Gulf of Mexico continental slope. *Organic Geochemistry* 30: 485-497.

- Sassen, R., H.H. Roberts, R. Carney, A. V. Milkov, D.A. DeFreitas, B. Lanoil, and C. Zhang. 2004. Free hydrocarbon gas, gas hydrate, and authigenic minerals in chemosynthetic communities of the northern Gulf of Mexico continental slope: relation to microbial processes. *Chemical Geology* 205: 195-217.

- Sato, K., H. Watanabe, and T. Sasaki. 2013. A new species of *Solemya* (Bivalvia: Protobranchia: Solemyidae) from a hydrothermal vent in the Iheya Ridge in the mid-Okinawa Trough, Japan. *Nautilus* 127: 93-100.

- Savazzi, E. 1995. Morphology and mode of life of the polychaete *Rotularia*. *Paläontologische Zeitschrift* 69: 73-85.

- Schlacher, T.A., and R.M. Connolly. 2014. Effects of acid treatment on carbon and nitrogen stable isotope ratios in ecological samples: a review and synthesis. *Methods in Ecology and Evolution* 5: 541-550.

- Schwarcz, H.P., and M.J. Schoeninger. 1991. Stable isotope analyses in human nutritional ecology. *American Journal of Physical Anthropology* 34: 283-321.

- Scott, K.M., J. Schwedock, D.P. Schrag, and C.M. Cavanaugh. 2004. Influence of form IA RubisCO and environmental dissolved inorganic carbon on the $\delta^{13}C$ of the clam-chemoautotroph symbiosis *Solemya velum. Environmental Microbiology* 6*:* 1210–1219*.*

- Shanks. W.C. 2001. Stable isotopes in seafloor hydrothermal systems: vent fluids, hydrothermal deposits, hydrothermal alteration, and microbial processes. *Reviews in Mineralogy and Geochemistry* 43: 469-525.

- Stewart, F.J., L.G. Newton, and C.M. Cavanaugh. 2005. Chemosymbiotic endosymbioises: adaptations to oxic-anoxic interfaces. *Trends in Microbiology* 13: 439-448.

- Schweitzer, M.H., R. Avci, T. Collier, and M.B. Goodwin. 2008. Microscopic, chemical and molecular methods for examining fossil preservation. *Comptes Rendus Palevol* 7: 159-184.

- Shimek, R.L. 1990. Diet and habitat utilization in a Northeastern Pacific Ocean scaphopod assemblage. *American Malacological Bulletin* 7: 147-169.

- Sibuet, M., and K. Olu. 1998. Biogeography, biodiversity and fluid dependence of deep-sea cold-seep communities at active and passive margins. *Deep Sea Research Part II: Topical Studies in Oceanography* 45: 517-567.

- Smith, A.M., and H.G. Spencer. 2015. Skeletal mineralogy of scaphopods: an unusual uniformity. *Journal of Molluscan Studies* 82: 344-348.

- Smith, K.R., R.A. McConnaughey, and C.E. Armistead. 2011. Benthi invertebrates of the eastern Bering Sea: A synopsis of the life history and ecology of snails of the genus *Neptunea*. U.S. Dep. Commer., NOAA Tech Memo NMFS-AFSC-231.

- Stanley, S.M. 1986. Population size, extinction, and speciation: the fission effect in Neogene Bivalvia. *Palaeobiology* 12: 89-110.

- Stein, J.L., M. Haygood, and H. Felbeck. 1990. Nucleotide sequence and expression of a deep-sea ribulose-1,5-bisphosphate carboxylase gene cloned from a chemoautotrophic bacterial endosymbiont. *Proceedings of the National Academy of Sciences* 87: 8850-8854.

- Streams, M., C.R. Fisher, A. FialaMedioni. 1997. Methanotrophic symbiont location and fate of carbon incorporated from methane in a hydrocarbon seep mussel. *Marine Biology* 129: 465–476.

- Suzuki, Y., T. Sasaki, M. Suzuki, Y. Nogi, T. Miwa, K. Takai, K.H. Nealson, and K. Horikoshi. 2005. Novel chemoautotrophic endosymbiosis between a member of the Epsilonproteobacteria and the hydrothermal-vent gastropod *Alviniconcha* aff. *hessleri* (Gastropoda: Provannidae) from the Indian Ocean. *Applied and environmental microbiology* 71: 5440-5450.

- Sykes, G.A., M.J. Collins, and D.I. Walton. The significance of a geochemically isolated intracrystalline fraction within biominerals. *Organic Geochemistry* 23: 1059-1065.

- Tabita, F.R., S. Satagopan, T.E. Hanson, N. Kreel, and S.S. Scott. 2008. Distinct form I, II, III, and IV Rubisco proteins from the three kingdoms of life provide clues about Rubisco evolution and structure/function relationships. *Journal of Experimental Botany* 59: 1515-1524.

- Taylor, J.D. 1969. The shell structure and mineralogy of the Bivalvia. Introduction. Nuculacea-Trigonacea. *Bulleting of the British Museum Natural History (Zoology)* 3: 1-125.

- Taylor, J.D., and E.A. Glover. 2010. Chemosymbiotic bivalves. In*:* S. Kiel (ed.), *The Vent and Seep Biota Aspects from Microbes to Ecosystems*, Topics in Geobiology 33, Springer*,* Heidelberg, p. 107-135.

- Taylor, J.D., and D.G. Reid. 1990. Shell microstructure and mineralogy of the Littorinidae: ecological and evolutionary significance. *Hydrobiologia* 193: 199-215.

- Templeton, A.S., K.H. Chu, L. Alvarez-Cohen, and M.E. Conrad. 2006. Variable carbon isotope fractionation expressed by aerobic CH_4-oxidizing bacteria. *Geochimica et Cosmochimica Acta* 70: 1739-1752.

- Trask, J.L., and C.L. Van Dover. 1999. Site-specific and ontogenetic variations in nutrition of mussels (*Bathymodiolus* sp.) from the Lucky Strike hydrothermal vent field, Mid-Atlantic Ridge. *Limnology and Oceanography* 44: 334-343.

- Tunnell, J.W., J. Andrews, N.C. Barrera, and F. Moretzsohn. 2010. *Encyclopedia of Texas seashells – identification, ecology, distribution and history*, Texas A&M University Press, College Station.

- Tunnicliffe, V., S.K. Juniper, and M. Sibuet. 2003. Reducing environments of the deep-sea floor. In: P.A. Tyler (ed.), *Ecosystems of the World*, Elsevier, Amsterdam, p. 81-110.

- Ullmann, C.V., N. Thibault, M. Ruhl, S.P. Hesselbo, and C. Korte. 2014. Effect of a Jurassic oceanic anoxic event on belemnite ecology and evolution. *Proceedings of the National Academy of Sciences* 111: 10073-10076.

- Van der Geest, M., A.A. Sall, S.O. Ely, R.W. Nauta, J.A. van Gils, and T. Piersma. 2014. Nutritional and reproductive strategies in a chemosymbiotic bivalve living in a tropical intertidal seagrass bed. *Marine Ecology Progress Series* 501: 113-126.

- Van der Heide, T., L.L. Glovers, J. de Fouw, H. Olff, M. van der Geest, M.M. van Katwijk, T. Piersma, J. van de Koppel, B.R. Silliman, A.J. Smolders, and J.A. van Gils. 2012. A three-stage symbiosis forms the foundation of seagrass ecosystems. *Science* 336: 1432-1434.

- Van Dover, C. 2000. *The ecology of deep-sea hydrothermal vents*, Princeton University press, Princeton.

- Van Dover, C.L. 2002. Evolution and biogeography of deep-sea vent and seep invertebrates. *Science* 295: 1253-1257.

- Van Dover, C.L. 2003. P. Aharon, J.M. Bernhard, E. Caylor, M. Doerries, W. Flickinger, W. GIlhooy, S.K. Goffredi, K.E. Knick, S.A. Macko, and S. Rapoport. 2003. Blake Ridge methane seeps: characterization of a soft-sediment, chemosynthetically based ecosystem. *Deep Sea Research Part I: Oceanographic Research Papers* 50: 281-300.

- Versteegh, E.A.A., D. P. Gillikin, and F. Dehairs. 2011. Analysis of $\delta^{15}N$ values in mollusk shell organic matrix by elemental analysis/isotope ratio mass spectrometry without acidification: an evaluation and effects of long-term preservation. *Rapid Communications in Mass Spectrometry* 25: 675-680.

- Vetter, R.D., and B. Fry. 1998. Sulfur contents and sulfur-isotope compositions of thiotrophic symbioses in bivalve molluscs and vestimentiferan worms. *Marine Biology* 132: 453-460.

- Vinn, O., and H. Furrer. 2008. Tube structure and ultrastructure of serpulids from the Jurassic of France and Switzerland, its evolutionary implications. *Neues Jahrbuch für Geologie und Paläontologie-Abhandlungen* 250: 129-135.

- Von Cosel, R. 2002. A new species of bathymodioline mussel (Mollusca, Bivalvia, Mytilidae) from Mauritania (West Africa), with comments on the genus *Bathymodiolus* Kenk & Wilson. *Zoosystema* 24: 259-272.

- Voigt, S. 2000. Stable oxygen and carbon isotopes from brachiopods of southern England and northwestern Germany: estimation of Upper Turonian palaeotemperatures. *Geological Magazine* 137: 687-703.

- Von Cosel, R., and B.A. Marshall. 2003. Two new species of large mussels (Bivalvia: Mytilidae) from active submarine volcanoes and a cold seep off the eastern North Island of New Zealand, with description of a new genus. *The Nautilus* 117: 31-46.

- Watanabe, S., M. Kodama, and M. Fukuda. 2009. Nitrogen stable isotope ratio in the manila clam, *Ruditapes philippinarum*, reflects eutrophication levels in tidal flats. *Marine Pollution Bulletin* 58: 1447-1453.

- Wells, R.J.D., and J.R. Rooker. 2009. Feeding ecology of pelagic fish larvae and juveniles in slope waters of the Gulf of Mexico. *Journal of Fish Biology* 75: 1719-1732.

- Whiticar, M.J. 1999. Carbon and hydrogen isotope systematics of bacterial formation and oxidation of methane. *Chemical Geology* 161: 291-314.

- Yonge, C.M. 1939. The protobranchiate Mollusca; a functional interpretation of their structure and evolution. *Philosophical Transactions of the Royal Society of London, Series B* 230: 79–147.

Appendix A

Does carbonate associated sulphate (CAS) record nutrition in lucinid and thyasirid bivalve shells from modern hydrocarbon seeps?

Robert J. Newton[a*], Crispin T.S. Little[a], Edine Pape[a], Fiona Gill[a], Clara F. Rodrigues[b] and Marina R. Cunha[b]

[a] School of Earth and Environment, University of Leeds, Leeds LS2 9JT, United Kingdom

[b]Departamento de Biologia & CESAM, Universidade de Aveiro, Campus Universitário de Santiago, 3810–193 Aveiro, Portugal

*Corresponding author at: School of Earth and Environment, University of Leeds, Leeds LS2 9JT, United Kingdom. *E-mail address*: r.j.newton@leeds.ac.uk (R. Newton).

Abstract

Here we test whether chemosymbiotic bivalves with sulphide-oxidizing bacteria record their nutritional strategy in the sulphur isotope composition of the carbonate associated sulphate (CAS) in their shells as a possible indicator of thiotrophic chemosymbiosis in the fossil record. The hypothesis rests on the possible incorporation of ^{34}S-depleted sulphate resulting from sulphide oxidation in sufficient quantity to affect the intra-shell sulphate-sulphur isotope mass balance and hence the isotopic composition of sulphate which is incorporated into carbonate with little or no fractionation. We analysed shell material of lucinid (*Lucinoma asapheus*) and thyasirid (*Thyasira vulcolutre*) bivalves from active mud volcanoes in the Gulf of Cadiz. Our results show that the CAS-$\delta^{34}S$ values of the bivalve shells do not reflect the variety of sulphur sources present at hydrocarbon seeps, but instead only record seawater sulphate values. Depleted $\delta^{34}S$ values were, however, measured in the animals' soft tissues and shell organic matter (SOM), both displaying a strong influence of the depleted sulphide used as nutrition by the chemosynthethic bacteria. Given its potential for long term preservation, SOM may therefore represent a more promising record of chemosymbiosis in the fossil record, whilst CAS from seep bivalves can be used to reconstruct local seawater sulphate.

Author contribution

RJN performed the experiments and analyses, and wrote a first draft of the paper. RJN and CTLS designed the research, and material was provided by CFR and MRC. EP worked on the manuscript from the first draft until completion, and incorporated comments from all other authors.

Keywords

Carbonate Associated Sulphate; Chemosymbiosis; Bivalve shell; Sulfur isotopes; Geochemical proxies

Highlights

Carbonate associated sulphate (CAS) from bivalve shells with sulphide-oxidizing symbionts is investigated to determine if it represents a possible indicator of this nutritional strategy.

The S-isotope composition of CAS only reflects seawater sulphate values in bivalves with sulphide-oxidizing symbionts.

Shell organic matter from bivalves with sulphide-oxidizing symbionts has depleted $\delta^{34}S$ values and therefore records the influence of their nutrition.

1. Introduction

Carbonate associated sulphate (CAS) is the trace sulphate incorporated into the lattice of carbonate minerals, and has been shown to record the sulphur isotopic composition ($\delta^{34}S$) of the solution from which the carbonate is formed (Kampschulte and Strauss, 2004). In most cases CAS from marine carbonates therefore reflects the isotope value of ambient seawater sulphate, currently +20‰ Vienna Cañon Diablo troilite (VCDT) (Bottrell and Raiswell, 2000). At modern hydrocarbon seeps elevated concentrations of hydrocarbons, most commonly methane, are emitted at an ambient seawater temperature (Van Dover et al., 2002). Anaerobic oxidation of methane (AOM) in the sediment is coupled to high rates of microbial sulphate reduction, producing abundant sulphide. This reaction causes the sulphide to become severely depleted in ^{34}S relative to seawater sulphate (e.g. Jørgensen et al., 2004), although direct measurements of the sulphur isotope effects of AOM in culture are lacking (Deusner et al., 2014). The depleted sulphide is then utilized by

sulphide-oxidizing (thiotrophic) bacteria that live in symbiosis with seep invertebrates, particularly bivalves, which house the bacteria in their gills. The bacteria oxidize sulphide to release energy for fixation of inorganic carbon from seawater and the production of organic molecules to provide nutrition for the bacteria and their bivalve host (Fisher, 1995, Vetter, 1991). Sulphide uptake by the bacteria is generally associated with limited fractionation and the tissues of the chemosymbiotic bivalves record the ^{34}S-depleted sulphide, with $\delta^{34}S$ values down to -30‰ (Vetter and Fry, 1998). Chemosymbiotic bivalves must bridge the oxic-anoxic interface to access both the reduced compounds and oxygen (as an electron acceptor). To avoid spontaneous oxidation they use specialized behavioural, anatomical or physiological mechanisms to bridge sulphidic and oxic zones, or sequester them simultaneously (Cavanaugh et al., 2006, Rodrigues et al., 2013). Sulphide is obtained from interstitial water, and transferred to the chemosynthethic bacteria that oxidize it via a number of pathways (Dreier et al., 2012, Bruser et al., 2000, Taylor and Glover, 2000), producing ^{34}S-depleted sulphate very similar to the sulphide source, since the oxidation step involves zero or very limited fractionation (in experiments: (Fry et al., 1988). If this ^{34}S-depleted sulphate is incorporated into the carbonate shells of molluscs via the extrapallial fluid, CAS from chemosymbiotic bivalves will be depleted in ^{34}S relative to seawater sulphate values. The presence of ^{34}S-depleted sulphate in CAS could therefore be construed as evidence of bacterial sulphide oxidation occurring within the shell, and thus a likely indicator of chemosymbiosis. To determine this, we analysed the CAS of the shells of two species of deep burrowing thiotrophic bivalves belonging to the families Lucinidae (*Lucinoma asapheus*) and Thyasiridae (*Thyasira vulcolutre*) (Rodrigues et al., 2013).

2. Materials and methods

Table 1. Sample collection of shells from the Gulf of Cadiz used for this study, with associated $\delta^{34}S$ soft tissue values. MV = mud volcano.

Specimen code	**Species**	**Locality**	**Material**	**Weight (g)**	**Soft tissue value ($\delta^{34}S$) VCDT** (Rodrigues et al., 2013)
AT569-BIG	*Lucinoma asapheus*	Mercator MV Gulf of Cadiz (358m depth)	Live collected specimen; both complete valves analysed	7.2343	-15.96 (+/- 2.55)
AT569-MED	*Lucinoma asapheus*	Mercator MV, Gulf of Cadiz (358m depth)	Live collected specimen; single complete valve analysed	2.8974	
AT569-1.19	*Lucinoma asapheus*	Mercator MV, Gulf of Cadiz (358m depth)	Dead shell; single complete valve analysed	1.0491	
AT615	*Thyasira vulcolutre*	Carlos Ribeiro MV, Gulf of Cadiz (2200m depth)	Live collected specimen; one complete and one incomplete valve analysed	0.7008	1.03 (+/- 0.45)
STN169	*Thyasira vulcolutre*	Carlos Ribeiro MV, Gulf of Cadiz (2199m depth)	Live collected specimen; both complete valves analysed	0.9579	-21.92 (+/- n/a)
AT615-0.97	*Thyasira vulcolutre*	Carlos Ribeiro MV, Gulf of Cadiz (2200m depth)	Dead shell; single complete valve analysed	0.8616	n/a

The taxa analysed were collected from active mud volcanoes in the Gulf of Cadiz (Table 1), that display relatively mild fluxes of methane and sulphide, with a methane-sulphate transition zone of 80cm at the Mercator mud volcano (MV) and 20-55cm at the Carlos Ribeiro MV (Van Rensbergen et al., 2005, Niemann et al., 2006). In the Gulf of Cadiz a large number of chemosymbiotic species have been

identified, including 11 bivalve species from four families with chemosymbiotic members (Solemyidae, Lucinidae, Thyasiridae and Mytilidae) (Rodrigues et al., 2010, Oliver et al., 2011, Rodrigues et al., 2013). The collected specimens of *Lucinoma asapheus* and *Thyasira vulcolutre* show no evidence of any sulphide staining in either live or dead specimens. This is an important observation since it makes the contamination of CAS by sulphide oxidation during extraction less likely. Previously published soft tissue values for our specimens are as follows: $\delta^{34}S$ lucinids = -15.96‰; thyasirids = -21.92 to + 1.03‰ (Rodrigues et al., 2013).

CAS and shell organic matter (SOM) extraction methods.

All soft tissue was removed from the live collected specimens, and the shell material from these and dead shells was cleaned in de-ionised water in an ultrasonic bath for 10 minutes to remove surface contamination before drying overnight at 70° C. The shell material was then powdered in an agate pestle and mortar and sieved to ensure all material was <150 µm. To extract sulphur bound to organic compounds powdered material was weighed and treated with a 5% (vol/vol) NaOCl solution overnight before vacuum filtering onto weighed glass fibre filter papers (Whatman GFA). The powder was dried and the weight loss from the NaOCl extraction was determined. The sample was then dissolved in 50% (6 M) HCl to liberate the carbonate associated sulphate. $BaSO_4$ for isotopic analysis was precipitated from both the NaOCl and HCl solutions by adjusting the pH to between 2.5 and 3 with either HCl or ammonium hydroxide before heating to ~70°C and adding 10% of the volume of the sample solution of 100g/L BaCl solution. Whereas the HCl precipitate contains the CAS, the NaOCl precipitate represents the SOM. The proteinaceous SOM is present as an organic framework around and within the carbonate crystals to guide nucleation and provide strengthening of the shell (Marin et al., 2012, Berman et al., 1990, Kamat et al., 2000). Because SOM is secreted by the mantle, it has been shown to reflect soft tissue values (O'Donnell et al., 2003, Dreier et al., 2012). The amount of sulphur from each extraction was determined by gravimetry. Because $BaSO_4$ precipitates are sometimes impure, the concentration of sulphur contained in the BaSO4 precipitate was determined during the isotope analyses and used to correct the weight of sulphur recovered.

Isotope analyses were performed using a Eurovector 3028HT elemental analyser coupled to an Isoprime mass spectrometer at the University of Leeds. Between 250 and 400 µg of $BaSO_4$ were weighed into tin cups and combusted at 1020°C in a pulse of pure oxygen (BOC, research grade N5.5) in a stream of helium (BOC, CP grade) at a flow rate of 80ml/min. The stream of gas was passed through tungstic

oxide, copper wire, and magnesium perchlorate to ensure quantitative conversion to SO_2, remove excess oxygen and water, before passing through a 1 meter chromatographic column designed for sulphur analyses (Elemental Microanalysis, part no E3002) held at 85°C. The isotopic ratio of the sample gas was determined relative to a pulse of pure SO_2 reference gas (BOC, 99.9%) and calibrated to the international VCDT scale using a $BaSO_4$ internal lab standard SWS-3A derived from seawater sulphate with a $\delta^{34}S$ value of +20.3‰ and an international chalcopyrite standard CP-1 with a $\delta^{34}S$ value of -4.56‰. Standards were run every 8-10 samples. The analytical precision is <0.3‰ (1 standard deviation). Sulphur isotopes are given as δ values in per mil (‰) relative to the Vienna Cañon Diablo troilite (VCDT) standard.

3. Results

Table 2. Sulphur and sulphate amounts present in the *Lucinoma asapheus* and *Thyasira vulcolutre* shells from the Gulf of Cadiz mud volcanoes, and their carbonate associated sulphate (CAS) and shell organic matter (SOM) sulphur isotopic values.

Specimen code	**% sample lost on bleaching**	**NaOCl-S (ppm in whole shell)**	**NaOCl-S (ppm in material removed)**	**$\delta^{34}S$-SOM**	**CAS-S (ppm in whole shell)**	**CAS-SO_4 (ppm in whole shell)**	**$\delta^{34}S$-CAS**
AT569-BIG	1.43	107	7461	-1.6	287	861	**19.8**
AT569-MED	1.73	93	5388	2.1	225	674	**19.2**
AT569-1.19	n/a	135	n/a	0.3	106	318	**17.8**
AT615	1.38	17	1260	8.4	478	1433	**19.2**
STN169	1.33	151	11418	1.6	413	1239	**17.6**
AT615-0.97	n/a	73	n/a	8.8	327	982	**21.3**

The mean CAS-$\delta^{34}S$ is +18.9 ±1.0‰ for the lucinids and +19.4 ±1.8‰ for the thyasirids (Table 2, Figure 1), showing no significant difference between the two taxa (ANOVA: p=0.737). A distinct difference was found in the CAS concentrations

(expressed as S in the whole shell powder) between the thyasirid shells (406 ±75 ppm, all precision figures are one standard deviation) and the lucinid shells (206 ±92 ppm) (ANOVA: p=0.043, cut-off p=0.050). The lowest concentrations of CAS were produced by the dead collected shells of both *Thyasira vulcolutre* and *Lucinoma asapheus*, but there is no correlation between CAS concentration and CAS-δ^{34}S values. Both the amount of organic material removed from the shell by bleaching (*T. vulcolutre* = -1.5% mean weight loss, *L. asapheus* = -1.35%, ANOVA: p=0.277), and the concentration of organic-S in the shell (ppm in untreated material: 111±21ppm S for lucinids and 81±67ppm S for thyasirids, ANOVA: p=0.159) were broadly similar. The δ^{34}S of the SOM bound sulphur released by the NaOCl leach for thyasirids ranged from +1.6 to +8.8‰ and for lucinids from -+1.6 to +2.1‰ (no significant difference between the groups, p=0.080), and is distinctly different from CAS-δ^{34}S for both *T. vulcolutre* (ANOVA: p=0.007) and *L. asapheus* (ANOVA: p= < 0.001). Soft tissue δ^{34}S values obtained from Rodrigues et al. (2013) (Table1) are also distinct from the CAS-δ^{34}S values (thyasirids ANOVA: p=0.043, lucinids ANOVA: p=0.001) (Figure 2).

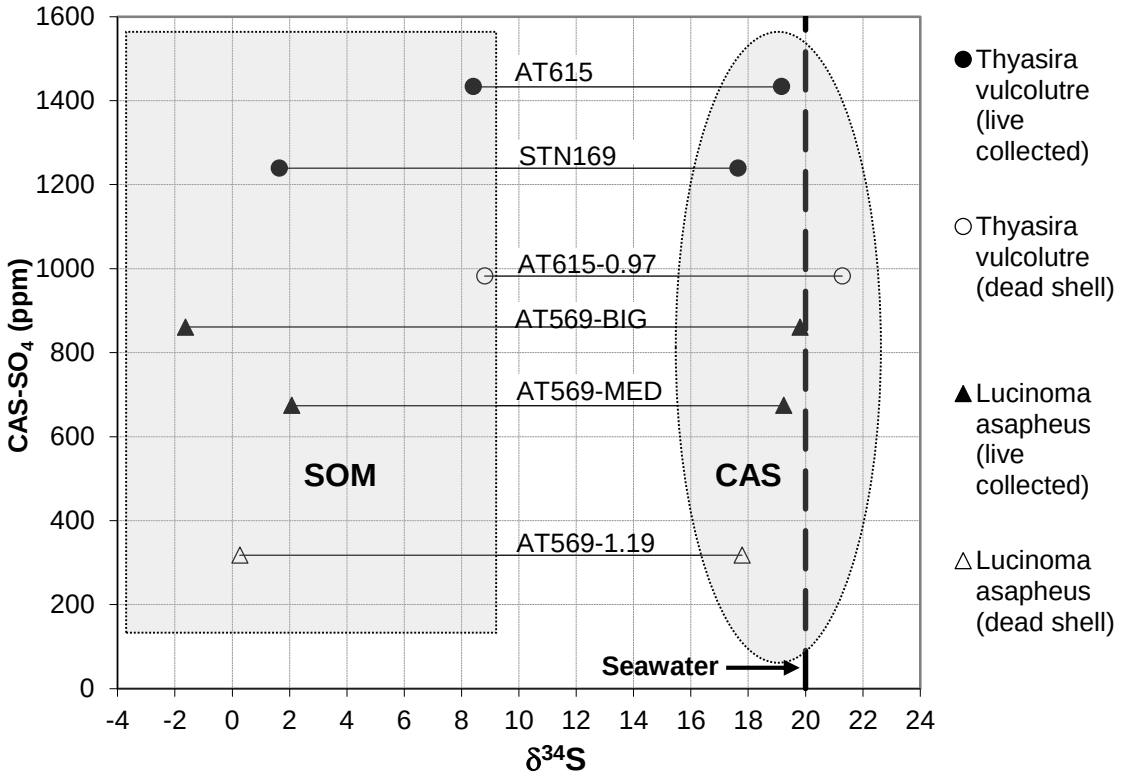

Figure 1. The sulphur isotopic composition of shell organic matter (SOM) and carbonate associated sulphate (CAS) vs. the concentrations of CAS in the shells of *Thyasira vulcolutre* and *Lucinoma asapheus* from the Gulf of Cadiz mud volcanoes. Seawater value from Bottrell & Raiswell (2000).

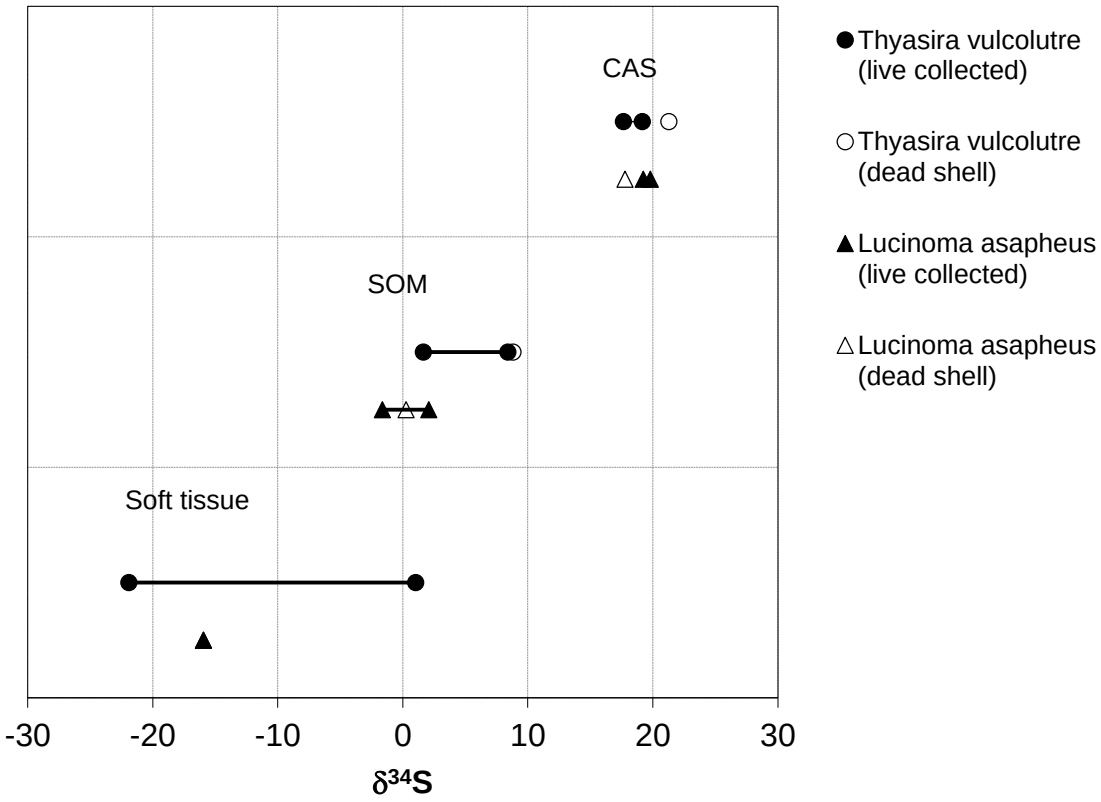

Figure 2. Range of values of CAS, SOM (both this study) and soft tissue values (Rodrigues et al., 2013) for *Thyasira vulcolutre* and *Lucinoma asapheus* from the Gulf of Cadiz mud volcanoes.

4. Discussion

The δ^{34}S-CAS values (range = +17.6 to +21.3, average = +19.15 ±1.4) from the chemosymbiotic bivalves are all very close to values of known seawater sulphate, (+20‰; Bottrell and Raiswell, 2000). The range of mean CAS values are within 2‰ of seawater, and this variability is comparable to modern non-seep shell material (+21.2 +/- 0.8‰; Kampschulte and Strauss, 2004). Thus, we conclusively show that the δ^{34}S-CAS in the carbonate shell of chemosymbiotic bivalves at active mud volcanoes is mostly derived from seawater sulphate, and does not incorporate depleted sulphate from sulphide oxidation. Therefore δ^{34}S-CAS from these bivalves does not record nutrition, and cannot be used as an indicator of chemosymbiosis. This observation is further supported by comparison of δ^{34}S-CAS values from both taxa (+17.6 to +21.3) to statistically different δ^{34}S-SOM (-1.6 to +8.8) and δ^{34}S-soft tissue data (-21.92 to +1.03), that imply a different sulphur source for the latter two.

For both thyasirids and lucinids, soft tissue and SOM $\delta^{34}S$ values reflect the contribution of the depleted sulphide used by the thiotrophic chemosynthethic bacteria (e.g. Fisher, 1995). The wide range of soft tissue $\delta^{34}S$ values for *Thyasira vulcolutre* has been attributed to local and regional variability of the sulphide pool (Rodrigues et al., 2013). Lack of incorporation of depleted sulphate in the shell carbonate could be explained by its insignificance in the mass balance of sulphur within the animal, which is dependent on behavioural strategies of the bivalves to obtain chemosymbiotic nutrition. Both lucinids and thyasirids are sediment dwellers that produce long ramified burrows spanning oxic–anoxic interfaces in the seafloor. They obtain sulphide from the sediments below and access oxygenated seawater circulating through the burrow and from above, via an anterior inhalant connection to the surface (Taylor and Glover, 2010, Taylor and Glover, 2000). Sulphide uptake from pore water in the burrows is not well understood, and could be transported to the symbionts via the foot tissue (Dufour, 2005), by diffusion up the burrow to the animal (Taylor and Glover, 2010), or possibly by entering the mantle cavity through the anterior gape (Addadi et al., 2006). The sulphur mass balance within the shell is determined by the relative supply of sulphate from seawater (related to shell pumping rate), and sulphate derived from symbiont controlled oxidation of sulphide, which is in turn linked to sulphide supply and symbiont oxidation rates. (Dando et al., 2004) found that the rates of sulphide oxidation were close to the rate of sulphide formation in a controlled experiment with *Thyasira sarsi*. Oxidation of the sulphide has a high oxygen requirement and rapid and continuous uptake of oxygenated water has been suggested (Childress and Girguis, 2011). This oxygenated water would contain abundant sulfate at seawater concentration and isotopic composition.It is also unknown whether the transport mechanisms for the sulphide brings additional pore water sulphate into the shell cavity, which can be present at equal or higher concentration to sulphide in the anoxic methane-sulphate transition zone (Niemann et al., 2006). It is likely that the amount of ^{34}S-depleted sulphate generated by the chemosymbiotic bacteria is too small to be detected isotopically in the CAS relative to the high concentrations of seawater sulphate. Even if isotopically depleted sulphate derived from the chemosymbiont bacteria is present in high enough abundance, it might not be transported through the mantle epithelia to the extrapallial fluid, and therefore would not be available to become incorporated within the shell (Wilbur 1964; Neff 1972). Whilst metabolic ions are known to be incorporated (e.g. metabolic carbon can make up to 10% of the total shell carbon (Duperron et al., 2008), the biosynthetic pathways for this process are not well known. Instead of being conducted to the calcification site, the depleted

sulphate could be treated as waste products and expelled via the posterior exhalant siphon (Lucinidae) or discharged into the sediment (Thyasiridae) (Raulfs et al., 2004, Jolly et al., 2004). A alternative explanation for the absence of depleted sulphate is a scenario whereby the sulphide is not completely oxidized to sulphate by the bacteria, but is stored in the bacterial cells as elemental sulphur (Lechaire et al., 2008, Vetter, 1985) or excreted as an intermittent oxidation state product. The δ^{34}S-CAS values we obtained in this study are mostly < 20‰, a little below the lower end of the range for modern bivalves reported in Kampschulte et al (2001) (+20.1; Kampschulte et al., 2001). It is possible that this indicates the effect of depleted sulphide, albeit a small contribution. Another possible explanation for this bias to lower δ^{34}S-CAS values is the incorporation of sulphur from intra-crystalline SOM. This is likely to also have the depleted isotopic values found in soft tissues and is not removed during the bleach step as it represents the small percentage of SOM bound within the lattice of the micro-crystals. This is in contrast to the inter-crystalline SOM extracted by the bleach procedure which forms a framework between the carbonate crystals. The incorporation of intracrystalline SOM sulphur into the CAS precipitate has been little investigated, but the depleted intercrystalline SOM values show the potential of this source for contamination of CAS. SOM can make up as much as 5% weight percent of the shell (Marin et al., 2012) and, in CAS studies excluding a bleach step, has the potential to affect sulphur stable isotope analysis if the δ^{34}S-CAS and δ^{34}S-SOM differ. In the case of heterotrophic bivalves both fractions generally reflect seawater sulphate and the isotopic effect of the incorporation of SOM-sulphur would be undetectable. It's possible that incorporation of sulphur from SOM is partially responsible for the wide range and variability of apparent CAS-sulphur concentrations in CAS studies that did not include a bleach step. For instance Kampschulte et al (2001) reported a range of 100 to 6700 ppm in biogenic carbonate, and 1238 +/- 795 ppm for heterotrophic bivalves (n=15). For future analyses it is important to understand the relationship between the CAS and SOM isotopic compositions, the concentrations of sulphur sources, and develop methods of analysis that effectively separate the organic and inorganic sulphur fractions in the shell.

This study presents the first δ^{34}S-SOM values from bivalves living at active mud volcanoes, and the Thyasiridae in general. Previously published results from thiotrophic bivalves (Lucinidae and Vesicomyidae) from hydrothermal vent sites and shallow reducing environments show δ^{34}S-SOM values ranging from -26.70 to -2.50 ‰ (n=8, (Mae et al., 2007, Dreier et al., 2012, Dreier et al., 2014). The isotopic difference between δ^{34}S -SOM and associated δ^{34}S-soft tissue from these studies

can be as high as 11.5‰, but with the SOM being generally more isotopically depleted than soft tissue values. Compared to previous studies, the enriched SOM-$\delta^{34}S$ values obtained in this study ($\delta^{34}S$ -1.6 to +8.8‰), and their enrichment compared to soft tissue data ($\delta^{34}S$ -21.92 to +1.32‰) could be explained through species-specific biological effects or differences in SOM extraction methods. With the available data it is not possible to distinguish between these two possibilities.

The $\delta^{13}C$ and $\delta^{18}O$ analysis of molluscs shell carbonate is well known to provide information about the isotopic composition of seawater dissolved inorganic carbon and temperature, whilst the isotopic analysis of soft tissue and SOM provides information on nutrition. Our work shows that the utility of CAS-sulphur isotopes follows this pattern as we show it is only of use in reconstructing the isotopic composition of local seawater sulphate, even when analysing chemosymbiotic bivalves. We also show that information about chemosymbiotic thiotrophic nutritional strategies can be derived from SOM of bivalves in a similar way to that of soft tissue. Given its potential for long term preservation, SOM therefore represents the more promising record of chemosymbiosis in the fossil record.

Acknowledgements

This work was partially funded by Fundação para a Ciência e Tecnologia (FCT) under the European Regional Development Fund through COMPETE (FCOMP-01-0124-FEDER-010569) and the projects PEst-C/MAR/LA0017/2013 and UID/AMB/50017/2013 CFR is supported by a postdoctoral fellowship (SFRH/BPD/64154/2009) from FCT. EP is supported by Leverhulme Trust research grant RPG-2012-470. The funding bodies played no role in the collection, analysis or interpretation of the data in this paper.

References

ADDADI, L., JOESTER, D., NUDELMAN, F. & WEINER, S. 2006. Mollusk Shell Formation: A Source of New Concepts for Understanding Biomineralization Processes. *Chemistry – A European Journal,* 12**,** 980-987.

BERMAN, A., ADDADI, L., KVICK, A., LEISEROWITZ, L., NELSON, M. & WEINER, S. 1990. Intercalation of sea urchin proteins in calcite: study of a crystalline composite material. *Science,* 250**,** 664-667.

BOTTRELL, S. & RAISWELL, R. 2000. Sulphur isotopes and microbial sulphur cycling in sediments. *Microbial Sediments.* Springer.

BRUSER, T., LENS, P. & TRUPER, H. 2000. The biological sulfur cycle. *In: Environmental Technologies to Treat Sulfur Pollution/PNL Lens and LW Hulshoff Pol.-London: IWA Publishing, 2000.-ISBN 1900222094*.

CAVANAUGH, C. M., MCKINESS, Z., NEWTON, I. L. & STEWART, F. J. 2006. Marine chemosynthetic symbioses. *The prokaryotes,* 1**,** 475-507.

CHILDRESS, J. & GIRGUIS, P. 2011. The metabolic demands of endosymbiotic chemoautotrophic metabolism on host physiological capacities. *The Journal of Experimental Biology,* 214**,** 312-325.

DANDO, P., SOUTHWARD, A. & SOUTHWARD, E. 2004. Rates of sediment sulphide oxidation by the bivalve mollusc Thyasira sarsi. *Marine Ecology Progress Series,* 280**,** 181-187.

DEUSNER, C., HOLLER, T., ARNOLD, G. L., BERNASCONI, S. M., FORMOLO, M. J. & BRUNNER, B. 2014. Sulfur and oxygen isotope fractionation during sulfate reduction coupled to anaerobic oxidation of methane is dependent on methane concentration. *Earth and Planetary Science Letters,* 399**,** 61-73.

DREIER, A., LOH, W., BLUMENBERG, M., THIEL, V., HAUSE-REITNER, D. & HOPPERT, M. 2014. The isotopic biosignatures of photo-vs. thiotrophic bivalves: are they preserved in fossil shells? *Geobiology,* 12**,** 406-423.

DREIER, A., STANNEK, L., BLUMENBERG, M., TAVIANI, M., SIGOVINI, M., WREDE, C., THIEL, V. & HOPPERT, M. 2012. The fingerprint of chemosymbiosis: origin and preservation of isotopic biosignatures in the nonseep bivalve Loripes lacteus compared with Venerupis aurea. *FEMS Microbiology Ecology,* 81**,** 480-493.

DUFOUR, S. C. 2005. Gill anatomy and the evolution of symbiosis in the bivalve family Thyasiridae. *The Biological Bulletin,* 208**,** 200-212.

DUPERRON, S., HALARY, S., LORION, J., SIBUET, M. & GAILL, F. 2008. Unexpected co-occurrence of six bacterial symbionts in the gills of the cold seep mussel Idas sp. (Bivalvia: Mytilidae). *Environmental Microbiology,* 10**,** 433-445.

FISHER, C. R. 1995. Toward an Appreciation of Hydrothennal-Vent Animals: Their Environment, Physiological Ecology, and Tissue Stable Isotope Values. *Seafloor hydrothermal systems: physical, chemical, biological, and geological interactions***,** 297-316.

FRY, B., GEST, H. & HAYES, J. S. 1988. 34S/32S fractionation in sulfur cycles catalyzed by anaerobic bacteria. *Applied and environmental microbiology,* 54**,** 250-256.

JOLLY, C., BERLAND, S., MILET, C., BORZEIX, S., LOPEZ, E. & DOUMENC, D. 2004. Zona Localization of Shell Matrix Proteins in Mantle of Haliotis tuberculata (Mollusca, Gastropoda). *Marine Biotechnology,* 6**,** 541-551.

JØRGENSEN, B. B., BÖTTCHER, M. E., LÜSCHEN, H., NERETIN, L. N. & VOLKOV, I. I. 2004. Anaerobic methane oxidation and a deep H 2 S sink generate isotopically heavy sulfides in Black Sea sediments. *Geochimica et Cosmochimica Acta,* 68**,** 2095-2118.

KAMAT, S., SU, X., BALLARINI, R. & HEUER, A. 2000. Structural basis for the fracture toughness of the shell of the conch Strombus gigas. *Nature,* 405**,** 1036-1040.

KAMPSCHULTE, A., BRUCKSCHEN, P. & STRAUSS, H. 2001. The sulphur isotopic composition of trace sulphates in Carboniferous brachiopods: implications for coeval seawater, correlation with other geochemical cycles and isotope stratigraphy. *Chemical Geology,* 175**,** 149-173.

KAMPSCHULTE, A. & STRAUSS, H. 2004. The sulfur isotopic evolution of Phanerozoic seawater based on the analysis of structurally substituted sulfate in carbonates. *Chemical Geology,* 204**,** 255-286.

LECHAIRE, J.-P., FRÉBOURG, G., GAILL, F. & GROS, O. 2008. In situ characterization of sulphur in gill-endosymbionts of the shallow water lucinid Codakia orbicularis (Linné, 1758) by high-pressure cryofixation and EFTEM microanalysis. *Marine Biology,* 154**,** 693-700.

MAE, A., YAMANAKA, T. & SHIMOYAMA, S. 2007. Stable isotope evidence for identification of chemosynthesis-based fossil bivalves associated with cold-seepages. *Palaeogeography, Palaeoclimatology, Palaeoecology,* 245**,** 411-420.

MARIN, F., LE ROY, N. & MARIE, B. 2012. The formation and mineralization of mollusk shell. *Front Biosci,* 4**,** 1099-1125.

NIEMANN, H., DUARTE, J., HENSEN, C., OMOREGIE, E., MAGALHAES, V., ELVERT, M., PINHEIRO, L., KOPF, A. & BOETIUS, A. 2006. Microbial methane turnover at mud volcanoes of the Gulf of Cadiz. *Geochimica et Cosmochimica Acta,* 70**,** 5336-5355.

O'DONNELL, T. H., MACKO, S. A., CHOU, J., DAVIS-HARTTEN, K. L. & WEHMILLER, J. F. 2003. Analysis of δ13C, δ15N, and δ34S in organic matter from the biominerals of modern and fossil Mercenaria spp. *Organic Geochemistry,* 34**,** 165-183.

OLIVER, G., RODRIGUES, C. F. & CUNHA, M. R. 2011. Chemosymbiotic bivalves from the mud volcanoes of the Gulf of Cadiz, NE Atlantic, with descriptions of new species of Solemyidae, Lucinidae and Vesicomyidae. *ZooKeys,* 113**,** 1-38.

RAULFS, E. C., MACKO, S. A. & VAN DOVER, C. L. 2004. Tissue and symbiont condition of mussels (Bathymodiolus thermophilus) exposed to varying levels of hydrothermal activity. *Journal of the Marine Biological Association of the United Kingdom,* 84**,** 229-234.

RODRIGUES, C., HILÁRIO, A. & CUNHA, M. 2013. Chemosymbiotic species from the Gulf of Cadiz (NE Atlantic): distribution, life styles and nutritional patterns. *Biogeosciences,* 10**,** 2569-2581.

RODRIGUES, C. F., WEBSTER, G., CUNHA, M. R., DUPERRON, S. & WEIGHTMAN, A. J. 2010. Chemosynthetic bacteria found in bivalve species from mud volcanoes of the Gulf of Cadiz. *FEMS Microbiology Ecology,* 73**,** 486-499.

TAYLOR, J. D. & GLOVER, E. A. 2000. Functional anatomy, chemosymbiosis and evolution of the Lucinidae. *Geological Society, London, Special Publications,* 177**,** 207-225.

TAYLOR, J. D. & GLOVER, E. A. 2010. Chemosymbiotic bivalves. *The Vent and Seep Biota.* Springer.

VAN DOVER, C. L., GERMAN, C., SPEER, K. G., PARSON, L. & VRIJENHOEK, R. 2002. Evolution and biogeography of deep-sea vent and seep invertebrates. *Science,* 295**,** 1253-1257.

VAN RENSBERGEN, P., DEPREITER, D., PANNEMANS, B., MOERKERKE, G., VAN ROOIJ, D., MARSSET, B., AKHMANOV, G., BLINOVA, V., IVANOV, M. & RACHIDI, M. 2005. The El Arraiche mud volcano field at the Moroccan Atlantic slope, Gulf of Cadiz. *Marine Geology,* 219**,** 1-17.

VETTER, R. 1985. Elemental sulfur in the gills of three species of clams containing chemoautotrophic symbiotic bacteria: a possible inorganic energy storage compound. *Marine Biology,* 88**,** 33-42.

VETTER, R. & FRY, B. 1998. Sulfur contents and sulfur-isotope compositions of thiotrophic symbioses in bivalve molluscs and vestimentiferan worms. *Marine Biology,* 132**,** 453-460.

VETTER, R. D. 1991. Symbiosis and the evolution of novel trophic strategies: thiotrophic organisms at hydrothermal vents. *Symbiosis as a source of evolutionary innovation: speciation and morphogenesis,* 219**,** 248.